ISSN 2413-5577

№ 2 Апрель – Июнь 2024

Экологическая безопасность прибрежной и шельфовой зон моря

Ecological Safety of Coastal and Shelf Zones of Sea

No. 2 April – June 2024

ecological-safety.ru

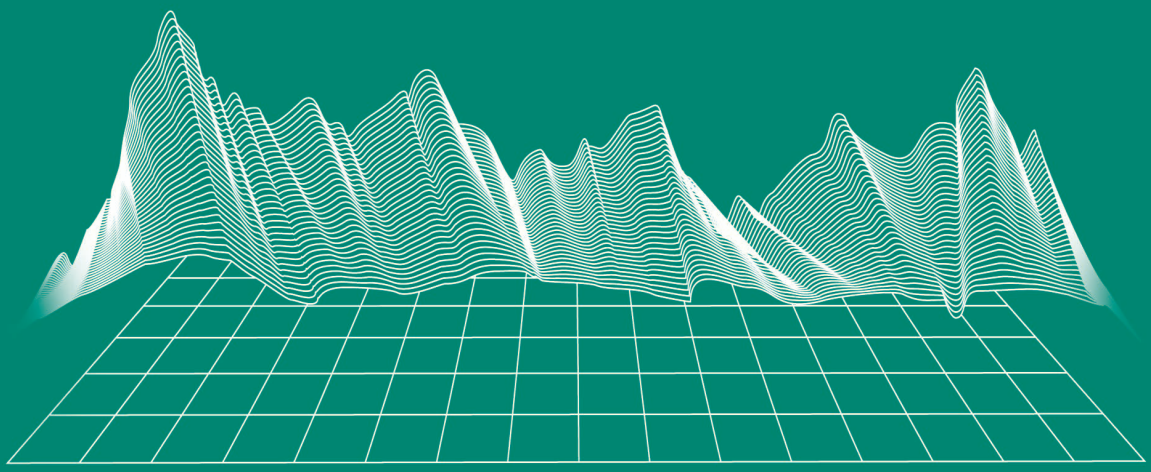

ISSN 2413-5577
No. 2, 2024
April – June

Publication frequency:
Quarterly
16+

ECOLOGICAL SAFETY OF COASTAL AND SHELF ZONES OF SEA

Scientific and theoretical peer reviewed journal

FOUNDER AND PUBLISHER:
Federal State Budget Scientific Institution
Federal Research Centre
"Marine Hydrophysical Institute of RAS"

The Journal publishes original research results, review articles (at the editorial board's request) and brief reports.

The Journal aims at publication of results of original scientific research concerning the state and interaction of geospheres (atmosphere, lithosphere, hydrosphere, and biosphere) within coastal and shelf areas of seas and oceans, methods and means of study thereof, ecological state of these areas under anthropogenic load as well as environmental protection issues.

The Journal's editorial board sees its mission as scientific, educational and regulatory work to preserve the ecological balance and restore the resource potential of coastal and shelf areas believing that despite the geographical limitations of the areas under study, the processes taking place within them have a significant impact on the waters of the seas and oceans and economic activity.

The Journal publishes original research materials, results of research performed by national and foreign scientific institutions in the coastal and shelf zones of seas and oceans, review articles (at the editorial board's request) and brief reports on the following major topics:
- Scientific basis for complex use of shelf natural resources
- Marine environment state and variability
- Coastal area state and variability; coast protection structures
- Monitoring and estimates of possible effects of anthropogenic activities
- Development and implementation of new marine environment control and monitoring technologies

The outcome of the research is information on the status, variability and possible effects of anthropogenic activities in the coastal and shelf marine areas, as well as the means to perform calculations and to provide information for making decisions on the implementation of activities in the coastal zone.

e-mail: ecology-safety@mhi-ras.ru

website: http://ecological-safety.ru

Founder, Publisher and Editorial Office address:
2, Kapitanskaya St.,
Sevastopol, 299011, Russia

Phone, fax: + 7 (8692) 54-57-16

EDITORIAL BOARD

РЕДАКЦИОННАЯ КОЛЛЕГИЯ

CONTENTS

№ 2. 2024 April – June, 2024

СОДЕРЖАНИЕ

№ 2. 2024 Апрель – Июнь, 2024

Original article

Anthropogenic Impact on the Coastal Zone of Koktebel Bay (Black Sea) over the Last 100 Years

Yu. N. Goryachkin

Marine Hydrophysical Institute of RAS, Sevastopol, Russia
e-mail: yngor@mhi-ras.ru

Abstract

In view of the problem of unsustainable nature management, the paper considers coastal dynamics of a popular Crimean resort. The work aims to provide a post-assessment of changes in the Koktebel Bay coastal zone under the anthropogenic influence. The paper uses materials of surveys, literary and archival sources, data on the digitization of coastlines in space images for 2011–2021. Physical, geographical and lithodynamic characteristics of the bay were given. Anthropogenic impact on the coastal zone and coastline response thereto were considered. It is shown that for the last 100 years, anthropogenic impact on Koktebel Bay has led to a reduction in the width or to disappearance of beaches, changes in their material composition, replacement of the natural landscape by the anthropogenic one and, therefore, its aesthetic attraction has decreased. Three periods were identified in the evolution of the coastal zone. The first one is characterized by a gradual increase in anthropogenic impact on the landscapes of the land and coastal zone. In the second period, the established dynamic balance was disturbed and the balance of sediments became negative. This was due to the regulation of the streamflows and the industrial development of sand, gravel and pebbles in the coastal zone. This led to a sharp decrease in the area of the beaches, up to their complete disappearance in certain areas. The third period is characterized by a dramatic increase in anthropogenic impact, which manifested itself in the active (often illegal) construction of various structures on the beaches and by erection of hydraulic structures in order to protect and restore the beaches. It was shown that to date, man-made coasts occupy about 3 km and here natural processes have transformed into natural-anthropogenic. Natural coastal landscapes have preserved only in the eastern (about 2 km long) and western (about 1.5 km long) parts of the bay with its total length of 7 km. The paper provides information on coastal protection projects: both those fulfilled earlier and those being currently implemented.

Keywords: Black Sea, Crimea, Koktebel Bay, anthropogenic impact, coastline, space images, coastal protection

Acknowledgments: The work was carried out under state assignment no. FNNN-2024-0016.

For citation: Goryachkin, Yu.N., 2024. Anthropogenic impact on the coastal zone of Koktebel Bay (Black Sea) over the last 100 years. *Ecological Safety of Coastal and Shelf Zones of Sea*, (2), pp. 6–22.

Антропогенное воздействие на береговую зону бухты Коктебель (Черное море) за последние 100 лет

Ю. Н. Горячкин

Морской гидрофизический институт РАН, Севастополь, Россия
e-mail: yngor@mhi-ras.ru

Аннотация
В связи с проблемой нерационального природопользования рассмотрена динамика берегов одного из популярных курортов Крыма. Цель работы – дать ретроспективную оценку изменений береговой зоны бухты Коктебель, подвергающейся антропогенному воздействию. Использованы материалы обследований, литературные и архивные источники, данные оцифровки береговых линий на космических снимках за 2011–2021 гг. Даны физико-географическая и литодинамическая характеристики бухты. Рассмотрено антропогенное воздействие на береговую зону и отклик береговой линии на него. Показано, что за последние 100 лет антропогенное воздействие на бухту Коктебель привело к сокращению ширины или исчезновению пляжей, изменению их вещественного состава, замене естественного ландшафта антропогенным, что снизило его эстетическую привлекательность. Выделено три периода в эволюции береговой зоны. Для первого характерно постепенное нарастание антропогенного воздействия на ландшафты суши и береговой зоны. Во второй период сложившееся динамическое равновесие нарушилось и баланс наносов стал отрицательным. Это было обусловлено зарегулированием стока водотоков и промышленной разработкой песка, гравия и гальки в береговой зоне. Такое воздействие привело к резкому уменьшению площади пляжей, вплоть до полного их исчезновения на отдельных участках. Третий период характеризуется резким увеличением антропогенного воздействия, которое выразилось в активном (часто незаконном) строительстве на пляжах различных сооружений, а также возведением гидротехнических сооружений с целью защиты и восстановления пляжей. Показано, что к настоящему времени техногенные берега занимают около 3 км, здесь природные процессы трансформировались в природно-антропогенные. Природные ландшафты берегов сохранились только в восточной (протяженностью около 2 км) и западной (около 1.5 км) частях бухты при общей ее длине 7 км. Приводятся сведения о проектах защиты берега, выполненных ранее и реализуемых в настоящее время.

Ключевые слова: Черное море, Крым, бухта Коктебель, антропогенное воздействие, береговая линия, космические снимки, берегозащита

Благодарности: работа выполнена в рамках выполнения государственного задания FNNN-2024-0016

Для цитирования: *Горячкин Ю. Н.* Антропогенное воздействие на береговую зону бухты Коктебель (Черное море) за последние 100 лет // Экологическая безопасность прибрежной и шельфовой зон моря. 2024. № 2. С. 6–22. EDN UTBCDW.

Introduction

The anthropogenic impact on the environment has reached such proportions that it has become one of the main global agenda issues. This impact has not bypassed the coastal zone of seas and oceans. As is known, about 40% of humanity lives in the regions adjacent to it, and the population density is twice as high as the average one [1)].

[1)] Available at: https://www.unep.org/ru/issleduyte-temy/okeany-i-morya/nasha-deyatelnost/rabota-po-regionalnym-moryam/upravlenie [Accessed: 20 May 2024].

The Black Sea is no exception. For thousands of years, its coastline has changed under the influence of natural factors, but remained a stable self-regulating system. However, constant anthropogenic impact on the coastal zone has brought it out of this state since the mid-20th century. The coastline has begun to retreat intensively over a considerable distance destroying some coastal objects and posing a threat to others. The reduction and disappearance of beaches, deterioration of their material composition have reduced the recreational attractiveness of the resort. In a number of regions, landscapes have changed from natural to man-made.

Researchers from different countries recognize the dominant role of the anthropogenic factor in changing the natural environment of the Black Sea coastal zone over the past 100 years [1–6]. The same can be said about the coastal zone of the Crimean Peninsula [7–10]. We classified the types of anthropogenic impact on the coastal zone of the Black Sea coast of Crimea in [10, 11]. In [12], changes in the coastal zone over the past 100 years were studied using the example of the resort of Yevpatoriya and it is shown that these changes were caused mainly by ill-considered actions in the past. Unfortunately, even now, when developing business projects, previously acquired experience is often ignored, which leads to negative consequences. In this sense, the stages of the development of the coastal zone in Koktebel Bay, which is a well-known resort area, are typical.

Koktebel became a popular summer holiday resting place at the end of the 19th century. As early as the 1890s, famous writers, artists and scientists visited the estate of Eduard Junge, the owner of the surrounding lands, which he sold for summer cottages. Despite such fame of Koktebel Bay, there are very few literary sources devoted to its nature. In our opinion, this is due to the proximity of the bay to the Kara Dag massif, which was given primary importance due to the uniqueness of its nature. Among the oldest ones, we can note publications [2), 3)] containing the information concerning the width and material composition of the Koktebel beaches.

The first scientific survey of the bottom of the bay by divers was carried out in 1939 under the leadership of Academician R. A. Orbeli, founder of the Russian underwater archeology [4)]. In the western part, the remains of an ancient underwater breakwall were discovered. Some of its masonry was removed and used in the construction of the pier and in 1933–1934 its remains were blown up. Presence of the ancient breakwall, absence of ancient Black Sea terraces on the shore, as well as shallow waters and configuration of the bay made it possible for V. P. Zenkovich to conclude that the shore of the bay was ingressive, experiencing modern submergence [4)]. This monograph published in 1954 and classified until 1992 contains only one and a half pages devoted to Koktebel Bay. The work mainly describes its eastern wing – Toprakh-Kaya Cape. The monograph dedicated to Kara Dag contains some information about the bay [13]. Work [14] examines the issues of morphology

---

[2)] Elpatievsky, S.Ya., 1913. [*Crimean Notes*]. Moscow, 149 p. (in Russian).

[3)] Voloshinov, I.M., 1929. [*Crimean Guide. Crimean Society of Naturalists and Nature Lovers*]. Simferepol: Krymskoe Gosudarstvennoe Idatelstvo, 614 p. (in Russian).

[4)] Zenkovich, V.P., 1954. [*Morphology and Dynamics of the Black Sea Coasts Within the Borders of the USSR. Part III. Section II (Southern Crimea, Kerch and Taman Peninsulas)*]. Moscow, 234 p. (in Russian).

and dynamics of the eastern coasts of Crimea. Some peculiar conclusions on the reasons for the reduction of beaches in Koktebel are given in [15]. The modern granulometric composition of sediments in Koktebel Bay based on the results of a survey by MHI in 2021 is considered in [16].

In our opinion, the most information about Koktebel Bay is contained in the monograph by A.A. Klyukin devoted mainly to the South-Eastern Crimea exogeodynamics [17]. However, the information is scattered across several chapters and does not provide a comprehensive picture of the natural conditions and coastal dynamics.

This work aims to provide post-assessment of changes in the Koktebel Bay coastal zone over the past 100 years under the anthropogenic impact.

Materials and methods

We analyzed the materials of the Koktebel Bay surveys in 2009 and 2021 carried out by Marine Hydrophysical Institute of Russian Academy of Sciences (MHI). The work used the data on the digitizing of coastlines in space images of the Google Earth service for 2011–2021. At the same time, to compare the coastlines, they were additionally referenced by clearly visible landmarks on the coast of the urban-type settlement of Koktebel due to insufficient reference accuracy for our purposes. Since there were no such landmarks outside the settlement, the images were referenced to coastal roads, which are fairly stable elements of the landscape. In addition, literary and archival sources were used, mainly departmental reports of liquidated organizations (Division of Landslide Protection, Yalta Team of KrymMorGeologiya Association, Institute of Mineral Resources of the Ministry of Geology of the Ukrainian SSR). An electronic archive of photographic images of the Crimean Peninsula coasts created at MHI was also used.

Physical, geographical and lithodynamic characteristics of Koktebel Bay

Koktebel Bay (here and below the official names of geographical objects are given) is located between Cape Planerny (formerly called Malchin) in the west and Cape Lagerny (formerly called Toprakh-Kaya) in the east (Fig. 1). The resort village (urban-type settlement) of Koktebel is located on the shore of the bay. The length of the bay coastline is about 7 km. The distance along the line connecting the above mentioned capes is about 4 km, with the largest perpendicular to this line being 2 km long. Thus, the bay forms an almost perfect semicircle.

In its southern part, the coastline is most indented and forms a series of small bays with boulder heaps on the edge and near the shore. The landslide of boulder heaps in the water stretches for 1.5 km, and they are also noted in the eastern part near Cape Lagerny. The coast in the western part is mountainous and abrasive, with small bays. In the eastern part, it is abrasive, with landslide and loose rocks. The central part of the coast can be classified as accumulative and man-made according to the prevailing modern exogenous processes [11].

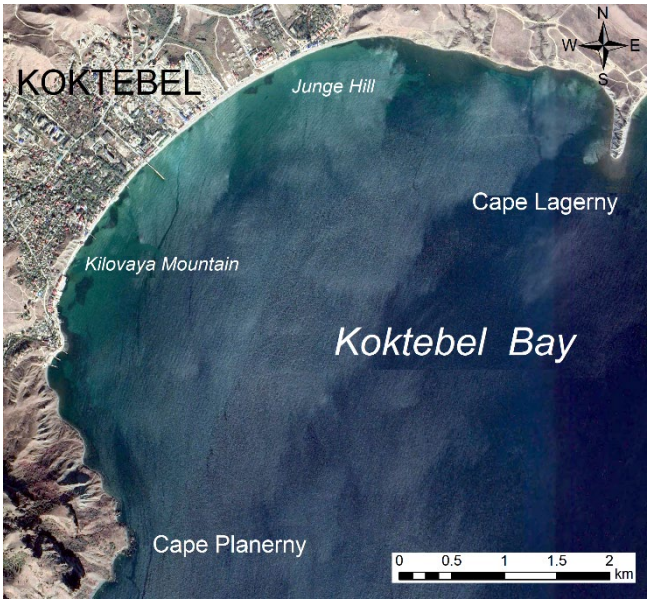

Fig. 1. Sketch-map of Koktebel Bay

The southern edge of the bay consists of cliffs of the Magnitny Ridge, which is part of the Kara Dag massif. The strong volcanic rocks of this part of the bay are replaced to the north, first by a long valley, on the shore of which there was previously a pier and now three groins, and then by a protrusion of an abrasive shore up to 30 m high composed of loose clay shales and marls (Kilovaya Mountain). Previously, the coast here was bordered by a wide pebble and sand beach. The open arc of the bay apex, 2 km long, borders an alluvial lowland, now almost completely developed. From the north, the slopes of Biyuk-Yanyshar Hill (up to 200 m high) approach the bay forming an active cliff about 10 m high near the shore. The cliff is composed of brown Quaternary and gray Jurassic clays. At the foot of the hill, in the western part adjacent to the Koktebel beaches, small (up to 3 m wide) boulder and block beaches are located, which gradually wedge out completely to the east. Cape Lagerny, which closes Koktebel Bay from the east, is an elongated narrow peninsula (more than half a kilometer long) made of gray Jurassic clays (Fig. 2). A narrow (2–3 m) platform lies at the foot of the cape cliffs. It is made up of exposed rock, in some places covered by small accumulations of rubble. This platform slopes down to the water gently and forms a wide bench. In front of the cape and on both sides of it, at a distance of up to 200 m from the water edge, blocks and plates of sandstone and clay shale washed out of the cape clay layer are scattered.

Koktebel Bay is shallow, with the 5 m isobath running on average at a distance of 200–300 m from the water edge and with depths of 10–15 m at the outer boundary of the bay. The western part of the bay is deeper, the shallowness of the bottom increases in its eastern part. Here, the 1 m isobath is located 100–120 m from the shore.

Fig. 2. View of Koktebel Bay from Biyuk-Yanyshar Hill

Further, the depth quickly increases, the distance between the 5 and 10 m isobaths is no more than 150 m. The source of beach material replenishment was previously the discharge of several watercourses flowing into the bay. In the central part, the mouth of the Yantiq River (the length and catchment area are about 10 km and 50 km^2, respectively) with the eponymous erosion gully and some temporary watercourses nearby.

Koktebel Bay is located to the east of the Southern Coast of Crimea (SCC), the border of which is considered to be Cape Planerny. The climate here, unlike the SCC subtropical Mediterranean climate, is coastal, moderately warm. The average annual air temperature is about 12°C, the average annual precipitation is about 400 mm. According to the data from the nearest hydrometeorological station Feodosia, the most frequent winds here are strong (10 m/s and more) ones from the northwest, northeast, south, southwest and west. The most frequent waves are those from the eastern, southeastern and southern directions. In total, waves from these directions account for 96% of all cases per year. Storms from the southern and eastern directions are most dangerous in terms of waves.

The beaches of Koktebel Bay are fed by the products of abrasion, erosion of landslides and rockslides, as well as biogenic material from the underwater coastal slope. Currently, the capes and wings of the bay are mainly subject to abrasive erosion. At the same time, it is mainly the eastern wing of the bay that is abraded (at the base of the cliffs and on the bench), while currently almost no abrasion is observed in the bay itself. Up to 90% of abrasion products arrive during the cold period, with the most active storms. In stormy years, which usually recur every 5–6 years, the volume of sediments exceeds the average value several times [17]. Sediments migrate along the coast from the capes to the bay and along the bay in both directions depending on the sea wave regime. When the proportion of relatively rare southern storms increases in the wave regime, sediments migrate from the southwestern and western parts to the northeastern and eastern parts of the bay, which is the main process in sediment dynamics.

The main source of beach material replenishment is stipulated by the erosion of landslide and rockslide tongues, where small ones are washed away during the storm season and relatively large ones – over the course of several years. Thus, the largest landslide from Cape Lagerny was completely washed away in eight years [17]. In 1913, the tongue of a large landslide located on the slope of the Kok-Kaya Ridge (western wing of the bay) protruded into the water area by more than 10 m and was washed away. In the spring of 1958, 6 m of the sliding tongue were cut off at the northeastern outskirts of Koktebel [15]. In 1980–1983, 5 thousand m^3 of loam were washed away from the sliding tongue extended into the water area near Cape Planerny [4]. At the same time, the drift products contain only 25% of the wave field sediments as they quickly become soaked and washed away. The drift increases in wet years and decreases in dry ones. The largest amount of sediments enters the coastal zone when wet years precede stormy years or coincide with them [17].

Anthropogenic impact and coastal dynamics

At the beginning of the 20th century, the shores of Koktebel Bay were a sparsely populated area. Old photographs show no significant construction (Fig. 3).

Works [2, 3] noted a beach with an incomplete profile and a width of up to 30 m along the coast. The bay bottom was sandy and shallow, the coastal shoal went tens of meters from the shore. The beach was predominantly composed of sand – a product of alluvial deposits carried away by watercourses. There was also a large amount of rounded pebbles from the solid rocks of the Kara Dag massif. On the back side of the beach, a clear ledge was observed everywhere, along which alluvial clays were washed away, so that the shore was not accumulative even at the top of the bay. In the western part of the bay shore, there were small sections of the beach cluttered with stones, with rocks of volcanic origin above them. It was noted that quite significant landslides sometimes occured in this area, traces of which were visible in the structure of the coastal slope [4].

Fig. 3. View of the western part of Koktebel Bay, photo 1914

The first significant intervention in the nature of the bay occurred in the 1920s. In 1925, a pier about 200 m long was built in its western part for loading trass (volcanic rock used to make a special type of cement) from a quarry developed nearby. The rock was extracted using blasting methods. When the material was delivered to the coast of the bay for crushing, rocks not related to trass were dumped into the water and accumulated in the coastal zone [5)]. The first embankment was built in the 1930s. During the Great Patriotic War, the German troops built up the coast with various anti-landing structures, including concrete ones, using local materials. They were dismantled after the war.

Until the mid-20th century, there were isolated small ponds in the gullies and valleys adjacent to Koktebel. In the second half of the century, most of the watercourses flowing into the bay were regulated, and about seventy reservoirs were formed, which sharply reduced the liquid and solid runoff. This was also facilitated by plowing, terracing and afforestation of the slopes adjacent to the bay. Here is a typical example: previously, an alluvial cone protruded into the water area from the mouth of the Yantiq River, the underwater continuation of which was traced on the bottom as evidenced by topographic maps of that time. Currently, this cone appears only after significant floods.

According to some data, before the regulation of the flow, the volume of removals from erosion forms had been comparable to the volume of abrasion products and erosion from coastal slopes, and it became half as much after the regulation, so less wave field sediments entered the coastal zone of the sea [17].

In the late 1950s, a new embankment with a breakwater wall was built in Koktebel, part of which was extended onto the beach. This design of the hydraulic structure subsequently played a negative role. At that time, there was still a sandy, gravel and pebble beach 20–30 m wide. It was distinguished by an unusual color due to the inclusion of pebbles from the Kara Dag rocks. It should be noted that the beach deposits were then and previously developed in an improvised manner for local construction needs, but in relatively small quantities. Beginning in 1954, industrial extraction of sand and gravel mixtures took place in the central part of the bay and on the beach. It was also carried out in neighboring areas: near the urban-type settlement of Kurortnoye, the urban-type settlement of Ordzhonikidze, in Tikhaya Bay (to the east of Cape Lagerny) and in the area of Feodosia.

The actual volumes of extraction, which continued until 1967, are unknown (according to estimates given in [14], they amounted to 1.5 million tons). As a result, the beaches began to shrink rapidly and their width in the western part of the bay was 5–10 m by the mid-1960s, and the water edge came right up to the cliff (Fig. 4).

The beach no longer provided any damping of the wave energy of even small storms. The beaches in the eastern part of the bay also became smaller. At Junge Hill, there was no beach at all and one could pass to the other side there with the help of footbridges in the water.

[5)] Rumanova, D.A., 1941. [*Report on Route Surveys of Coloured Stone Deposits and Experimental Mining of them on Mount Karadag and its Vicinity*]. Simferopol: Azchergeolupravlenie Krym. Geolbyuro, 66 p. (in Russian).

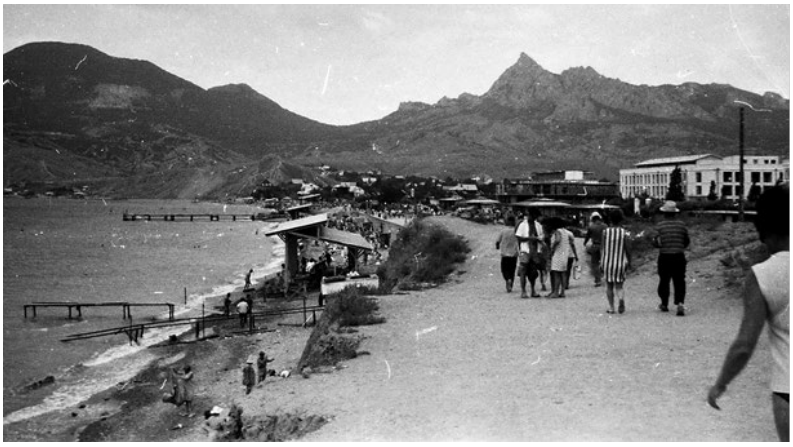

Fig. 4. A beach in Koktebel. Photo 1965

As a result of the use of beach material for economic and construction purposes lasted for more than 10 years, an emergency situation took place on the coast of the bay. Thus, in some places, the foundation of the retaining breakwater wall was washed away. Article [15] stated that the reduction of the beaches was caused by tectonic subsidence of the Koktebel Bay land. The velocity was determined as 2 m/year based on the fact that the beaches between 1963–1967 decreased by an average of 8 m. This statement contradicts clearly existing ideas about the velocity of the Earth crust vertical movements in this area, which is approximately three orders of magnitude less.

A strong storm in January 1967 washed away the remains of the beach, collapsed the retaining walls and destroyed the embankment (Fig. 5). The coast was washed away over a stretch of more than 2 km. The Koktebel beach practically ceased its existence and the buildings located behind the embankment were under threat of destruction.

Fig. 5. Consequences of the storm dated 13 January 1967. Photo 1967

In 1967, the Yalta Department of the GIPROKommunStroy Institute developed a project for emergency coastal protection measures, which envisaged partial restoration of the beaches by backfilling the water edge zone with imported material. The material was backfilled on the western wing of the bay in the amount of 150 thousand m^3 in approximately equal proportions of limestone rubble from the quarry of Mount Agarmysh (near the town of Stary Krym) and granite from the Donbass deposits. Taking into account the content of clay impurities, the actual volume was about 90 thousand m^3. Over 12 years, the rubble turned into pebbles. Its roundness was from 2.4 to 3.4 points on a four-point scale [6)].

As a result of the backfilling carried out in the coast sections where the width of the beach had been 2–4 m in 1966, by 1969 it had increased to 30–35 m, but the recreational properties of the previously existing beach were lost. The project envisaged the delivery of 360 thousand m^3 of beach-forming material more, but this stage of the project was not implemented.

Over a period of 13 years (1968–1981), the artificial beach material shifted almost entirely toward the center of the bay exposing the shore in the area of the municipal beach and the beach of the Koktebel Art Center. The width of the beaches in the western wing of the bay decreased significantly and the coastal zone experienced a significant increase in depth. Exposure and erosion of the bedrock were observed. The risk of destruction of the embankment in the western section of the bay arose again. To remedy the situation, several proposals were considered and an option was adopted that included the construction of coastal protection structures in six sections of the bay and the creation of a reserve backfill zone to replenish the beach in a specially designated area in the western wing of the bay. The expediency of such a solution was confirmed by the experience of 1967.

According to the 1984–1990 project of the Yalta Department of the UkrYuzhGIPROKommunStroy Institute, embankments with a stepped slope structure designed to dampen residual wave energy were built and an artificial beach was created. In addition, reserve filling of crushed stone in the amount of 144 thousand m^3 was carried out in the westernmost section of the coast. The width of the beach area along the entire length of the bay was restored. In 1988, the western section of the bay represented an artificial pebble beach leaning against the foot of the coastal slope; the width of the above-water part of the beach here reached 43 m (Fig. 6).

The implemented scheme of coastal protection structures performed its functions until the beginning of the 21st century, until capital construction began on the reserve filling area, accompanied by the degradation of the beaches. Thus, if the width of the beach on the western wing of the bay in 2002 was 22 m, then by 2004 it had decreased to 4–9 m. Let us give several examples of unauthorized construction.

In 2005, in the area northeast of the rescue station, where there was an artificial pebble beach and a prefabricated stepped slope structure made of flight slabs, part of the stepped slope structure was dismantled without permission and

---

[6)] Romanyuk, O.S., 1988. [*Report on Topic "Drawing up an Inventory of the Overwater Part of the Crimean Coastline at a Scale of 1:200,000". KKGRE, IMR*]. Simferopol, 497 p. (in Russian).

Fig. 6. An artificial beach in the western part of Koktebel Bay. Photo 1988

a vertical wall was erected. Here, part of the embankment was expanded by means of a stepped slope structure – a vertical reinforced concrete wall was erected along the abutment of the flight slabs, the sinus was filled with soil, a concrete covering was installed and later concrete tiles were laid on top of the concrete. The vertical wall installed instead of the existing slope structure contributed to the degradation of the beach, which subsequently led to its erosion and destruction. In the central part, to the west of the Voloshin House Museum, two platforms protruding into the sea were built illegally. Such transverse structures represent an obstacle to the existing flow of sediments and cause the accumulation of beach material in front of the structure and erosion behind the structure (in the direction of the flow). By 2009, this process had already been quite pronounced. Since the sediment flow is directed toward the center of the bay, the width of the above-water part of the beach northeast of the above mentioned platforms (in the area of the Voloshin House Museum) has decreased by 6–8 m in two years since the start of construction of the sites (2006); at the same time, beach material accumulated to the southwest. The structures built in the waterfront zone and extended into the sea prevented the natural movement of material and they were subjected to the intense wave action, as a result of which some of them were destroyed (Fig. 7).

When the Autonomous Republic of Crimea was a Ukrainian region, applications were repeatedly sent to administrative bodies indicating the inadmissibility of construction on the reserve filling area and the inevitability of the destruction of the constructed structures, but no effective measures were taken (Fig. 8).

Altogether, the general nature of the lithodynamic processes occurring in the bay remained unchanged throughout the 1990s and 2000s: the beach remained fairly stable in the central part of the bay; seasonal changes in the width of the above-water part of the beach were within 5 m with a beach width of up to 45 m; steady degradation of the beach was observed in the southwestern part (the reserve filling area).

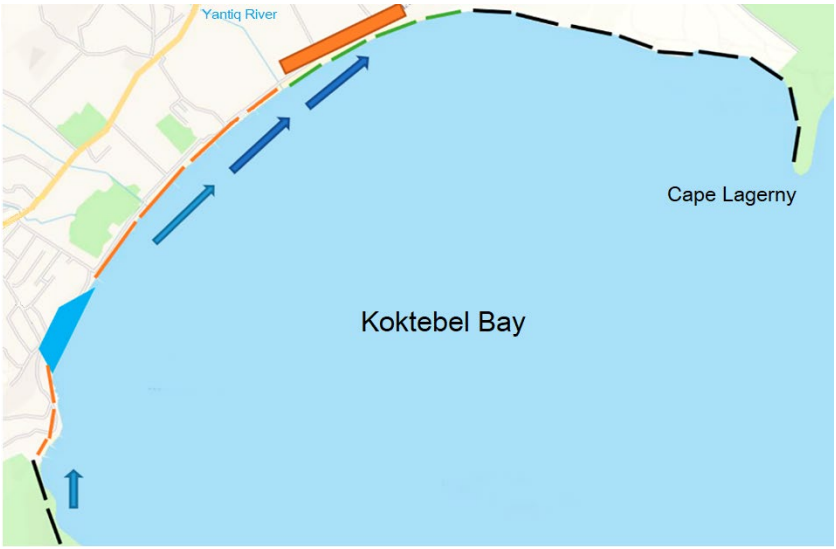

Fig. 7. Lithodynamics diagram. Black dashed line – areas of abrasion, orange one – coast retreat, green one – a relatively stable coast. Orange rectangle – place of sand extraction, blue trapezoid – place of reserve filling. Arrows – average long-term direction of sediment movement

Fig. 8. Reserve filling area. Photo 2021

In the last decade, it has become possible to analyze changes in the coastline using satellite images. To determine the change in beach width between 2009 and 2021, we use satellite images from this time and the results of surveys conducted in September 2009 and November 2021. A total of 15 images with a resolution of 0.6 m per pixel were used for the analysis.

The width of the beach to the west of the reserve filling area has hardly changed. Over the past period, it has fluctuated within 1–3 m, i.e. at the threshold of the method accuracy. It was difficult to determine the seaward boundary due to the boulders in the watershed zone. The reserve filling area is a pile of remains of reinforced concrete structures built at different times. The natural and later artificial beaches that existed here disappeared without a trace. By 2017, the buildings at the foot of Kilovaya Mountain had been almost completely destroyed by the sea. To the west of the Koktebel embankment, the width of the beaches was 9–13 m in 2009; in 2021, it remained unchanged. In fact, the beach has shrunk on the embankment from 9–18 m to 2 m (in the area of the illegally constructed platform), and in the eastern part of the embankment – to 8–12 m. At the same time, the interannual variability of the beach width in this section of the coast was about 5–6 m.

An analysis of the change in the beach area reduced to its length showed that for the period 2009–2021, on average, the width of the beaches along the embankment decreased by 4.8 m. In 2021, the width of the beach near the Voloshin monument was 10 m. To the east of the embankment, according to satellite images for 2008–2020, the configuration and width of the beach remained almost unchanged; in 2021, the beach was 15–20 m wide.

Further east, to Junge Hill and further east, the width of the above-water part of the beach ranged from 33 to 42 m according to a 2009 survey and satellite images. During this time, the width of the beach changed insignificantly (1–2 m). By 2021, the configuration of the coastline and the width of the beaches had hardly changed.

Further east, right up to the beginning of the cliff, the beach has gradually decreases. Its width and configuration of the coastline remained almost unchanged over the period 2009–2021 according to satellite images and survey materials from November 2021. In the area of the beginning of the cliff, the beach width in 2021 was 12 m, which corresponds to the 2021image. Further east, over a distance of 1 km, the abrasion coast in 2011–2021 retreated at an average rate of 0.7 m/year (Fig. 9). The rate of retreat of the coastline of the western part of Cape Lagerny during the same period was two times less – about 0.3 m/year.

Summarizing the results of the analysis of satellite images for 2011–2021 in comparison with the survey data of 2009 and 2021, it can be said that there were no changes along the greater length of the coastline of the urban-type settlement of Koktebel. At the same time, the beach completely disappeared in the reserve filling area and it decreased by 6–8 m in the area of the embankment.

During this period, the beach material of the central part of the bay was replenished due to the erosion of the bottom in the western section in the area of Kilovaya Mountain. This material moved in the eastern direction and as a result, the water line in the area of Voloshin house was relatively stable, while the depth

Fig. 9. Satellite image of the eastern part of Koktebel Bay in the area of the observation deck (September 2011). Red line – coastline in August 2021. Black lines – roads in August 2021

in the collapse zone in the area of Kilovaya Mountain increased significantly. It can be said that after the artificially created deficit of beach-forming sediments and the subsequent creation of artificial beaches in the coastal zone, a new state of dynamic balance was established, in which the volume of sediments on natural beaches in the long-term regime remains more or less constant and changes in either direction are temporary.

Conclusion

Thus, the anthropogenic impact on Koktebel Bay over the last 100 years has led to a reduction or disappearance of beaches, change in their material composition and replacement of the natural landscape with an anthropogenic one, which has reduced its aesthetic attraction.

Three periods can be distinguished in the evolution of the coastal zone of Koktebel Bay. In the first (starting from the 1920s), anthropogenic impact on the landscapes of the land and coastal zone increased gradually. In the incoming part of the sediment balance, solid runoff of watercourses and coastal abrasion prevailed, and sediment accumulation prevailed in the outgoing part. Some increase in solid runoff associated with anthropogenic impact on landscapes and the development of accelerated erosion was compensated by periodic removal of small volumes of sediment from the beaches for local construction needs.

During the second period (from the middle of the 20th century), the established dynamic balance was disrupted and the sediment balance became negative. This was stipulated by the regulation of the runoff and industrial extraction of sand, gravel

and pebbles in the coastal zone. This impact led to a sharp decrease in the width of the beaches, up to their complete disappearance in some areas.

The third period (from the last quarter of the 20th century to the present) is characterized by a sharp increase in anthropogenic impact, which was expressed in the active (often illegal) construction of various structures on the beaches to protect and restore the beaches by erecting hydraulic structures. In the incoming part of the sediment balance, such a component as artificial beach filling appeared, which partially compensates for the sediment deficit. A new dynamic balance has been established in the coastal zone over the past 10 years. By now, man-made shores occupy about 3 km, where natural processes have transformed into natural-anthropogenic ones. Natural coastal landscapes have been preserved only in the eastern (about 2 km) and western (about 1.5 km) parts of Koktebel Bay. The engineering load coefficient (the ratio of the total length of engineering structures to the length of the coast) for Koktebel Bay is currently 0.4.

It should be noted that artificial beaches remained the only way to preserve the coast of Koktebel Bay. However, they also have some disadvantages. Thus, the operation of artificial beaches must be accompanied by long-term additional costs for backfilling the material. Concrete structures reduce the aesthetic attraction of the coast and worsen water exchange in the water area (for example, three groins in the western part of the bay). The ability of water to self-purify in the bay is limited, especially in summer, which significantly worsens the quality of sea water and sanitary and epidemiological situation. Coarse debris of artificial beaches is less comfortable for recreation. Abrasion of crushed stone is accompanied by additional flow of suspended matter into the water area, decrease in water transparency and change in the composition of bottom sediments, which also affects the benthos negatively.

Therefore, when developing a new project for the reconstruction of the embankment and restoration of the beaches of Koktebel Bay with a total length of 1850 m, these provisions were taken into account. Thus, the original project provided for the construction of a system of groins. As a result of numerous discussions, including ones with the participation of employees of MHI, this project was rejected and another version was adopted. It provides for the construction of one groin 70 m long and backfilling of the beach with a width of 35 to 45 m. The groin located in the western part of the bay should limit the movement of beach material in the western direction and at the same time should not distort the natural landscape of Koktebel Bay significantly. Taking into account the movement of beach material, the criterion for assessing the need to replenish the beach area will be the width of the beach in the groin area. The beach material recommended by the project is gravel with a fraction of no more than 40 mm. Reconstruction of the embankment began in 2023 and is expected to be completed at the end of 2024.

In conclusion, we want to note that the number of vacationers to Koktebel Bay and consequently the economy of the region will depend on the ecological state of the coastal zone of the sea and its provision with comfortable beach resources, landscape diversity and coast attractiveness. Under the conditions of land private

ownership, the state must regulate issues related to the strengthening of the coast, protection of the coastal zone and coast of resort and recreational regions. It is necessary to use modern effective methods and technologies to protect the coast that do not violate the landscape appearance of the territory and the ecological state of coastal waters.

REFERENCES

1. Stãnicã, A., Panin, N. and Caraivan, G., 2012. Romania. In: E. Pranzini and A. Williams, eds., 2013. *Coastal Erosion and Protection in Europe*. London: Routledge, pp. 396–412.
2. Stancheva, M., 2013. Bulgaria. In: E. Pranzini and A. Williams, eds., 2013. *Coastal Erosion and Protection in Europe*. London: Routledge, pp. 378–395. https://doi.org/10.4324/9780203128558
3. Ozsahin, E., 2011. Human Impact (N Turkey) on the Black Sea Shore. In: Yu. Makogon, D. Ekinci and I. Mangaltepe, eds., 2011. *Black Sea Basin Studies*. Donetsk: Donetsk National University Publishing, pp. 381–412.
4. Tătui, F., Pîrvan, M., Popa, M., Aydogan, B., Ayat, B., Görmüş, T., Korzinin, D., Văidianu, N., Vespremeanu-Stroe, A. [et al.], 2019. The Black Sea Coastline Erosion: Index-Based Sensitivity Assessment and Management-Related Issues. *Ocean and Coastal Management*, 182, 104949. https://doi.org/10.1016/j.ocecoaman.2019.104949
5. Kosyan, R.D. and Krylenko, V.V., 2014. *The Current State of Marine Accumulative Shores of Krasnodar Region and their Use*. Moscow: Nauchnyy Mir, 256 p. (in Russian).
6. Krylenko, M.V., Krylenko, V.V. and Krylenko, D.V., 2022. Impact of Anthropogenic Factors on the Anapa Bay-Bay Relief. In: KGU, 2022. [*Proceedings of the 10th Scientific and Practical Conference "Tourist-Recreational Complex in the System of Regional Development". Sukhum, 11–15 April 2022*]. Krasnodar: Kubansky Gosudarstvenny Universitet, pp. 190–194 (in Russian).
7. Efremova, T.V. and Goryachkin, Yu.N., 2021. Anthropogenic Impact on the Coastal Zone of the Southern and Western Black Sea Coast (Review). *Ecological Safety of Coastal and Shelf Zones of Sea*, (2), pp. 5–29. https://doi.org/10.22449/2413-5577-2021-2-5-29 (in Russian).
8. Goryachkin, Yu.N. and Efremova, T.V., 2022. Anthropogenic Impact on the Lithodynamics of the Black Sea Coastal Zone of the Crimean Peninsula. *Ecological Safety of Coastal and Shelf Zones of Sea*, (1), pp. 6–30. https://doi.org/10.22449/2413-5577-2022-1-6-30
9. Efremova, T.V. and Goryachkin, Yu.N., 2023. Morphodynamics of the Sevastopol Bays under Anthropogenic Impact. *Ecological Safety of Coastal and Shelf Zones of Sea*, (1), pp. 31–47. https://doi.org/10.29039/2413-5577-2023-1-31-47
10. Goryachkin, Yu.N., 2010. Anthropogenic Impact on the Black Sea Coast of Crimea. In: MHI, 2010. *Ekologicheskaya Bezopasnost' Pribrezhnoy i Shel'fovoy Zon i Kompleksnoe Ispol'zovanie Resursov Shel'fa* [Ecological Safety of Coastal and Shelf Zones and Comprehensive Use of Shelf Resources]. Sevastopol: ECOSI-Gidrofizika. Issue 23, pp. 193–198 (in Russian).
11. Goryachkin, Yu.N. and Dolotov, V.V., 2019. *Sea Coasts of Crimea*. Sevastopol: Colorit, 256 p. (in Russian).
12. Goryachkin, Yu.N., 2020. Changes in the Yevpatoria Coastal Zone in the Last 100 Years. *Ecological Safety of Coastal and Shelf Zones of Sea*, (1), pp. 5–21. https://doi.org/10.22449/2413-5577-2020-1-5-21 (in Russian).
13. Morozova, A.L. and Vronsky, A.A., eds., 1989. [*Nature of Karadag*]. Kiev: Naukova Dumka, 288 p. (in Russian).

14. Zakharzhevsky, Ya.V., 1968. [Some Features of Morphology and Dynamics of Eastern Crimean Coasts near Planerskoe]. In: I. Ya. Yatsko, 1968. [*Geology of Coasts and Bottom of the Black Sea and the Sea of Azov within the Ukrainian Soviet Socialistic Republic*]. Kiev: Izd-vo Kievskogo Universiteta. Vol. 2, pp. 150–156 (in Russian).
15. Gavrilov, V.P., 1968. [Koktebel Bay Warping]. *Priroda*, (8), pp. 70–71 (in Russian).
16. Gurov, K.I., 2023. Granulometric Composition of Sediments in the Coastal Zone of Koktebel Bay (Crimea). *Ecological Safety of Coastal and Shelf Zones of Sea*, (4), pp. 34–45.
17. Klyukin, A.A., 2007. [*Exogeodynamics of Crimea*]. Simferopol, 320 p. (in Russian).

Submitted 12.01.2024; accepted after review 01.02.2024;
revised 27.03.2024; published 25.06.2024

About the author

Yuri N. Goryachkin, Chief Research Associate, Marine Hydrophysical Institute of RAS (2 Kapitanskaya St., Sevastopol, 299011, Russian Federation), Dr.Sci. (Geogr.), **ORCID ID: 0000-0002-2807-201X, ResearcherID: I-3062-2015,** *yngor@mhi-ras.ru*

The author has read and approved the final manuscript.

Original article

Seasonal Variability of Horizontal Gradients in the North Atlantic Large-Scale Thermohaline Frontal Zones

I. G. Shokurova *, N. V. Nikolsky, E. D. Chernyshova

Marine Hydrophysical Institute of RAS, Sevastopol, Russia
* *e-mail: igshokurova@mail.ru*

Abstract
The paper examines seasonal variability in the spatial distribution and magnitude of horizontal gradients of temperature, salinity and density in large-scale surface frontal zones in the North Atlantic Ocean. Monthly average temperature and salinity data at the 0.5 m horizon from the ORAS5 oceanic reanalysis (1958–2021) are used. High gradients of temperature exceeding 2 °C/100 km, those of salinity exceeding 1 PSU/100 km, and those of density exceeding 1 kg·m^{-3}/100 km were observed in the subpolar and temperate regions in fronts along large-scale currents carrying warm salty waters from the southern latitudes (Gulf Stream, North Atlantic Current) and cold waters with low salinity from the Arctic regions (Labrador Current, East Greenland Current). These fronts occur throughout the year. High salinity and density gradients are also observed in the tropical summer in the front at the edge of the Amazon River plume, resulting from seasonal river flow. In these five frontal zones, areas were identified for which quantitative estimates of seasonal variability of gradients are provided. In the subpolar and temperate latitudes, maximum temperature gradients are observed in winter. Warming up of water in the summer season is accompanied by a decrease in gradients. The greatest range of seasonal variability of temperature gradients was noted in the frontal zones of the Gulf Stream and the East Greenland Current. In summer, in the fronts of subpolar regions, salinity gradients increase due to the melting of Arctic and continental ice and an increase in the influx of waters with low salinity. In the frontal zone of the East Greenland Current, as well as at the boundary of the Amazon River plume, the highest range of seasonal changes in salinity and density gradients was noted. In these areas, the contribution of salinity to seasonal changes in density at the ocean surface increases.

Keywords: frontal zone, horizontal gradients, temperature gradient, salinity gradient, density gradient, seasonal variability, Atlantic Ocean

Acknowledgements: The study was carried out under state assignment FNNN-2024-0014 “Fundamental studies of interaction processes in the sea-air system that form the physical state variability of the marine environment at various spatial and temporal scales”.

For citation: Shokurova, I.G., Nikolsky, N.V. and Chernyshova, E.D., 2024. Seasonal Variability of Horizontal Gradients in the North Atlantic Large-Scale Thermohaline Frontal Zones. *Ecological Safety of Coastal and Shelf Zones of Sea*, (2), pp. 23–38.

Сезонная изменчивость горизонтальных градиентов в крупномасштабных термохалинных фронтальных зонах в Северной Атлантике

И. Г. Шокурова *, Н. В. Никольский, Е. Д. Чернышова

Морской гидрофизический институт РАН, Севастополь, Россия
* *e-mail: igshokurova@mail.ru*

Аннотация
Рассматривается сезонная изменчивость пространственного распределения и величины горизонтальных градиентов температуры, солености и плотности в крупномасштабных поверхностных фронтальных зонах в северной части Атлантического океана. Используются среднемесячные данные о температуре и солености на горизонте 0.5 м океанического реанализа ORAS5 (1958–2021 гг.). Получено, что высокие градиенты температуры, превышающие 2 °С/100 км, солености – 1 ЕПС/100 км, плотности – 1 кг·м$^{-3}$/100 км, наблюдаются в субполярной и умеренной зонах во фронтах вдоль крупномасштабных течений, переносящих теплые соленые воды из южных широт (Гольфстрим, Северо-Атлантическое течение) и холодные воды с низкой соленостью из арктических районов (Лабрадорское течение, Восточно-Гренландское течение). Эти фронты выделяются в течение всего года. Высокие градиенты солености и плотности также отмечаются летом в тропической зоне во фронте на границе плюма Амазонки, возникающего в результате сезонного стока реки. В указанных пяти фронтальных зонах были выделены области, для которых приводятся количественные оценки сезонной изменчивости градиентов. В субполярной и умеренной зонах максимальные градиенты температуры отмечаются в зимнее время. Прогрев воды в летний сезон сопровождается уменьшением градиентов. Наибольший размах сезонной изменчивости градиентов температуры наблюдается во фронтальных зонах Гольфстрима и Восточно-Гренландского течения. Летом во фронтах субполярных районов происходит повышение градиентов солености вследствие таяния арктических и материковых льдов и увеличения поступления вод с пониженной соленостью. Во фронтальной зоне Восточно-Гренландского течения, а также на границе плюма реки Амазонки отмечается наиболее высокий размах сезонных изменений градиентов солености и плотности. В этих районах возрастает вклад солености в сезонные изменения плотности на поверхности океана.

Ключевые слова: фронтальные зоны, горизонтальные градиенты, градиент температуры, градиент солености, градиент плотности, сезонная изменчивость, Атлантический океан

Благодарности: работа выполнена в рамках государственного задания ФГБУН ФИЦ МГИ по теме № FNNN-2024-0014 «Фундаментальные исследования процессов взаимодействия в системе океан-атмосфера, формирующих изменчивость физического состояния морской среды на различных пространственно-временных масштабах».

Для цитирования: *Шокурова И. Г., Никольский Н. В., Чернышова Е. Д.* Сезонная изменчивость горизонтальных градиентов в крупномасштабных термохалинных фронтальных зонах в Северной Атлантике // Экологическая безопасность прибрежной и шельфовой зон моря. 2024. № 2. С. 23–38. EDN MWVISQ.

Introduction

Frontal zones are areas in the ocean where water masses with different physical, chemical and biological properties are encountered as a result of water transport by currents, river flow, upwellings and other dynamic processes [1, 2]. Boundaries between water masses are characterized by high horizontal gradients of temperature, salinity, density and other characteristics which makes it possible to determine the position of fronts [1]. Frontal zones are areas of high biodiversity, while oceanic frontal interface separate zones with different habitat conditions for marine organisms, that is why the analysis of changes in frontal characteristics is important for marine biology [2–4]. The greatest number of studies of surface frontal zones are currently being conducted in this field. What is more, long-term changes in the characteristics of frontal zones can serve as indicators of climate change in the ocean, which manifests itself differently in different seasons, which determines the importance of studying them [1, 5, 6].

The study of processes in frontal zones began in the mid-20th century [1, 7], but the emergence of satellite data, drifting buoy data and creation of modern ocean reanalyses at the end of the century expanded the possibilities for studying fronts in the ocean [8]. These data made it possible to study fronts on various time and spatial scales [1, 6, 9].

Currently, the characteristics of frontal zones are analyzed based on satellite data on ocean surface temperature [10–12], salinity [13, 14], sea level [15, 16]. Modern ocean reanalyses with high spatial resolution make it possible to consider spatiotemporal changes in temperature and salinity frontal zones comprehensively.

The features of the seasonal course of the North Atlantic Ocean have been studied most closely for temperature frontal zones [17–22]. Therefore, it is of interest to consider the seasonal variability of the characteristics of frontal zones in the salinity and density fields. This paper examines the seasonal variability of climatic frontal zones associated with large-scale movements in the ocean. The position of the fronts is determined based on calculations of horizontal gradients of temperature, salinity and density.

The work aims at a comprehensive study of seasonal variability of horizontal gradients in the fields of temperature, salinity and density in large-scale frontal zones in the North Atlantic Ocean.

Research data and methods

Monthly average data from the ORAS5 ocean reanalysis for 1958–2021 on potential temperature θ (°C) and salinity S (PSU) at a depth of 0.5 m on a grid with a spatial resolution of about 0.25° (up to 9 km in polar regions) were used in this paper [23]. The potential density anomaly was calculated based on salinity and potential temperature values according to the algorithms of the international equation of seawater (TEOS-10) [1)].

[1)] UNESCO, 2010. *The International Thermodynamic Equation of Seawater – 2010: Calculation and Use of Thermodynamic Properties*. UNESCO, 196 p.

To determine the position and characteristics of frontal zones, horizontal gradients of potential temperature $\nabla\theta$ (°C/100 km), salinity ∇S (PSU/100 km) and potential density anomaly $\nabla\sigma_\theta$ (kg·m^{-3}/100 km) were calculated for each month of all the years:

$$\nabla\varphi = \left(\frac{\partial\varphi}{\partial x}, \frac{\partial\varphi}{\partial y}\right), \quad |\nabla\varphi| = \sqrt{\left(\frac{\partial\varphi}{\partial x}\right)^2 + \left(\frac{\partial\varphi}{\partial y}\right)^2},$$

where φ is potential temperature θ, salinity S or potential density anomaly σ_θ. The gradient vector components were calculated using the method of central finite differences. When calculating, the local latitude was taken into account.

Spatial distribution of thermohaline fields and their gradients is presented for winter (December–February) and summer (June–August). Quantitative evaluation of seasonal variability of temperature, salinity and density gradients was performed for frontal zones with the gradients of temperature exceeding 2 °C/100 km, salinity – 1 PSU/100 km, density – 1 kg·m^{-3}/100 km. The calculations were carried out for five separate areas identified in frontal zones along large-scale currents and at the edge of the Amazon River plume. Area *1* was identified in the frontal zone of the Gulf Stream (41.5°–43° N, 58°–64° W); area *2* – of the North Atlantic Current (49°–53° N, 28°–42° W); area *3* – of the Labrador Current (59°–63° N, 60°–61° W); area *4* – of the East Greenland Coastal Current (65.5°–67° N, 29°–35° W); and area *5* – of the Amazon River plume (8°–11° N, 48°–52° W) (Fig. 1, *d*). Thermohaline characteristics were averaged within the area edges.

An analysis of the seasonal variability of the frontal zone position and size was carried out for areas *1*, *3* and *4*. Meridional sections were identified along 61° and 34° W, respectively, in the zonally oriented areas of the frontal zones of the Gulf Stream and the East Greenland Current. A zonal section along 59° N was identified on the meridionally oriented section of the Labrador Current frontal zone (Fig. 1, *d*). In this case, the gradient values were pre-averaged with a step of 0.25° along the section in areas with a finer grid.

Results and discussion

Temperature frontal zones

Waters with different thermohaline characteristics enter the North Atlantic with ocean currents, which determines the presence of oceanic fronts at their boundaries [1]. The temperature frontal zones are observed on the ocean surface in the vicinity of all such large-scale currents as the Gulf Stream, Labrador, West Greenland, East Greenland, Norwegian Currents, as well as in the area of coastal upwelling off the western coast of Africa and in summer in the eastern part of the equatorial region due to equatorial upwelling (Fig. 1).

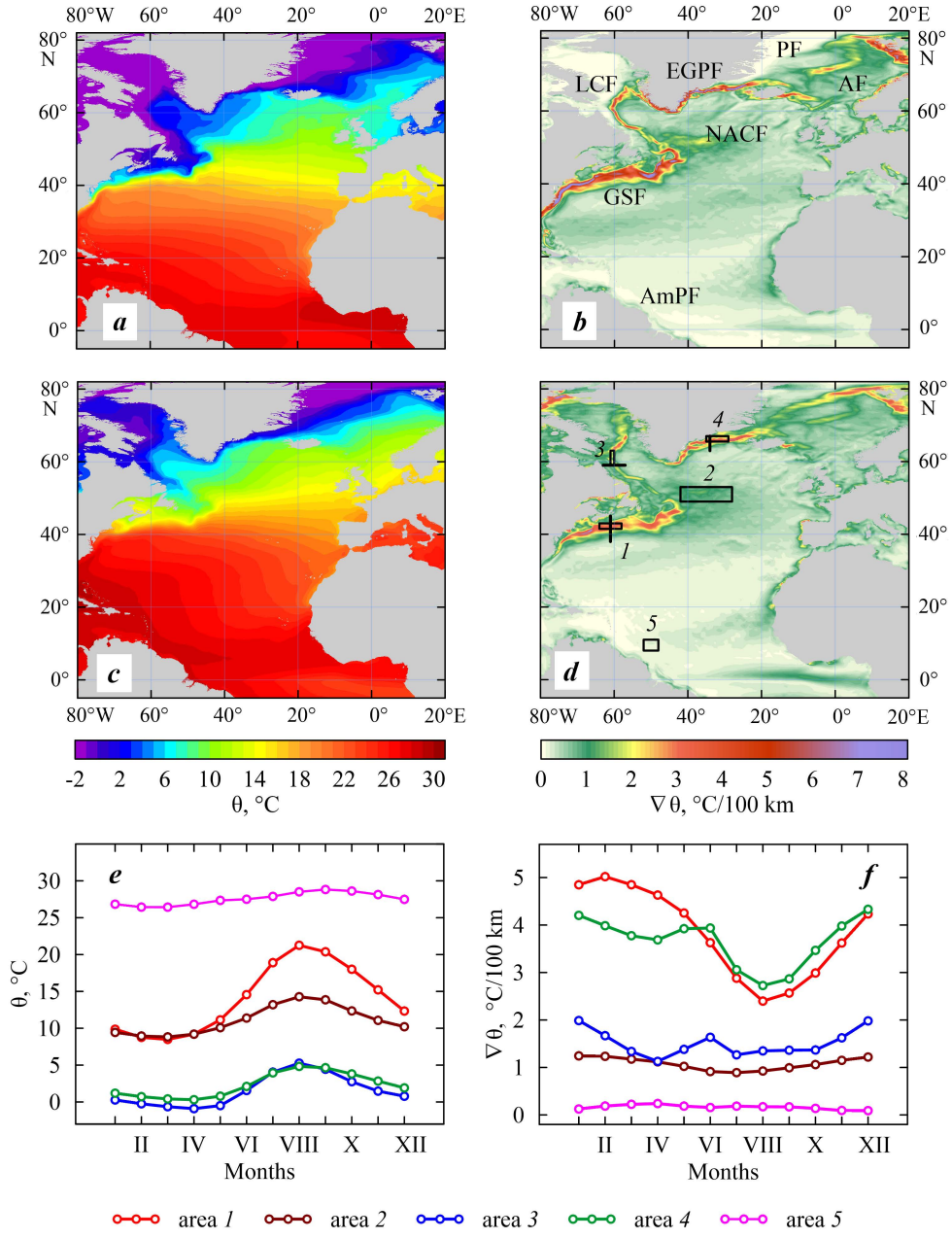

Fig. 1. Spatial distribution of potential temperature θ (*a*, *c*) and its horizontal gradients ∇θ (*b*, *d*) at a depth of 0.5 m in winter (*a*, *b*) and summer (*c*, *d*); seasonal variability of mean values θ (*e*) and ∇θ (*f*) in areas *1*–*5*. Frontal zones: GSF – Gulf Stream, NACF – North Atlantic Current, LCF – Labrador Current, EGCF – East Greenland Current, AmPF – Amazon River plume, PF – East Greenland Polar Front, AF – Arctic Front

The temperature frontal zone along the Gulf Stream is observed throughout the year. It separates the warm waters carried by the Gulf Stream from the southern latitudes and the cold waters of the Labrador Current off the Nova Scotia coast (Fig. 1, *a* – *d*) [24, 25]. Temperature gradients reach 13 °C/100 km in this frontal zone. Mean temperature gradients in area 1 in winter are 4 °C/100 km with their maxima up to 6.5 °C/100 km. (Fig. 1, *b*, *f*; Table). By summer, this front weakens due to the seasonal increase in water temperature in the surrounding waters and the gradients decrease, but remain quite high exceeding 2 °C/100 km (Fig. 1, *c*, *d*, *f*; Table).

Statistical characteristics of frontal zone gradients in areas *1–5*

Value	Area *1*	Area *2*	Area *3*	Area *4*	Area *5*
			$\nabla\theta$, *°C/100 km*		
Mean	3.8	1.0	1.5	3.7	0.16
Maximum	5.0	1.2	2.0	4.3	0.2
Minimum	2.4	0.9	1.1	2.7	0.09
Range	2.6	0.3	0.9	1.6	0.11
			∇S, *PSU/100 km*		
Mean	1.8	0.22	1.0	1.3	0.8
Maximum	2.0	0.24	1.6	2.3	1.7
Minimum	1.6	0.19	0.7	0.9	0.2
Range	0.4	0.05	0.9	1.4	1.5
			$\nabla\sigma_\theta$, *kg·m^{-3}/100 km*		
Mean	0.8	0.15	0.8	0.8	0.6
Maximum	1.0	0.22	1.1	1.6	1.3
Minimum	0.7	0.1	0.5	0.5	0.2
Range	0.3	0.12	0.6	1.1	1.1

The mean gradients do not exceed 1 °C/100 km in area *2* of the North Atlantic Current frontal zone. They increase in winter and decrease in summer. Low gradient values can be associated with the branching of the current and the seasonal displacement of branches [18].

The Labrador and East Greenland Currents transport cold waters into the North Atlantic from the Arctic Ocean. The frontal zones of the Labrador and East Greenland Coastal Currents are present in all seasons. The winter decrease in temperature lasts until April in these areas, with temperatures increasing towards summer, with its maximum in August (Fig. 1, *e*). Maximum gradients in areas *3* and *4* are observed in December and January, then they decrease from winter to summer (Fig. 1, *f*; Table). The local minimum in April corresponds to the minimum water temperature in the seasonal cycle. The local maximum in June is observed at the beginning of the summer warming, when the difference between the water temperature in the coastal and sea areas is still large.

Summer ice edge retreat in the Atlantic sector of the Arctic leads to the East Greenland Polar Temperature Front strengthening [26]. Here, the maximum gradients reach 4 °C/100 km in summer. The Arctic Front (Jan Mayen – Mohns Ridge [27]) extending from Iceland to Svalbard intensifies in winter and weakens in summer. Maximum temperature gradients are observed in the frontal area in winter and spring reaching 3 °C/100 km (Fig. 1, *b*, *d*). In summer, gradients decrease and do not exceed 2 °C/100 km.

Along the African coast, the upwelling frontal zone is present south of 20° N in winter and spring and north of 20° N in summer and autumn, which is associated with seasonal changes in the wind regime [21]. Gradients in the equatorial upwelling frontal zone increase in summer and autumn (Fig. 1, *b*, *d*).

The obtained position of large-scale temperature frontal zones and seasonal variability of gradients are in good agreement with the results of previous studies conducted using different types of data: satellite data on the surface temperature of the entire World Ocean [2, 19], the North Atlantic subtropical zone [28], the Gulf Stream front [6, 20], *in situ* measurement hydrological data [17, 27] and satellite altimetry data for the North Atlantic [22].

Salinity frontal zones

The salinity frontal zones with gradients exceeding 1 PSU/100 km are located in the areas of the Gulf Stream, Labradorand East Greenland Currents, as well as of the Polar Front and at the edge of the Amazon River plume (Fig. 2).

In the Gulf Stream frontal zone, the maximum salinity gradients are found in the area of the Gulf Stream North Wall throughout the year [29] (Fig. 2, *b*, *d*). Their values reach 5 PSU/100 km in winter and 4 PSU/100 km in summer. In area *1*, maximum salinity is observed in spring [30] and gradients are minimum at this time (Fig. 2, *e*, *f*). High salinity gradients are observed in autumn and winter, when seasonal intensification of transport of

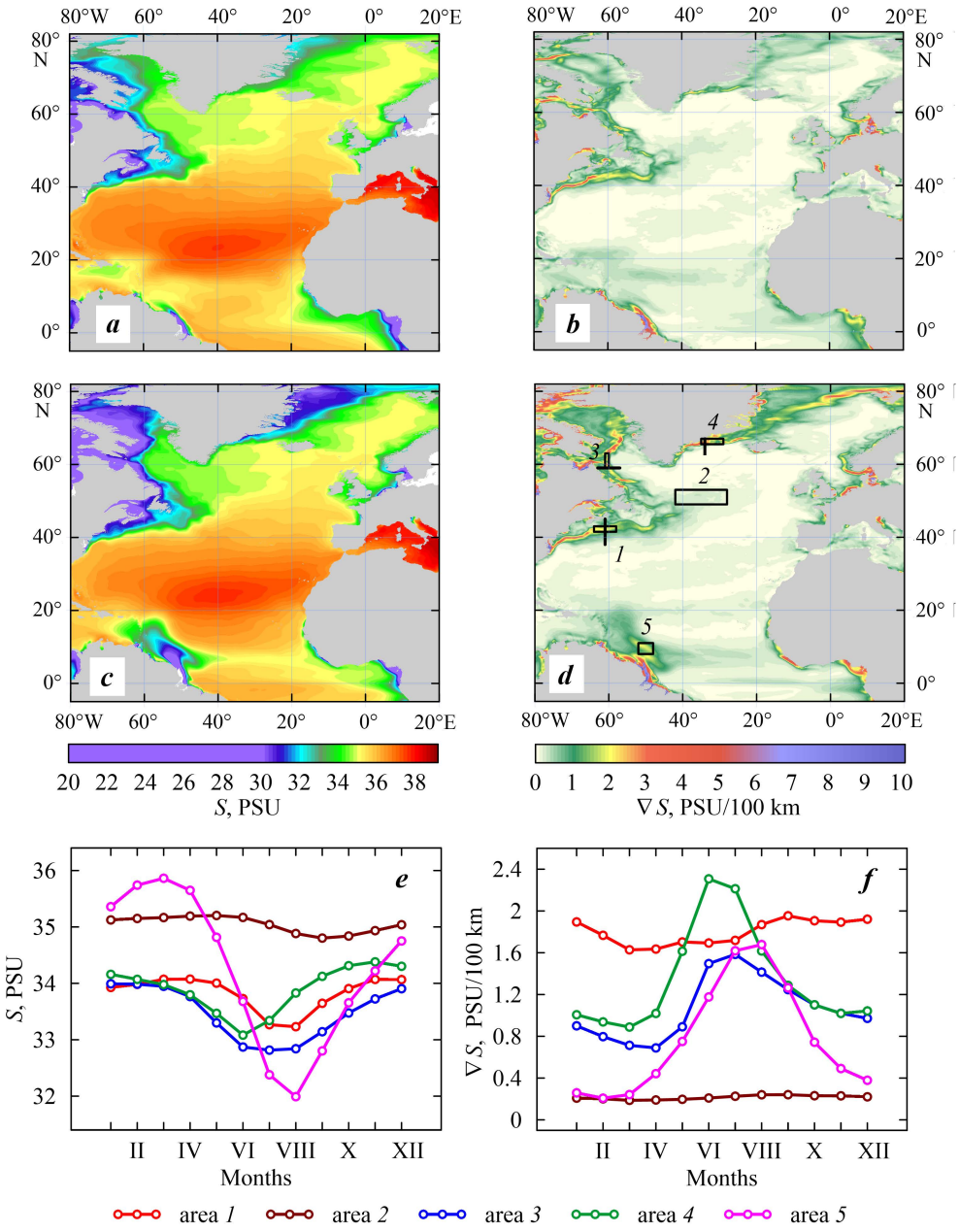

Fig. 2. Spatial distribution of salinity S (*a*, *c*) and horizontal salinity gradients ∇S (*b*, *d*) at a depth of 0.5 m in winter (*a*, *b*) and summer (*c*, *d*); seasonal variability of mean values S (*e*) and ∇S (*f*) in areas 1–5

the Labrador Current and its branch spreading along the Nova Scotia coast occur [24, 31, 32]. The influence of fresh water flow from the Gulf of St. Lawrence and the salinity of the Gulf Stream water are also important [33].

Despite the fact that the Labrador Current intensifies in autumn and winter [31], and the East Greenland Current – in winter and spring [34], the gradients in the frontal zones of these currents (areas *3* and *4*) increase in summer, which is associated with the seasonal melting of the Arctic ice and removal of freshened water from the Arctic Ocean, as well as with the melting of coastal and continental ice. Minimum gradients are observed in March and April at minimum temperature, after which gradient values increase and reach their maximum at the beginning of summer (Fig. 2, *f*; Table).

In the Atlantic sector of the Arctic, the East Greenland Polar Salinity Front is significantly strengthened in summer. This is also stipulated by the Arctic ice melting and influx of freshened waters, the salinity of which is significantly lower than that of the subpolar regions [26]. The maximum values of horizontal salinity gradients in summer are 3.5 PSU/100 km.

In the tropical Atlantic Ocean, an extensive salinity frontal zone is located at the edge of the Amazon River plume [35]. Freshened waters are distributed by the North Brazil Current to the north to 15° N in spring and summer. Salinity decreases in area *5* from March (36 PSU) to August (32 PSU) and gradients increase from 0.2 to 1.7 PSU/100 km.

Density frontal zones

The density frontal zones with gradients exceeding 1 kg·m^{-3}/100 km are located in the areas of the Gulf Stream, Labrador, East Greenland Currents (Fig. 3, *b, d*). In summer, a large estuarine frontal zone is observed in the Amazon River plume area (Fig. 3, *c*, *d*). In summer, a frontal zone associated with equatorial upwelling also occurs along the equator.

The density in areas *1–4* decreases in summer, while the density gradients increase at this time (Fig. 3, *e*, *f*). Gradients exceeding 4 kg·m^{-3}/100 km are observed locally in certain areas of the frontal zones of the Labrador Current in the Davis Strait, the East Greenland Coastal Current, the Polar Front and in the Amazon estuarine zone (Fig. 3, *b*, *d*).

Minimum density gradients in areas *1–4* of the North Atlantic frontal zones are observed in March. The minimum density gradient in the frontal zone of the Amazon River plume (area *5*) is observed in February.

In areas *1* (the Gulf Stream frontal zone) and *2* (the North Atlantic Current frontal zone), the minimum and maximum density in the seasonal cycle are observed at the maximum and minimum temperatures, respectively (Fig. 4, *a*, *b*). Here (in the open ocean), the contribution of temperature exceeds the contribution of salinity to seasonal density changes.

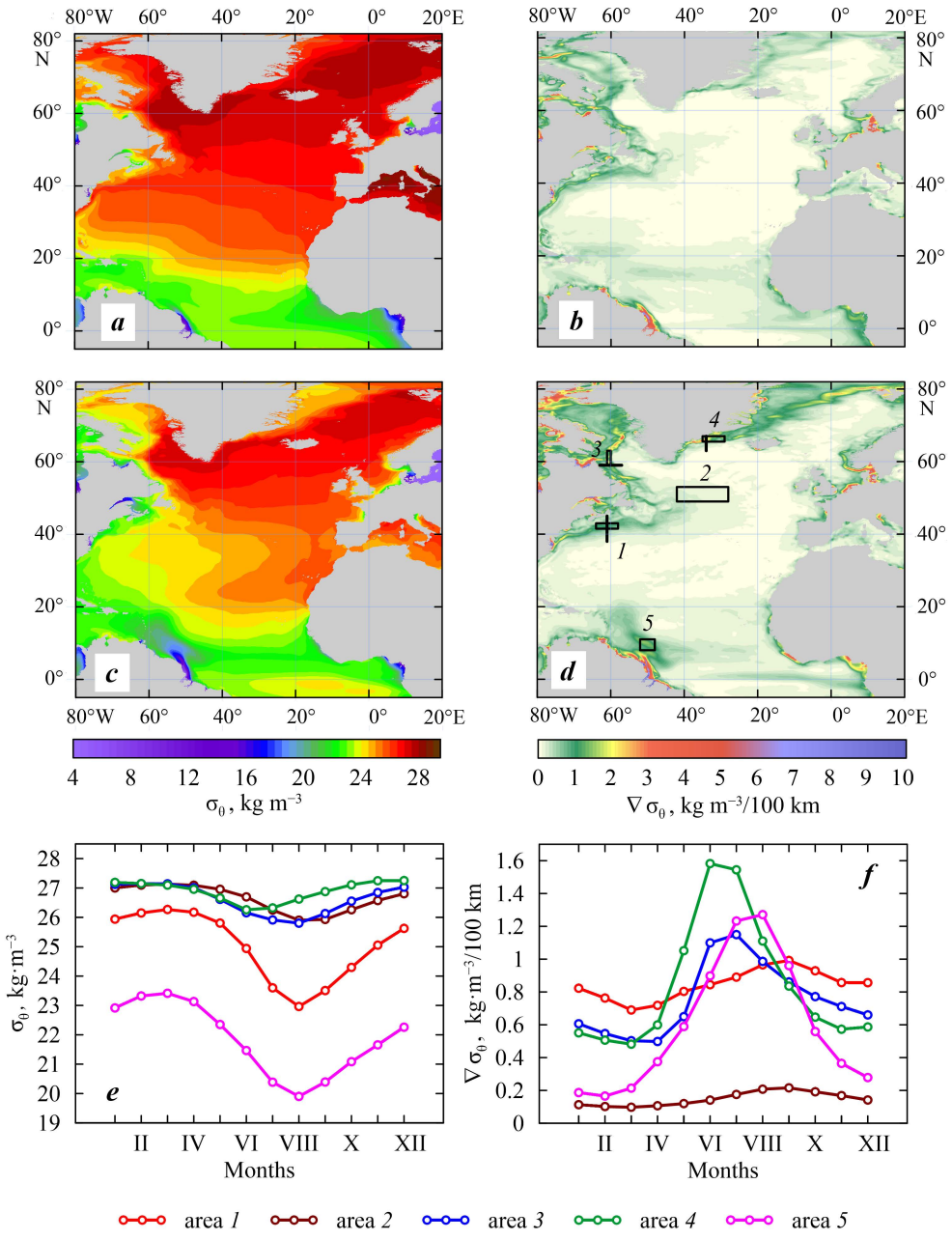

Fig. 3. Spatial distribution of potential density anomaly σ_θ (*a*, *c*) and horizontal potential density gradients $\nabla\sigma_\theta$ (*b*, *d*) at a depth of 0.5 m in winter (*a*, *b*) and summer (*c*, *d*) seasons; seasonal variability of mean values σ_θ (*e*) and $\nabla\sigma_\theta$ (*f*) in areas *1–5*

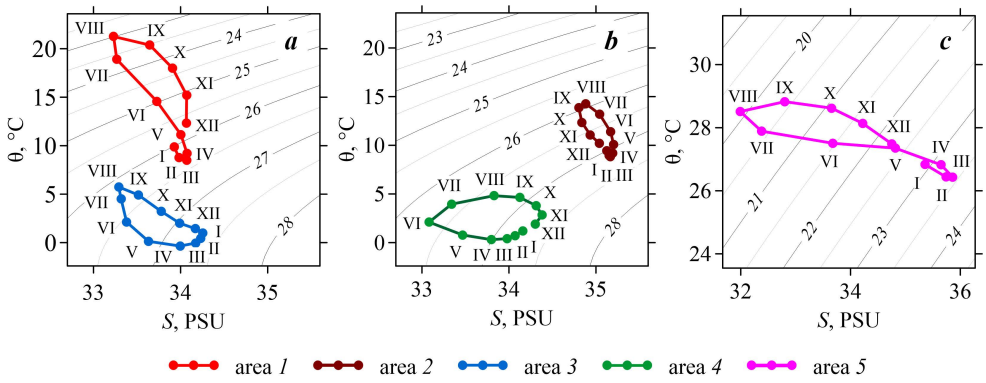

Fig. 4. TS diagrams of seasonal variability of temperature and salinity at a depth of 0.5 m in areas *1*, *3* (*a*), *2*, *4* (*b*), *5* (*c*)

In areas where less saline waters flow from the Arctic Ocean (the Labrador and East Greenland Currents) and in the area of the Amazon River flow, the contribution of salinity to seasonal density changes increases. This is clearly illustrated by density changes in the frontal zone of the East Greenland Coastal Current (area *4*). Here, the lowest density is achieved in June with the lowest salinity, rather than with the maximum temperature, which is observed in August (Fig. 4, *b*). The maximum density is observed in November and December with high salinity. The minimum temperature in this area is observed in April. In the frontal zone of the Labrador Current (area *3*), the maximum density is observed in February and March, while the minimum temperature is in April.

In area *5* of the Amazon River plume frontal zone, the maximum temperature is observed in September [36], while the minimum density is obtained for August, when the salinity is minimum (Fig. 4, *c*).

Seasonal variability of the size of frontal zones

Seasonal temperature and salinity changes in currents and surrounding waters, as well as changes in river flow, can lead to shifts in the edges or changes in the size of the frontal zone. Thus, the salinity and density frontal zones of the Amazon River plume (Figs. 2, 3) are observed only during the increase in seasonal flow in spring and summer, not in the winter months.

The seasonal variability of the position and magnitude of gradients along the meridional section crossing the Gulf Stream frontal zone at 61° W (area *1*) is well expressed. Here, the front with temperature gradients exceeding 2 °C/100 km narrows in August and September with the decrease of gradients (Fig. 5, *a*). The zone of high salinity gradients (more than 2 PSU/100 km) shifts southward from winter to summer and back northward in autumn (Fig. 5, *b*). The zone of high density gradients shifts in a similar manner (Fig. 5, *c*). It should be noted that the change in the width of frontal zones obtained from average long-term data for individual seasons can be associated with the shifts of these zones in separate years.

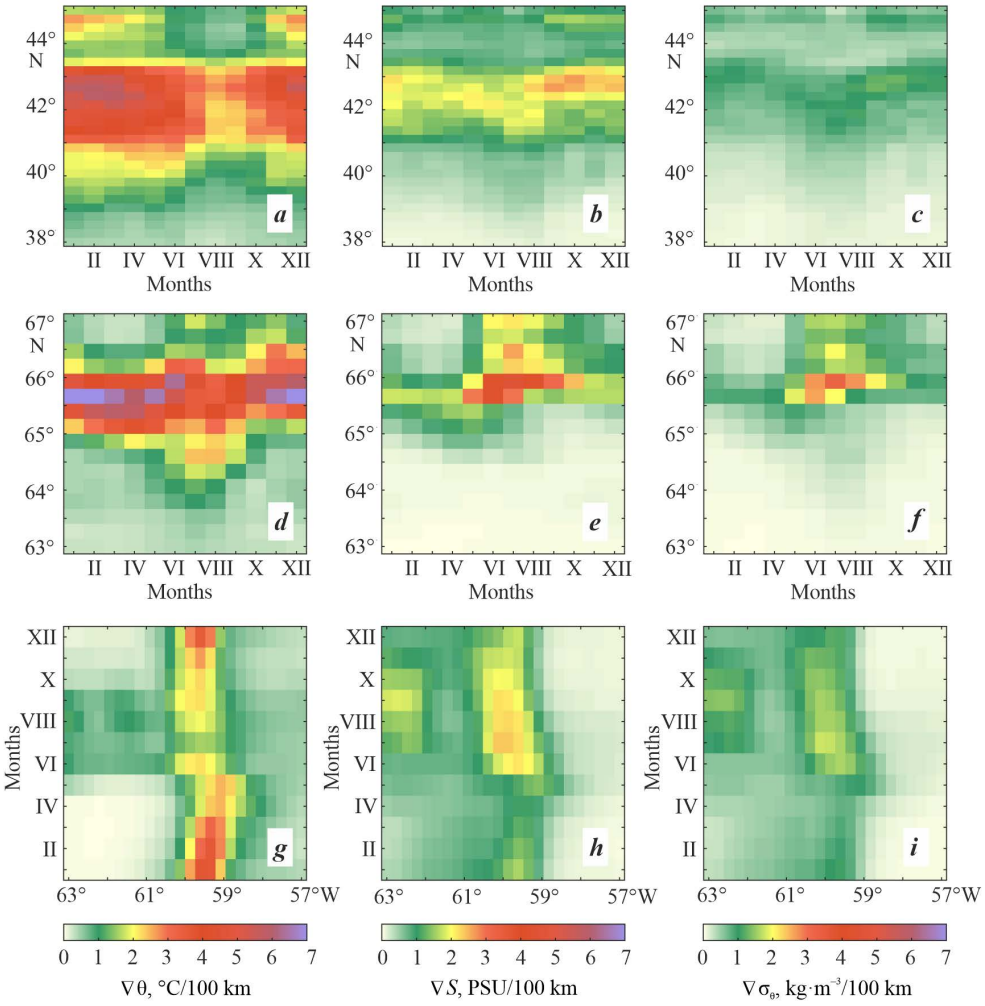

Fig. 5. Seasonal variability of gradients of potential temperature $\nabla\theta$ (*a*, *d*, *g*), salinity ∇S (*b*, *e*, *h*) and potential density anomaly $\nabla\sigma_\theta$ (*c*, *f*, *i*) on meridional sections along 61° W in area *1* of the northern section of the Gulf Stream frontal zone (*a*, *b*, *c*), along 34° W in area *4* of the East Greenland Coastal Current (*d*, *e*, *f*) and on the zonal section along 59° N in area *3* of the Labrador Current frontal zone (*g*, *h*, *i*)

In area *4* of the East Greenland Coastal Current frontal zone, the meridional section along 34° W was chosen. The meridional size of the temperature frontal zone expands southward in July and August and northward in October and December (Fig. 5, *d*). The width of the salinity and density frontal zones increases in summer due to the increase of gradients at the northern edge (Fig. 5, *e, f*).

In the meridional section of the Labrador Current frontal zone (area *3*), the zonal section along 59° N was considered. In this area, the zone of high gradients (more than 2 °C/100 km) shifts eastward from January to April. In May, the gradients decrease and the zone shifts westward (Fig. 5, *g*). The gradients in the salinity (Fig. 5, *f*) and density (Fig. 5, *i*) frontal zones increase in summer and early autumn. At the same time, the zones shift westward.

Conclusion

This paper gives a comprehensive understanding of the position of large-scale surface thermal, salinity and density frontal zones in the North Atlantic Ocean and seasonal variability of their gradients based on the use of ORAS5 ocean reanalysis data on temperature and salinity at the 0.5 m horizon. Quantitative evaluation of seasonal variability of gradients in frontal zones in individual areas of large-scale currents and at the edge of the Amazon River plume is provided.

The analysis of seasonal variability of spatial distribution and magnitudes of horizontal gradients in thermohaline frontal zones showed the following. Frontal zones on the ocean surface located along such large-scale currents as the Gulf Stream, North Atlantic, Labrador and East Greenland Currents, which carry waters differing in temperature and salinity from the surrounding waters, are observed throughout the year. Temperature gradients in these zones decrease from winter to summer due to seasonal warming of the waters. The maximum range of seasonal changes in temperature gradients is observed in the regions of the Gulf Stream and the East Greenland Current.

Significant seasonal variability of salinity and density gradients is observed in the frontal zones of the Labrador and East Greenland Currents. Minimum gradients are observed in late winter and early spring at minimum temperatures. Gradients increase in summer due to the melting of coastal, continental and Arctic ice.

In the Tropical Atlantic, high intra-annual variability of salinity and density gradients is observed in the Amazon River frontal zone. Here, maximum gradients are observed in summer at the edge of the plume that occurs due to the seasonal increase in river flow. No frontal zone is observed in winter.

The obtained magnitudes of seasonal changes in gradients in frontal zones can be used when studying the biological productivity of marine waters. They can also be taken into account in climate studies since as a rule, the amplitude of the seasonal cycle of the ocean surface layer characteristics exceeds interannual changes.

References

1. Fedorov, K.N., 1986. *The Physical Nature and Structure of Oceanic Fronts*. New York: Springer-Verlag, 333 p.
2. Belkin, I.M., Cornillon, P.C. and Sherman, K., 2009. Fronts in Large Marine Ecosystems. *Progress in Oceanography*, 81(1–4), pp. 223–236. https://doi.org/10.1016/j.pocean.2009.04.015
3. Taylor, J.R. and Ferrari, R., 2011. Ocean Fronts Trigger High Latitude Phytoplankton Blooms. *Geophysical Research Letters*, 38(23), L23601. https://doi.org/10.1029/2011GL049312
4. Olson, D.B., 2002. Biophysical Dynamics of Ocean Fronts. In: A. R. Robinson, J. J. McCarthy, B. J. Rotschild, Eds., 2002. *The Sea: Ideas and Observations on Progress in the Study of the Seas*. Harvard University Press. Vol. 12: Biological-Physical Interactions in the Sea, pp. 187–218.
5. Yang, K., Meyer, A., Strutton, P.G. and Fischer, A.M., 2023. Global Trends of Fronts and Chlorophyll in a Warming Ocean. *Communications Earth & Environment*, 4, 489. https://doi.org/10.1038/s43247-023-01160-2
6. Kida S., Mitsudera, H., Aoki, S., Guo, X., Ito, S., Kobashi, F., Komori, N., Kubokawa, A., Miyama, T. [et al.], 2016. Oceanic Fronts and Jets around Japan: a Review. In: H. Nakamura, A. Isobe, S. Minobe, H. Mitsudera, M. Nonaka, T. Suga, eds., 2016. *"Hot Spots" in the Climate System: New Developments in the Extratropical Ocean-Atmosphere Interaction Research*. Tokyo: Springer, pp. 1–30. https://doi.org/10.1007/978-4-431-56053-1_1
7. Cromwell, T. and Reid Jr., J. L., 1956. A Study of Oceanic Fronts1. *Tellus*, 8(1), pp. 94–101. https://doi.org/10.3402/tellusa.v8i1.8947
8. Ferrari, R., 2011. A Frontal Challenge for Climate Models. *Science*, 332(6027), pp. 316–317. https://doi.org/10.1126/science.1203632
9. Swart, S., du Plessis, M.D., Thompson, A.F., Biddle, L.C., Giddy, I., Linders, T., Mohrmann, M. and Nicholson, S.-A., 2020. Submesoscale Fronts in the Antarctic Marginal Ice Zone and Their Response to Wind Forcing. *Geophysical Research Letters*, 47(6), e2019GL086649. https://doi.org/10.1029/2019GL086649
10. Kostianoy, A.G., Ginzburg, A.I., Frankignoulle, M. and Delille, B., 2004. Fronts in the Southern Indian Ocean as Inferred from Satellite Sea Surface Temperature Data. *Journal of Marine Systems*, 45(1–2), pp. 55–73. https://doi.org/10.1016/j.jmarsys.2003.09.004
11. Konik, A.A. and Zimin, A.V., 2022. Variability of the Arctic Frontal Zone Characteristics in the Barents and Kara Seas in the First Two Decades of the XXI Century. *Physical Oceanography*, 29(6), pp. 659–673. https://doi.org/10.22449/1573-160X-2022-6-659-673
12. Artamonov, Yu.V., Skripaleva, E.A. and Nikolsky, N.V., 2022. Climatic Structure of the Dynamic and Temperature Fronts in the Scotia Sea and the Adjacent Water Areas. *Physical Oceanography*, 29(2), pp. 117–138. https://doi.org/10.22449/1573-160X-2022-2-117-138
13. Belkin, I.M., 2021. Remote Sensing of Ocean Fronts in Marine Ecology and Fisheries. *Remote Sensing*, 13(5), 883. https://doi.org/10.3390/rs13050883
14. Yu, L., 2015. Sea-Surface Salinity Fronts and Associated Salinity-Minimum Zones in the Tropical Ocean. *Journal of Geophysical Research: Oceans*, 120(6), pp. 4205–4225. https://doi.org/10.1002/2015JC010790
15. Kostianoy, A.G., Ginzburg, A.I., Lebedev, S.A., Frankignoulle, M. and Delille, B., 2004. Oceanic Fronts in the Southern Indian Ocean as Inferred from the NOAA SST, TOPEX/Poseidon and ERS-2 Altimetry Data. *Gayana (Concepción)*, 68(2, Suppl.), pp. 333–339. https://dx.doi.org/10.4067/S0717-65382004000300003

16. Akhtyamova, A.F. and Travkin, V.S., 2023. Investigation of Frontal Zones in the Norwegian Sea. *Physical Oceanography*, 30(1), pp. 62–77. https://doi.org/10.29039/1573-160X-2023-1-62-77
17. Galerkin, L.I., Gritsenko, A.M., Panfilova, S.G. and Yampol'skii, A.D., 2002. Seasonal Variations in Horizontal Temperature Gradients of Water in the North Atlantic. *Doklady Earth Sciences*, 384(4), pp. 473–477.
18. Miller, P.I., Read, J.F. and Dale, A.C., 2013. Thermal Front Variability along the North Atlantic Current Observed Using Microwave and Infrared Satellite Data. *Deep Sea Research Part II: Topical Studies in Oceanography*, 98(B), pp. 244–256. https://doi.org/10.1016/j.dsr2.2013.08.014
19. Kazmin, A.S., 2017. Variability of the Climatic Oceanic Frontal Zones and Its Connection with the Large-Scale Atmospheric Forcing. *Progress in Oceanography*, 154, pp. 38–48. https://doi.org/10.1016/j.pocean.2017.04.012
20. Artamonov, Yu.V. and Skripaleva, E.A., 2005. The Structure and Seasonal Variability of the Large-Scale Fronts in the Atlantic Ocean on the Basis of Satellite Data. *Issledovaniye Zemli iz Kosmosa*, (4), pp. 62–75 (in Russian).
21. Santos, A.M.P., Kazmin, A.S. and Peliz, A., 2005. Decadal Changes in the Canary Upwelling System as Revealed by Satellite Observations: Their Impact on Productivity. *Journal of Marine Research*, 63(2), pp. 359–379.
22. Novikova, I.S. and Bashmachnikov, I.L., 2018. Seasonal and Interannual Dynamics of Frontal Zones in the North Atlantic. In: IO RAS, 2018. *Proceedings of the II Russian National Conference "Hydrometeorology and Ecology: Scientific and Educational Achievements and Perspectives"*. Saint Petersburg: HIMIZDAT, pp. 496–498 (in Russian).
23. Zuo, H., Balmaseda, M.A., Tietsche, S., Mogensen, K. and Mayer, M., 2019. The ECMWF Operational Ensemble Reanalysis-Analysis System for Ocean and Sea Ice: a Description of the System and Assessment. *Ocean Science*, 15(3), pp. 779–808. https://doi.org/10.5194/os-15-779-2019
24. Seidov, D., Mishonov, A., Reagan, J. and Parsons, R., 2019. Eddy-Resolving in situ Ocean Climatologies of Temperature and Salinity in the Northwest Atlantic Ocean. *Journal of Geophysical Research: Oceans*, 124(1), pp. 41–58. https://doi.org/10.1029/2018JC014548
25. Daniault, N., Mercier, H., Lherminier, P., Sarafanov, A., Falina, A., Zunino, P., Pérez, F.F., Ríos, A.F., Ferron, B. [et al.], 2016. The Northern North Atlantic Ocean Mean Circulation in the Early 21st Century. *Progress in Oceanography*, 146, pp. 142–158. https://doi.org/10.1016/j.pocean.2016.06.007
26. Liu, Y., Wang, J., Han, G., Lin, X., Yang, G. and Ji, Q., 2022. Spatio-Temporal Analysis of East Greenland Polar Front. *Frontiers in Marine Science*, 9, 943457. https://doi.org/10.3389/fmars.2022.943457
27. Kostianoy, A.G., Nihoul, J.C.J. and Rodionov, V.B., 2004. *Physical Oceanography of Frontal Zones in the Subarctic Seas*. Amsterdam: Elsevier, 2004. 316 p.
28. Ullman, D.S., Cornillon, P.C. and Shan, Z., 2007. On the Characteristics of Subtropical Fronts in the North Atlantic. *Journal of Geophysical Research: Oceans*, 112(C1), C01010. https://doi.org/10.1029/2006JC003601
29. Taylor, A.H. and Stephens J.A., 1998. The North Atlantic Oscillation and the latitude of the Gulf Stream. *Tellus A: Dynamic Meteorology and Oceanography*, 50(1), pp. 134–142. https://doi.org/10.3402/tellusa.v50i1.14517
30. Richaud, B., Kwon, Y., Joyce, T.M., Fratantoni, P.S. and Lentz, S.J., 2016. Surface and Bottom Temperature and Salinity Climatology along the Continental Shelf off the Canadian and U.S. East Coasts. *Continental Shelf Research*, 124, pp. 165–181. https://doi.org/10.1016/j.csr.2016.06.005

31. Han, G., Lu, Z., Wang, Z., Helbig, J., Chen, N. and de Young, B., 2008. Seasonal Variability of the Labrador Current and Shelf Circulation off Newfoundland. *Journal of Geophysical Research: Oceans*, 113(C10), C10013. https://doi.org/10.1029/2007JC004376
32. Grodsky, S.A., Reul, N., Chapron, B., Carton, J. A. and Bryan, F.O., 2017. Interannual Surface Salinity on Northwest Atlantic Shelf. *Journal of Geophysical Research: Oceans*, 122(5), pp. 3638–3659. https://doi.org/10.1002/2016JC012580
33. Ohashi, K. and Sheng, J., 2013. Influence of St. Lawrence River Discharge on the Circulation and Hydrography in Canadian Atlantic Waters. *Continental Shelf Research*, 58, pp. 32–49. https://doi.org/10.1016/j.csr.2013.03.005
34. Bacon, S., Marshall, A., Holliday, N.P., Aksenov, Y. and Dye, S.R., 2014. Seasonal Variability of the East Greenland Coastal Current. *Journal of Geophysical Research: Oceans*, 119(6), pp. 3967–3987. https://doi.org/10.1002/2013JC009279
35. Liang, Y.C., Lo, M.H., Lan, C.W., Seo, H., Ummenhofer, C.C., Yeager, S., Wu, R.J. and Steffen, J.D., 2020. Amplified Seasonal Cycle in Hydroclimate over the Amazon River Basin and Its Plume Region. *Nature Communications*, 11, 4390. https://doi.org/10.1038/s41467-020-18187-0
36. Yu, L., Jin, X. and Weller, R.A., 2006. Role of Net Surface Heat Flux in Seasonal Variations of Sea Surface Temperature in the Tropical Atlantic Ocean. *Journal of Climate*, 19(23), pp. 6153–6169. https://doi.org/10.1175/JCLI3970.1

Submitted 13.02.2024; accepted after review 15.03.2024;
revised 27.03.2024; published 25.06.2024

About the authors:

Irina G. Shokurova, Senior Research Associate, Marine Hydrophysical Institute of RAS (2 Kapitanskaya St., Sevastopol, 299011, Russian Federation), Ph.D. (Geogr.), **ORCID ID: 0000-0002-3150-8603**, *igshokurova@mail.ru*

Nikolay V. Nikolsky, Junior Research Associate, Marine Hydrophysical Institute of RAS (2 Kapitanskaya St., Sevastopol, 299011, Russian Federation), **ORCID ID: 0000-0002-3368-6745**, *n.nikolsky@mhi-ras.ru*

Elena D. Chernyshova, Research Engineer, Marine Hydrophysical Institute of RAS (2 Kapitanskaya St., Sevastopol, 299011, Russian Federation), **ORCID ID: 0009-0005-4607-8190**, *alenaksendzik@rambler.ru*

About the authors:

Irina G. Shokurova – original text, literature review, editing, analyzing and summarizing of results

Nikolay V. Nikolsky – calculations, visualization, original text, editing, analyzing and summarizing of results

Elena D. Chernyshova – visualization, original text, literature review, analyzing and summarizing of results

All the authors have read and approved the final manuscript.

Original article

Interannual Variability of Physical and Biological Characteristics of Crimean Shelf Waters in Summer Season (2010–2020)

S. A. Piontkovski [1]*, Yu. A. Zagorodnyaya [2], I. M. Serikova [2], I. A. Minski [1, 2], I. V. Kovaleva [2], E. Yu. Georgieva [2]

[1] *Sevastopol State University, Sevastopol, Russia*
[2] *A. O. Kovalevsky Institute of Biology of the Southern Seas of RAS, Sevastopol, Russia*
* *e-mail: spiontkovski@mail.ru*

Abstract
The coastal zone and shelf of Crimea are the objects of long-term comprehensive research predetermined by the significant role these zones play in the economic life of the peninsula. The purpose of the research is to identify trends in inter-annual variability in the structural and functional characteristics of the pelagic community. Data on remote sensing (from satellites), *in situ* measurements (on board a research vessel) and computed parameters were employed to identify the variability of physical and biological characteristics of the Crimean shelf waters from 2010 to 2020. It was shown that after the environmental cataclysms of the 1990s, associated with shelf eutrophication and trophic impact of plankton invasive species, the planktonic community entered a period of relative stability. The inter-annual variability of its key structural and functional characteristics (namely, phytoplankton biomass, the intensity of its bioluminescence, zooplankton biomass, net primary production and the ratio of production to biomass) could be characterized rather by inter-annual fluctuations due to hydrophysical dynamics than statistically significant trends of long-term variability. The hydrophysical dynamics was assessed by two parameters: the kinetic energy density and cross-shelf mass transfer in the upper layers.

Keywords: phytoplankton, zooplankton, bioluminescence, pollution, sea surface temperature, Black Sea

Acknowledgments: The work was funded by the Russian Science Foundation (grant no. 23-24-00007), state assignment no. 121040600178-6 ("Structural-functional organization, productivity, and stability of marine pelagic ecosystems"), no. 121030100028-0 ("Trends of formation and anthropogenic transformation of biodiversity and bioresources of the Azov-Black Sea basin and other regions of the World's Ocean"), no. 121041400077-1 ("Functional, metabolical, and toxicological aspects of hydrobiont and their population persistence across biotopes with different physical-chemical mode"), and state assignment to SevSU no. FEFM-2023-0005. The expeditions were carried out onboard R/V *Professor Vodyanitsky*. The authors are grateful to A. Akpinar (Middle East Technical University,

Turkey) for the water mass transport data, to V. V. Suslin for the data for primary production calculation, to V. V. Gubanov for gelatinous macrozooplankton data, and to A. N. Korshenko for oil hydrocarbon data.

For citation: Piontkovski, S.A., Zagorodnyaya, Yu.A., Serikova, I.M., Minski, I.A., Kovaleva, I.V. and Georgieva, E.Yu., 2024. Interannual Variability of Physical and Biological Characteristics of Crimean Shelf Waters in Summer Season (2010–2020). *Ecological Safety of Coastal and Shelf Zones of Sea*, (2), pp. 39–59.

Межгодовая изменчивость физических и биологических характеристик вод Крымского шельфа в летний сезон (2010–2020 годы)

С. А. Пионтковский [1]*, Ю. А. Загородняя [2], И. М. Серикова [2], И. А. Минский [1, 2], И. В. Ковалева [2], Е. Ю. Георгиева [2]

[1] *ФГАОУ ВО Севастопольский государственный университет, Севастополь, Россия*
[2] *ФГБУН ФИЦ «Институт биологии южных морей им. А. О. Ковалевского», Севастополь, Россия*
* *e-mail: spiontkovski@mail.ru*

Аннотация
Прибрежная зона Крыма и его шельф являются объектами многолетних комплексных исследований, предопределенных той значимой ролью, которую эти зоны играют в экономической жизни полуострова. Цель работы состоит в выявлении трендов межгодовой изменчивости структурных и функциональных характеристик пелагического сообщества. Данные дистанционных измерений (со спутников), контактных измерений (с борта научно-исследовательского судна) и расчетные параметры использованы для выявления изменчивости физических и биологических характеристик шельфовых вод Крыма в 2010–2020 гг. Показано, что после экологических катаклизмов 1990-х гг., связанных с эвтрофикацией шельфа и трофическим прессом планктонных видов-вселенцев, планктонное сообщество вступило в период относительной стабильности. Межгодовая изменчивость его ключевых структурных и функциональных характеристик (биомассы фитопланктона, интенсивности его биолюминесценции, биомассы зоопланктона, чистой первичной продукции и отношения продукции к биомассе) характеризуется не столько статистически значимыми трендами многолетней изменчивости, сколько межгодовыми колебаниями, обусловленными гидрофизической динамикой. Эта динамика оценивалась двумя параметрами: величиной плотности кинетической энергии и кросс-шельфовым массопереносом в верхних слоях.

Ключевые слова: фитопланктон, зоопланктон, биолюминесценция, загрязнение, температура поверхности моря, Черное море

Благодарности: работа выполнена при финансовой поддержке Российского научного фонда (проект № 23-24-00007) и в рамках государственных заданий ФГБУН ФИЦ ИнБЮМ № 121040600178-6 («Структурно-функциональная организация, продуктивность и устойчивость морских пелагических экосистем»), № 121030100028-0 («Закономерности формирования и антропогенная трансформация биоразнообразия и биоресурсов Азово-Черноморского бассейна и других районов Мирового океана»), № 121041400077-1 («Функциональные, метаболические и токсикологические аспекты

существования гидробионтов и их популяций в биотопах с различным физико-химическим режимом») и государственного задания СевГУ № FEFM-2023-0005. Полевые исследования были выполнены в Центре коллективного пользования НИС “Профессор Водяницкий” ФГБУН ФИЦ ИнБЮМ им. А.О.Ковалевского РАН. Авторы благодарны A. Akpinar (Middle East Technical University, Turkey) за данные по массопереносу вод, В. В. Суслину за данные для расчета первичной продукции, В. В. Губанову за данные по желетелому макрозоопланктону и А. Н. Коршенко за данные по нефтяным углеводородам.

Для цитирования: Межгодовая изменчивость физических и биологических характеристик вод Крымского шельфа в летний сезон (2010–2020 годы) / С. А. Пионтковский [и др.] // Экологическая безопасность прибрежной и шельфовой зон моря. 2024. № 2. С. 39–59. EDN CUBYXI.

Introduction

The coastal zone of Crimea and its shelf are the objects of many years of complex research by Roshydromet, VNIRO and the Russian Academy of Sciences, predetermined by the significant role these zones play in the economic life of the peninsula. Gas production (about 1.6 billion cubic meters) [1)], development of aquaculture (with cultivation of mussels, oysters, shrimps and other organisms with a volume of about 2,700 tons per year) [2), 3)], fisheries (with a catch of about 40,000 tons per year) [4)], tourism and recreation (with a load of about 8 million holidaymakers per year) are important components of economic activity; and investments in the development of the fishery complex of the Southern Federal District are estimated at about 60 billion rubles in the first two decades of the 21st century [1, 2].

As part of this multidisciplinary activity, the monitoring based on multiple-year measurements of key parameters enhances the understanding of the resource dynamics and ecological state of the shelf [3]. It should be noted that an anthropogenic load on the Crimean shelf is high due to its small width, high population density along the coast, developed agriculture and industrial complex, forming about 30% of the consolidated budget of the Republic of Crimea. As a consequence, in 1998–2018, the *Yuzhnye* sewage treatment facilities, producing 76% of the total volume of domestic sewage in the region, discharged 468,000 cubic meters per year in the Sevastopol region alone [4]. Measurements of petroleum hydrocarbon

---

1) *Rambler/finance*. 2024. [online] Available at: https://finance.rambler.ru/markets/41621705-dobycha-gaza-v-krymu-snizilas-v-2018-godu-na-3-do-1-6-mlrd-kubometrov [Accessed: 5 June 2024] (in Russian).

2) Government of the RF, 2022. *On Approval of the Strategy for the Development of the Fishery Sector of the Russian Federation for the Period until 2030 (together with the Action Plan for the Implementation of the Strategy for the Development of the Fishery Sector of the Russian Federation for the Period until 2030)*. Resolution of the RF Government no. 2798-p as of 26 November 2019 (as amended on 12 May 2022) (in Russian).

3) Federal Agency for Fisheries. *Crimean farmers plan to start supplying oysters to Armenia and Kazakhstan in 2020*. 2020. [online] Available at: https://fish.gov.ru/obzor-smi/2020/01/22/fermery-kryma-v-2020-godu-planiruyut-nachat-postavki-ustrits-v-armeniyu-i-kazakhstan [Accessed: 5 June 2024] (in Russian).

4) Government of the City of Sevastopol, 2020. Strategy for the Development of the Black Sea Anchovy Fishery in the Black Sea for 2021–2030. In: GSS, 2020. *Minutes of the Meeting of the Azov-Black Sea Basin Scientific and Fisheries Council*. Sevastopol, pp. 8–26 (in Russian).

concentrations by the SOI staff in 2023 at eight stations in Karkinitsky and Kalamitsky Bays showed that the maximum permissible concentrations were exceeded at all eight stations.

In oceanological studies, the shelf boundary is usually delineated by a 200-metre isobath [5]. According to its morphostructural characteristics, the western area (from Tarkhankut Bay to Laspi Bay and Sarych Bay), the southern coastal area (from Sarych Bay to Meganom Bay) and the eastern area, including the area of Feodosia Bay and the Kerch-Taman shelf, are distinguished [6]. The bottom relief is spatially heterogeneous: while in the north of the western shelf of the peninsula the 60 m isobath is located at a distance of 10–15 km from the shore, in the south it passes in close proximity to the water's edge. In the main part of the shelf, its width is 90 km [7] and increases in the northwestern direction, reaching 220 km in the area of the Gulf of Karkinit.

Regional peculiarities of the shelf geomorphology determine proximity of the Rim Current (RC) to the coastline. It comes close the coast at the southern tip of the peninsula. The RC velocity with a flow width of up to 80 km is 40–150 cm/s [5], which is several times higher than that of the coastal current.

The geostrophic dynamics of waters is subject to interannual variability, due to which the circulation may have a "basin" (with a pronounced RC) or an "eddy" mode [8]. The change of modes affects physical and biological characteristics of the pelagic ecosystem. The thermohaline structure of waters, their physical dynamics, phyto- and zooplankton production affect fishery stocks of small pelagic fish (anchovy *Engraulis encrasicolus* (Linnaeus, 1758) and sprat *Sprattus sprattus* (Linnaeus, 1758)), which form the basis of fisheries in Crimean waters [9].

The purpose of our research was to identify trends in the interannual variability of structural and functional characteristics of the pelagic community in the first decades of the 21st century, since the processes that occurred in the previous decades were covered in a number of overviews [10, 11].

Material and methods

To identify multiyear trends, we used the results of remote measurements (by *MODIS-Aqua/Terra* satellite scanners), contact measurements (from the R/V *Professor Vodyanitsky*) and calculations of structural and functional relationships, such as the ratio of primary production to forage zooplankton biomass and the ratio of gelatinous biomass to forage zooplankton fraction (Table 1).

The geographical contours of the study area are defined by a multiyear grid of oceanographic stations carried out during the expeditions of the R/V *Professor Vodyanitsky* (Fig. 1) within the scope of different projects.

Due to the diverse objectives of these projects, the set of measured parameters, the number of stations and their location varied over years. The bulk of the contact measurements of biological characteristics took place in 2010–2020. Some plankton samples from later expeditions remain unprocessed. The examples of field surveys with vertical soundings at stations and their distribution are given in Fig. 1 and Table 2.

Table 1. Analyzed characteristics

Parameter	Measurement type	Source
Wind speed at the sea surface ($m \cdot s^{-1}$)	Products of models *MERRA*-2 / *M2TMNXOCN* v.5.12.4; *NCEP*/*NCAR Reanalysis*	URL: https://giovanni.gsfc.nasa.gov/giovanni; URL: https://psl.noaa.gov/data/timeseries/
Sea surface temperature (°C)	Remote sensing (*MODIS-Aqua*)	URL: https://giovanni.gsfc.nasa.gov/giovanni/
Mass transport in the 0–200 m layer (Sv)	NEMO model v.3.6 calculation results	[12]
Concentration of petroleum hydrocarbons ($mg \cdot dm^{-3}$)	IR radiometry	Archive materials of SOI [5)]
Chlorophyll a concentration ($mg \cdot m^{-3}$)	Remote sensing (*MODIS-Aqua/Terra*)	URL: https://oceancolor.gsfc.nasa.gov; model calculation [13]
Phytoplankton biomass ($mg \cdot m^{-2}$)	Processing of samples collected in expeditions	Archive materials of IBSS
Primary production ($mg\ C \cdot m^{-3} \cdot day^{-1}$)	Calculation results from remote sensing data	[14]
Bioluminescent potential ($10^{-8}\ W \cdot s^{-2} \cdot L^{-1}$)	Sounding in the 0–50 м layer	Archive materials of IBSS [6)]

[5)] Korshenko, A.N., ed., 2023. *Marine Water Quality by Hydrochemical Indicators. Annual Report 2021*. Moscow: GOIN, pp. 70–105 (in Russian).

[6)] Zhuk, V.F., Belogurova, Yu.B., Vasilenko, V.I. and Melnik, A.V., 2023. *Bioluminescence of the Black Sea. Atlas*. Sevastopol: IBSS, 371 p. (in Russian).

Parameter	Measurement type	Source
Forage zooplankton biomass ($mg \cdot m^{-3}$)	Catching in the 0–100 m layer with a Juday net	Archive materials of IBSS
Gelatinous zooplankton biomass ($mg \cdot m^{-3}$)	Catching in the 0–100 m layer with a Bogorov Rass net	Archive materials of IBSS
Ratio of primary production to forage zooplankton biomass	Calculation results from measured parameters	Archive materials of IBSS
Stocks and catches of small pelagic fish on the Crimean shelf	Results of calculation of trawl catch parameters	Archive materials of VNIRO, Azov and Black Sea Basin Scientific and Fishery Council, https://fish.gov.ru and works [13, 15, 16]

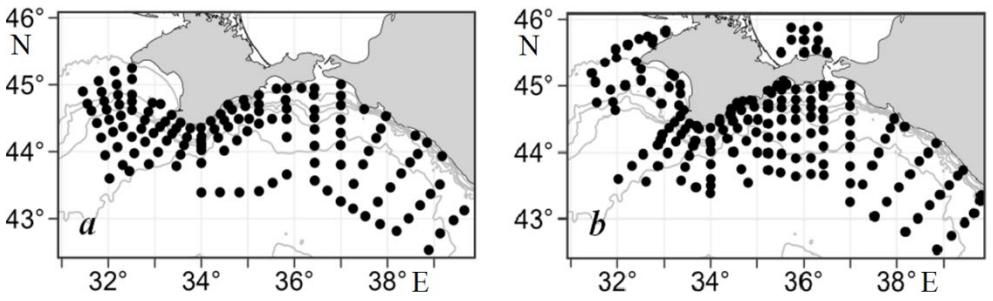

Fig. 1. Examples of oceanographic station grids carried out on board R/V *Professor Vodyanitsky*: 102nd cruise, June–July, 2018 (*a*); 108th cruise, July–August, 2019 (*b*)

Table 2. The R/V *Professor Vodyanitsky* expeditions, from 2010 to 2022

Year	Cruise number	Number of oceanographic stations
2010	64, 68	16, 23
2011	70	41
2013	72	50
2015	81	52
2016	86	63
2017	93, 94, 95, 96, 97	39, 104, 132, 93, 22
2018	102, 103,105	137, 155, 114
2019	106, 107,108, 110, 111	106, 2, 174, 120, 142
2020	113, 114,115	163, 130, 97
2021	116, 117, 118, 119	134,145, 49, 146
2022	120, 121, 122, 123,124, 125-1	124, 221, 189, 113, 56, 128

Remote measurements. A time series of monthly mean sea surface temperatures was constructed from *MODIS-Aqua* upwelling spectroradiometer measurements. Level 3 (L3) data obtained with a spatial resolution of 4 km and further averaged for the Crimean shelf were used. Two time series were constructed: one with monthly average resolution and one with interannual temperature averaging over the entire summer season. Both time series are presented in units of deviation from the multiyear average for each of the time series.

The same satellite also obtained time series of chlorophyll *a* concentration in the surface layer and photosynthetically active radiation. The time series of monthly mean values of wind speed above the sea surface (at a height of 10 m) and a zonal component of wind speed were downloaded from the *MERRA-2* and *NCEP/NCAR* reanalysis databases.

Computational characteristics. The net integral primary production in the euphotic layer was calculated using an algorithm where surface temperature and photosynthetically active radiation are remotely measured parameters [14]. The chlorophyll *a* concentration values (from *MODIS-Aqua* scanner measurements) used to calculate primary production underwent correction to separate chlorophyll and dissolved colored matter [13]. The calculations of lateral mass transfer of water in the direction from the shelf to the seaward part in the 0–50, 50–200 and 0–200 m layers were carried out by A. Akpınar and co-authors and detailed in their works [17, 18].

Contact measurements. Phytoplankton was studied according to the data of bathometric water samples (2 liters in volume) taken from the R/V *Professor Vodyanitsky*. The samples were thickened by reverse filtration through track membrane

filters with a pore diameter of 1 μm. The resulting concentrate was preserved with Lugol's solution (0.1 mL per 50 mL of sample). Phytoplankton species composition and cell sizes were determined in a Naumann chamber under a *XY-B2* trinocular microscope. The cell volumes and biomass were calculated according to the generally accepted methodology [7)].

Measurements of the bioluminescence intensity of the plankton community (its bioluminescence potential) were taken from aboard the ship. The bioluminescence potential (BP) characterizes the maximum luminescence energy of organisms: $BP = \int B(t)\,dt$, where $B(t)$ – light emission intensity during a bioluminescent flash (t) [19]. For BP measurements the *Salpa-M* submersible instrument complex was used, which in the vertical sounding mode enables synchronous measurements of mechanically stimulated bioluminescence of planktonic organisms (in the range from 10^{-13} to 10^{-8} W·cm^{-2}·L^{-1} with precision ±10%), hydrostatic pressure, temperature, conductivity, turbidity and photosynthetically active radiation. The resolution of measurements when the device was immersed at a velocity of 1.2 m·s^{-1}, was 0.25 m. The method of work was described in detail earlier [19].

Zooplankton were collected using a Juday plankton net with an inlet diameter of 36 cm (mesh size 140 μm). The obtained samples were condensed to 100 mL and preserved with neutral formaldehyde solution to 4% concentration. The samples were processed by standard counting in the Bogorov chamber: taxonomic composition, age stages, size of hydrobionts and their number in the sample were determined. The size-weight relationships known for the Black Sea species were used to convert the size characteristics of individuals to biomass units [20]. Based on the results of sample processing, the biomass of zooplankton in a meter cubic and under a meter square of the sampled layer was calculated.

The data on the concentration of petroleum hydrocarbons and stocks and catches of small pelagic fishes on the Crimean shelf were retrieved from the archival materials of SOI, VNIRO, reports of the Azov-Black Sea Basin Scientific and Fisheries Council and the published articles (Table 1). *Statistica v.9* and *PAST v.13* software products were used for graphical representation and statistical processing. In particular, the nonparametric Mann–Kendall test, used in the analysis of time series in hydrophysics and hydrometeorology [21], was applied to test the statistical significance of the monotonic interannual trend.

Results and discussion

Interannual variability was analyzed for the summer season as the most abundant with biological measurements.

Wind speed. In the summer season, the wind field in the near-surface layer over the Crimean shelf is spatially heterogeneous both in the direction and in the values of the meridional and zonal components of speed, which was noted earlier [22]. In June–August 2002–2020, the mean wind speed was 5.1 ± 0.2 m·s^{-1}

[7)] Radchenko, I.G., Kapkov, V.I. and Fedorov, V.D., 2010. [*A Practical Guide to Collecting and Analysing Marine Phytoplankton Samples*]. Moscow: Mordvintsev, 60 p. (in Russian).

and had no statistically significant monotonic interannual trend (Mann–Kendall test $S = -23$, $Z = 0.77$, $p = 0.44$). It was also absent in the time series of summer values of the zonal velocity component dominating in the formation of alongshore water mass transfer on the Crimean shelf ($S = -87$, $Z = 1.28$, $p = 0.20$).

Physical water dynamics. A characteristic property of the pelagic community biotope is its mobility (mass transfer). From a regional perspective, mass transfer is determined by the direction of both the RC and the coastal current. In the area of the southern coast of Crimea, the latter is a wind-modulated large-scale alongshore flow of west-south-west direction, parallel to the coastline, with a mean annual velocity modulus of ~ 8 cm·s^{-1} [23] with maximum values up to 35 cm·s^{-1} [24]. Meandering currents, mesoscale and submesoscale eddies (Fig. 2) form mass transfer anomalies, including transverse mass transfer of waters from the coastal area beyond the shelf [25–27]. The multicomponent dynamics is most clearly represented in the animation of the *NEMO-eNATL60* model *.

Both physical and biological parameters are sensitive indicators of cross-shelf mass transfer. Thus, the tongue of warm water directed from the shore to the seaward part can be seen in the spatial distribution of sea surface temperature far beyond the shelf (Fig. 2, *b*).

Coastal upwelling is manifested in the sea surface temperature field by tongues of cold water directed from the coast to the seaward part. Summer surface temperature in the Crimean shelf can be 10–12 °C. The data of expedition and satellite measurements contain numerous episodes of coastal upwelling during the summer period. The time series of cross-shelf mass transfer on the scales of seasonal and interannual variability were obtained from the three-dimensional circulation model *NEMO v.3.6*, which has 61 vertical layers with zonal and meridional spatial resolution of 3 km (Fig. 3).

Transverse mass transfer showed relative stability in the upper 0–50 m and integral 0–200 m sea layer (no interannual trend: Mann–Kendall test for the 0–200 m layer, $S = 110$, $Z = 1.33$, $p = 0.18$). The trend was also absent in the interannual variability of the kinetic energy density in the upper 30 m layer, which characterizes the intensity of currents in it [28].

The interannual temperature changes in the upper layers are ecologically significant, as key structural and functional characteristics of the coastal pelagic community are correlated with temperature [19, 29, 30]. The multiyear trend in the Black Sea surface temperature (from 1993 to 2021) is generally positive (0.07 °C year^{-1}),

* The model shows details of the macroscale turbulence of the entire basin at hourly resolution Available at: https://www.youtube.com/watch?v=IaWycRF5Zho [Accessed: 30 May 2024].

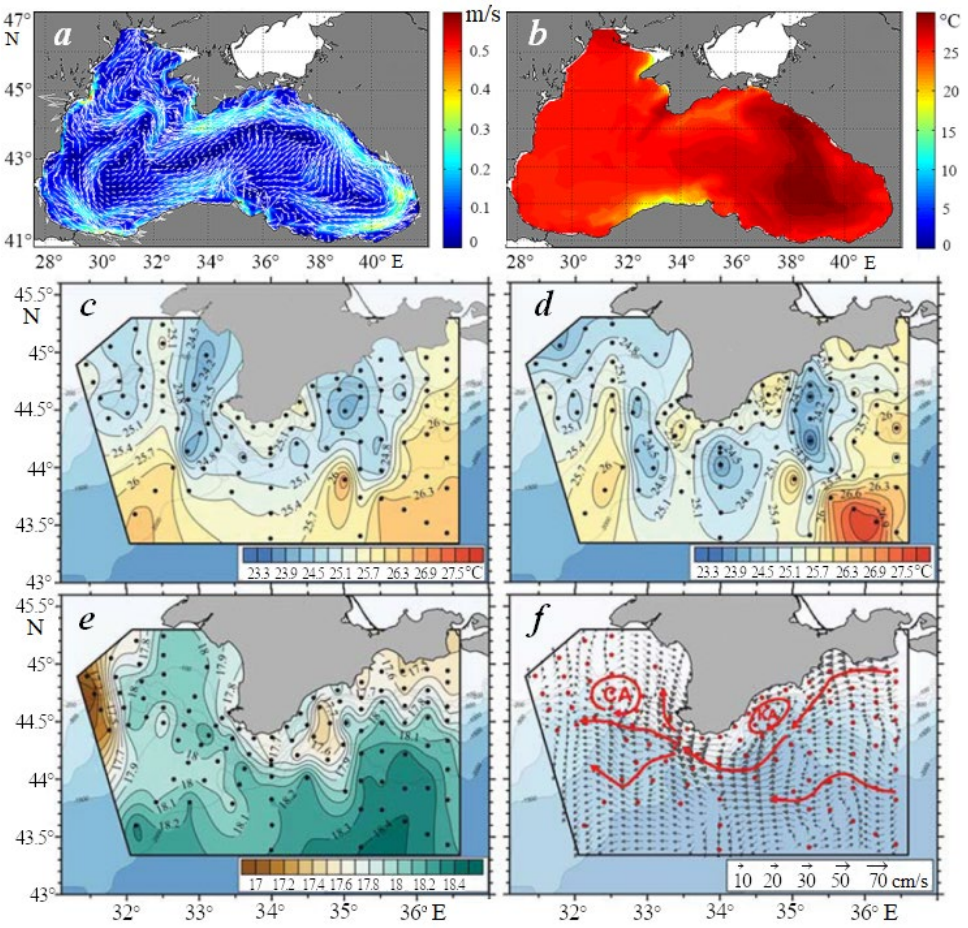

F i g . 2 . Large scale (*a, b*) and mesoscale (*c – f*) spatial structure of hydrophysical fields: the direction and geostrophic current velocity in the upper layer, in August 2018 (*a*) and the sea surface temperature (*b*) (available at: https://dekosim.ims.metu.edu.tr/BlackSeaModels/BlackSeaModels.shtml); examples of mesoscale heterogeneities of sea surface temperature (*c*), temperature at 1 m depth (*d*), salinity at 1 m depth (*e*). Vectors of currents from instrumental measurements (*f*). Red arrows indicate the Rim Current. The Sevastopol anticyclonic eddy (CA) and Crimean anticyclonic eddy (KA) are highlighted with red ovals [26]

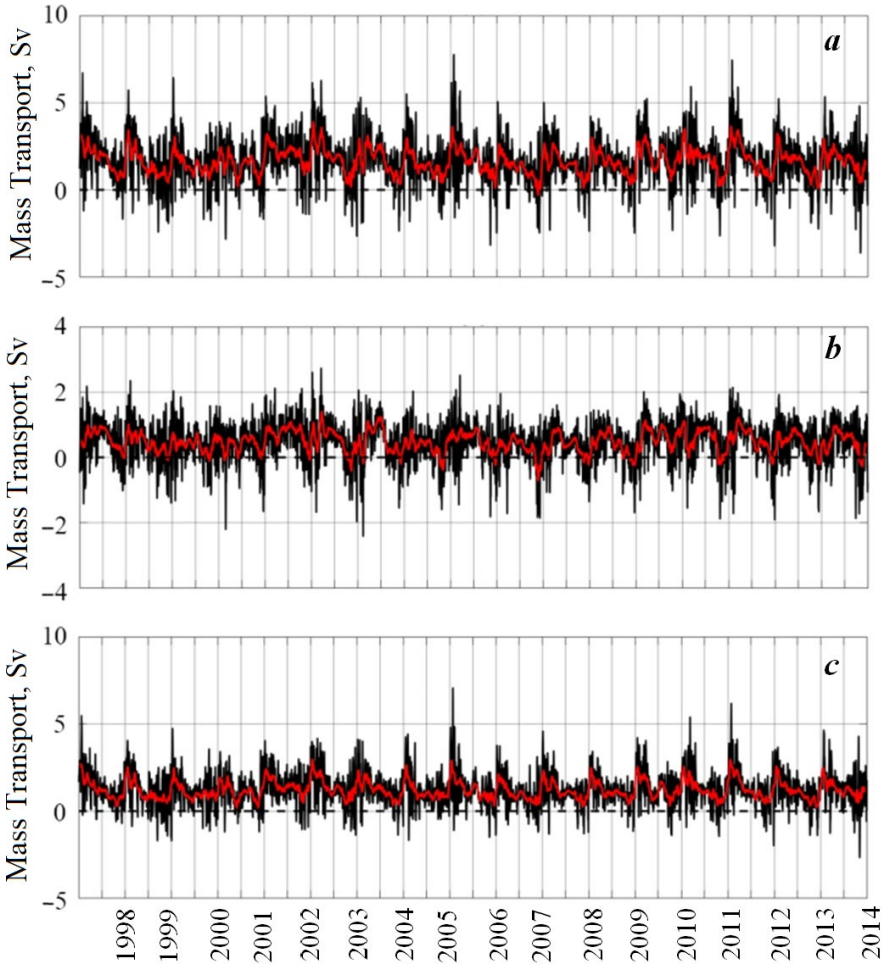

Fig. 3. Cross-shelf water mass transport (Sv) in the layers: 0–200 m (*a*), 0–50 m (*b*) and 50–200 m (*c*). Positive values stand for the transport directed off the shelf seawards. The red curve stands for the trend based on a running mean, with a 30-day smoothing window [12]

although the rate of increase becomes less pronounced from 2011 to 2022 (Fig. 4, *a*). On the Crimean shelf, there was no interannual trend of sea surface temperature anomalies in 2011−2022 (Fig. 4, *b*, *c*; Mann−Kendall test, $S = 1652$, $Z = 1.32$, $p = 0.19$). This is clearly represented by the interannual variability of the summer season anomalies (Fig. 4, *c*).

Pollution. River, storm and municipal runoffs make a significant contribution to the pollution of coastal waters of Crimea. Thus, on the seaside of Sevastopol, the average concentrations of petroleum hydrocarbons in 2016–2021 were approximately twice as high as the maximum permissible concentrations [31]. The increase in the concentration of ammonia nitrogen and petroleum products in the city wastewater in the first decades of the 21st century was reported in [32].

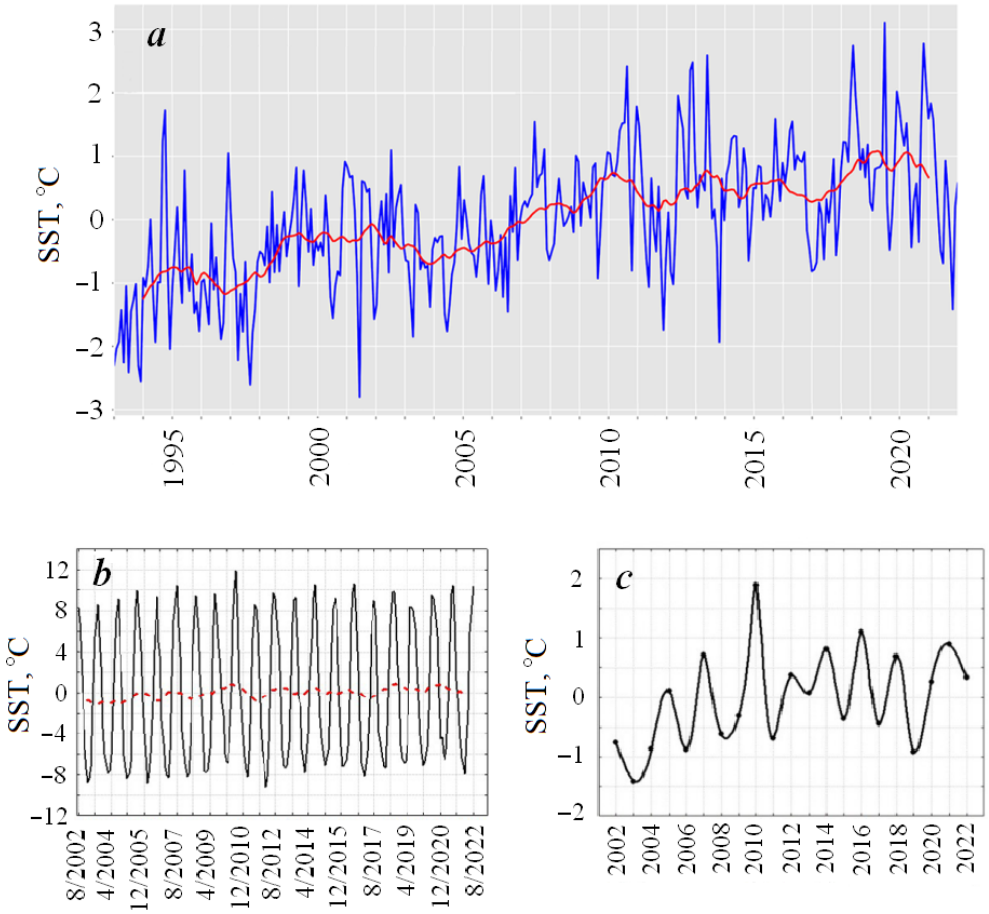

Fig. 4. Temporal variability of the sea surface temperature (SST): sea surface temperature deviations from the mean, on a basin scale (https://data.marine.copernicus.eu/product/BLKSEA_OMI_TEMPSAL_sst_area_averaged_anomalies/description) (*a*); the Crimean shelf sea surface temperature anomalies in monthly time series. The red dashed curve stands for the running mean (with a 12-month window) (*b*); the Crimean shelf sea surface temperature anomalies of the summer season (in 2002–2022), smoothed by a cubic spline (*c*)

Planktonic organisms are known to be sensitive to high concentrations of petroleum hydrocarbons, which adversely affects the growth rates of phytoplanktonic algae [33, 34], the intensity of their bioluminescence [19, 35] and zooplankton reproduction [36].

There is no statistically significant trend (Mann–Kendall test, $S = -24$, $Z = 0.61$, $p = 0.54$) in the multiyear SOI data on the mean annual concentration of petroleum hydrocarbons in the coastal waters of Crimea as a whole (in 2000–2022) (Fig. 5).

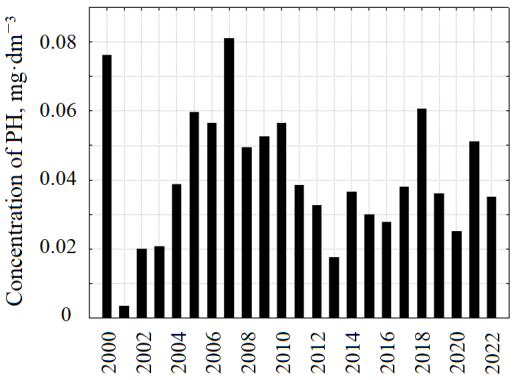

F i g . 5 . Interannual variability of the annual concentration of petroleum hydrocarbons (PH, mg·dm^{-3}) on the Crimean shelf according to SOI data

A likely reason for the absence of an interannual trend in the concentration of petroleum hydrocarbons within the Crimean shelf may be the combination of a narrow shelf with a stable interannual cross-shelf mass exchange (Fig. 3), which can offset the interannual increase in hydrocarbon concentration due to exchange with open waters, but maintain its high average level due to incoming high-volume runoff.

Another explanation for the presented dynamics could be the lack of data, as the coverage of the shelf by measurements was spatially uneven and weak due to the fragmented nature of monitoring, especially in the first decade of the 21st century owing to insufficient funding [32]. It should also be noted that the infrared radiometric concentration measurement used by SOI is less sensitive to the concentration of natural petroleum hydrocarbons compared to the fluorimetric measurement method. As a consequence, the concentration level of petroleum hydrocarbons in coastal waters is recognized as being below the maximum permissible concentration established for water bodies of fishery significance, while the fluorescent analysis data show that this level is exceeded by 1.4 times [37].

Input of ~ 80% of runoff into coastal waters without treatment and increase in the volume of wastewater [4] will worsen the sanitary condition of the shelf. Probably, in the summer season we should expect an increase in the cases of gastrointestinal (bacterial-viral) infections, the cause of which is the sea. However, hypothesis testing needs appropriate preparation of time series of parameters for their statistical analysis.

Phytoplankton and primary production. Eutrophication of shelf waters as a result of runoff affects the structure and productivity of the phytoplankton community. This has been shown by studies of the broad and shallow northwestern Black Sea shelf on the scale of multiyear variability [10]. The productivity of shelf waters of Crimea is much lower and the taxonomic composition of phytoplankton is very diverse: Dinophyceae alone are represented by 156 taxa of species and intraspecific rank. The genera *Protoperidinium*, *Gymnodinium* and *Dynophysis* dominate by the number of species [38]. In 2010–2019, the genera Dinophyceae made the greatest contribution (~ 46%) to phytoplankton biomass formation. The share of other groups (Bacillariophyceae and Prymnesiophyceae) was ~ 39 and 15%, respectively.

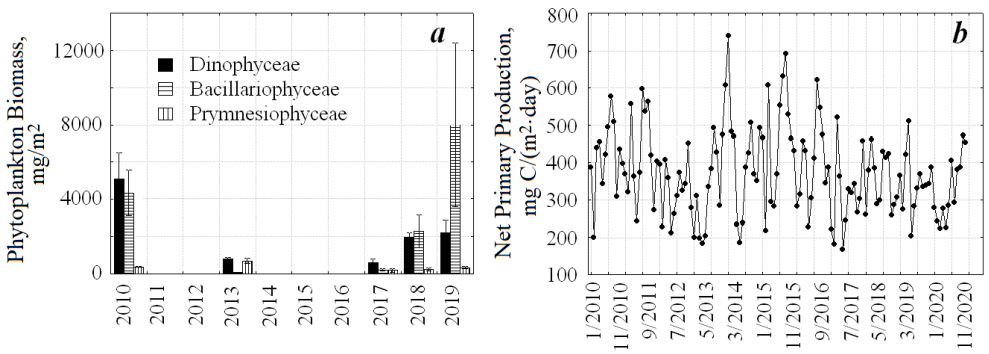

Fig. 6. Interannual variability of phytoplankton biomass (*a*) and net primary production (*b*). The vertical whickers stand for the error mean

Their contribution in different years differed by an order of magnitude. In the interannual variability of biomasses of Dinophyceae, Bacillariophyceae and Prymnesiophyceae of the integral layer, no statistically significant trends of interannual variability were revealed (Fig. 6).

Calculation of the values of integral net primary production on the scale of the Crimean shelf showed the absence of an interannual trend (Mann–Kendall test, $S = 924$; $Z = 1.82$; $p = 0.07$). It was also absent in the time series based on summer values only ($S = –19$; $Z = 1.40$; $p = 0.16$). The absence of trend was observed on the shelf of the Anatolian coast and in the eastern part of the Black Sea for the earlier period of 1998–2015 [39]. In the time series of net primary production plotted against monthly averages, a decrease in the range of fluctuations can be observed, highlighting the interannual stabilization of the process (Fig. 6).

Bioluminescence of plankton. Bioluminescent potential has a dual nature. On the one hand, it is regulated by the abundance and biomass of bioluminescent organisms (primarily phytoplankton, which dominates the integral mechanically stimulated bioluminescence in the Black Sea), and on the other hand, it serves as an indicator of the functional (physiological) state of these organisms, since the characteristics of their bioluminescence depend on temperature, salinity, oil pollution and other factors [19].

No monotonic trend was observed in the time series of integral layer BP values (Fig. 7). It can be assumed that the interannual ("non-trend") variability of BP is regulated by the dynamics of Dinophyceae biomass. Thus, during the four-year period of studies at the coastal station near Sevastopol (in 2010–2013), the value of the sample correlation coefficient between BP and biomass of luminous Dinophyceae in monthly time series was 0.91 at $p = 0.01$ [40].

The next group (Bacillariophyceae) is not bioluminescent in terms of its contribution to the total phytoplankton biomass, but its multiyear dynamics is given

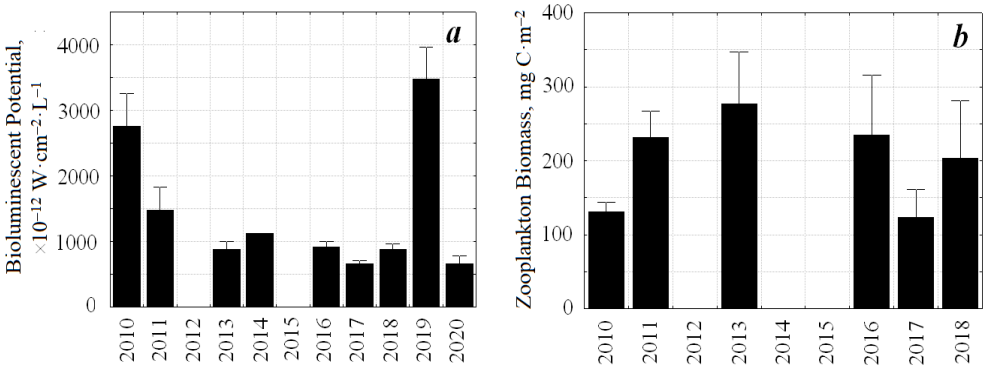

Fig. 7. Interannual variability of the bioluminescent potential, 10^{-12} W·cm^{-2}·L^{-1} (*a*) and the forage zooplankton biomass, mg C·m^{-2}, (*b*) on the Crimean shelf. The vertical whickers stand for the error mean

in this section (Fig. 5) to state that there is no multiyear trend in biomass at the level of individual phytoplankton taxonomic groups (at $p = 0.24$).

Zooplankton. Interannual fluctuations in the taxonomic composition and biomass of phytoplankton are reflected in the characteristics of spatial and temporal variability of the biomass of zooplankton consuming phytoplankton. The basis of the biomass of feeding zooplankton in the summer period in all years was formed by Copepoda (41–48%) and bristlefishes, represented by one species – *Parasagitta setosa* (J. Muller, 1847) with the share varying in the range of 12–49%. There was no trend in the long-term dynamics of zooplankton biomass (Fig. 7). It was not detected in the dynamics of gelatinous zooplankton biomass according to eight years of observations (2010–2018). We should note a large range of fluctuations in the biomass of forage zooplankton with the average number of stations for the summer season equal to 16 for each of the expeditions. Apparently, this range is modulated by the mesoscale and submesoscale spatial heterogeneity of the biotope, elements of which can be seen in Fig. 2.

The zooplankton of the Black Sea includes indicator species of coastal waters. These include branchiopod crustaceans (Cladocera), which develop extensively during the summer months. Their presence in offshore waters may be considered as a consequence of cross-shelf mass transfer. Thus, the analysis of samples showed the presence of species of *Penilia avirostris, Pleopsis polyphemoides, Pseudevadne tergestina* above the depths of 1800–2120 m. Cladocera abundance in coastal areas (151–303 eq/m^3) was one or two orders of magnitude higher than in deep waters. Interannual variability is also significant. For example, in 2014–2020, fluctuations in total abundance in the deep water and on the shelf reached one or two orders of magnitude without pronounced interannual trends.

As for the non-feeding, i. e., gelatinous zooplankton (jellyfish, comb and noctiluca), its crude biomass (in 2010, 2011, 2013, 2016, 2018) exceeded the crude biomass of the feeding zooplankton by tens and sometimes hundreds of times. The ratio of gelatinous to foraging zooplankton biomass converted to organic carbon units was markedly lower. However, the two- to threefold dominance of gelatinous in this respect was preserved, indirectly indicating the predominance of the detrital (rather than grazing) pathway of organic carbon transfer in the pelagic ecosystem of the shelf.

Among the set of structural and functional relations characterising the plankton community as a whole, we should mention the ratio of net primary production to biomass of forage zooplankton, which is interpreted as the rate of turnover of primary production through zooplankton [41, 42]. The calculation of this ratio showed no interannual trend in 2010–2018 with its mean value of 2.3 and coefficient of variation of 36%. In general, the twofold coverage of the available biomass of forage zooplankton by net primary production indicates favourable feeding conditions for zooplankton organisms on the shelf.

Small pelagic fishes. Multiyear dynamics of sea surface temperature and biomass of forage zooplankton is important for the formation of the commercial stock of its mass consumers (anchovy and sprat) and interannual fluctuations of this stock [43]. In 2016–2018, their catches accounted for 96% of the total catches in Russian waters [9]. In the current regulatory framework, stock and catch estimates are separated by fishing area. For example, in August 2023, average sprat catches per vessel, according to AzNIIRKH data, varied between ~ 36 tons in the western part of the shelf (the Kalamitsky Gulf) and ~ 42 tons in the eastern part (the Gulf of Feodosia) with the maximum allowable exploitation of the resource estimated at 18–20 thousand tons in 2023–2024 [15].

On the scale of interannual variability (in 2010–2019), the dynamics of the commercial stock of Azov anchovy (east of Cape Sarych) had a statistically significant negative trend (Mann–Kendall test, $S = -25$, $p = 0.01$), which is regulated by both physical and anthropogenic factors (with the dominance of the latter). The probability of wintering aggregations forming along the Crimean coast is considered to be extremely low in the context of continuing stock decline. The unregulated catch of seasonally migratory anchovy and sprat by fishing vessels from Turkey (whose catches account for about 62% of the total in the Black Sea basin) is one of the factors in the long-term decline of fish stocks, including Crimean fish stocks [44]. It probably reduces the positive impact of the extended spawning season for small pelagic fish, which has been noted in connection with the long-term increase in temperature in the upper layers [45, 46].

Conclusion

After the cataclysms of the 1990s associated with eutrophication and trophic pressure of planktonic omnivores *Mnemiopsis leidyi* A. Agassiz, 1865 and *Beroe ovata* Mayer 1912, the interannual structure of the pelagic plankton community of the Crimean shelf became relatively stable. Since in complex systems (in particular, ecosystems) the structure of the system regulates its function, the relative stability

of structural characteristics (primarily biomass) determined the absence of interannual trends in the functional properties of the community: i.e. net primary production, phytoplankton bioluminescence intensity, and the ratio of primary production to biomass of forage zooplankton (i. e., the rate of turnover of primary production through zooplankton).

Thus, the pelagic ecosystem of the Crimean shelf in the second decade of the 21st century is characterized not so much by monotonic trends of interannual variability as by interannual fluctuations of its structural and functional properties against the background of relatively stable large-scale hydrophysical dynamics estimated by kinetic energy density and cross-shelf mass transfer of water in the upper layers.

REFERENCES

1. Kozhurin, E.A., Shlyakhov, V.A. and Gubanov, E.P., 2018. Crimea Commercial Fish Dynamics in the Black Sea. *Trudy VNIRO*, 171, pp. 157–169 (in Russian).
2. Golovanov, V.I., Anfimova, A.Yu. and Melnichenko, N.F., 2021. Improving the Mechanisms for Managing the Environmental Situation in the Republic of Crimea on the Eve of the 2021 Tourist Season. *Municipal Academy*, (2), pp. 162–169. https://doi.org/10.52176/2304831X_2021_02_162 (in Russian)
3. Sovga, E.E., Korshenko, A.N., Mezentseva, I.V., Khmara, T.V. and Pogozheva, M.P., 2022. Environmental Monitoring System in the Azov and Black Sea Basin. *Ecological Safety of Coastal and Shelf Zones of Sea*, (2), pp. 19–37.
4. Verzhevskaya, L.V. and Minkovskaya, R.Ya., 2020. Structure and Dynamics of Anthropogenic Load on the Coastal Zone of the Sevastopol Region. *Ecological Safety of Coastal and Shelf Zones of Sea*, (2), pp. 92–106. doi:10.22449/2413-5577-2020-2-92-106 (in Russian).
5. Ivanov, V.A. and Belokopytov, V.N., 2013. *Oceanography of the Black Sea*. Sevastopol: EKOSI-Gidrofizika, 210 p.
6. Myslivets, V.I., Rimsky-Korsakov, N.A., Korotaev, V.N., Pronin, A.A. and Porotov, A.V., 2021. [Geophysical and Geomorphological Studies of the Crimean Shelf]. In: GeoEurasia, 2021. [*Proceedings of the International Geological and Geophysical Conference and Exhibition "GeoEurasia-2021. Geological Exploration in the Today's Reality". 2–4 March, 2021*]. Tver: OOO "PoliPRESS". Vol. II, pp. 244–247 (in Russian).
7. Rimsky-Korsakov, N.A., Korotaev, V.N., Myslivets, V.I., Porotov, A.V., Pronin, A.A. and Ivanov, V.V., 2019. The Geomorphology and History Formation of Western Shelf of Crimea. *Journal of Oceanological Research*, 47(4), pp. 161–176. https://doi.org/10.29006/1564-2291.JOR-2019.47(4).11 (in Russian).
8. Demyshev, S.G., Dymova, O.A. and Miklashevskaya, N.A., 2022. Spatio-Temporal Variability of Hydrophysical and Energy Characteristics of the Black Sea Circulation During Prevalence Movements of Different Scale. *Journal of Oceanological Research*, 50(3), pp. 27–50. https://doi.org/10.29006/1564-2291.JOR-2022.50(3).2 (in Russian).
9. Balykin, P.A., Kutsyn, D.N. and Startsev, A.V., 2021. Fishing Under Climate Change: Dynamics of Composition and Structure of Catches in the Russian Black Sea in the XXI Century. *Marine Biological Journal*, 6(3), pp. 3–14. https://doi.org/10.21072/mbj.2021.06.3.01
10. Yunev, O.A., Konovalov, S.K. and Velikova, V., 2019. *Anthropogenic Eutrophication in the Black Sea Pelagic Zone: Long-Term Trends, Mechanisms, Consequences*. Moscow: GEOS, 164 p. https://doi.org/10.34756/GEOS.2019.16.37827 (in Russian).

11. Zaitsev, Yu. and Mamaev, V., 1997. *Marine Biological Diversity in the Black Sea. A Study of Change and Decline*. New York: United Nations Publications, 208 p. Available at: https://digitallibrary.un.org/record/245415?ln=ru [Accessed: 14 April 2024].
12. Akpinar, A., Sadighrad, E., Fach, B.A. and Arkin, S., 2022. Eddy Induced Cross-Shelf Exchanges in the Black Sea. *Remote Sensing*, 14(19), 14881. https://doi.org/10.3390/rs14194881
13. Suslin, V.V. and Churilova, T.Ya., 2016. A Regional Algorithm for Separating Light Absorption by Chlorophyll-a and Coloured Detrital Matter in the Black Sea, Using 480–560 nm Bands from Ocean Colour Scanners. *International Journal of Remote Sensing*, 37(18), pp. 4380–4400. https://doi.org/10.1080/01431161.2016.1211350
14. Kovalyova, I.V. and Suslin, V.V., 2022. Integrated Primary Production in the Deep-Sea Regions of the Black Sea in 1998–2015. *Physical Oceanography*, 29(4), pp. 404–416. https://doi.org/10.22449/1573-160X-2022-4-404-416
15. Piatinskii, M.M., Shlyakhov, V.A. and Afanasiev, D.F., 2022. Crimean-Caucasian Black Sea Sprat Updated Stock Assessment Results During the Period 2001–2021. In: MSU, 2022. *Proceedings of the XI International Conference Marine Research and Education. MARESEDU-2022. Moscow, 24–28 October 2022. Vol. III (IV)*. Tver: PoliPRESS, pp. 393–397 (in Russian).
16. Stafikopulo, A.M. and Negoda, S.A., 2021. Dynamics of the Industrial Fishing Indices of the European Anchovy in the Azov and Black Sea Basin in Recent Years. *Aquatic Bioresources and Environment*, 4(1), pp. 50–70. https://doi.org/10.47921/2619-1024_2021_4_1_50 (in Russian).
17. Akpinar, A., Sadighrad, E., Fach, B.A. and Arkin, S., 2022. Eddy Induced Cross-Shelf Exchanges in the Black Sea. *Remote Sensing*, 14, 14881. https://doi.org/10.3390/rs14194881
18. Akpınar, A. and Bingölbali, B., 2016. Long-Term Variations of Wind and Wave Conditions in the Coastal Regions of the Black Sea. *Natural Hazards*, 84, pp. 69–92. https://doi.org/10.1007/s11069-016-2407-9
19. Tokarev, V.N., Evstigneev, P.V. and Mashukova, O.V., 2016. [*Plankton Bioluminescents of the World Ocean: Species Diversity, Light Emission Characteristics Under Normal Conditions and Anthropogenic Impact*]. Simferopol: N. Orianda, 340 p. (in Russian).
20. Petipa, T.C., 1957. [On Average Weight of Main Zooplankton Forms of the Black Sea]. In: Academy of Sciences of the USSR, 1957. *Trudy Sevastopolskoy Biologicheskoy Stantsii*, 9, pp. 39–57 (in Russian).
21. Wang, F., Shao, W., Yu, H., Kan, G., He, X., Zhang, D., Ren, M. and Wang, G., 2020. Re-Evaluation of the Power of the Mann-Kendall Test for Detecting Monotonic Trends in Hydrometeorological Time Series. *Frontiers in Earth Science*, 8, https://doi.org/10.3389/feart.2020.00014
22. Polonskii, A.B. and Muzyleva, M.A., 2016. Modern Spatial-Temporal Vartiability of Upwelling in the North-Western Black Sea and Off the Crimea Coast. *Izvestiya RAN. Seriya Geograficheskaya*, (4), pp. 96–108. https://doi.org/10.15356/0373-2444-2016-4-96-108 (in Russian).
23. Kuznetsov, A.S., Zima, V.V. and Shcherbachenko, S.V., 2020. Variability of Characteristics of the Coastal Current at the Southern Coast of Crimea in 2017–2019. *Ecological Safety of Coastal and Shelf Zones of Sea*, (3), pp. 5–16. https://doi.org/10.22449/2413-5577-2020-3-5-16 (in Russian).
24. Yurovsky, Yu.Yu., Malinovsky, V.V., Korinenko, A.E., Glukhov, L.A. and Dulov, V.A., 2023. Prospects for Radar Monitoring of Wind Speed, Wind Wave Spectra and Velocity of Currents from an Oceanographic Platform. *Ecological Safety of Coastal and Shelf Zones of Sea*, (3), pp. 40–54.

25. Artamonov, Yu.V., Alekseev, D.V., Skripaleva, E.A., Shutov, S.A., Deryushkin, D.V., Zavyalov, D.D., Kolmak, R.V., Shapovalov, R.O., Shapovalov, Yu.I., Fedirko, A.V. and Shcherbachenko, S.V., 2017. Thermohaline Structure of Water near the Crimea Coast and Adjacent Open Water Area of the Black Sea at Summer 2016. In: MHI, 2017. *Ecological Safety in Coastal and Shelf Zones of the Sea*. Sevastopol: ECOSI-Gidrofizika. Iss. 3, pp. 20–31 (in Russian).
26. Artamonov, Yu.V., Fedirko, A.V., Skripaleva, E.A., Shutov, S.A., Deryushkin, D.V., Kilmak, R.V., Zavyalov, D.D., Shapovalov, R.O., Shapovalov, Yu.I. and Shcherbachenko, S.V., 2019. Water Structure in the Ara of the Rim Black Sea Current in Spring and Summer 2017 (94th, 95th Cruises of the R/V "Professor Vodyanitsky"). *Ecological Safety in Coastal and Shelf Zones of the Sea*, (1), pp. 16–28. EDN ABVXOP. https://doi.org/10.22449/2413-5577-2019-1-16-28 (in Russian).
27. Kubryakov, A., Aleskerova, A., Plotnikov, E., Mizyuk, A., Medvedeva, A. and Stanichny, S., 2023. Accumulation and Cross-Shelf Transport of Coastal Waters by Submesoscale Cyclones in the Black Sea. *Remote Sensing*, 15(18), 4386. https://doi.org/10.3390/rs15184386
28. Dorofeev, V.L. and Sukhikh, L.I., 2023. Analysis of Long-Term Variability of Hydrodynamic Fields in the Upper 200-Meter Layer of the Black Sea Based on the Reanalysis Results. *Physical Oceanography*, 30(5), pp. 581–593.
29. Panov, B.N., Spiridonova, E.O., Piatinskii, M.M. and Stytsyuk, D.R., 2020. On the Role of Temperature as a Factor Influencing the Behavior of the European Sprat and the Efficiency of its Fishing. *Aquatic Bioresources and Environment*, 3(1), pp. 106–113. https://doi.org/10.47921/2619-1024_2020_3_1_106 (in Russian).
30. Seregin, S.A. and Popova, E.V., 2019. Different-Scale Variations in the Abundance and Species Diversity of Metazoan Microzooplankton in the Coastal Zone of the Black Sea. *Water Resources*, 46(5), pp. 769–779. https://doi.org/10.1134/S009780781905018X
31. Gruzinov, V.M., Dyakov, N.N., Mezenceva, I.V., Malchenko, Y.A., Zhohova, N.V. and Korshenko, A.N., 2019. Sources of Coastal Water Pollution near Sevastopol. *Oceanology*, 59(4), pp. 523–532. https://doi.org/10.1134/S0001437019040076
32. Dyakov, N.N., Korshenko, A.N., Malchenko, Yu.A., Lipchenko, A.E., Zhilyaev, D.P. and Bobrova, S.A., 2018. Hydrological and Hydrochemical Conditions of the Crimean and Caucasus Shelf Zones in 2016–2017. In: Kabatchenko, I.M., ed., 2018. *Proceedings of N.N. Zubov State Oceanographic Institute*. Moscow. Vol. 219, pp. 66–87 (in Russian).
33. Stelmakh, L.V. and Mansurova, I.M., 2021. Functional State of the Marine Microalgae Cultures as an Indicator of the Water Pollution Level of the Sevastopol Bay. *Monitoring Systems of Environment*, (4), pp. 83–90. https://doi.org/10.33075/2220-5861-2021-4-83-90 (in Russian).
34. Rudneva, I.I., 2022. Assessment of Mazut Toxicity for Embryos of Two Sea Fish Species. *Ecological Safety of Coastal and Shelf Zones of Sea*, (2), pp. 118–127. https://doi.org/10.22449/2413-5577-2022-2-118-127
35. Lapota, D., Osorio, A.R., Liao, C. and Bjorndal, B., 2007. The Use of Bioluminescent Dinoflagellates as an Environmental Risk Assessment Tool. *Marine Pollution Bulletin*, 54(12), pp. 1857–1867. https://doi.org/10.1016/j.marpolbul.2007.08.008
36. Seuront, L., 2011. Hydrocarbon Contamination Decreases Mating Success in a Marine Planktonic Copepod. *PLOS One*. 2011. Vol. 6, iss. 10, e26283. https://doi.org/10.1371/journal.pone.0026283
37. Temerdashev, Z.A, Pavlenko, L.Ph., Karpokova, I.G., Ermakova, Ya.S. and Ekilik, V.S., 2016. Some Methodological Aspects of Oil Pollution Evaluation of Water Bodies Based on the Degradation of Petroleum Products over Time. *Analytics and Control*, 20(3), pp. 225–235. https://doi.org/10.15826/analitika.2016.20.3.006 (in Russian).

38. Bryantseva, Yu.V., Krahmalnyi, A.F., Velikova, V.N. and Sergeeva, O.V., 2016. Dinoflagellates in the Sevastopol coastal zone (Black Sea, Crimea). *International Journal of Algae*, 18(1), pp. 21–32. https://doi.org/10.1615/InterJAlgae.v18.i1.20

39. Kovalyova, I.V., Finenko, Z.Z. and Suslin, V.V., 2021. Trends of Long-Term Changes in Chlorophyll Concentration, Primary Production of Phytoplankton and Water Temperature in the Shelf Regions of the Black Sea. *Sovremennye Problemy Distantsionnogo Zondirovaniya Zemli iz Kosmosa*, 18(4), pp. 228–235. https://doi.org/10.21046/2070-7401-2021-18-4-228-235 (in Russian).

40. Bryantseva, Yu.V., Serikova, I.M. and Suslin, V.V., 2014. Interannual Variability of the Dinoflagellates Diversity and Bioluminescence Fields off the Coast of Sevastopol In: TNU, 2014. *Optimization and Protection of Ecosystems*. Simferopol: TNU. Iss. 11, pp. 158–164 (in Russian).

41. Vinogradov, M.E. and Shushkina, E.L., 1987. [*Functioning of Plankton Communities in the Epipelagial Ocean*]. Moscow: Nauka, 240 p. (in Russian).

42. Piontkovski, S.A., Williams, R. and Melnik, T.A., 1995. Spatial Heterogeneity, Biomass and Size Structure of Plankton of the Indian Ocean: Some General Trends. *Marine Ecology Progress Series*, 117(1/3), pp. 219–227. https://doi.org/10.3354/meps117219

43. Glushchenko, T.I., 2011. Nutrition and Assessment of Black Sea Sprat in 2009–2010. In: YugNIRO, 2011. *YugNIRO Proceedings*. Kerch: YugNIRO. Vol. 49, pp. 34–39 (in Russian).

44. Latun, V.S., 2017. Influence of Connatural and Anthropogenous Factors on Trade Stores Dynamics of the Black Sea Anchovy. In: MHI, 2017. *Ecological Safety of Coastal and Shelf Zones of the Sea*. Sevastopol : ECOSI-Gidrofizika. Iss. 1, pp. 79–86 (in Russian).

45. Klimova, T.N., Subbotin, A.A., Melnikov, V.V., Serebrennikov, A.N., Podrezova, P.S., 2019. Spatial Distribution of Ichthyoplankton near the Crimean Peninsula in the Summer Spawning Season 2013. *Marine Biological Journal*, 4(1), pp. 63−80. https://doi.org/10.21072/mbj.2019.04.1.06 (in Russian).

46. Podrezova, P.S., Klimova, T.N. and Vdodovoch, I.V., 2021. Shifts in the Spawning Phenology of the Black Sea Mass Short-Cycle Species (Sprattus Sprattus and Engraulis Encrasicolus) Against the Background of Climatic Changes. In: MSU, 2021. *Proceedings of the X International Conference Marine Research and Education. MARESEDU-2021. Moscow, 25–29 October 2021. Vol. II (III)*. Tver: PoliPRESS, pp. 293–296 (in Russian).

Submitted 30.11.2023; accepted after review 19.02.2024;
revised 27.03.2024; published 25.06.2024

About the authors:

Sergey A. Piontkovski, Leading Research Associate, Sevastopol State University (33 Universitetskaya St., 299053, Sevastopol, Russian Federation), DSc (Biol.), **ORCID ID: 0000-002-6472-9701, Scopus Author ID: 6602165194, ResearcherID: ABB-9334-2020,** *spiontkovski@mail.ru*

Yulia A. Zagorodnyaya, Leading Research Associate, A.O. Kovalevsky Institute of Biology of the Southern Seas of RAS (2 Nakhimova Ave., Sevastopol, 299011, Russian Federation), PhD (Biol.), **ORCID ID 0000-0002-9502-4923, Scopus Author ID: 6506214138, ResearcherID: E-3325-2018**, *artam-ant.yandex.ru*

Irina M. Serikova, Senior Research Associate, A.O. Kovalevsky Institute of Biology of the Southern Seas of RAS (2 Nakhimova Ave, Sevastopol, 299011, Russian Federation), PhD (Biol.), **ORCID ID: 0000-0001-6604-2594, Scopus Author ID: 57148098700, ResearcherID: AAO-4117-2020**, *irasimwin@yandex.ru*

Ivan A. Minski, Junior Research Associate, Sevastopol State University (33 Universitetskaya St., 299053, Sevastopol, Russian Federation), Leading Engineer, A.O. Kovalevsky Institute of Biology of the Southern Seas of RAS (2 Nakhimova Ave, Sevastopol, 299011, Russian Federation), **ORCID ID: 0009-0009-6539-303X, Scopus Author ID: 58168623600**, *ivansimfer@yandex.ru*

Ilona V. Kovaleva, Research Associate, A.O. Kovalevsky Institute of Biology of the Southern Seas of RAS (2 Nakhimova Ave, Sevastopol, 299011, Russian Federation), PhD (Biol.), **ORCID ID: 0000-0001-5430-2002, Scopus Author ID: 56405274600, ResearcherID: AAB-4397-2019**, *ila.82@mail.ru*

Elena Yu. Georgieva, Leading Engineer, A.O. Kovalevsky Institute of Biology of the Southern Seas of RAS (2 Nakhimova Ave, Sevastopol, 299011, Russian Federation), **ORCID ID: 0000-0002-8177-0781, Scopus Author ID: 57193546928**, *e-georgieva@mail.ru*

Contribution of the authors:

Sergey A. Piontkovski – statement of the study objectives, formation of the article structure, analysis and interpretation of the results, preparation of the graphical materials, statistical analyses

Yulia A. Zagorodnyaya – statement of the study objectives, analysis and interpretation of the results, preparation of the graphical materials on zooplankton

Irina M. Serikova – preparation of the graphical materials, analysis and interpretation of the results on bioluminescence

Ivan A. Minski – preparation of the graphical materials, analysis and interpretation of the results on bioluminescence

Ilona V. Kovaleva – preparation of the graphical materials, analysis and interpretation of the results on primary production

Elena Yu. Georgieva – preparation of the graphical materials, analysis and interpretation of the results on phytoplankton

All the authors have read and approved the final manuscript.

ISSN 2413-5577, Ecological Safety of Coastal and Shelf Zones of Sea, 2024, No.2, pp. 60–75.

Original article

Characteristics of Storm Waves in Laspi Bay (Black Sea) Based on Results of Numerical Modeling

A. Yu. Belokon *, V. V. Fomin

Marine Hydrophysical Institute of RAS, Sevastopol, Russia
** e-mail: aleksa.44.33@gmail.com*

Abstract

This paper studies the characteristics of storm waves in Laspi Bay (Crimean Peninsula) using the numerical hydrodynamic model SWASH with a spatial resolution of 5 m. The wave reanalysis data obtained from the spectral model SWAN were set as boundary conditions. The fields of significant wave heights and wave current velocities in the bay were analyzed for storms of various regime conditions. It was established that the maximum values in the bay could reach 2.5–3.0 m, 4.0–4.5 m, 5.0–5.5 m and 6.0–6.5 m during storms that are possible once a year, once every 5, 10 and 25 years, respectively. An increase in wave velocities to 1.5–3.0 m/s occurred near the coast at depths of less than 10 m during storms that are possible once every 25 years. The influence of the protective breakwater, built in the 1980s, on the waves was local and manifested itself in the formation of a shadow zone on its downwind side. The possible influence of storm waves on the reduction of bottom vegetation in Laspi Bay was discussed. An analysis of the wave load on the bottom of the bay showed that during periods of extreme storms in its waters, the slopes most susceptible to the effects of waves were in the depth range from 2 to 12 m where the kinetic energy density increased to 500–2000 J/m^3. At the same time, the density could reach 3000–4500 J/m^3 in the western end of the bay. The energy load values were low in the middle part of the bay. Therefore, the disappearance of bottom vegetation here could be not due to storm impact, but an increase in water turbidity caused by anthropogenic factors. The obtained results are of great practical importance for the safety of navigation, engineering and exploitation of coastal infrastructure.

Keywords: storm waves, Black Sea, Southern Coast of Crimea, Laspi Bay, numerical modeling, SWASH

Acknowledgments: The work was carried out under MHI topic no. FNNN-2021-0005 “Coastal Research”. Calculations were carried out on the MHI computing cluster.

For citation: Belokon, A.Yu. and Fomin, V.V., 2024. Characteristics of Storm Waves in Laspi Bay (Black Sea) Based on Results of Numerical Modeling. *Ecological Safety of Coastal and Shelf Zones of Sea*, (2), pp. 60–75.

Характеристики штормового волнения в бухте Ласпи (Черное море) по результатам численного моделирования

А. Ю. Белоконь *, В. В. Фомин

Морской гидрофизический институт РАН, Севастополь, Россия
** e-mail: aleksa.44.33@gmail.com*

Аннотация
Исследуются характеристики штормового волнения в бухте Ласпи (Крымский полуостров) с использованием численной гидродинамической модели *SWASH* с пространственным разрешением 5 м. В качестве граничных условий задаются данные реанализа волнения, полученные на основе спектральной модели *SWAN*. Анализируются поля значимых высот волн h_s и скоростей волновых течений в бухте при штормах различной режимной обеспеченности. Установлено, что при штормах, возможных 1 раз в год, 1 раз в 5, 10 и 25 лет максимальные значения h_s в бухте могут достигать 2.5–3.0, 4.0–4.5, 5.0–5.5 и 6.0–6.5 м соответственно. При этом при штормах, возможных 1 раз в 25 лет, усиление волновых скоростей до 1.5–3.0 м/с происходит вблизи берега на глубинах менее 10 м. Влияние на волны защитного мола, построенного в 1980-х гг., является локальным и проявляется в формировании теневой зоны с его подветренной стороны. Обсуждаются вопросы возможного влияния штормового волнения на сокращение донной растительности в бухте Ласпи. Анализ волновой нагрузки на дно бухты показал, что в период экстремальных штормов в ее акватории наиболее подверженными воздействию волн оказываются склоны в области глубин от 2 до 12 м, где значения плотности кинетической энергии увеличиваются до 500–2000 Дж/м^3. При этом в западной оконечности бухты плотность может достигать 3000–4500 Дж/м^3. В средней части бухты значения энергетической нагрузки невелики. Поэтому к исчезновению здесь донной растительности могло привести не штормовое воздействие, а увеличение мутности воды, вызванное антропогенными факторами. Полученные результаты имеют большое практическое значение для безопасности мореплавания, проектирования и эксплуатации объектов береговой инфраструктуры.

Ключевые слова: ветровое волнение, Черное море, Южный берег Крыма, бухта Ласпи, численное моделирование, *SWASH*

Благодарности: работа выполнена в рамках темы МГИ № FNNN-2021-0005 «Прибрежные исследования». Расчеты проводились на вычислительном кластере МГИ.

Для цитирования: *Белоконь А. Ю., Фомин В. В.* Характеристики штормового волнения в бухте Ласпи (Черное море) по результатам численного моделирования // Экологическая безопасность прибрежной и шельфовой зон моря. 2024. № 2. С. 60–75. EDN PMPNVZ.

Introduction

In the last decade, many areas of the Southern Coast of Crimea (SCC) have been actively working on design, reconstruction of existing ones and construction of new coastal protection structures for the development of recreational activities. Regime and climatic information on wind waves and wave currents with high spatial resolution is necessary to carry out these works. Laspi Bay is one of such areas of the SCC.

Laspi Bay is one of the warmest areas of the SCC [1]. This is an open bay located between Cape Aya and Cape Sarych with the length of its coastline of about 4 km. The Laspi Bay area is aesthetically significant and attractive for the development of recreational activities [2].

The shores of the bay are of the abrasion and abrasion-landslide types, for which gravitational processes are well developed. The coast is formed by a fairly wide, about 20 m, pebble beach. To the west and south, small beaches alternate with piles of blocks. Low cliffs are located near the shores of the bay [1]. The underwater slope is deep, its most part is pronounced block bench, which drops steeply to a considerable depth. The central part of the bay is a sloping plain with sand and silt deposits [3]. In the coastal zone from Cape Aya to Cape Sarych, stable alongshore anticyclonic currents with velocities of up to 0.6 m/s are formed for most of the year. The hydrological regime of Laspi Bay is determined by the influence of these currents, influx of deep waters into surface layers during surge phenomena and water exchange with the open sea [4].

In 1983, as field studies showed [5], Laspi Bay was in a natural or close to natural state, in which the ecological balance of the coastal zone was maintained. The bay was characterized by an abundance of unique habitats of bottom vegetation – Cystoseira, phyllophora, eelgrass.

In the late 1980s, a hydraulic structure was built in the eastern part of Laspi Bay, which partially blocked the coastal sediment flows at its top [6]. In 2009, the *Dream Bay* hotel complex was built in the southeastern part of the bay. The construction was accompanied by large-scale coastal protection works which led to a change in the configuration of the coast and the underwater coastal slope. However, the embankment and breakwater wall of the complex were partially destroyed after the first strong storms [7]. Anthropogenic impact has led to additional influx of terrigenous material and its sedimentation in the coastal area [2]. As is known [8], the construction of hydraulic structures can lead to disruption of the hydrodynamic regime and changes in areas of abrasion and accumulation. Thus, studies in the Peter the Great Gulf (Sea of Japan) showed [8] that the construction of hydraulic structures had led to a significant reduction in bottom vegetation in the coastal zone.

The construction of a protective breakwater in Laspi Bay and the destruction of its coastal slope as a result of active coastal development could cause a disruption of the hydrodynamic regime of the bay, which, in turn, led to the erosion of pebble bench and additional influx of terrigenous material formed due to construction [2]. During the study at the bay top in 1998, silt and sandy bottom sediments were discovered starting at a depth of 3 m [6]. The bay, which in the 1980s was a model of the natural ecosystem of the Black Sea, has lost this status. A bottom natural complex devoid of vegetation has been formed in its central part [9]. Over a period of more than 30 years, the bay has undergone significant structural changes in the vegetation species composition and changes in the configuration

of coastal boundaries [10]. In general, the stocks of macrophytobenthos in the bay decreased by 1.5 times, phyllophores – by 35 times and Zostera – by 4 times during this period [9].

The formation of the bottom natural topography of Laspi Bay could be influenced by both economic activity on the coast and natural factors. In terms of climate, the rise of the Black Sea level leads to an increase in depth near the coast and increases the influence of waves on it [11]. The average annual storm activity in the Black Sea increased by 10–15% for the period of 1991–2016 [12]. An extreme storm that occurred in November 2007 could also contribute to the partial destruction of the bay bottom vegetation. This assumption is supported by the fact that vegetation was completely destroyed at depths of up to 10 m during an extreme storm in the area of Karadag in 1992 [9]. Such consequences can be explained by the fact that strong bottom wave currents and intense turbulent mixing create movements in the upper layers of the bottom soil during storms and the plants rooted here are gradually washed out of it [8, 13].

Taking into account the above, this work aims at studying the wave regime of Laspi Bay and the degree of its influence on the phytocenosis of bottom vegetation. It should be noted that such studies have not been conducted to date.

The objectives of the work included obtaining and analyzing fields of wave heights and wave current velocities in Laspi Bay during storms of various regime conditions. The calculations were carried out taking into account the protective breakwater built in the late 1980s and without regard to it. The obtained wave characteristics can be used in developing recommendations for economic activities in the bay water area and assessing the influence of storm waves on the bottom vegetation phytocenosis.

Mathematical model and input data

Modeling of wave fields in the Laspi Bay waters was carried out with a two-dimensional version of the numerical wave model Simulating WAves till SHore (SWASH) [14]. The model makes it possible to carry out calculations of hydrodynamic fields in the coastal zone in a wide range of spatial and temporal scales, taking into account nonlinearity, refraction, diffraction and reflection of waves. The initial equations of the model are as follows:

$$\frac{\partial \zeta}{\partial t} + \frac{\partial hu}{\partial x} + \frac{\partial hv}{\partial x} = 0, \tag{1}$$

$$\frac{\partial u}{\partial t} + u\frac{\partial u}{\partial x} + v\frac{\partial u}{\partial y} + g\frac{\partial \zeta}{\partial x} + \frac{1}{h}\int_{-d}^{\zeta}\frac{\partial q}{\partial x}dz + c_f\frac{u\sqrt{u^2+v^2}}{h} = \frac{1}{h}\left(\frac{\partial h\tau_{xx}}{\partial x} + \frac{\partial h\tau_{xy}}{\partial y}\right), \tag{2}$$

$$\frac{\partial v}{\partial t} + u\frac{\partial v}{\partial x} + v\frac{\partial v}{\partial y} + g\frac{\partial \zeta}{\partial y} + \frac{1}{h}\int_{-d}^{\zeta}\frac{\partial q}{\partial y}dz + c_f\frac{v\sqrt{u^2+v^2}}{h} = \frac{1}{h}\left(\frac{\partial h\tau_{yx}}{\partial x} + \frac{\partial h\tau_{yy}}{\partial y}\right), \tag{3}$$

$$\tau_{xx} = 2\nu_t\frac{\partial u}{\partial x}, \quad \tau_{xy} = \tau_{yx} = \nu_t\left(\frac{\partial u}{\partial y} + \frac{\partial v}{\partial x}\right), \quad \tau_{yy} = 2\nu_t\frac{\partial v}{\partial y}.$$

Here, t is time; x, y are Cartesian coordinates; axis z is directed upwards; $\zeta(x, y, t)$ is deviation of free surface from undisturbed level; $h = d + \zeta$ is total depth equal to the sum of free surface deviation and depth d in the undisturbed state of liquid; u and v are x and y velocity components averaged by depth; $q(x, y, z, t)$ is non-hydrostatic pressure; g is gravity acceleration; $c_f = gm^2/h^{1/3}$ is bottom friction coefficient, m is Manning's roughness coefficient; τ_{xx}, τ_{xy}, τ_{yx}, τ_{yy} are turbulent stress tensor components; ν_t is horizontal turbulent viscosity coefficient.

A rectangular computational grid of the bay water depths with a resolution of 5 m obtained on the basis of digitizing navigation charts was used for the numerical solution of system of equations (1)–(3). The dimensions of the computational domain were 3500 × 2500 m. To optimize the numerical algorithm, a coordinate system was used with the x axis directed from northwest to southeast (Fig. 1).

At the seaside boundary of the computational domain (at $y = 0$), significant wave height h_s and average wave period $\bar{\tau}$, which could occur once every n years, were specified. These parameters were obtained based on wave reanalysis data for the period 1979–2021 using the spectral model SWAN [15, 16] (Table 1).

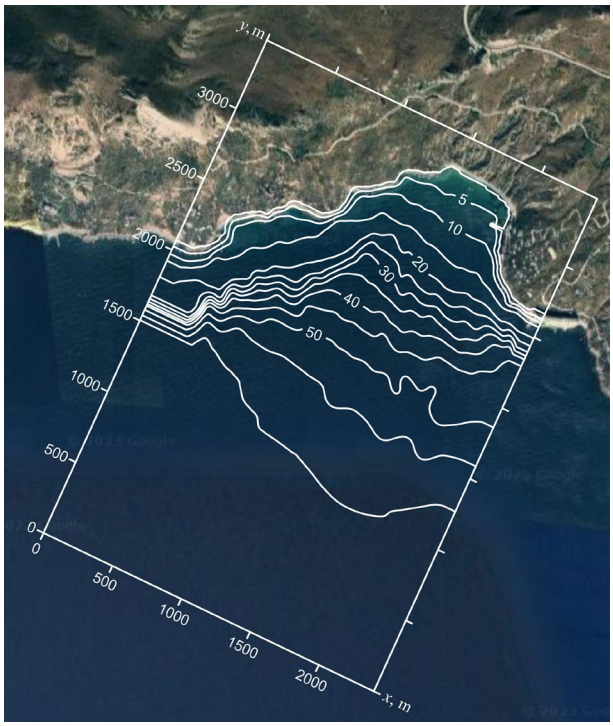

F i g . 1 . Bottom topography of the calculation area (available at: https://www.google.com/maps/@44.3927988,33.7329232,12998m/data=!3m1!1e3?entry=ttu

Table 1. Wave parameters

T, year	$\bar{h}$, m	h_s, m	$\bar{\tau}$, s
1	3.3	5.2	9.3
5	4.1	6.5	10.1
10	4.5	7.1	10.5
25	5.0	7.9	11.1

Note: Average wave height $\bar{h}$, significant wave height h_s and average wave period $\bar{\tau}$ in the seaside of Laspi Bay at a depth of 65 m, possible once a year, once every 5, 10 and 25 years according to retrospective calculations of waves in the Black Sea for the period 1979–2021 [15, 16].

At the liquid lateral boundaries of the computational domain (at x = 0 and x = 2500 m), the radiation condition was set. The horizontal turbulent viscosity coefficient was determined using the Smagorinsky formula with constant C = 0.2. Manning's roughness coefficient is m = 0.022 s/m$^{1/3}$. The integration time step was 0.05 s.

Results of modeling and discussion

As a result of numerical experiments, significant wave heights and wave current velocities in Laspi Bay during storms of various regime conditions were obtained. Calculations were carried out taking into account the protective breakwater and without regard to it. Wave fields were constructed based on numerical modeling data averaged over 100 periods of the incoming wave (~ 20 min). In each calculation node, the significant wave height was calculated using the following formula: $h_s = 4\sqrt{D}$, where D is free surface elevation variance ζ.

As a result of the analysis of spatial structure h_s it was found that during storms possible once a year, once every 5, 10 and 25 years, significant wave heights can reach 2.5–3.0, 4.0–4.5, 5.0–5.5 and 6.0–6.5 m, respectively (Figs. 2 and 3). When comparing the calculation results obtained taking into account the protective breakwater and without regard to it, it is clear that the structure has a local influence on wave dynamics. Near the breakwater, on its downwind side, a shadow zone of about 90 × 110 m is formed. Significant wave heights in this zone were 0.9 and 1.8 m during storms possible once a year and once every 25 years, respectively. During a storm possible once a year, the waves on the downwind side of the breakwater are 3.5–4 m high. In the case of a storm possible once in 25 years, the wave heights were 4–6 m, and in the wave shadow zone the wave heights decreased to 1.5–2.0 m.

The wave current patterns during storms of various regime conditions in Laspi Bay are considered. Figs. 4 and 5 show velocity and direction of wave currents in the bay during storms possible once a year and once every 25 years. It is evident that the zones of maximum wave velocities are located along the lateral boundaries of the bay. During a storm possible once a year, the values of wave velocities were 0.5–1.5 m/s at depths of less than 10 m. During storms possible once every 25 years, the velocities can increase to 1.5–3.0 m/s in these zones and the wave velocities do not exceed 1 m/s in the shadow zones. Thus, the construction of the protective breakwater in Laspi Bay led to a decrease in wave velocities in the eastern part of its top. The breakwater leads to a decrease in wave velocities in the shadow zone by 4–6 times.

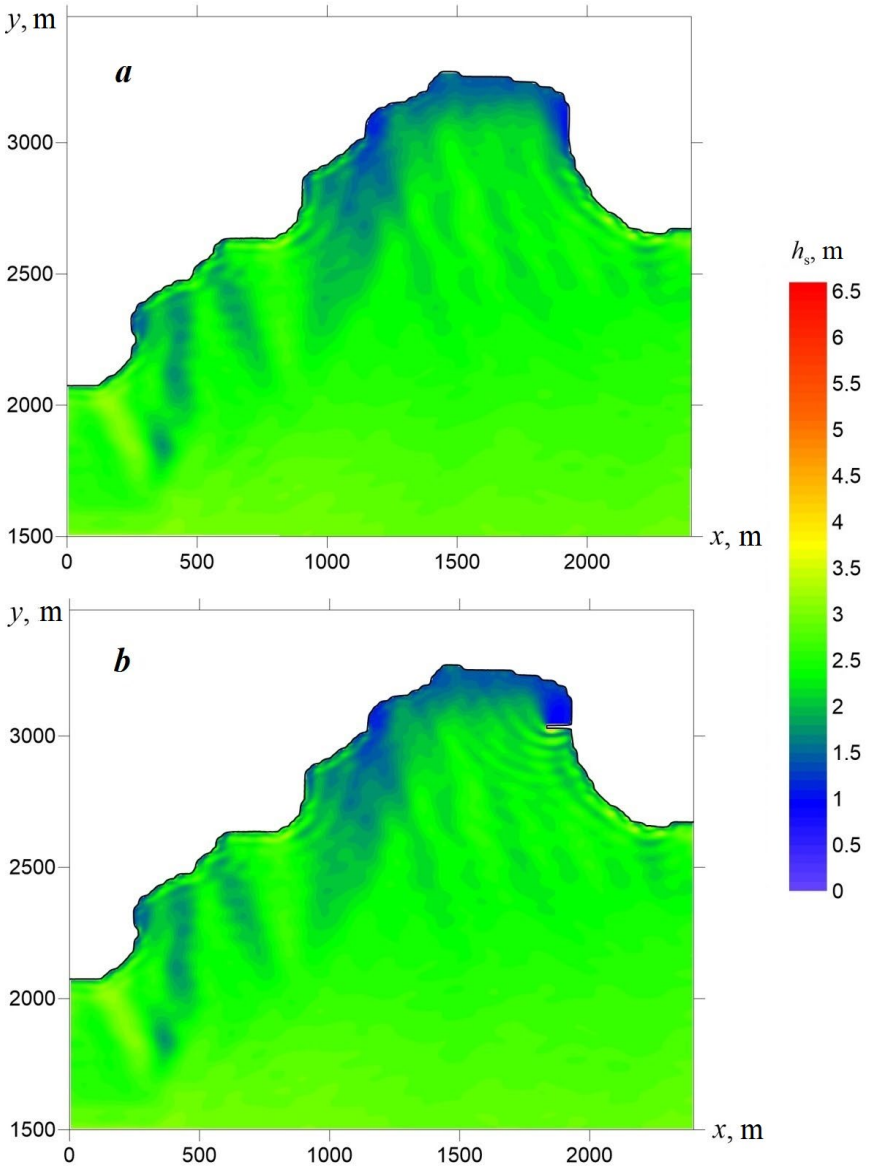

F i g . 2 . Significant wave heights in Laspi Bay for storms possible once a year: without taking into account the hydraulic structure (*a*); taking into account the hydraulic structure (*b*)

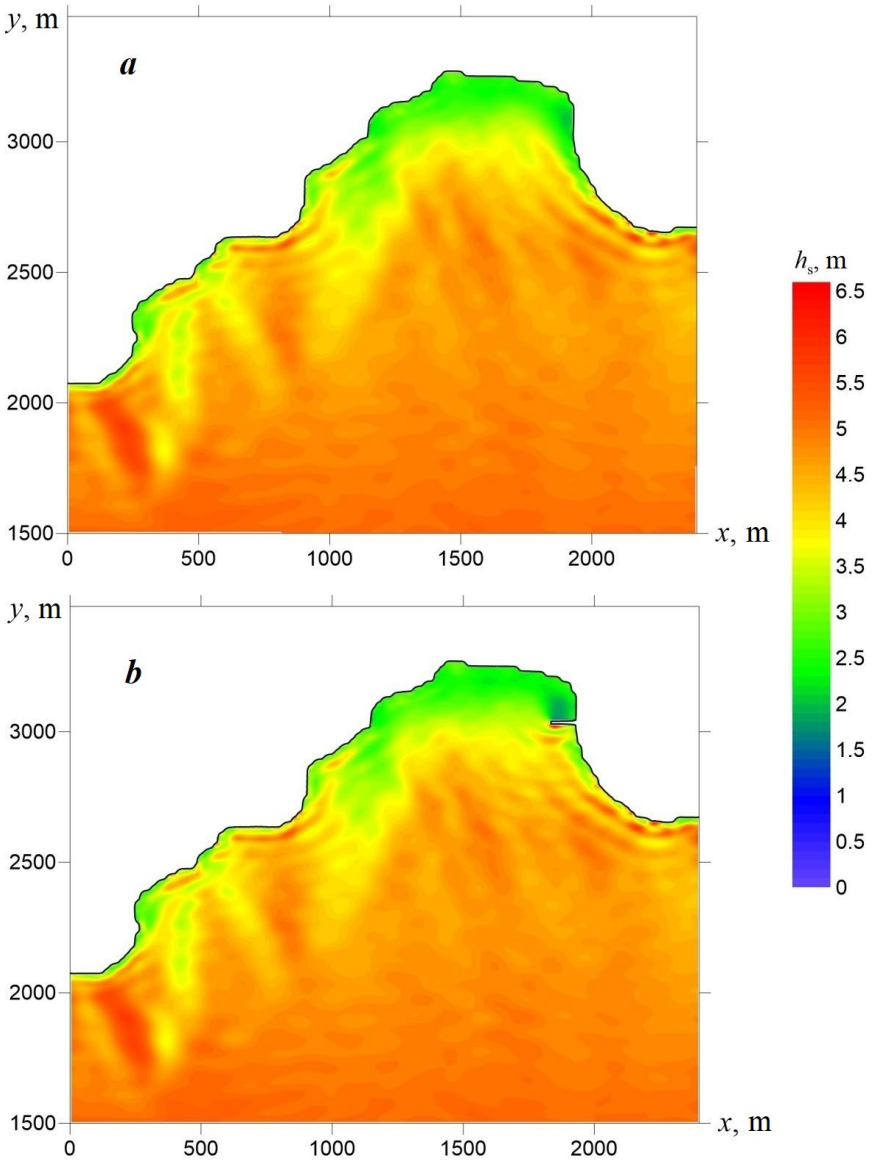

Fig. 3. Significant wave heights in Laspi Bay for storms possible once every 25 years: without taking into account the hydraulic structure (*a*); taking into account the hydraulic structure (*b*)

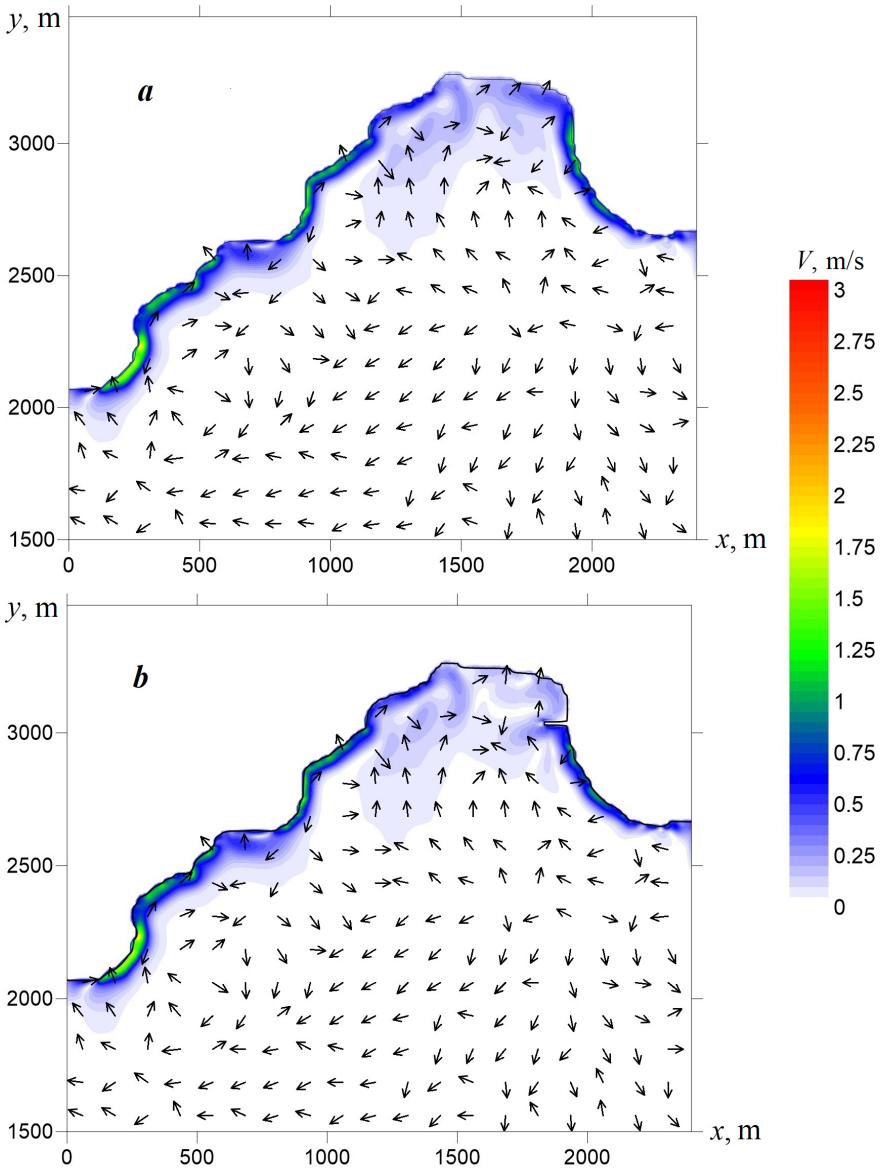

Fig. 4. Wave currents in Laspi Bay for storms possible once a year: without taking into account the hydraulic structures (*a*); taking into account the hydraulic structure (*b*)

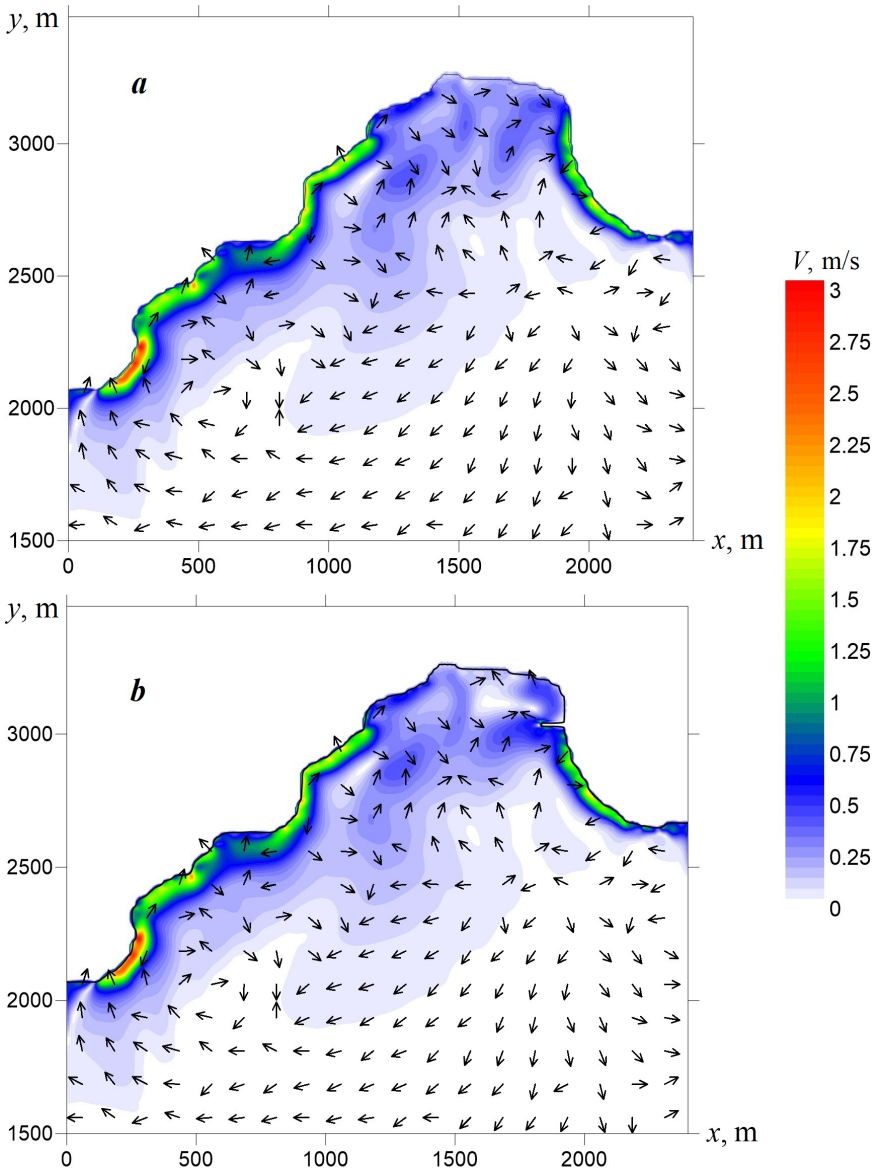

F i g . 5 . Wave currents in Laspi Bay for storms possible once every 25 years: without taking into account the hydraulic structures (*a*); taking into account the hydraulic structure (*b*)

An assessment of the wave load on the bottom of Laspi Bay was carried out. For this purpose, the density fields of kinetic energy of the waves E were calculated. Fig. 6 shows the distribution of kinetic energy density in the bay during a storm possible once in 25 years. As can be seen, the intensity of the influence of wind waves increases as the depth decreases. In areas with depths of 10–20 m throughout the entire Laspi Bay water area and in shallower areas at its top, where the depth increases relatively smoothly, the kinetic energy density does not exceed 300 J/m^3. The same density values are typical for the central part of the bay down to depths of 35 m. Steep slopes are located almost along the entire perimeter of the bay at depths of 2–7 m. Here, the kinetic energy density increases to 500–2000 J/m^3 and it can reach 3000–4500 J/m^3 in the western end of the bay.

Fig. 6 highlights in bold the sections where the study of the bottom topography of Laspi Bay was carried out [2]. The sections are located perpendicular to the shore and cover all types of landscape identified in the bay. Section I is located in the western part of the bay, section II connects the top and the middle of the bay, sections III and IV are located in the eastern part of the bay. Concerning these sections, kinetic energy density profiles were obtained for a storm possible once a year, once every 5, 10 and 25 years (Figs. 7–9). These figures also show the bottom topography for each section, and the types of landscapes studied in [2] are indicated by numbers.

Fig. 7 shows kinetic energy density distribution and bottom topography for section I. It is evident that the energy loads for the storms under consideration are insignificant near the shore itself, where the block bench is located (number *1* in Fig. 7) [2]. With increasing depth, they increase sharply and reach a maximum value at a distance of about 15 m from the shore at depths of 2–7 m. In this area, a steep underwater abrasive coastal slope is located where Cystoseira dominates (number *3* in Fig. 7) [2]. During storms possible once a year, the maximum wave load is ~ 500 J/m^3; once every 5 years – ~ 1000 J/m^3; once every 10 years – ~ 1300 J/m^3; once every 25 years – about 1700 J/m^3. Then, at a distance of 30 m or more from the shore, at depths of 7–12 m, a gradual decrease in the energy load by 2–3 times occurs. Here, the underwater coastal abrasion slope with a predominance of Cystoseira and Zostera marina species extends (number *4* in Fig. 7) [2]. At depths greater than 12 m, the energy load effect is insignificant.

The energy load for section II, which is located at the Laspi Bay top, is minimal along the entire profile (Fig. 8). This is due to the small slopes of the bottom, as a result of which the dissipation of wave energy occurs at a fairly large distance from the shore.

For sections III and IV (the eastern part of the bay) (Fig. 9), the energy load is insignificant near the shore, then it increases to its maximum at depths of 2–6 m, where also a fairly steep underwater slope with a predominance of Cystoseira is located (number *3* in Fig. 9). For section III, in case of storms possible once a year, the maximum energy load is about 500 J/m^3; during storms possible once every 5, 10, 25 years, it reaches 1100, 1300, 1600 J/m^3, respectively. For section IV,

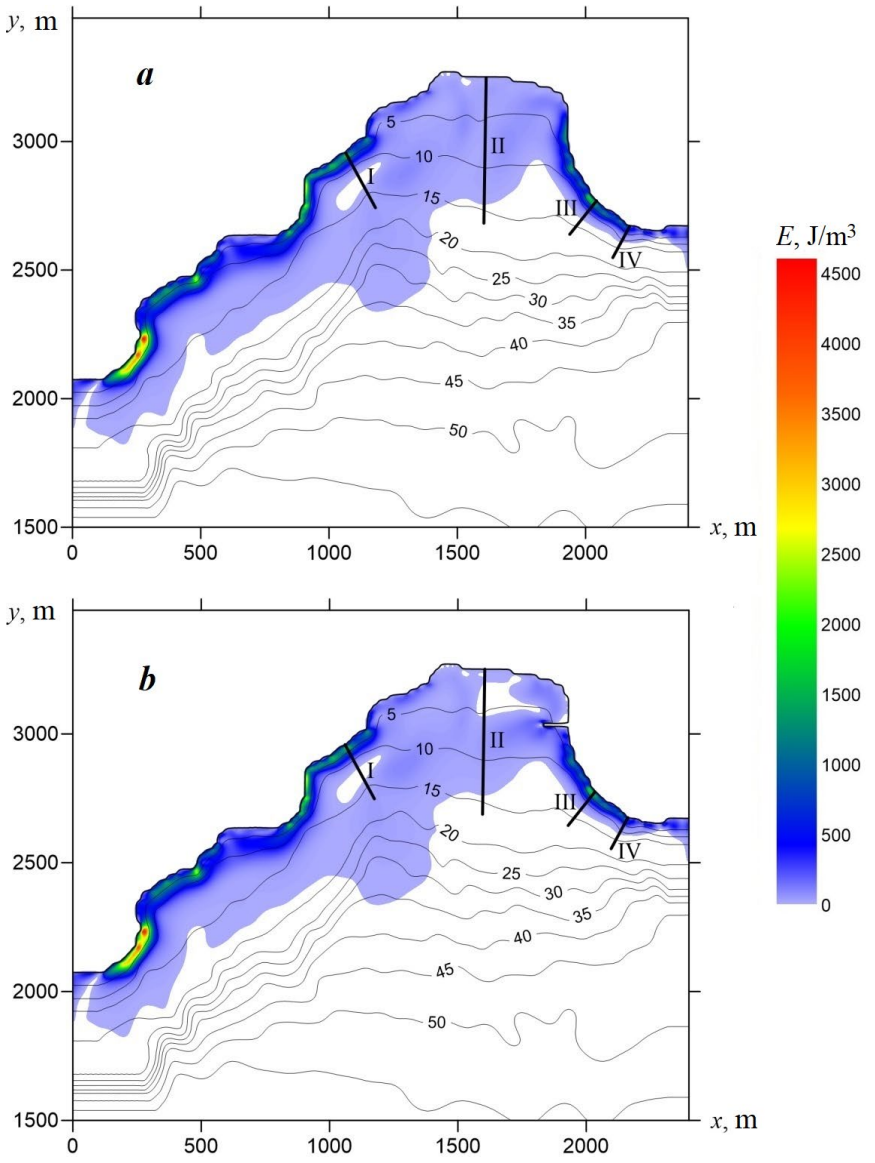

Fig. 6. Distribution of kinetic energy density in Laspi Bay for a storm possible once every 25 years: without taking into account the hydraulic structures (*a*); taking into account the hydraulic structure (*b*). Numbers I–IV indicate section numbers [2]

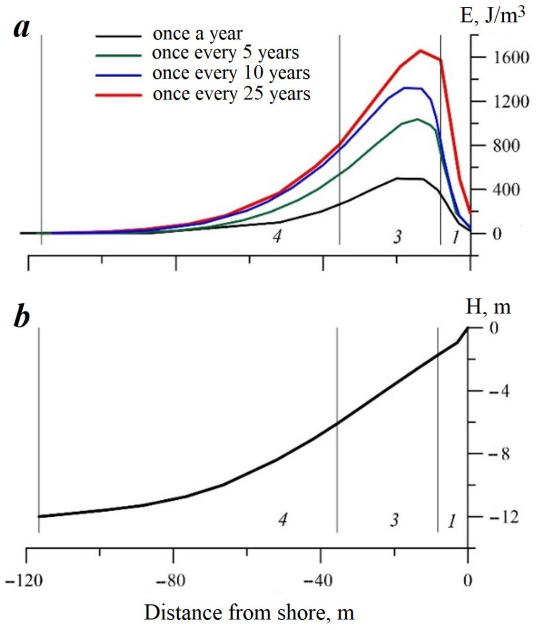

Fig. 7. Profiles of kinetic energy density (*a*) and bottom topography (*b*) for section I. The numbers indicate bottom natural complexes from [2]

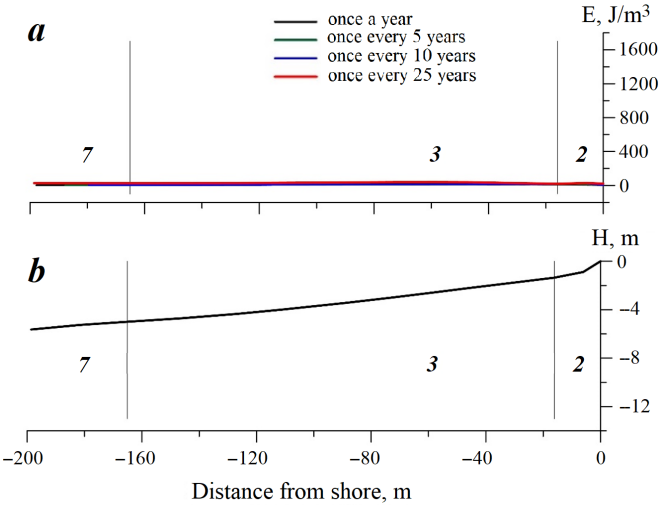

Fig. 8. Profiles of kinetic energy density (*a*) and bottom topography (*b*) for section II. The numbers indicate bottom natural complexes from [2]

the wave load decreases significantly, with 150 J/m^3 once a year and 500, 550, 700 J/m^3 once every 5, 10, 25 years, respectively.

Analysis of all obtained profiles of the kinetic energy density of waves (Figs. 7–9) shows that the wave load increases with distance from the shore reaching maximum values in the depth range of 2–7 m. Then, at depths of 7–12 m, a gradual decrease in wave load is observed. At depths greater than 10–12 m, wave load decreases sharply. The highest wave load values were obtained for sections I and III where they amounted to about 1600–1700 J/m^3, and slightly lower values were found in section IV (about 700 J/m^3). The minimum wave load values were obtained for section II where they did not exceed 50 J/m^3.

It can be concluded that during periods of extreme storms in the waters of Laspi Bay, the strongest wave effect occurs at depths of up to 10–12 m near coastal slopes with fairly steep bottom slopes. The middle part of the bay, devoid of bottom vegetation, is shallow, but is not subject to intense wave effect. It appears that the reason for the disappearance of bottom natural complexes in this area can be an increase in water turbidity caused by an increase in the influx of finely dispersed fractions due to anthropogenic impact on the shores of the bay.

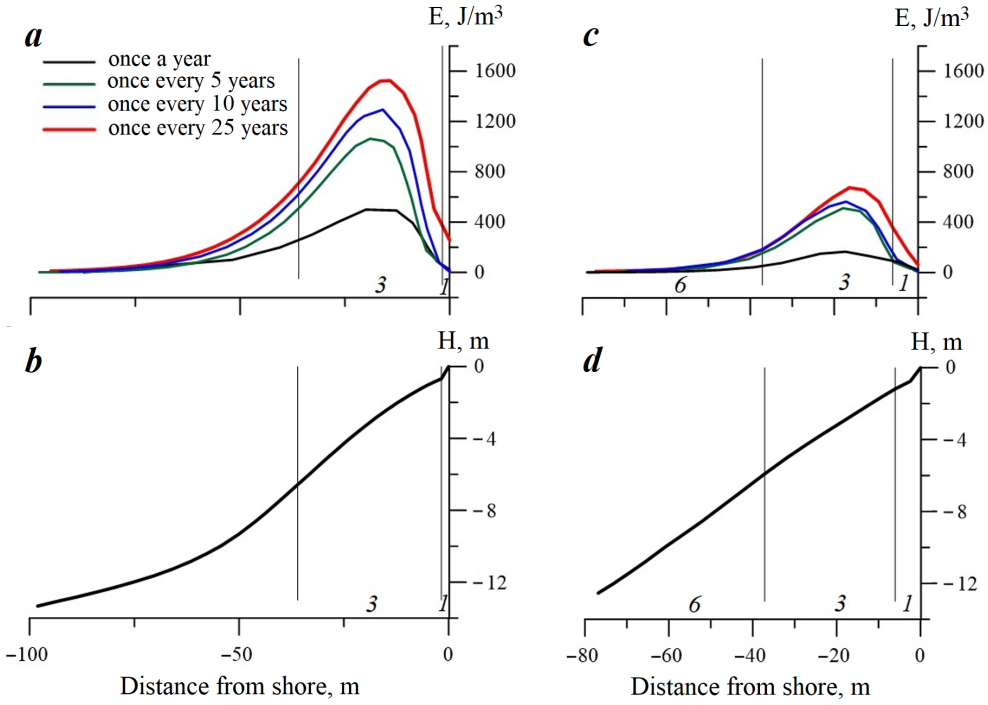

Fig. 9. Profiles of kinetic energy density (*a*) and bottom topography (*b*) for section III; profiles of kinetic energy density (*c*) and bottom topography (*d*) for section IV. The numbers indicate bottom natural complexes from [2]

Conclusion

Calculations of wave fields for the Laspi Bay water area were performed with the numerical model SWASH. Data obtained from wave reanalysis were specified at the boundary of the computational domain. As a result of numerical experiments, significant wave heights and wave current velocities were obtained for storms that are possible once a year, once every 5, 10, 25 years in Laspi Bay. The calculations were carried out taking into account the protective breakwater built in the late 1980s and without regard to it.

During storms possible once a year, once every 5, 10 and 25 years, significant wave heights in the bay can reach 2.5–3.0, 4.0–4.5, 5.0–5.5 and 6.0–6.5 m, respectively. The zones of maximum wave velocities are located along the lateral boundaries of the bay. During storms possible once every 25 years, the increase in velocities to 1.5–3.0 m/s occurs along the coast at depths less than 10 m. Maximum wave loads on the bottom occur at depths of 2–7 m.

An assessment of the wave load on the Laspi Bay bottom showed that during storms of various regime conditions, the coastal slopes in the depth range from 2 to 12 m, where the kinetic energy density values increased to 500–2000 J/м^3, were most susceptible to wave effect. At this, the density can reach 3000–4500 J/m^3 in the western end of the bay. In the middle part of the bay, the energy load values are small. Therefore, the disappearance of bottom vegetation here could be not due to storm impact, but an increase in water turbidity caused by anthropogenic factors.

References

1. Goryachkin, Yu.N. and Dolotov, V.V., 2019. *Sea Coasts of Crimea*. Sevastopol: COLORIT, 256 p. (in Russian).
2. Pankeeva, T.V., Mironova, N.V. and Parkhomenko, A.V., 2019. Bottom Natural Complexs of Laspi Bay (Black Sea, Sevastopol). *Geopolitics and Ecogeodynamics of Regions*, 5(4), pp. 319–332 (in Russian).
3. Pankeeva, T.V. and Mironova, N.V., 2018. Organization and Optimization of the Territorial Structure of the Nature Reserve (Zakaznik) "Laspi" (Sevastopol). *Biota and Environment of Natural Areas*, (4), pp. 124–139 (in Russian).
4. Atsikhovskaya, Zh.M. and Chekmenyova, N.I., 2002. Water Dynamic Activity Estimation in the Laspi Bay Area (the Black Sea). *Ecology of the Sea = Ekologiya Morya*, 59, pp. 5–8 (in Russian).
5. Kalugina-Gutnik, A.A., 1989. Variations in the Species Composition of Phytobenthos in the Laspi Bay over 1964-1983. *Ecology of the Sea = Ekologiya Morya*, 31, pp. 7–12 (in Russian).
6. Pankeeva, T.V. and Mironova, N.V., 2019. Spatiotemporal Changes in the Macrophytobenthos of Laspi Bay (Crimea, Black Sea). *Oceanology*, 59(1), pp. 86–98. https://doi.org/10.1134/S0001437019010168
7. Goryachkin, Yu.N., 2016. Coast Protections of Crimea: South Coast. *Hydrotechnika,* 3(44), pp. 34–39 (in Russian).
8. Preobrazhensky, B.V., Zharikov, V.V. and Dubeikovsky, L.V., 2000. *Basics of Underwater Landscape Studies (Management of Marine Ecosystems)*. Vladivostok: Dalnauka, 352 p. (in Russian).

9. Mironova, N.V. and Pankeeva, T.V., 2018. Long Time Changes of Spatial Distribution of Phytomasses Stock of Seaweeds in the Laspi Bay (the Black Sea). *Ekosistemy*, 16, pp. 33–46 (in Russian).
10. Pankeeva, T.V., Mironova, N.V. and Novikov, B.A., 2020. Experience in Mapping Bottom Vegetation (for Example of Laspi Bay, Black Sea). *Geopolitics and Ecogeodynamics of Regions*, 6(4), pp. 154–169. https://doi.org/10.37279/2309-7663-2020-6-4-154-169
11. Goryachkin, Yu.N. and Ivanov, V.A., 2006. [*Black Sea Level: Past, Present and Future*]. Sevastopol: MHI NAS of Ukraine, 210 p. (in Russian). EDN XXXSRN.
12. Divinsky, B.V. and Kos'yan, R.D., 2016. The Black Sea and Sea of Azov Wave Regime: Results of Numerical Simulation. *Ecological Safety of Coastal and Shelf Zones of Sea*, (1), pp. 14–21 (in Russian).
13. Denny, M., 1995. Predicting Physical Disturbance: Mechanistic Approaches to the Study of Survivorship on Wave-Swept Shores. *Ecological Monographs*, 65(4), pp. 371–418. https://doi.org/10.2307/2963496
14. Zijlema, M., Stelling, G. and Smit P., 2011. SWASH: An Operational Public Domain Code for Simulating Wave Fields and Rapidly Varied Flows in Coastal Waters. *Coastal Engineering*, 58(10), pp. 992–1012. https://doi.org/10.1016/j.coastaleng.2011.05.015
15. Divinskii, B., Fomin, V., Kosyan, R. and Lazorenko, D., 2019. Maximum Waves in the Black Sea. In: E. Özhan, ed., 2019. *Proceedings of the Fourteenth International MEDCOAST Congress on Coastal and Marine Sciences, Engineering, Management and Conservation. MEDCOAST 2019, 22-26 October 2019, Marmaris, Turkey.* Ortica, Mŭgla, Turkey: Mediterranean Coastal Foundation. Vol. 2, pp. 799–810.
16. Divinsky, B.V., Fomin, V.V., Kosyan, R.D. and Ratner, Y.D., 2020. Extreme Wind Waves in the Black Sea. *Oceanologia*, 62(1), pp. 23–30. https://doi.org/10.1016/j.oceano.2019.06.003

Submitted 12.01.2024; accepted after review 30.01.2024;
revised 27.03.2024; published 25.06.2024

About the authors:

Aleksandra Yu. Belokon, Research Associate, Department of Computational Technologies and Computational Modeling, Marine Hydrophysical Institute of RAS (2 Kapitanskaya St., Sevastopol, 299011, Russian Federation), Ph.D. (Phys.-Math.), **ORCID ID: 0000-0002-1299-0983, ResearcherID: M-6839-2018**, *aleksa.44.33@gmail.com*

Vladimir V. Fomin, Chief Research Associate, Head of Department of Computational Technologies and Computational Modeling, Marine Hydrophysical Institute of RAS (2 Kapitanskaya St., Sevastopol, 299011, Russian Federation), Dr.Sci. (Phys.-Math.), **ORCID: 0000-0002-9070-4460, ResearcherID: H-8185-2015**, *v.fomin@mhi-ras.ru*

Contribution of the authors:

Aleksandra Yu. Belokon – review of the literature on the research problem, processing and description of the research results, writing the text of the article

Vladimir V. Fomin – performing numerical experiments, analyzing modeling results, writing the text of the article

All the authors have read and approved the final manuscript.

ISSN 2413-5577, Ecological Safety of Coastal and Shelf Zones of Sea, 2024, No.2, pp. 76–90.

Original article

Analysis of Hydrological and Hydrochemical Factors of Bottom Phytocenosis Transformation near Cape Kosa Severnaya (Black Sea, Sevastopol)

A. V. Parkhomenko *, E. F. Vasechkina, A. A. Latushkin

Marine Hydrophysical Institute of RAS, Sevastopol, Russia
** e-mail: avparkhomenko52@gmail.com*

Abstract

Macrophytes act as important bioindicators of environmental conditions and long-term changes in water quality allowing their use in studying the dynamics of bottom natural complexes. The purpose of the work is to identify the main hydrophysical and hydrochemical factors leading to changes in the biomass of bottom phytocenoses near Cape Kosa Severnaya. The paper analyzes and summarizes literary sources and results of landscape and hydrobotanical studies (summer 1964, 1997, 2006 and 2017) carried out in the coastal zone between Cape Kosa Severnaya and Cape Tolsty. We used data on water temperature, concentrations of nitrates, nitrites, ammonium, phosphates and total suspended matter in water from 1998 to 2021. We also used simulation results of macrophytobenthos biomass dynamics in the area from 1998 to 2002. Several bottom natural complexes were distinguished in the landscape structure of this area at different periods. Their composition and quantity changed over time. In the *Ericaria-Gongolaria* phytocenosis (0.5–5 m), by 2006 there was an increase in the biomass of the dominant species characterized by an increase in the proportion of epiphytes. In 2017, there was a restoration of the dominant species, and the total biomass almost tripled. The *Ericaria-Gongolaria-Phyllophora* phytocenosis (5–10 m) had completely disappeared by 2006, and *Dictyota* spp. took its place in 2017. The *Phyllophora* phytocenosis (depths over 10 m) significantly degraded in 1997, and its biomass decreased almost to zero. In 2006, *Phyllophora crispa* was not recorded at these depths, but by 2017, there appeared separate areas of the bottom where *Phyllophora crispa* was present, with biomass an order of magnitude lower compared to that in 1964. It was concluded that the recorded transformations of benthic communities were caused mainly by changes in water transparency associated with the content of total suspended matter. To monitor the situation, it is advisable to regularly conduct hydrobotanical surveys at intervals of several years.

Keywords: macrophytobenthos, bottom phytocenosis, Black Sea, simulation model, bottom natural complex, eutrophication, water transparency

Acknowledgments: This work was carried out under state assignment of Marine Hydrophysical Institute of RAS no. FNNN-2024-0016 “Studies of spatial and temporal variability of oceanological processes in the coastal, near-shore and shelf zones of the Black Sea influenced by natural and anthropogenic factors on the basis of in situ measurements and numerical modelling” and FNNN-2024-0012 “Analysis, diagnosis and real-time forecast of the state of hydrophysical and hydrochemical fields of marine water areas based on mathematical modelling using data from remote and in situ methods of measurements”.

For citation: Parkhomenko, A.V., Vasechkina, E.F. and Latushkin, A.A., 2024. Analysis of Hydrological and Hydrochemical Factors of Bottom Phytocenosis Transformation near Cape Kosa Severnaya (Black Sea, Sevastopol). *Ecological Safety of Coastal and Shelf Zones of Sea*, (2), pp. 76–90.

Анализ гидролого-гидрохимических факторов трансформации донных фитоценозов в районе мыса Коса Северная (Черное море, Севастополь)

А. В. Пархоменко *, Е. Ф. Васечкина, А. А. Латушкин

Морской гидрофизический институт РАН, Севастополь, Россия
** e-mail: avparkhomenko52@gmail.com*

Аннотация
Макрофиты выступают в качестве важных биоиндикаторов условий окружающей среды и долгосрочных изменений качества воды, что позволяет использовать макрофитов при изучении динамики донных природных комплексов. Цель работы – выявление основных гидрофизических и гидрохимических факторов, приводящих к изменениям биомассы донных фитоценозов в районе м. Коса Северная. Проанализированы и обобщены литературные источники, результаты ландшафтных и гидроботанических исследований (летний период 1964, 1997, 2006 и 2017 гг.) в прибрежной зоне м. Коса Северная – м. Толстый с использованием данных о температуре воды, содержании в воде нитратов, нитритов, аммония, фосфатов и общего взвешенного вещества в 1998–2021 гг., а также результаты имитационного моделирования динамики биомассы макрофитобентоса в этом районе в 1998–2002 гг. В ландшафтной структуре прибрежной зоны района исследования в разные периоды времени выделялись несколько донных природных комплексов, причем с течением времени их состав и количество менялись. В эрикариево-гонголариевом фитоценозе (0.5–5 м) к 2006 г. произошло увеличение биомассы доминирующих видов, характеризующееся ростом доли эпифитов. В 2017 г. наблюдалось восстановление доминирующих видов, а общая биомасса возросла почти в три раза. Эрикариево-гонголариево-филлофоровый фитоценоз (5–10 м) полностью исчез к 2006 г., а на его месте в 2017 г. была зафиксирована *Dictyota* spp. Филлофоровый фитоценоз (глубины свыше 10 м) существенно деградировал в 1997 г., его биомасса сократилась почти до нуля. В 2006 г. *Phyllophora crispa* на этих глубинах не регистрировалась, но к 2017 г. появились отдельные участки дна, где представлена *Phyllophora crispa* с биомассой, меньшей на порядок по сравнению с 1964 г. Сделан вывод, что зафиксированные трансформации донных сообществ были вызваны в основном изменениями прозрачности воды, связанными с содержанием общего взвешенного вещества. Для слежения за развитием ситуации целесообразно регулярно с частотой раз в несколько лет проводить гидроботанические съемки.

Ключевые слова: макрофитобентос, донный фитоценоз, Черное море, имитационная модель, донные природные комплексы, эвтрофикация, прозрачность воды

Благодарности: исследование выполнено в рамках государственного задания ФГБУН ФИЦ МГИ № FNNN-2024-0016 «Исследование пространственно-временной изменчивости океанологических процессов в береговой, прибрежной и шельфовой зонах Черного моря под воздействием природных и антропогенных факторов

на основе контактных измерений и математического моделирования» и FNNN-2024-0012 «Анализ, диагноз и оперативный прогноз состояния гидрофизических и гидрохимических полей морских акваторий на основе математического моделирования с использованием данных дистанционных и контактных методов измерений».

Для цитирования: *Пархоменко А. В., Васечкина Е. Ф., Латушкин А. А*. Анализ гидролого-гидрохимических факторов трансформации донных фитоценозов в районе мыса Коса Северная (Черное море, Севастополь) // Экологическая безопасность прибрежной и шельфовой зон моря. 2024. № 2. С. 76–90. EDN CMHLRP.

Introduction

Upper underwater shorefaces and shallow marine areas occupy a very small part of the ocean, but it is here that production processes are most active, with a great diversity of species and ecosystems, habitats of hydrobionts and bottom natural complexes [1].

The bottom natural complex (BNC) is a multicomponent developing system. Even minor changes in one of the components of this system can lead to unpredictable transformations of the environment. In this regard, studies of the landscape and morphological structure of the coastal zone have been and are currently carried out actively in the Black Sea [1)] [2–6]. Thus, physical and geographical zoning was carried out [7–9] and characteristics of deep-sea landscapes of the continental slope were given [10]. In addition, approaches to determining the resistance of the Black Sea bottom landscapes to natural and anthropogenic factors were considered [3, 11], the concept of “marine anthropogenic landscape” was introduced and its typification according to the prevailing types of economic activity was proposed [12]. Material fluxes in the coastal zone of the Crimean Peninsula are actively studied highlighting exogenous and endogenous processes that influence the transformation of BNC components [6, 13].

An analysis of BNC studies conducted in the Black Sea led to the conclusion that a negative transformation of the BNC occurs along the entire Black Sea coast.

In this work, we will focus on the identification of possible causes of bottom phytocenosis negative transformations as the main components of the BNC. Macrophytobenthos is considered to be one of the most important and at the same time vulnerable components of the BNC and plays a leading role in the stabilization of coastal ecosystems ensuring the implementation of a number of ecosystem functions and services. The function of macrophytes in an ecosystem is related to their structural characteristics, such as species composition, distribution, abundance and diversity. In their turn, these characteristics depend on various environmental factors: illumination, water temperature, substrate composition, competitive interactions, water level fluctuations, seawater quality and the concentration of nutrients in water and bottom sediments.

[1)] Petrov, K.M., 1969. [Methods of Landscape Research of the Marine Coastal Zone]. In: B. P. Manteyfel, ed., 1969. [*Marine Underwater Research*]. Moscow: Nauka, pp. 136–148 (in Russian).

Macrophytes act as important bioindicators of environmental conditions and long-term changes in water quality, which makes it possible to use them when studying the BNC dynamics [14].

The positive effects of macroalgae and sea grasses on the ecosystem have been well studied. In spring, the growth of established species begins, which leads to a maximum biomass of macrophytobenthos in summer. The primary production of macrophytobenthos is limited mainly by water transparency, epiphyte biomass and nutrient availability, which can act as indicators of increasing anthropogenic load on coastal areas [14–17].

Over the past few decades, a decrease in macrophyte biomass has accelerated due to anthropogenic load on the coast. The main factors resulting in this decrease in biomass are a decrease in illumination caused by an increase in the content of total suspended matter (TSM) and dissolved organic matter in water, as well as pollution by nutrients, mainly nitrates and phosphates. An excess of nutrients causes undesirable changes in the hydrochemical and hydrobiological regimes of water bodies and is the main reason for increasing the level of eutrophication [17]. Under eutrophication conditions, the availability of light in the water column decreases due to an increase in phytoplankton biomass, which leads to macrophytobenthos degradation [14].

Complex interactions among such factors as light availability, nutrient concentrations, storm exposure, macrophyte release and sediment transport can be studied with mathematical modeling. Given the significant role that macrophytes play in marine ecosystems, understanding and quantification of the environmental factors that influence the structure of benthic macrophyte communities are necessary to develop sustainable management practices for these ecosystems.

The purpose of the work is to identify the main hydrophysical and hydrochemical factors leading to changes in the biomass of bottom phytocenosis near Cape Kosa Severnaya.

Materials and methods of study

Changes in macrophytobenthos in 1964–2017

The paper analyzes and summarizes materials from literary sources, landscape and hydrobotanical studies (summer 1964, 1997, 2006 and 2017) carried out in the coastal zone between Cape Kosa Severnaya and Cape Tolsty [18, 19]. Fig. 1 shows the schematic map of the profiles along which observations were made.

Statistical data processing was performed in MS Excel. In the landscape structure of the coastal zone Cape Kosa Severnaya – Cape Tolsty, several BNCs were identified at different periods of time. Moreover, their composition and quantity changed over time. Thus, four BNCs were observed in 1964, only three in 1997. Then, the number of BNCs under study decreased to two in 2006 and increased again to four in 2017. The dominant macrophyte species were *Ericaria crinite* (Duby)

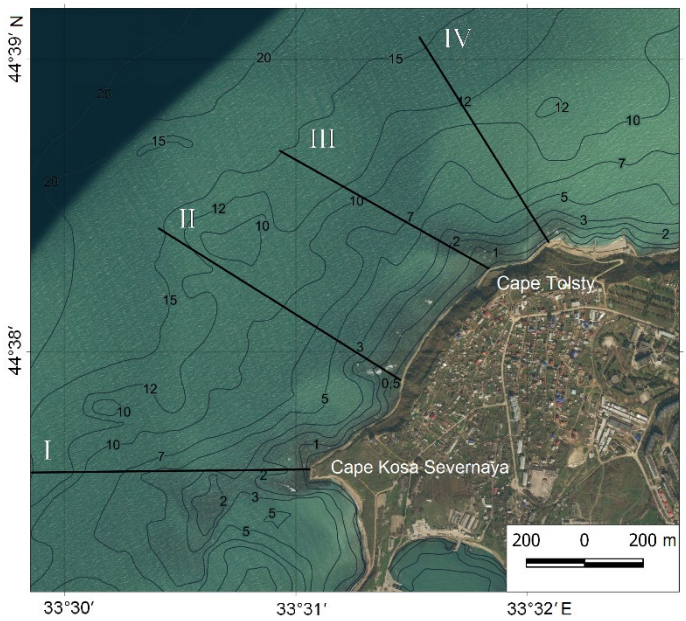

Fig. 1. Schematic map of the location of landscape and hydrobotanical profiles in the coastal zone Cape Kosa Severnaya – Cape Tolsty (Roman numerals stand for profiles). The image is adapted from Bing (available at: https://www.bing.com/map)

Molinari & Guiry = *Cystoseira crinita*, *Gongolaria barbata* (Stackhouse) Kuntze = *Cystoseira barbata* and *Phyllophora crispa* (Huds.) P.S. Dixon.

Qualitative and quantitative changes that occurred in the coastal zone BNCs are described in detail in [19]. In our work, we focus on changes in the relative contributions of dominant species, associated species and epiphytes, as such changes accompanied the restructuring of the BNCs during the period under review.

Hydrochemical and hydrophysical indicators of the aquatic environment state (concentration of nutrients, TSM, water temperature, current velocity) affect the growth rate of macrophytes significantly. To identify the connection between the BNC dynamics and changes in the chemical and biological state of the coastal zone near Cape Kosa Severnaya, all available hydrophysical and hydrochemical observation data for 1998–2021 were analyzed. For the purposes of this study, data on water temperature and content of nitrates, nitrites, ammonium, phosphates and TSM in water were used. Based on the available data, the average monthly values of the listed characteristics were calculated. Depth averaging was also carried out; two layers of 0–10 m (upper layer) and 10–20 m (lower layer) were identified.

Determination of illumination at the depth of macrophyte growth

According to existing notions, the most important characteristic for the growth of macroalgae is water transparency, which determines the amount of light energy available for photosynthesis at the depth of algae growth. Standard measurements at coastal stations provide information on TSM content, which can be used to estimate illumination level at depth. *In situ* synchronous measurements of vertical profiles of the 660 nm beam attenuation coefficient (BAC 660) and photosynthetically active radiation (PAR) were carried out at drift stations off Sevastopol Bay using *Kondor* probing hydrophysical complex. The concentration of TSM in water was determined based on the data on BAC 660 using empirical relationship $C_{TSM} = 0.78 \cdot \text{BAC } 660$.

The decrease in the PAR intensity with depth is most realistic when described by exponential function

$$I_z = I_0 \exp(\beta z), \qquad (1)$$

where I_0 is sea surface illumination; β is coefficient of light absorption in water depending on the TSM content in water; z is depth. To estimate β as function C_{TSM}, we found the relationship between coefficients β obtained as a result of applying approximation (1) to PAR *in situ* profiles and the average TSM content in the upper mixed layer (Fig. 2, *a*). The thickness of this layer was determined using the temperature profile data. The least squares method yielded two formulas that can be used to determine the light absorption coefficient β knowing the average TSM content in the upper mixed layer of water (C_{TSM}):

$$\beta = \begin{cases} -1.1818 C_{TSM}^3 + 1.6298 C_{TSM}^2 - 0.7207 C_{TSM} - 0.0264, & C_{TSM} < 1 \text{ mg/L}, \\ -0.6649 \ln C_{TSM} - 0.309, & C_{TSM} > 1 \text{ mg/L}, \end{cases} \qquad (2)$$

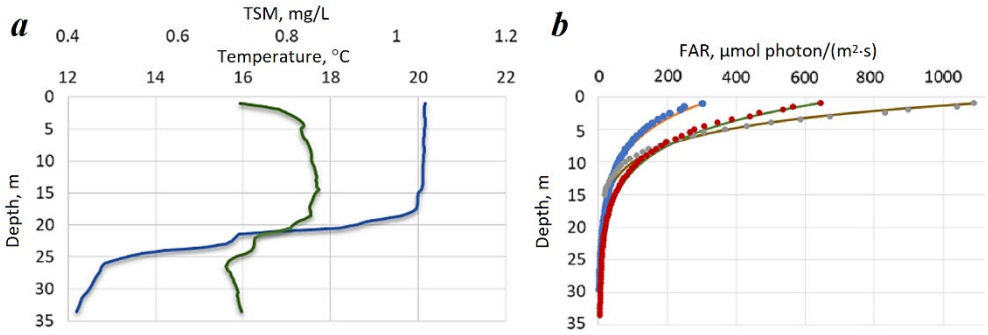

F i g . 2 . Example of vertical profiles of water temperature and total suspended matter content at one of the stations (*a*); vertical profiles of PAR (dots) and their approximations (colour lines) using models (1) and (2) at three profiles (*b*)

Using these approximations and knowing the intensity of solar radiation at the water surface, it is possible to determine the amount of light reaching the depth of algae growth for given water turbidity in the upper layer. Fig. 2, *b* shows the quality of resulting model (2). Here, the dots represent the *in situ* data on the vertical profiles of PAR at the control stations and lines represent model approximations using expressions (1) and (2). Relative root-mean-square error of the models lies in the range from 7 to 15% of the average illumination in the 0–25 m layer.

It should be noted that model (2) is regional and cannot claim to be universal. Obviously, to obtain more generalized dependencies, it is necessary to have more data from different water areas. However, to analyze the variability of bottom phytocenosis near Cape Kosa Severnaya, we consider the found dependencies to be sufficiently representative.

Using this model, we can also estimate the potential lower limit of the distribution of a particular alga depending on the average coefficient of light attenuation in water. We will define this limit at a depth where the light intensity is such that the alga photosynthesis rate is equal to its dark respiration:

$$(P_{\max} + R_d) \cdot \mathrm{th}\left(\frac{\alpha I_0 \exp(\beta z)}{P_{\max} + R_d} \right) = R_d,$$

where $P_{\max}$ is maximum photosynthesis rate; R_d is dark respiration; α is slope of the photosynthetic curve in the low light area. From this we get

$$z = \frac{1}{\beta} \ln\left(\alpha \cdot \mathrm{th}\left(\frac{R_d}{P_{\max} + R_d} \right) (P_{\max} + R_d) \Big/ \alpha I_0 \right). \qquad (3)$$

By setting C_{TSM} = 1 mg/L, we obtain an estimate of the maximum growth depth of bottom phytocenosis of 10–14 m; the lower limit will move to 25–35 m with a decrease in C_{TSM} to 0.5 mg/L. This estimate is a function of the photosynthetic parameters of the alga, water turbidity and intensity of light at the water surface. This is the potential maximum depth distribution of algae in the sea, but for a more accurate assessment it is necessary to take into account the sufficiency of the concentration of dissolved biogenic substances, as well as the release of organic substances by the alga both during its growth and during the process of thalli dying off or consumption of the alga by marine hydrobionts. It can be said that the observed biomass of algae at a given depth is the result of a balance between its formation during photosynthesis, assimilation of inorganic substances and elimination during excretion, decay or consumption. Therefore, the actual lower boundary of growth of a particular alga will be at a shallower depth than that calculated by formula (3).

Simulation model of the dynamics of bottom phytocenosis

The work uses a model previously tested during studies of the dynamics of macrophyte biomass in Kruglaya Bay and Donuzlav Bay [20, 21]. The proposed

model of dynamic energy balance makes it possible to estimate the growth rate of sea grasses, amount of absorbed biogenic elements, released oxygen, produced and released organic matter, concentration of nitrogen and phosphorus in plant tissues. The dynamics equations of the biomass of macroalgae and sea grasses are written in the form of balance relationship

$$dB/dt = (P_r - eG_r - m)B, \quad (4)$$

where B is biomass of all plant tissues: roots, root stocks and leaves, g DW /m^2 or g DW/m^3; t is time, h; P_r is specific rate of net primary production, 1/h; G_r is specific rate of gross primary production, 1/h; e is ratio of the released dissolved organic matter during the life of the alga to the gross production for the same time; m is coefficient of biomass loss due to mechanical damage, tissue death and consumption by marine animals, 1/h.

Results and discussion

Based on the data of hydrobotanical surveys published in [18, 19], the structure of bottom phytocenoses was studied and the dynamics of the relative distribution of dominant species (basifites), associated species and epiphytes was revealed (Fig. 3).

Structural changes in bottom phytocenosis

The *Ericaria-Gongolaria* phytocenosis on boulder benches up to 1 m deep with an area of 14.7 ha changed quantitatively only in the last observation period of 2006–2017: its biomass increased more than twofold. At the same time, the proportion of epiphytes decreased from 11 to 5%, although their mass increased by 1.3 times. The *Ericaria-Gongolaria* phytocenosis located on a shoreface up to 5 m deep underwent significant changes throughout the entire observation period. From 1964 to 1997, the biomass of the phytocenosis decreased and the proportion of associated species and epiphytes increased to 42%. These changes continued in 1997–2006 when the proportion of *Ericaria crinita* and *Gongolaria barbata* (basifites) in the phytocenosis decreased to 48%. Epiphytes made up 50% of the macrophyte biomass indicating the extreme distress of the ecosystem. After 2006, the situation improved, which led to an increase in the biomass of the entire phytocenosis and an increase in the mass of the dominant macrophytes *Ericaria crinita* and *Gongolaria barbata* to 98%.

The *Erikaria-Gongolaria-Phyllophora* phytocenosis at depths of up to 10 m also degraded throughout the entire observation period. If in 1964 the community included only basiphytes *Ericaria crinita*, *Gongolaria barbata* and *Phyllophora crispa*, then in 1997 a decrease in the total biomass of the phytocenosis was observed and a proportion of epiphytes became noticeable. By 2017, in place of *Ericaria crinita*, *Gongolaria barbata* and *Phyllophora crispa*, a new community had emerged in which the dominant role was played by *Dictyota* spp.

On a gently dipping plain with depths of 10–15 m, the *Phyllophora* phytocenosis that had existed in the middle of the last century with a fairly large biomass (870 g/m^2) with a small proportion of associated species and epiphytes (6 and 5%, respectively) almost disappeared. In 2017, only separate bottom areas were recorded

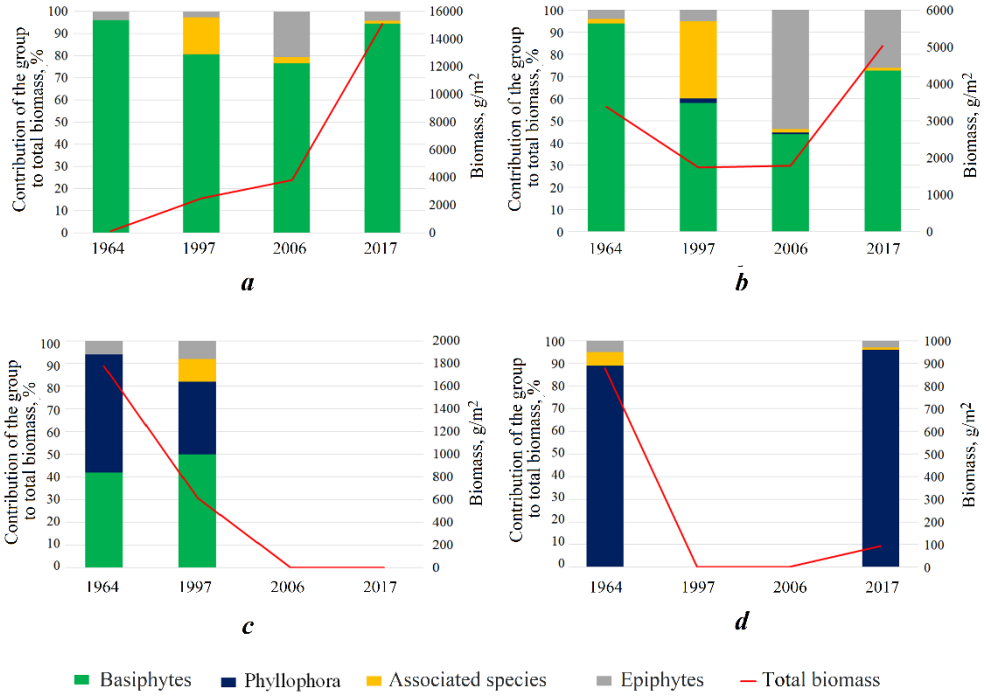

Fig. 3. Dynamics of the total biomass of bottom phytocenosis located near Cape Kosa Severnaya and its structure: *a* – boulder benches with a predominance of *Ericaria crinita* and *Gongolaria barbata* (0.5–1 m); *b* – upper shoreface dominated by *Ericaria crinita* and *Gongolaria barbata* (1–5 m); *c* – upper shoreface with alternating areas dominated by *Ericaria crinita, Gongolaria barbata* and *Phyllophora crispa* (5–10 m); *d* – gently dipping plain dominated by *Phyllophora crispa* (10–15 m). The total algal mass of the phytocenosis is shown for 1964–2017

where *Phyllophora crispa* was present with an average biomass of 90 g/m^2. However, the restoration of the *Phyllophora* phytocenosis indicates the onset of favorable conditions, the main one of which is increased water transparency.

Changes in hydrochemical state of waters

Let us now analyze the data available in the MHI database on the variability of water temperature, as well as measurements of hydrochemical parameters of the aquatic environment near Cape Kosa Severnaya: the content of dissolved inorganic compounds of nitrogen and phosphorus, as well as TSM, in water. Significant heterogeneity in the distribution of observation data over time prevents

us from calculating average annual values of hydrochemical indicators or constructing a reliable series of average monthly observations. To assess their dynamics, we will consider the variability of these indicators in the warm period of the year characterized by the maximum number of observations and the most intensive growth of macrophytes. Fig. 4 shows the TSM content in September during 1998–2021 (in several cases, data for August were used due to the lack of data for September). This month marks the peak of macroalgae biomass and the maximum number of measurements of water hydrochemical parameters in different years. As we can see, from 1998 to 2017, the water turbidity in the upper layer decreased noticeably, which can explain the significantly increased biomass of phytobenthos at depths of up to 5 m. A slight tendency towards decreasing turbidity was observed in the lower layer also, but it was not nearly as pronounced. By 2006, the *Ericaria-Gongolaria-Phyllophora* phytocenosis at depths over 5 m and the *Phyllophora* phytocenosis at depths of 10–15 m had completely disappeared. According to available data, the average TSM content during the vegetation period in 2006 varied within the range of 1.5–2 mg/L, which limited the thickness of the photic layer to 5–7 m according to equation (3).

The analysis of the temporal variability of the hydrochemical state of waters in the area under study showed no significant trends in the content of biogenic substances during the period under consideration. The concentration values of inorganic nitrogen and phosphorus compounds fluctuated within the limits typical for the Sevastopol coastal waters ($[NO_3]+[NO_2]$ from 0.03 to 3.54; $[NH_4]$ from 0.02 to 2.95; $[PO_4]$ from 0.001 to 0.9 μmol/L). As shown by numerical experiments with a phytocenosis model, the average value of phosphate concentration of 0.11 μmol/L is insufficient for the growth of macroalgae. Thus, the content of inorganic phosphorus in water is a limiting factor. With an increase in this aquatic environment parameter, intensive growth of macroalgae is observed.

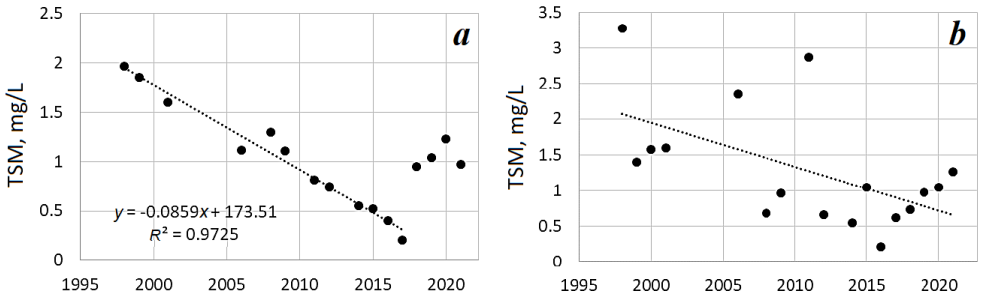

Fig. 4. TSM content in the upper (*a*) and lower (*b*) layers of water in September during 1998–2021 near Cape Kosa Severnaya

Model studies

With the available data on the hydrochemical state of waters near Cape Kosa Severnaya, it is impossible to carry out a detailed calculation of the dynamics of phytocenoses biomass throughout the entire period. Therefore, we chose the most data-rich period from May 1998 to February 2002 for our experiments. With a discreteness of one month, the data were interpolated at gaps. The time step of the model was 24 h. In addition to hydrochemical parameters, the model control variables were water temperature in the 0–10 m layer and average daily solar radiation intensity at the sea surface (Fig. 5, *a* – *c*).

Fig. 5, *d* shows simulation results (at a depth of 4 m) with input variable series. At the beginning of the analyzed period, the content of TSM in the upper layer was

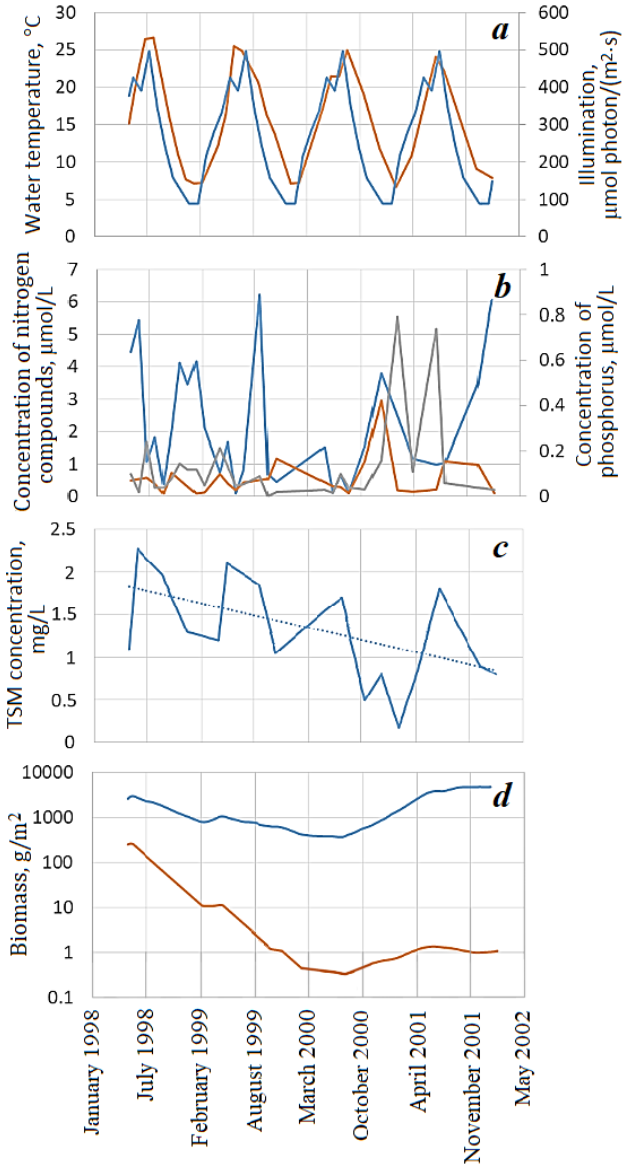

F i g . 5 . External conditions of the model and results of model calculations for 4 years in Cape Kosa Severnaya: *a* – water temperature (red line) and illumination of the sea surface (blue line); *b* – concentrations of ammonium compounds (blue line), nitrates and nitrites (red line) and phosphorus (grey line) in water; *c* – TSM concentration (solid line) and trend line (dotted line); *d* – biomass of *Ericaria crinita*, *Gongolaria barbata* (blue line) and *Phyllophora crispa* (red line)

1.5 mg/L or more. With such water turbidity, *Phyllophora crispa* could grow at depths of no more than 4 m. We see that as a result of a slight decrease in the amount of suspended matter, the *Ericaria-Gongolaria* phytocenosis was restored and *Phyllophora crispa* almost completely disappeared over four years of model calculation. According to observations, the *Phyllophora* phytocenosis had begun to recover at depths of 10–15 m by 2017, although in 2017 its biomass reached a value 10 times less than that recorded at the beginning of the observation period. It is safe to assume that the restoration was possible due to the water quality improvement. The concentration of TSM in the warm period of the year has a negative trend (Fig. 4, *a*).

Of interest is the analysis of the variability of model functions reflecting the relative content of nitrogen and phosphorus in the tissues of macroalgae (Fig. 6):

$$f(Q_N) = \frac{Q_N - Q_N^{min}}{Q_N^{max} - Q_N^{min}}, \qquad f(Q_P) = \frac{Q_P - Q_P^{min}}{Q_P^{max} - Q_P^{min}}, \tag{5}$$

where Q_P and Q_N, μmol/g, are concentrations of phosphorus and nitrogen in alga tissues; Q_P^{min}, Q_P^{max}, Q_N^{min}, Q_N^{max}, μmol/g, are minimum and maximum concentration values (species-specific characteristics of algae). According to the model equations [22], the level of reserves of inorganic nitrogen and phosphorus compounds in algae cells influences the rate of assimilation of biogenic compounds from sea water and the rate of photosynthesis. Thus, functions (5) limit the macroalgae growth. Fig. 6 shows that the limiting effect of nitrogen and phosphorus was manifested alternately over four years of the model time, but phosphorus was the limiting element for macrophytobenthos for most of the time.

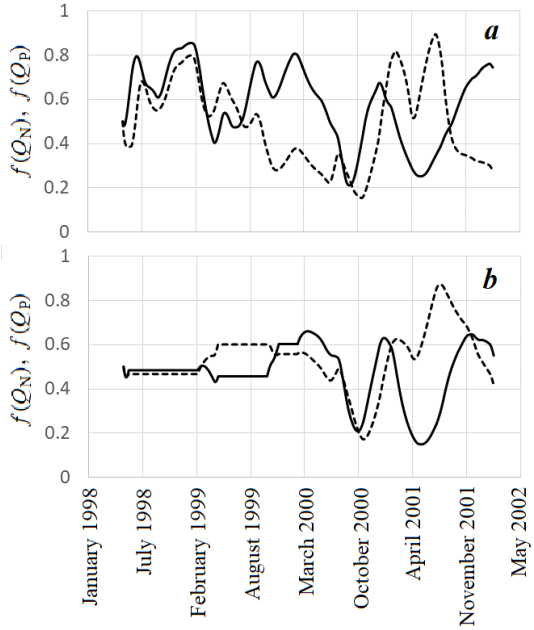

Fig. 6. Temporal variability of functions $f(Q_N)$ (solid line) and $f(Q_P)$ (dashed line) limiting the growth of *Ericaria crinita, Gongolaria barbata* (*a*) and *Phyllophora crispa* (*b*) near Cape Kosa Severnaya

Conclusion

Significant changes in the biomass of phytocenosis of the Black Sea dominant species were identified. These changes manifest themselves differently depending on the depth of bottom vegetation growth. In the *Ericaria-Gongolaria* phytocenosis occupying shallow waters with depths of up to 5 m, by 2006 there had been an increase in the biomass of *Ericaria crinita* and *Gongolaria barbata* characterized by an increase in the proportion of epiphytes from 5 to 50%. In 2017, a recovery of dominant species was observed while the total biomass increased almost threefold. At the same time, species of bottom vegetation growing deeper than 5 m underwent catastrophic degradation. The *Erikaria-Gongolaria-Phyllophora* phytocenosis located at depths of 5–10 m had completely disappeared by 2006, and *Dictyota* spp. took its place in 2017. The *Phyllophora* phytocenosis located at depths over 10 m degraded significantly in 1997, and its biomass decreased almost to zero. In 2006, *Phyllophora crispa* was not recorded at these depths. However, separate areas of the bottom where *Phyllophora crispa* was present, with biomass an order of magnitude lower compared to that in 1964, had appeared by 2017.

Having analyzed the changes in the hydrochemical regime for 1998–2021, we came to the conclusion that the recorded transformations of benthic communities were caused mainly by changes in water transparency associated with the TSM content. Hydrochemical indicators of water quality varied during the period under review, but no noticeable trends in changes in the concentrations of biogenic compounds were identified. In 1998–2017, water transparency increased in the summer period (August–September), but an increase in water turbidity was recorded again in 2018–2021. The processes of restoration of the biomass of *Phyllophora crispa* at depths greater than 10 m can stop with further reduction in transparency, which will lead to the disappearance of this macroalga in the area under study with conservation value. The analysis of model functions characterizing the influence of the concentration of inorganic nitrogen and phosphorus compounds in water on the growth of macroalgae showed that the growth of macroalgae was alternately limited by nitrogen and phosphorus inorganic compounds.

To organize monitoring studies of the transformation of bottom phytocenosis, it is advisable to conduct regularly hydrobotanical surveys in combination with hydrochemical and hydrophysical studies of the coastal zone at intervals of several years.

References

1. Zharikov, V., Bazarov, K. and Egidarev, E., 2017. Use of Remotely Sensed Data in Mapping Underwater Landscapes of Srednyaya Bay (Peter the Great Gulf, Sea of Japan). *Geography and Natural Resources*, 38(2), pp. 188–195. https://doi.org/10.1134/S187537281702010X
2. Petrov, K.M., 1989. [*Subaquatic Landscapes: Theory, Research Methods*]. Leningrad: Nauka, 124 p. (in Russian).
3. Mitina, N.N., 2005. [*Geoecological Studies of Marine Shallow-Water Landscapes*]. Moscow: Nauka, 197 p. (in Russian).
4. Pankeeva, T.V., Milchakova, N.A., Mironova, N.V., Aleksandrov, V.V., Kashirina, E.S., Kovardakov, S.A. and Ryabogina, V.G., 2014. [Landscape Approach to Assessment of

Macrophytobenthos Condition Under Conflict Nature Management]. In: MHI, 2014. *Ekologicheskaya Bezopasnost' Pribrezhnoy i Shel'fovoy Zon i Kompleksnoe Ispol'zovanie Resursov Shel'fa* [Ecological Safety of Coastal and Shelf Zones and Comprehensive Use of Shelf Resources]. Sevastopol: MHI. Iss. 29, pp. 70–79 (in Russian).

5. Pankeeva, T.V., Mironyuk, O.A. and Pankeeva, A.Ur., 2014. Researches of Bottom Landscapes of the Coastal Zone Tarkhankut Peninsula (Crimea, Black sea). *Geopolitics and Ecogeodynamics of Regions*, 10(1), pp. 800–805 (in Russian).
6. Agarkova-Lyakh, I.V. and Skrebets, G.N., 2009. Landscapes of the Black Sea Coastal Zone. In: E. A. Pozachenyuk, ed., 2009. *Modern Landscapes of the Crimea and Adjacent Water Areas*. Simferopol: Business-Inform, pp. 250–279 (in Russian).
7. Mitina, N.N. and Chuprina, E.V., 2012. *Subaquatic Landscapes of the Black and Azov Seas: Structure, Hydroecology, Protection*. Moscow: FGUP "Tipographya" Rosselhozakademii, 320 p. (in Russian).
8. Tamaychuk, A.N., 2009. Landscapes of the Black Sea. In: E. A. Pozachenyuk, ed., 2009. *Modern Landscapes of the Crimea and Adjacent Water Areas*. Simferopol: Business-Inform, pp. 497–529 (in Russian).
9. Tamaychuk, A.N., 2017. The Space Heterogeneity of Natural Conditions and the Division of the Black Sea. *Proceedings of the Russian Geographical Society*, 149(2), pp. 30–50 (in Russian).
10. Pasynkova, L.A., 2008. Landscapes of Continental Slope of the Black Sea: Principles of It's Single Out and Description. *Scientific Notes of Tavrida National V.I. Vernadsky University. Geography*, 21(3), pp. 266–273 (in Russian).
11. Pasynkova, L.A., 2010. [The Problem of Sustainability of Underwater Landscapes in the Yalta Bay Area]. *Scientific Notes of Tavrida National V.I. Vernadsky University. Geography*, 23(3), pp. 331–333 (in Russian).
12. Pozachenjuk, E. and Penno, M., 2013. To the Substantiation of Highlighting the Marine Anthropogenic Landscapes. In: VSPU, 2013. *Scientific Notes of Vinnytsya State Pedagogical University Named After Michailo Kotzubynsky. Series: Geography*. Vinnytsa. Iss. 25, pp. 142–148 (in Russian).
13. Bondarev, I.P., 2008. The Problem of Instability of the Underwater Landscape (on the Example of Northern Part of the Black Sea). *Scientific Notes of Tavrida National V.I. Vernadsky University. Geography*, 21(2), pp. 128–133 (in Russian).
14. Dar, N., Pandit, A. and Ganai, B., 2014. Factors Affecting the Distribution Patterns of Aquatic Macrophytes. *Limnological Review*, 14(2), pp. 75–89. https://doi.org/10.2478/limre-2014-0008
15. Teubner, K., Teubner, I.E., Pall, K., Tolotti, M., Kabas, W., Drexler, S.-S., Waidbacher, H. and Dokulil, M.T., 2022. Macrophyte Habitat Architecture and Benthic-Pelagic Coupling: Photic Habitat Demand to Build Up Large P Storage Capacity and Bio-Surface by Underwater Vegetation. *Frontiers in Environmental Science*, 10, pp. 1–20. https://doi.org/10.3389/fenvs.2022.901924
16. Vila-Costa, M., Pulido, C., Chappuis, E., Calviño, A., Casamayor, E.O. and Gacia, E., 2015. Macrophyte Landscape Modulates Lake Ecosystem-Level Nitrogen Losses Through Tightly Coupled Plant-Microbe Interactions. *Limnology and Oceanography*, 61(1), pp. 1–11. https://doi.org/10.1002/lno.10209
17. Kalra, T., Ganju, N. and Testa, J., 2020. Development of a Submerged Aquatic Vegetation Growth Model in the Coupled Ocean-Atmosphere-Wave-Sediment Transport (COAWST v 3.4) Model. *Geoscientific Model Development*, 13(11), pp. 5211–5228. https://doi.org/10.5194/gmd-13-5211-2020

18. Pankeeva, T.V. and Mironova, N.V., 2022. Long-term Dynamics of Underwater Landscapes of the Coastal Zone Cape Kosa Severnaya – Cape Tolsty (Sevastopol). *Ecological Safety of Coastal and Shelf Zones of Sea*, (2), pp. 70–85. https://doi.org/10.22449/2413-5577-2022-2-70-85
19. Pankeeva, T.V. and Mironova, N.V., 2023. Spatio-Temporal Changes of Macrophyto-benthos in Coastal Landscapes at Cape Kosa Severnaya (Sevastopol). *Theoretical and Applied Ecology*, (2), pp. 66–72. https://doi.org/10.25750/1995-4301-2023-2-066-072 (in Russian).
20. Vasechkina, E.F. and Filippova, T.A., 2020. Simulation of Bottom Phytocenosis in the Crimean Coastal Zone. *Physical Oceanography*, 27(3), pp. 317–334. https://doi.org/10.22449/1573-160X-2020-3-317-334
21. Filippova, T.A. and Vasechkina, E.F., 2022. Simulation of Chemical and Biological Processes of Seagrass Growth. *Physical Oceanography*, 29(6), pp. 674–687. https://doi.org/10.22449/1573-160X-2022-6-674-687
22. Vasechkina, E.F. and Filippova, T.A., 2019. Modeling of the Biochemical Processes in the Benthic Phytocenosis of the Coastal Zone. *Physical Oceanography*, 26(1), pp. 47–62. https://doi.org/10.22449/1573-160X-2019-1-47-62

Submitted 09.01.2024; accepted after review 19.03.2024;
revised 27.03.2024; published 25.06.2024

About the authors:

Anastasia V. Parkhomenko, Postgraduate Student, Marine Hydrophysical Institute of RAS (2 Kapitanskaya St., Sevastopol, 299011, Russian Federation), **ORCID ID: 0000-0002-2378-7067, ResearcherID: 5090-2023,** *avparkhomenko52@gmail.com*

Elena F. Vasechkina, Deputy Director for Research, Methodology and Education, Marine Hydrophysical Institute of RAS (2 Kapitanskaya St., Sevastopol, 299011, Russian Federation), DrSci (Geogr.), **ORCID ID: 0000-0001-7007-9496, Scopus Author ID: 6507481336, ResearcherID: P-2178-2017**, *vasechkina.elena@gmail.com*

Aleksandr A. Latushkin, Research Associate, Marine Hydrophysical Institute of RAS (2 Kapitanskaya St., Sevastopol, 299011, Russian Federation), PhD (Geogr.), **ORCID ID: 0000-0002-3412-7339, Scopus Author ID: 56298305600, ResearcherID: U-8871-2019**, *sevsalat@gmail.com*

Contribution of the authors:

Anastasia V. Parkhomenko – selection, systematisation and analysis of literature sources, analysis of hydrochemical observation data, preparation of the article text, cartographic materials and the list of references

Elena F. Vasechkina – problem statement, numerical modelling, analysis of study results, preparation of the article text and the list of references

Aleksandr A. Latushkin – expeditionary hydro-optical studies, data processing and analysis

All the authors have read and approved the final manuscript.

Original article

Biogenic Elements in the Waters of the Eastern Gulf of Finland According to the Results of Studies 2020–2022

M. A. Siniakova [1, 2] *, J. V. Krylova [3], L. V. Bronnikova [2]

[1] *Saint Petersburg Branch of VNIRO (GosNIORKH named after L.S. Berg), Saint Petersburg, Russia*

[2] *Saint-Petersburg State Marine Technical University, Saint Petersburg, Russia*

[3] *Papanin Institute for Biology of Inland Waters Russian Academy of Sciences, Borok, Russia*

* *e-mail: kafischem@yandex.ru*

Abstract

The paper studies the dynamics of biogenic elements (mineral (phosphate) and total phosphorus and ammonium) content based on the results of annual monitoring surveys of water in the eastern Gulf of Finland conducted in 2020–2022. Information on the horizontal and vertical distribution of the indicators was analysed, so samples were taken in the surface, bottom and middle (at deep-water stations) layers of water. The content of elements was determined by the spectrophotometric method. The results are compared and analysed by median values. During the study period, phosphate phosphorus concentrations in the absolute majority of cases did not exceed the maximum permissible concentration (0.15 mg/dm^3), total phosphorus concentrations on average corresponded to the mesotrophic status, although there were cases of its concentration increase to values characteristic of the eutrophic status of a water body. Namely, in 2020, the concentrations amounted up to 0.091 mg P/dm^3 in the bottom and surface water layers in June (mainly at the coastal stations) and in September (mainly in the bottom layer at the central offshore stations). In summer 2021, the concentrations reached 0.147 mg P/dm^3 (surface layer) and 0.171 mg P/dm^3 (bottom layer) at the coastal stations and 0.163 mg P/dm^3 at the central station. Ammonia nitrogen concentrations were mainly within the MPC (0.5 mg/dm^3). In June 2021, local areas along the southern and northern shores of the Gulf of Finland with relatively high levels of ammonia nitrogen (up to 0.285 mg/dm^3) in surface and bottom water layers were identified. In general, despite the high anthropogenic load, concentrations of mineral phosphorus and ammonium in the waters of the Gulf of Finland were within the MPC, with exceedances recorded rarely, usually in Neva Bay, Koporye Bay and near the coast of the Kurortny district. Elevated concentrations of total phosphorus at the central stations can apparently be explained by transport of the substance from the western part of the Gulf and diffusion from bottom sediments. On average, higher concentrations of total phosphorus were found in bottom water layers than in surface water layers. In general, concentrations of biogenic elements correspond to the mesotrophic status of the water body.

Key words: mineral phosphorus, total phosphorus, ammonium ions, Gulf of Finland, biogenic elements, trophic state

Acknowledgments: The work was carried out under state assignment of VNIRO no. 076-00005-20-02.

For citation: Siniakova, M.A., Krylova, J.V. and Bronnikova, L.V., 2024. Biogenic Elements in the Waters of the Eastern Gulf of Finland According to the Results of Studies 2020–2022. *Ecological Safety of Coastal and Shelf Zones of Sea*, (2), pp. 91–106.

Биогенные элементы в водах восточной части Финского залива по результатам исследований 2020–2022 годов

М. А. Синякова [1, 2] *, **Ю. В. Крылова** [3], **Л. В. Бронникова** [2]

[1] *Санкт-Петербургский филиал Всероссийского научно-исследовательского института рыбного хозяйства и океанографии (Государственный научно-исследовательский институт озерного и речного рыбного хозяйства им. Л. С. Берга), Санкт-Петербург, Россия*

[2] *Санкт-Петербургский государственный морской технический университет, Санкт-Петербург, Россия*

[3] *Институт биологии внутренних вод им. И.Д. Папанина Российской академии наук, Борок, Россия*

* *e-mail: kafischem@yandex.ru*

Аннотация

Изучена динамика содержания биогенных элементов (минерального (фосфатного) и общего фосфора и аммония) по результатам ежегодных мониторинговых исследований воды восточной части Финского залива, проводившихся в 2020–2022 гг. Анализировалась информация о распределении показателей по горизонтали и по вертикали, поэтому пробы отбирали в поверхностном, придонном, а на глубоководных станциях и в срединном слоях воды. Содержание элементов определяли спектрофотометрическим методом. Сопоставляются и анализируются результаты по среднемедианным значениям. В период исследований концентрация фосфатного фосфора в абсолютном большинстве случаев не превышала ПДК (0.15 мг/дм^3), концентрации общего фосфора в среднем соответствовали мезотрофному статусу, хотя наблюдались случаи повышения его концентрации до значений, характерных для эвтрофного статуса водоема: в 2020 г. в придонном и поверхностном слоях воды (в июне в основном на прибрежных станциях (0.091 мг Р/дм^3) и в сентябре преимущественно в придонном слое на центральных станциях, удаленных от берега), в 2021 г. летом концентрации достигали 0.147 мг Р/дм^3 (поверхностный слой) и 0.171 мг Р/дм^3 (придонный слой) на прибрежных станциях, 0.163 мг Р/дм^3 на центральной станции. Концентрации аммонийного азота в основном находились в пределах ПДК (0.5 мг/дм^3). В июне 2021 г. выделялись локальные области вдоль южного и северного берега Финского залива с относительно высоким содержанием аммонийного азота (до 0.285 мг/дм^3) в поверхностном и придонном слоях воды. В целом, несмотря на высокую антропогенную нагрузку, концентрации минерального фосфора и аммония в водах Финского залива находились в пределах ПДК, превышения фиксировались редко, обычно в Невской Губе, Копорской Губе, у побережья Курортного района. Повышенные концентрации общего фосфора на центральных станциях, по-видимому, можно объяснить переносом вещества из западной части залива и диффузией из донных отложений. В среднем в придонных слоях воды обнаруживается более высокое содержание общего фосфора, чем в поверхностных. В целом концентрации биогенных элементов соответствуют мезотрофному статусу водоема.

Ключевые слова: фосфор минеральный, фосфор общий, ионы аммония, Финский залив, биогенные элементы, трофность

Благодарности: работа выполнена в рамках государственного задания ФГБНУ «ВНИРО» № 076-00005-20-02.

Для цитирования: *Синякова М. А., Крылова Ю. В., Бронникова Л. В.* Биогенные элементы в водах восточной части Финского залива по результатам исследований 2020–2022 годов // Экологическая безопасность прибрежной и шельфовой зон моря. 2024. № 2. С. 91–106. EDN EDSGSE.

Introduction

The Baltic Sea belongs to the Atlantic Ocean basin. The sea is deeply incised into the land, it has a long coastline and complex coastal contours [1)].

Within the Baltic Sea, several relatively isolated zones can be distinguished, including the Gulf of Finland. The area of the Gulf of Finland is 29.5 thousand km^2; the average depth is 38 m, the maximum one is 115 m. The rivers Neva, Luga, Narva, and Sestra flow into the Gulf. The part of the Gulf between the mouth of the Neva River and Kotlin Island is called Neva Bay; a fairway for the passage of ships was dug along its bottom [1)]. The coast of the Gulf of Finland is characterized by a high concentration of anthropogenic objects: settlements, ports, agricultural complexes, as well as nature reserves and historical monuments. A nuclear power plant is located in the town of Sosnovy Bor, and the second most important city in Russia, Saint Petersburg, was founded at the mouth of the Neva River.

Thus, the Gulf of Finland is of great importance for the functioning of the economy of the North-West region of Russia and experiences high anthropogenic load. This determines the need for careful monitoring of its ecological state. The Leningrad Region Committee on Natural Resources publishes collections containing information on the state of the atmospheric air and water of water bodies in the region regularly, including information on the state of the waters of the Gulf of Finland [2), 3), 4), 5)]. The hydrochemical characteristics of the Gulf are studied in [1–5].

The parameters under control include concentrations of total phosphorus, mineral phosphorus and ammonium nitrogen. Phosphorus and nitrogen are among the elements necessary for the development of living organisms as can be seen, for example, from the formula of organic matter according to Redfield $(CH_2O)_{106}(NH_3)_{16}H_3PO_4$ and the C:N:P ratio as 106:16:1 [6]. In natural conditions, it is the lack of phosphorus that often limits the development of hydrobionts. At the same time, when phosphorus enters water bodies, uncontrolled growth of plant

---

1) Zonn, I.S., Kostyanoy, A.G., Semenov, A.V. and Zhiltsov, S.S., 2015. [*The Baltic Sea: Encyclopedia*]. Moscow: Mezhdunarodnye Otnosheniya, 570 p. (in Russian).

2) Natural Resources Committee of Leningrad Region, 2018. [*State of Environment in Leningrad Region*]. Saint Peterburg, 372 p. (in Russian).

3) Natural Resources Committee of Leningrad Region, 2019. [*State of Environment in Leningrad Region in 2018*]. Saint Peterburg, 448 p. (in Russian).

4) Natural Resources Committee of Leningrad Region, 2022. [*State of Environment in Leningrad Region*]. Saint Peterburg, 528 p. (in Russian).

5) Natural Resources Committee of Leningrad Region, 2023. [*State of Environment in Leningrad Region in 2022*]. Saint Peterburg: Papirus, 320 p. (in Russian).

biomass begins, eutrophication of the water body occurs with the change of its trophic status and the number of phytoplankton and bacteria increases. According to trophicity criteria [7], oligotrophic water bodies are characterized by phosphate concentrations (for phosphorus) from 0 to 0.012 mg P/dm^3, mesotrophic ones – from 0.012 to 0.024 mg P/dm^3 and eutrophic water bodies – from 0.024 to 0.096 mg P/dm^3. Higher values correspond to hypereutrophic waters.

The content of phosphorus compounds is subject to significant seasonal fluctuations since it depends on the ratio of the intensity of photosynthesis and biochemical oxidation of organic matter. Minimum concentrations of phosphates in surface fresh waters are usually observed in spring and summer, maximum ones – in autumn and winter. Maximum concentrations in sea waters are more typical for spring and autumn and minimum ones – for summer and winter [6)].

Ammonium ions are absorbed by plants turning into glutamic acid, on the basis of which α–amino acids are synthesized and then proteins, nucleic acids and other nitrogen-containing substances [6]. They are necessary for the development of aquatic organisms. At the same time, the NH_4^+ excess has a negative impact, thus causing fish intoxication [7)] [8]. Increased concentration of ammonium ions can be used as an indicator reflecting the deterioration of the sanitary condition of a water body and the pollution of surface and ground waters. Significant amounts of phosphorus and nitrogen compounds enter water bodies with wastewater from agricultural enterprises [7)], including livestock complexes [8, 9], domestic wastewater from populated areas and a result of the activities of some industrial enterprises.

The aim of this study is to investigate the dynamics of the content of mineral (phosphate) and total phosphorus and ammonium in the waters of the Gulf of Finland according to the results of monitoring studies 2020–2022.

Materials and methods of study

The content of various forms of phosphorus and ammonium ions in the waters of the eastern Gulf of Finland is monitored as part of the studies conducted annually by the Saint Petersburg Branch of VNIRO (GosNIORKH named after L.S. Berg). As a rule, two cruises are carried out under these studies: in spring and early summer, as well as in late summer and early autumn. More specific dates depend on weather conditions. During the cruises, samples are taken at stations distributed throughout the water area from several layers of water: surface, bottom and also middle layers of water at deep-water stations. This is done in order to describe the distribution of indicators not only horizontally, but also vertically. The number of sampling points can vary from cruise to cruise.

As a rule, the content of total phosphorus, mineral (phosphate) phosphorus and ammonium ions is determined in water samples by the spectrophotometric

---

[6)] World Water Technologies. [*Water Chemistry. Total Phosphorus*]. 2024. [online] Available at: https://wwtec.ru/index.php?id=213 [Accessed: 28 May 2024].

[7)] World Water Technologies. [*Water Chemistry. Total Nitrogen*]. 2024. [online] Available at: https://wwtec.ru/index.php?id=212#8.2 [Accessed: 28 May 2024].

method in accordance with regulatory documents [8), 9)]

Results and discussion

2020

In 2020, two cruises were carried out as part of the monitoring studies: in June and September. The cruises were carried out according to the VNIRO state assignment No. 076-00005-20-02. Samples were collected at 15 stations during the cruises (Fig. 1, *b*).

a

b

F i g . 1 . Gulf of Finland (the rectangular on the map shows the study area in the eastern part of the Gulf) (*a*) and an enlarged image of the selected area with a sampling station grid (*b*) [3, 10]. Google Maps image (available at: https://www.google.ru/maps)

[8)] Guideline RD 52.24.387-2019; Guideline RD 52.24.382-2019; Guideline RD 52.24.486-2009.

[9)] Ministry of Agriculture of Russia, 2016. *On the Approval of Water Quality Standards for Water Bodies of Commercial Fishing Importance, Including Standards for Maximum Permissible Concentrations of Harmful Substances in the Waters of Water Bodies of Commercial Fishing Importance*: Order of the Ministry of Agriculture of Russia dated December 13, 2016, No. 552. Moscow: Ministry of Agriculture of Russia (in Russian).

Table 1 shows results of determination of total and mineral phosphorus content. According to the obtained results, the concentrations of mineral phosphorus in the studied areas of the Gulf of Finland in June and September differed slightly. In September, compared to June, the concentration of mineral phosphorus at many points decreased,

Table 1. Results of determination of phosphorus (in terms of phosphorus) in water samples in 2020

Station	Water layer	Mineral phosphorus, mg P/dm^3		Total phosphorus, mg P/dm^3	
		June	September	June	September
1	S	0.001	0.005	0.006	0.013
	M	0	0.005	0	0.018
	B	0.003	0.008	0.013	0.042
2	S	0	0.002	0.005	0.011
	B	0.004	0.008	0.011	0.044
3	S	0	0.004	0.008	0.021
	M	0.008	0.002	0.015	0.020
	B	0.010	0.009	0.037	0.021
3k	S	0.005	0.004	0.005	0.012
	B	0.006	0.005	0.018	0.016
4	S	0.003	0.002	0.023	0.007
	B	0.005	0.004	0.040	0.019
6k	S	0.008	0.004	0.028	0.014
	B	0.015	0.006	0.076	0.009
6L	S	0.007	0.006	0.014	0.023
	B	0.005	0.004	0.023	0.013

Station	Water layer	Mineral phosphorus, mg P/dm^3		Total phosphorus, mg P/dm^3	
		June	September	June	September
18L	S	0.009	0.005	0.044	0.016
	B	0.007	0.004	0.010	0.016
19	S	0.001	0.003	0.033	0.013
	B	0	0.005	0.003	0.015
20	S	0.002	0.003	0.007	0.011
	B	0.006	0.002	0.013	0.013
21	S	0.001	0.004	0.005	0.010
	B	0.005	0.004	0.028	0.014
22	S	0.004	0.002	0.012	0.018
	B	0.002	0.005	0.036	0.009
24	S	0.003	0.006	0.019	0.037
	B	0.012	0007	0.091	0.007
26	S	0.009	0.004	0.073	0.017
	B	0.006	0.003	0.013	0.017
A	S	0.005	0.005	0.027	0.013
	M	0.002	0.002	0.021	0.021
	B	0.006	0.005	0.072	0.039
Median value		0.005	0.004	0.018	0.016

Note: S – surface water layer (0–0.3 m); M – middle layer (equidistant from the surface and bottom); B – bottom layer; mg P/dm^3 – concentration of mineral and total phosphorus expressed as phosphorus. Maximum permissible concentration (MPC) of mineral phosphorus – 0.15 mg/L. MPC of total phosphorus is absent.

which corresponds to the expectations and can be explained by the increased consumption of mineral phosphorus by photosynthetic organisms in the summer. The exceptions were deep-water stations and stations *1*, *2* and *4* located far from the shore.

Total phosphorus concentrations were naturally higher and varied from 0 (i.e. below the detection limit), which corresponds to the oligotrophic status of the water body, to 0.091 mg P/dm^3, which corresponds to its eutrophic status. Total phosphorus concentration levels characterising the eutrophic status of the water body were also noted at central stations far from anthropogenic sources (stations *2–4*). However, such concentrations are more typical for the stations where water quality can be affected by man-made, domestic and agricultural wastewater (stations *19*, *21*, *24*, *26*, *A*, *6k*, *18L*). It should be noted that in September, high values of total phosphorus concentration were observed mainly in the bottom layers of water, including at station *2*, where its maximum value (0.044 mg P/dm^3) was recorded. This can be stipulated by the sedimentation of suspended organic matter and its destruction, transfer of phosphorus compounds from the western part of the Gulf and their entry from bottom sediments.

The current regime in the Gulf of Finland is determined by the water exchange of the Gulf of Finland and the Gulf of Riga with the main part of the Baltic Sea. The currents are significantly influenced by the runoff of water from the land. There is a more or less stable constant current directed to the west and explained by the runoff of the Neva River (Fig. 2). In addition, temporary wind currents arise under the influence of winds [10)].

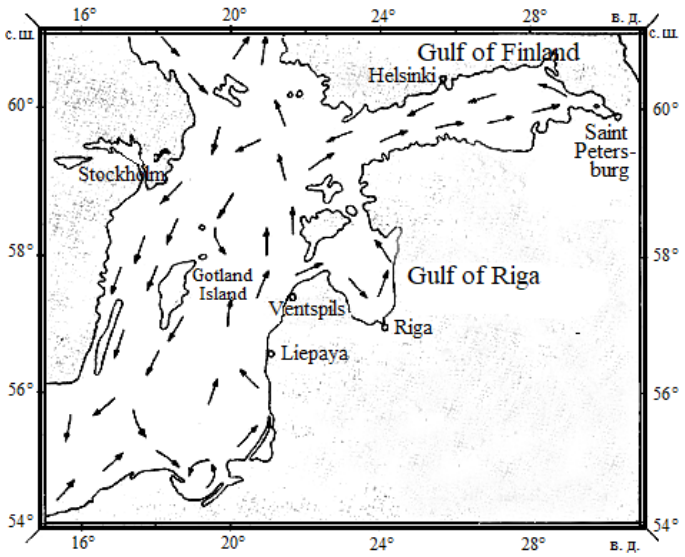

F i g . 2 . Diagram of main constant currents in the Gulf of Finland. The arrows show current directions

[10)] Department of Navigation and Oceanography, 2007. [*The Baltic Sea Sailing Directions. Part 1. Eastern Part of the Sea with the Gulf of Finland and the Gulf of Riga*]. Saint Petersburg, 656 p. 9in Russian).

According to literature data, phosphorus accumulation occurs actively in the deep-water western part of the Gulf where the biogenic regime is determined by the internal load on the water body, when additional phosphorus compounds are supplied from bottom sediments under conditions of oxygen deficiency [11]. Permanent currents transport the released phosphorus compounds from the western Gulf of Finland to the eastern one.

A decrease in the concentration of dissolved oxygen in the water and the development of hypoxic zones are less typical for the eastern Gulf of Finland due to its shallower waters. However, such phenomena are observed precisely in the area of deep-water station *4* (according to [11], oxygen concentration can vary from 5 to 2 mg/dm^3).

On average, the level of total phosphorus (based on the median values) indicates a mesotrophic status, which is why the MPC for mesotrophic water bodies was used in Table 1 [9]. As follows from the data in Table 1, the mineral phosphorus MPC was not exceeded either in June or in September.

2021

In 2021, sampling was carried out in May and June, as well as in August and September, according to the standard sampling scheme from the stations showed in Fig. 1, *a*.

This year, not only phosphate (mineral) phosphorus and total phosphorus were determined, but also ammonium nitrogen.

Table 2 shows the results of water sample analysis.

In spring and early summer 2021, mineral phosphorus concentrations were very low (lower than in June of the previous year). This can have been stipulated by the clear sunny weather during that period and, as a result, the intensive development of biota, which consumed mineral phosphorus rapidly. On the contrary, the values of total phosphorus concentration were on average higher than in the same period last year, and at the same time the median values in May and June were at the eutrophic level. At stations *3к* (surface), *4* (middle), *20* (bottom), they exceeded 0.096 mg P/dm^3 – the upper limit of the eutrophic level. Station *3k* is located in Koporye Bay, station *20* – near the coast of the Kurortny district (the town of Zelenogorsk). It is logical to assume that increased concentrations of total phosphorus are explained by anthropogenic influence. On the contrary, station *4* is located far from the coast, though a significant content of total phosphorus was observed in the area of this station earlier, which gives reason to assume the influx of phosphorus from bottom sediments and with water masses coming from the western part of the Gulf, as was already noted above [10].

In May and June 2021, the mineral phosphorus MPC was exceeded at station *4* in the middle layer of waters and at station *20* in the bottom layer.

Unusually high levels of ammonium nitrogen were recorded at a number of stations (*6k*, *6L*, *18L*) located along the southern coast of the Gulf within Koporye Bay and neighboring Luga Bay, as well as at stations *19* and *20* located near the northern coast of the Gulf within the boundaries of the Kurortny district of Saint Petersburg. It is noteworthy that high content of NH_4^+ was characteristic of both surface and bottom layers of water. Areas of ammonium nitrogen increased concentrations in Koporye and Luga Bays can be associated with the influx of biogen-rich river waters, and near the northern coast – with the anthropogenic load of the Kurortny district.

Table 2. Results of determination of phosphorus and ammonium nitrogen in water samples in 2021

Station	Water layer	Mineral phosphorus, mg P/dm^3		Total phosphorus, mg P/dm^3		Ammonium, mg/dm^3	
		May – June	August – September	May – June	August – September	May – June	August – September
1	S	N/D	N/D	0.004	N/D	<0.03	N/D
	M	N/D	N/D	0.009	N/D	0.06	N/D
	B	0.005	N/D	0.017	N/D	0.09	N/D
2	S	0.004	0.003	0.029	0.003	< 0.03	< 0.03
	M	0.004	0	0.095	0.0055	< 0.03	< 0.03
	B	0.005	0.003	0.037	0.005	< 0.03	< 0.03
3	S	0	0.003	0.042	0.003	< 0.03	< 0.03
	M	0.005	0.004	0.005	0.0065	< 0.03	< 0.03
	B	0.002	0.003	0.032	0.006	< 0.03	< 0.03
3k	S	0	0.003	0.147	0.005	< 0.03	< 0.03
	B	0.002	0.004	0.039	0.005	< 0.03	< 0.03
4	S	0.003	0.002	0.017	0.036	< 0.03	< 0.03
	M	0.006	0.002	0.163	0.039	< 0.03	< 0.03
	B	0.009	0.002	0.034	0.006	< 0.03	< 0.03
6k	S	0.001	0.001	0.042	0.027	0.130	< 0.03
	B	0.005	0.002	0.024	0.004	0.285	< 0.03
6L	S	0.002	0.004	0.002	0.013	0.055	< 0.03
	B	0.003	0.002	0.021	0.008	0.075	< 0.03

Station	Water layer	Mineral phosphorus, mg P/dm^3		Total phosphorus, mg P/dm^3		Ammonium, mg/dm^3	
		May – June	August – September	May – June	August – September	May – June	August – September
18L	S	0.0008	0.0040	0.0008	0.012	0.150	< 0.03
	B	0.0010	0.0030	0.0016	0.0055	0.055	< 0.03
19	S	0.0030	0.0065	0.0060	0.008	0.155	< 0.03
	B	0.0030	0.0060	0.0050	0.006	0.055	< 0.03
20	S	0.0030	0.0040	0.0260	0.005	0.075	< 0.03
	B	0.0030	0.0035	0.1710	0.006	0.170	< 0.03
21	S	0.0020	0.0150	0.0360	0.015	< 0.03	< 0.03
	B	0.0020	0.0065	0.0080	0.0065	< 0.03	< 0.03
22	S	0.0016	0.0080	0.0080	0.029	< 0.03	< 0.03
	B	0.0030	0.0120	0.0240	0.016	< 0.03	< 0.03
24	S	0.0020	0.0040	0.0500	0.013	< 0.03	< 0.03
	B	0.0020	0.0040	0.0440	0.004	< 0.03	< 0.03
26	S	0.0030	0.0050	0.0090	0.005	< 0.03	< 0.03
	B	0.0010	0.0050	0.0630	0.010	< 0.03	< 0.03
A	S	0.0004	0.0020	0.0120	0.021	< 0.03	< 0.03
	M	0.0030	0.0016	0.0030	0.009	0.030	< 0.03
	B	0.0065	0.0030	0.0680	0.031	0.070	< 0.03
Median value		0.0020	0.0040	0.0290	0.008	< 0.03	< 0.03

Note: N/D – not determined. See designations to Table 1. MPC of ammonium – 0.5 mg/L.

Moreover, high content of NH_4^+ was recorded at station *4* in the upper water layer. Thus, it is possible to assume the formation of local areas ("spots") with a relatively high content of ammonium nitrogen, which correlate partially with areas with an increased level of total phosphorus. Despite the recorded high level of ammonium concentrations, all values of this indicator were below the MPC.

At the end of August and in September of the same year, the concentrations of mineral phosphorus changed insignificantly compared to June. The concentrations of total phosphorus decreased significantly and ranged from 0.003 to 0.039 mg P/dm^3. Values corresponding to hypereutrophic status were completely absent; values exceeding the upper limit of the mesotrophic level were recorded only at stations *4* (surface and middle), *22* (surface) and *A* (bottom). Ammonium nitrogen concentrations were either below the detection limit or negligible.

2022

In 2022, samples were taken in June and September from the stations shown in Fig. 1, *a*.

As in 2021, phosphate (mineral) phosphorus, total phosphorus and ammonium nitrogen were determined.

Table 3 shows the results of water sample analysis.

Table 3. Results of determination of phosphorus and ammonium nitrogen in water samples in 2022

Station	Water layer	Mineral phosphorus, mg P/dm^3		Total phosphorus, mg P/dm^3		Ammonium, mg/dm^3	
		May – June	August – September	May – June	August – September	May – June	August – September
1	S	0.0008	0.0008	0.007	0.0008	< 0.03	< 0.03
	M	0.0040	0.0040	0.001	0.0200	< 0.03	< 0.03
	B	0.0070	0.0070	0.002	0.0390	< 0.03	< 0.03
2	S	0.0004	0.0004	0.027	0.0020	< 0.03	< 0.03
	M	0.0003	0.0003	0.008	0.0004	< 0.03	< 0.03
	B	0.0003	0.0003	0.041	0.0003	< 0.03	< 0.03

Continued Table 3

Station	Water layer	Mineral phosphorus, mg P/dm^3		Total phosphorus, mg P/dm^3		Ammonium, mg/dm^3	
		May – June	August – September	May – June	August – September	May – June	August – September
3	S	0.0007	0.0007	0.0170	0.0007	< 0.03	< 0.03
	M	0.0040	0.0040	0.0013	0.0670	< 0.03	< 0.03
	B	0.0030	0.0030	0.0120	0.0030	< 0.03	< 0.03
3k	S	0.0016	0	0.0016	0.0020	< 0.03	< 0.03
	B	0.0010	0.0020	0.0030	0.0024	< 0.03	< 0.03
4	S	0.0013	0	0.0060	0.0003	< 0.03	< 0.03
	M	0.0013	0.0030	0.0740	0.0030	< 0.03	< 0.03
	B	0.0070	0.0070	0.1140	0.0240	< 0.03	< 0.03
6k	S	0.0010	0.0008	0.0080	0.0008	< 0.03	< 0.03
	B	0.0050	0.0040	0.0010	0.0120	< 0.03	< 0.03
6L	S	0.0080	0.0030	0.0010	0.0100	< 0.03	< 0.03
	B	0.0013	0.0040	0.0160	0.0040	< 0.03	< 0.03
18L	S	0.0016	0.0040	0.0120	0.0200	< 0.03	< 0.03
	B	0.0016	0.0030	0.0390	0.0065	< 0.03	< 0.03
19	S	0.0020	0.0030	0.0020	0.0060	< 0.03	< 0.03
	B	0.0020	0.0040	0.0050	0.0130	< 0.03	< 0.03
20	S	0.0013	0.0003	0.0016	0.0130	< 0.03	< 0.03
	B	0.0010	0.0040	0.0160	0.0290	< 0.03	< 0.03
21	S	0.0013	0.0010	0.0070	0.0310	< 0.03	< 0.03
	B	0.0013	0.0080	0.0016	0.0340	< 0.03	< 0.03

Station	Water layer	Mineral phosphorus, mg P/dm^3		Total phosphorus, mg P/dm^3		Ammonium, mg/dm^3	
		May – June	August – September	May – June	August – September	May – June	August – September
22	S	0.0013	0.0030	0.0013	0.0030	< 0.03	<0.03
	B	0.0003	0.0050	0.0013	0.0090	< 0.03	< 0.03
24	S	0.0013	0.0010	0.0013	0.0120	< 0.03	< 0.03
	B	0.0010	0.00070	0.0220	0.0120	0.04	< 0.03
26	S	0.0013	0.0016	0.0100	0.0040	0.06	< 0.03
	B	0.0140	0.0016	0.0410	0.0050	< 0.03	< 0.03
A	S	0.0008	0.0008	0.0016	0.0008	< 0.03	< 0.03
	M	0.0013	0.0016	0.0100	0.0070	< 0.03	< 0.03
	B	0.0030	0.0340	0.0590	0.0430	< 0.03	< 0.03
Median value		0.0010	0.0030	0.007	0.0070	< 0.03	< 0.03

Note: N/D – not determined. See designations to Table 1. MPC of ammonium – 0.5 mg/L.

In June 2022, mineral phosphorus concentrations were at traditionally low levels. Ammonium nitrogen concentrations were also insignificant. The total phosphorus content varied from 0.001 to 0.074 mg P/dm^3. It exceeded 0.024 mg P/dm^3 at stations *2* (bottom), *4* (middle), *18L* (bottom), *26* (bottom) and *A* (bottom). A similar picture was observed in September, only the content of total phosphorus was from 0.002 to 0.067 mg P/dm^3 and the overflow of the mesotrophic state was recorded at stations *1* (bottom), *3* (middle), *20* (bottom), *21* (bottom) and *A* (bottom). As in September 2020, total phosphorus was accumulated in the bottom layer. In general, the content of biogenic elements in the Gulf water this year was lower than in 2020 and 2021, and the median values of total phosphorus concentrations in both seasons were even at the oligotrophic level.

Conclusion

A comparison of the 2020–2022 measurement results makes it possible to draw a number of conclusions.

Despite high anthropogenic load, the concentrations of mineral phosphorus and ammonium in the waters of the Gulf of Finland are within the MPC limits, and exceedances have been recorded quite rarely.

Over the period under discussion (three years for phosphorus, two years for ammonium), the concentrations of the studied biogenic elements fluctuated within relatively narrow ranges of values showing no obvious trends toward increase or decrease. Significant concentrations of total phosphorus are usually observed in such areas as Neva Bay, Koporye Bay, the area near the coast of the Kurortny district, that is, in the areas with the greatest anthropogenic impact. Once in 2021, an elevated, compared to normal, level of NH_4^+ was recorded in Koporye and Luga Bays, as well as near the coast of the Kurortny district. Stations *4* (deep-water) and *A* (remote from the coast) deserve special attention as there, elevated concentrations of total phosphorus have been periodically recorded. Apparently, this can be explained both by the transport of the substance from the western part of the Gulf and diffusion from bottom sediments.

On average, higher concentrations of total phosphorus were found in bottom water layers than in surface water layers.

Generally, concentrations of biogenic elements correspond to the mesotrophic status of the water body.

REFERENCES

1. Belkina, N.A., Ryzhakov, A.V. and Timakova, T.M., 2008. The Distribution and Transformation of Oil Hydrocarbons in Onega Lake Bottom Sediments. *Water Resources*, 35(4), pp. 472–481. https://doi.org/10.1134/S0097807808040088
2. Kondratev, S.A., Basova, S.L., Ershova, A.A., Efremova, L.V., Markova, E.G. and Shmakova, M.V., 2009. [A Method to Assess Biogenic Load on Water Bodies of the Northern-Western Part of Russia]. *Proceedings of the Russian Geographical Society*, 141(2), pp. 53–63 (in Russian).
3. Ipatova, S.V., 2017. [Sea Water and Bottom Sediment Quality in the Eastern Gulf of Finland According to Monitoring Data of Severo-Zapadnoye UGMS]. In: UGMS, 2017. [*Specialised Provision of Information on the State and Pollution of the Environment in Large Cities: All-Russian Meeting. September 7–8, 2017, Yaroslavl*]. Yaroslavl, 12 p. (in Russian).
4. Kulakov, D.V., Makushenko, M.E. and Vereshchagina, Y.A., 2015. Influence of the Leningrad Nuclear Power Plant on Zooplankton and Zoobenthos of the Gulf of Finland Koporskaya Guba. *Water Sector of Russia: Problems, Technologies, Management*, (1), pp. 42–54 (in Russian).
5. Litina, E.N., Zakharchuk, E.A. and Tikhonova, N.A., 2018. Dynamics of Hypoxia in the Baltic Sea at the Turn of the XX–XXI Centuries. In: P.P. Shirshov Institute of Oceanology, 2018. *Proceedings of the II Russian National Conference "Hydrometeorology and ecology: scientific and educational achievements and perspectives". St. Petersburg, December 19–21, 2018*. St. Petersburg: HIMIZDAT, pp. 404–407 (in Russian).

6. Khmelnitskaya, O.K., 2011. Principal Hydrochemical Parameters of Intermediate and Bottom Water Masses of the North Atlantic. *Vestnik Moskovskogo Universiteta. Seria 5. Geografia*, (6), pp. 60–66 (in Russian).
7. Carlson, R.E., 1977. A Trophic State Index for Lakes. *Limnology and Oceanography*, 22(2), pp. 361–369. Available at: https://aslopubs.onlinelibrary.wiley.com/doi/abs/10.4319/lo.1977.22.2.0361 [Accessed: 31 May 2024].
8. Briukhanov, A.Yu., Kondratyev, S.A., Vasilev, E.V., Minakova, E.A., Terekhov, A.V. and Oblomkova, N.S., 2018. Assessment of Agricultural Nutrient Load Generated on the River Catchment Areas Within the Kuybyshev Reservoir Basin. *Technologies, Machines and Equipment for Mechanised Crop and Livestock Production*, 96, pp. 175–186. https://doi.org/10.24411/0131-5226-2018-10071 (in Russian).
9. Korkishko, N.N., Kulish, T.P., Petrova, T.N. and Chernykh, O.N., 2002. [Aquatic Humic Matter in Lake Water and its Transformation]. In: V. A. Rumyantsev, and V. G. Drabkova, eds., 2002. [*Ladoga Lake: Past, Present, Future*]. Saint Petersburg: Nauka, pp. 111–117 (in Russian)].
10. Siniakova, M.A., Ponomarenko, A.M. and Krylova, U.V., 2022. Seasonal Changes in the Concentrations of Phosphorus and Petroleum Hydrocarbons in the Water of the Eastern Part of the Gulf of Finland. *Ekologicheskaya Khimiya*, 31(2), pp. 92–98 (in Russian).
11. Ershova, A.A., Korobchenkova, K.D. and Agranova, Ju.S., 2018. Assessment of the State of the Gulf of Finland Based on HELKOM Indicators of Eutrophication. *Proceedings of the Russian State Hydrometeorological University*, 51, pp. 137–149 (in Russian).

Submitted 01.02.2024; accepted after review 26.02.2024;
revised 27.03.2024; published 25.06.2024

About the authors:

Mariia A. Siniakova, Leading Research Associate, Laboratory of Fishery Ecology, Saint Petersburg Branch of VNIRO (GosNIORKH named after L.S. Berg) (26 Makarova Emb., Saint Petersburg, 199053, Russian Federation); Lecturer of the Department of Ergonomics, Ecology and Labor Law, Saint-Petersburg State Marine Technical University (3 Lotsmanskaya St., Saint Petersburg, 190121, Russian Federation), Ph.D. (Chem.), **ORCID ID: 0000-0001-9352-2083,** *kafischem@yandex.ru*

Julia V. Krylova, Senior Research Associate, Papanin Institute for Biology of Inland Waters Russian Academy of Sciences (109, Borok, Nekouzskiy District, Yaroslavskaya Region, 152742, Russian Federation), Ph.D. (Geogr.), **ORCID ID: 0000-0002-4274-2358**

Liliya V. Bronnikova, Head of the Department of Ergonomics, Ecology and Labor Law, Saint-Petersburg State Marine Technical University (3 Lotsmanskaya St., Saint Petersburg, 190121, Russian Federation), Ph.D. (Econ.), **ORCID ID: 0000-0002-8710-5328**

Contribution of the authors:

Mariia A. Siniakova – article concept development, study results processing and description, literature review

Julia V. Krylova – aim statement, study results processing and description, literature review

Liliya V. Bronnikova – qualitative analysis of results and their interpretation, literature review

All the authors have read and approved the final manuscript.

ISSN 2413-5577, Ecological Safety of Coastal and Shelf Zones of Sea, 2024, No.2, pp. 107–121.

Original article

Environmental Hazard Assessment of Storage Conditions of Wastes from Mining and Processing of Arsenopyrite Minerals

Le Thu Thuy [1]*, Tran Hong Con [2], Nguyen Trong Hiep [3], Vu Thi Minh Chau [3], Le Minh Tuan [4], Do Hoang Linh [2]

[1] *Hanoi University of Natural Resources and Environment, Hanoi, Vietnam*

[2] *Hanoi University of Science, Vietnam National University, Hanoi, Vietnam*

[3] *Southern Branch of Joint Vietnam-Russia Tropical Science and Technology Research Center, Ho Chi Minh, Vietnam*

[4] *Institute of science and technology for energy and environment, Vietnam Academy of Science and Technology, Ho Chi Minh, Vietnam*

* *e-mail: ltthuy.mt@hunre.edu.vn*

Abstract

Arsenopyrite is a common mineral of the sulphide class, belonging to minerals of hydrothermal genesis. On anthropogenic dumps, arsenopyrite is exposed to weathering agents and releases arsenic into the environment. In areas, where Cu, Pb, Zn minerals are mined, arsenic contamination of the environment is a serious problem. The results of this study show that arsenopyrite ores are capable of releasing arsenic and heavy metals during weathering on dumps under seepage and flooding conditions. The paper presents the results of a laboratory experiment on a developed simulation model of substance change in ore mine dumps under two conditions: seepage (modelling open ore dumps through which rainwater seeps) and flooding (modelling ore dumps stored in flooded lowland areas). The modelling conditions were consistent with the real ones. The ratio of arsenopyrite and sand was 1:20. The duration of the experiment was 60 days, which allowed determining arsenic in different chemistries. During the experiment under water seepage conditions, pH decreased and redox potential varied from 5 to 50 mV. With decreasing pH, release of metals and arsenic into the environment increased over time. Once pH reached values characterising an acidic environment (2.0–4.5), weathering markedly accelerated. Under conditions of excess water with high dissolved oxygen content, metals released faster. When pH was between 5.5 and 6.0, the rate of metal release decreased. When the ore was oxidised, iron in the divalent form Fe(II) slowly oxidised to Fe(III) at the pH value above. Under these conditions, Fe(III) was hydrolysed in the column. Thus, the released arsenic was adsorbed on Fe(III) and the resulting iron hydroxide $Fe(OH)_3$ coated the ore particles. Due to the reduced contact of the waste ore with the aqueous medium, the arsenic concentration continued to decrease. Under both seepage and flooding conditions, As(III) dominated As(V) in the flow exiting the ore column. As(III) can be highly toxic to the environment, therefore care should be taken to ensure that conditions are provided for its conversion to less toxic As(V).

Keywords: arsenic pollution, arsenic transformation, arsenopyrite, ore mining, toxic waste, industrial waste, anthropogenic pollution

Acknowledgements: We express our sincere gratitude to the Hanoi University of Natural Resources and Environment, Hanoi University of Science, the Southern Branch of the Joint Russian-Vietnamese Tropical Research and Technology Centre and the Institute of Environmental Technology, Vietnam Academy of Science and Technology, which created the conditions for the study and helped the research team in its implementation.

For citation: Le Thu Thuy, Tran Hong Con, Nguyen Trong Hiep, Vu Thi Minh Chau, Le Minh Tuan and Do Hoang Linh, 2024. Environmental Hazard Assessment of Storage Conditions of Wastes from Mining and Processing of Arsenopyrite Minerals. *Ecological Safety of Coastal and Shelf Zones of Sea*, (2), pp. 107–121.

Оценка экологической опасности условий хранения отходов добычи и переработки арсенопиритных минералов

Ле Тху Тхуи [1]*, Чан Хонг Кон [2], Нгуен Чонг Хиеп [3], Ву Тхи Минь Чау [3], Ле Минь Туан [4], До Хоанг Линь [2]

[1] *Ханойский университет природных ресурсов и окружающей среды, Ханой, Вьетнам*

[2] *Ханойский Университет естественных наук, Ханой, Вьетнам*

[3] *Южное отделение Совместного Российско-Вьетнамского Тропического научно-исследовательского и технологического центра, Хошимин, Вьетнам*

[4] *Институт экологических технологий, Вьетнамская академия наук и технологий, Хошимин, Вьетнам*

* *e-mail: ltthuy.mt@hunre.edu.vn*

Аннотация

Арсенопирит – распространенный минерал класса сульфидов, относящийся к минералам гидротермального происхождения. На техногенных отвалах арсенопирит подвергается воздействию агентов выветривания и выделяет мышьяк в окружающую среду. В районах, где разрабатываются минералы Cu, Pb, Zn, загрязнение окружающей среды мышьяком является серьезной проблемой. Результаты настоящего исследования показывают, что при выветривании на отвалах в условиях просачивания и затопления арсенопиритные руды способны выделять мышьяк и тяжелые металлы. Представлены результаты лабораторного эксперимента на разработанной имитационной модели изменения вещества в рудных отвалах шахт при двух условиях: при просачивании (моделирование открытых отвалов руды, через которые просачивается дождевая вода) и затоплении (моделирование отвалов руды, хранящихся в затопленных низинных районах). Модельные условия соответствуют реальным. Соотношение арсенопирита и песка 1:20. Продолжительность эксперимента составляет 60 сут, что позволяет определить мышьяк в различных химических веществах. В ходе эксперимента в условиях инфильтрации воды pH снижается, а окислительно-восстановительный потенциал варьирует от 5 до 50 мВ, при снижении pH выделение металлов и мышьяка в окружающую среду с течением времени увеличивается. По достижении pH значений, характеризующих кислую среду (2.0–4.5), выветривание

заметно ускоряется. В условиях избытка воды при высоком содержании растворенного кислорода металлы высвобождаются быстрее. Когда pH находится в диапазоне от 5.5 до 6.0, скорость высвобождения металлов снижается. При окислении руды железо в двухвалентной форме Fe(II) медленно окисляется до Fe(III) при pH, указанном выше. В этих условиях Fe(III) гидролизуется в колонке. Таким образом, выделяющийся мышьяк адсорбируется на Fe(III), а образующийся гидроксид железа $Fe(OH)_3$ покрывает частицы руды.

Ключевые слова: загрязнение мышьяком, трансформация мышьяка, арсенопирит, добыча руды, токсичные отходы, промышленные отходы, антропогенное загрязнение

Благодарности: авторы выражают искреннюю благодарность Ханойскому университету природных ресурсов и окружающей среды, Ханойскому университету естественных наук, Южному отделению Совместного российско-вьетнамского тропического научно-исследовательского и технологического центра и Институту экологических технологий, Вьетнамской академии наук и технологий, которые создали условия для проведения исследования и помогли исследовательской группе в его реализации.

Для цитирования: Оценка экологической опасности условий хранения отходов добычи и переработки арсенопиритных минералов / Ле Тху Тхуи [и др.] // Экологическая безопасность прибрежной и шельфовой зон моря. 2024. № 2. С. 107–121. EDN WCMKJB.

Introduction

Arsenopyrite is a compound of iron and arsenic sulphide (FeAsS) and one of the most common minerals among sulphides today. The chemical composition of arsenopyrite, according to microprobe analysis, is usually as follows: Fe = 34.05%; As = 43.87%; S = 21.76% [1]. Samples of waste arsenopyrite ore for this study were taken from tin ore mining and processing waste in the upper reaches of the Nam Huong River (Quy Hop district, Nghe An province, Vietnam).

Mining has a negative impact on the environment and poses a danger to the ecosystem in general and to humans in particular [2]. It is a significant problem in many countries around the world, including Vietnam.

The mining and processing of natural resources increases the rate at which heavy metals enter the environment, including aquatic ecosystems. Waste arsenopyrite ore stored in dumps is exposed to the atmosphere and slowly oxidises. In the process, arsenic converts to more water-soluble oxides, which through natural transformation leads to the release of sulphur. These sulphide minerals oxidise to form acid mine discharges and alter the properties and toxicity of the metals. Despite the risk of arsenic and heavy metal pollution from mine acid wastewaters and ore dumps, little attention has been paid to this problem.

High levels of arsenic have been found in the area of ore mining, possibly due to the weathering of FeAsS arsenopyrite and its leaching in water, especially in an old tin mine in the Ron Phibun area of Thailand (5000 μg/L). In the USA, the mining district of Fairbanks County (Alaska) has an arsenic concentration of 104 μg/L, and arsenic concentrations in groundwater in Coeur d'Alene County (Idaho) are as high as 1400 μg/L [3].

G. S. Kamm et al. [4] found in their study that arsenic in the form of methylated compounds is transformed to a lesser extent than inorganic arsenic (As^{3+} and As^{5+}). Inorganic arsenic in soil can undergo various transformations including oxidation decrease, functional degradation and biotransformation. The flooded soil is dominated by arsenite with low redox potential, and at pH equal to 5–8, As^{+5} is mostly transformed as As^{3+}, while in a reducing environment and at low pH, As(III) will dominate.

Some studies on geochemical characteristics of arsenic in mining operations showed that the release of arsenic into the environment strongly depends on the pH value, redox potential and heavy metal content [5, 6].

Today, there are limited studies on arsenic transformation in Vietnam, so studying the release of heavy metals, As(III) and As(V) on ore dumps is of great importance. This will improve the environmental protection of mining operations and storage of their waste in natural conditions.

The purpose of this study is to use the results of laboratory experiments to assess the impact level of waste from arsenopyrite minerals mining and processing on the environment under different conditions of their storage (seepage and flooding).

Experimental part

Design and construction of experimental models, preparation of reagents

To study the release of arsenic and heavy metals from arsenopyrite ore dumps and the transformation of As(III) into As(V), it is first of all necessary to develop a simulation model of substance change in mine ore dumps under conditions of seepage (an open ore dump into which rainwater seeps is modelled) and flooding (ore dumps stored in flooded lowland areas are modelled) [7]. The structure of the experimental model is presented in Fig. 1, the main elemental composition in a sample of a 1:20 mixture of arsenopyrite ore and sand is given in Table.

Element composition (mg/kg) of arsenopyrite ore samples and mixture of arsenopyrite ore with sand (1:20)

Material	As	Cr	Mn	Fe	Ni	Cu	Zn	Cd
Arsenopyrite ore	164.73	9.32	1253.52	21377.45	47.96	5257.54	576.45	14.20
Mixture of arsenopyrite ore with sand	8.12	0.51	60.32	987.16	2.81	646.64	26.43	1.46

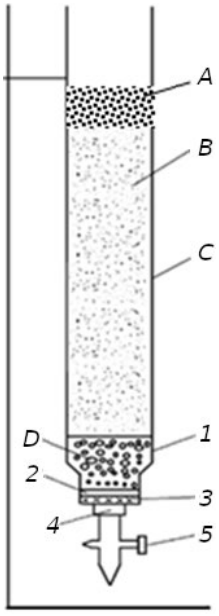

Fig. 1. Equipment scheme: 1 – plastic lid; 2 – fine mesh; 3 – plastic sheet (PE); 4 – rubber buttons; 5 – valve in the lower part; A – layer of gravel and soil taken from dump; B – sample of pyrite ore mixed with sand; C – column; D – gravel layer

The mixture of arsenopyrite ore and quartz sand in the ratio of 1:20 (this ratio is similar to that in the ore dump) is packed into a test column of 45 × 1000 mm (particle size 0.5–2.0 mm) and void volume of about 250 ml is left (Fig. 1). The order of the layers in the filled column is as follows. The first layer (*A*), 20 mm thick, is a mixture of soil debris and gravel removed from the mine to create conditions close to real ones (organic matter from 1.5%) [8]. The second layer (*B*) is an ore–sand mixture 650 mm thick, weighing 878 g. The third layer (*D*) is a supporting layer of gravel with a diameter of 3–5 mm. The composition of the used aqueous phase is similar to that of natural rainwater [9].

The composition of the used aqueous phase (in mg/L) is similar to natural rainwater (pH = 6.5):

Ca^{2+}	2.4	Cl^-	3.90	NH_4^+	1.5	NO_3^-	4.44
Na^+	8.5	SO_4^{2-}	5.35	Mg^{2+}	1.9	HCO_3^-	24.40

Reagents. As(III) 0.1 M (7500 ppm) standard solution: a mixture of 0.9902 g arsenic (III) oxide and 2.5 g NaOH (chemically pure) was placed in a 100 mL measuring flask, then 70 mL of hypoxic water was added and shaken. Then 10 mL of 2 M solution of HCl in hypoxic water was added, brought to the mark with hypoxic water and stirred. The experiments were carried out under nitrogen atmosphere.

Standard solutions of As(V) and metal ions Cu^{2+}, Cd^{2+}, Mn^{2+}, Fe^{2+}, Ni^{2+}, Zn^{2+} were prepared from Merck standard solutions.

Procedure

Seepage conditions. Water with the composition given above was poured into the column (Fig. 1), with the mouth of the column and the valve at the bottom open for two days. Then 120 mL of water simulating natural rainwater was poured into the column. The valve was opened and the seepage rate in the column was maintained at 8.5 cm/h (normal rate of water seepage through a waste ore layer) [10].

The solution that had passed through the column was collected in full. Then 20 mL of the collected solution was taken to analyse the content of Fe, Mn, Ni, Cu, Zn, total As, As(III) and As(V), which are the major ions often accompanying the weathering process of arsenopyrite. The remainder of the sample was saved for the following experiments. The valve and the column mouth were opened.

In five days, 120 mL of water simulating natural rainwater was added to the stored solution, then it was passed through the column and sampled. This sampling process was repeated once a day for five days (simulation of natural processes).

Flooding conditions. The research equipment was set up as shown in Fig. 1, and the effect of horizontal flow was not considered in the experiment due to its less influence on the weathering process. The arsenopyrite ore from the dump and the used aqueous phase had the same composition as in the seepage conditions.

First, the aqueous phase was oxygenated using an aerator to ensure a dissolved oxygen concentration of about 8 mg/L. After loading the ore, the column was continuously kept filled. The water level was 25 cm above the upper boundary of the ore–sand layer. The samples were left for five days after collection. At the same time, 20 mL of the newly collected solution were carefully withdrawn to analyse the same parameters that were determined under seepage conditions. The amount of water lost during sampling was replenished.

Under both seepage and flooding conditions, the experiment was conducted for 60 days [1]. An aliquot of the sample was taken at the same time to analyse for heavy metal content. The modelling experiments were repeated three times.

To further investigate the ability to release iron and arsenic in an acidic medium under real conditions, the authors conducted experiments at pH values from 4.5 to 2.5. The course of the experiment was the same as under seepage conditions: 120 mL of aqueous phase with the above composition was added in a pre-stored solution. A 4 M HCl solution was used to adjust the pH value of the water before each wash through the column and 20 mL of sample was taken for analysis. The above procedure was repeated (pH adjustment for five days and sampling).

Methods of As(III) and As(V) separation and quality indicator in a sample

The method of As(III) and As(V) separation in a solution of ethanol and water with a ratio of 30:70 involves single filtration using Lewatit MonoPlus M 500 ion exchange resin [11]. All experiments were performed in the nitrogen atmosphere to prevent arsenic oxidation. The process of arsenic extraction is shown in Fig. 2.

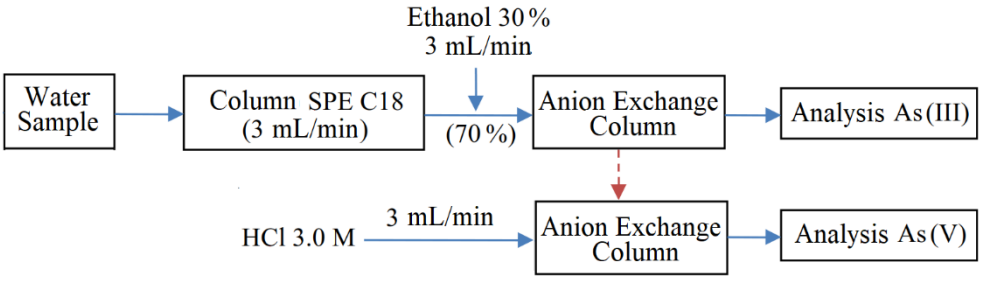

F i g . 2 . Scheme of separation of As(III) and As(V) [11]

The content of Ni^{2+}, Cu^{2+}, Pb^{2+}, Zn^{2+}, Fe^{2+}, As(III) and As(V) ions was analysed on an atomic absorption spectrometer, As was analysed by the cold vapour method.

Sample processing and analysis

The liquid samples were treated using HNO_3 and HCl acids at a volume ratio of HNO_3:HCl as 1:3, at a rate of 50 mL of acid mixture per 100 mL of the sample. Then, As and heavy metals were measured using an atomic absorption spectrophotometer (model iCE 3500, Thermo Scientific, USA), Fe^{2+} was analysed according to the Vietnamese standard TCVN on a DR 5000 device (HACH), whereas pH, Eh and dissolved oxygen content were measured using Hanna HI98304 electrodes (Romania).

Solutions of HCl, HNO_3 with different concentrations were prepared from 37% concentrated perchloric acid HCl and 65% nitric acid HNO_3 (chemically pure, Merck) in distilled water or in hypoxic distilled water, depending on the requirements of each experiment.

After separation of As(III) and As(V) by single filtration using Lewatit MonoPlus M 500 ion exchange resin. A solution of ethanol and water (30:70% vol.) [1)] was used as a reference solution [10], and the method reproducibility, the limit of detection (LOD) and the limit of quantification (LOQ) were evaluated [12].

The method reproducibility was calculated using the following formula:

$$S_r = SD = \sqrt{\frac{1}{n-1}\sum_{i=1}^{n}(X_i - \overline{X})^2}, \qquad RSD\% = \frac{S_r}{\overline{X}} \times 100,$$

where S_r – standard deviation of repeatability; $\overline{X}$ – average concentration of the analysed substance in the test sample; X_i – concentration of the sample of the i-th test; n – number of repetitions (10 times); RSD – relative standard deviation.

Limit of detection: LOD = 3 × SD.

Limit of quantification: LOQ = 10 × SD.

According to the experimental results, the LOD, LOQ values for As(III) were 0.06 and 0.1, respectively, and for As(V) were 0.05 and 0.08, respectively. These low values show that the analysis allows separation of As(III) and As(V) even for samples with low arsenic content.

[1)] Le Tu Hai, 2016. *Study of separation and determination method for anorganic arsenic(III) and arsenic(V) forms in natural water samples*. Abstract of doctoral thesis. Vietnam National University, Hanoi.

Results and discussion

Rate of metal and arsenic release in seepage conditions

Change in the pH and redox potential Eh values in seepage conditions

The experiment was conducted as described in Section 2.2, with the thickness of the ore dump layer being 65 cm. But in fact, the exposed waste ore dumps can be tens of metres thick. Thus, the experimental model gradually accumulates weathering products. Fig. 3 shows the changes of pH and Eh after 60 days of testing.

The results of the studies, presented in Fig. 3, showed that pH tends to decrease gradually and Eh tends to increase gradually, but for 60 days of observation the change in the model was insignificant. The decrease in pH in the aqueous phase was due to the weathering of sulphur minerals (mainly iron sulphide) with the formation of H^+ ions,

$$2FeS_2 + 5O_2 + 2H_2O \leftrightarrow 2Fe^{2+} + 4SO_3^{2-} + 4H^+$$

and hydrolysis of metal ions (mainly Fe^{3+})

$$Fe^{3+} + 3H_2O \leftrightarrow Fe(OH)_3 + 3H^+.$$

A small amount of Fe(II) was released in the first few days, and the oxidation of Fe(II) to Fe(III) consumed H^+ ions:

$$2Fe^{2+} + {}^1/_2O_2 + 2H^+ \leftrightarrow 2Fe^{3+} + H_2O.$$

Thus, the pH value did not change significantly. When iron was released in larger amounts, the hydrolysis occurring in the column along with oxidative weathering led to an increase in the concentration of H^+ ions, so the pH always tended to decrease [13].

At the same time, the redox potential of the solution (Eh) seeping through the waste ore column tended to increase gradually. This may be due to the fact that initially arsenopyrite particles are less bound, so their contact with dissolved oxygen and air oxygen causes oxygen to diffuse through the aqueous film. Therefore,

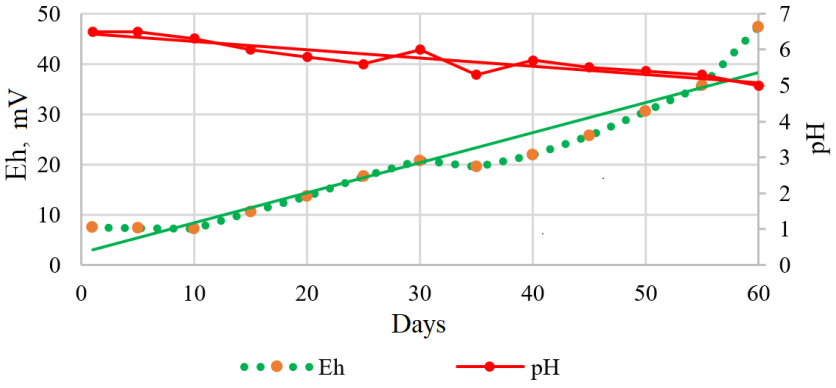

Fig. 3. Dynamics of pH и Eh under seepage conditions

more oxygen is consumed. Over time, the surface of ore grains decreases due to adhering layers of iron hydroxide, which hinder the oxidative weathering process. But under the experimental conditions, the total amount of air oxygen entering the waste ore column during sampling was almost the same.

Consequently, the concentration of dissolved oxygen increased. This led to an increase in Eh of the aqueous phase passing through the column. Throughout the experiment, the pH of the aqueous phase was always between 5 and 6, so it can be considered that the concentration of Fe^{3+} was only within the solubility product of $Fe(OH)_3$ at the corresponding pH value. Consequently, Fe^{3+} has an insignificant effect on the redox potential of the aqueous phase.

Release rate of arsenic and heavy metals in the aqueous phase

Changes in the concentrations of arsenic and some major heavy metals in arsenopyrite ore accumulated in the aqueous phase during 60 days are shown in Fig. 4.

During the first 30 days of the experiment, when the waste ore was exposed to air and water oxygen, the release of iron and arsenic from the ore tended to increase gradually and pH of the aqueous phase was about 6.0. At this pH value, Fe(II) was oxidised to Fe(III) due to dissolved air oxygen in water, simultaneously Fe(III) was hydrolysed to form a sparingly soluble $Fe(OH)_3$ precipitate and remained on the waste ore column. The released arsenic is also adsorbed on $Fe(OH)_3$, so the arsenic concentration in the aqueous phase increased slowly.

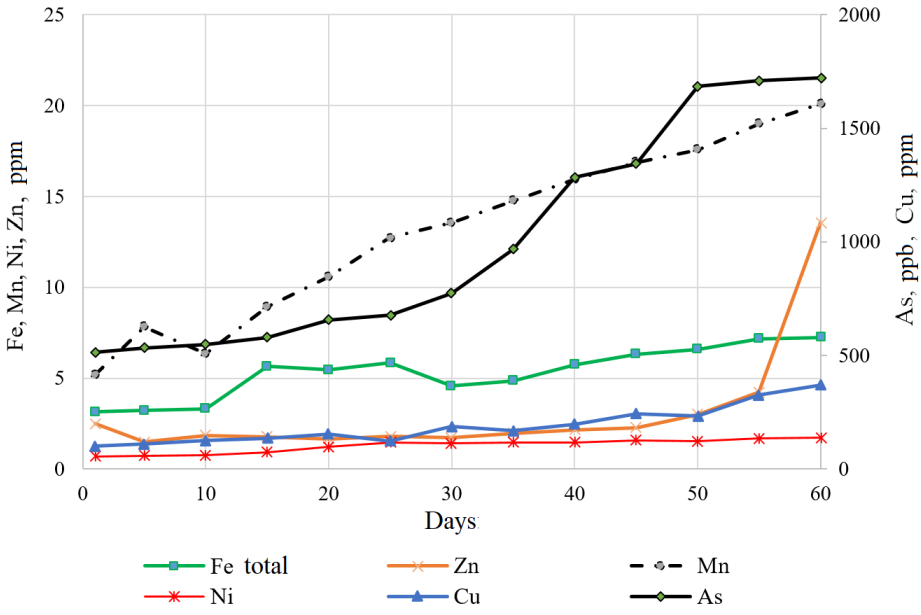

Fig. 4. Release of arsenic and some metals into the water phase

After 30 days, when pH of the aqueous phase decreased below 6 and continued to decrease below 5, the concentration of total iron in the aqueous phase increased markedly due to a decrease in the oxidising capacity of air oxygen and the precipitation of $Fe(OH)_3$ decreased. In parallel with this process, the total arsenic concentration was increasing rapidly as the percentage of this element, adsorbed on $Fe(OH)_3$, was decreasing.

The content of iron and arsenic in the aqueous phase at this stage is also affected by the increased rate of ore weathering along with an increase in H^+ concentration in the aqueous phase. The content of other metals increased markedly only during the first week of weathering; thereafter, it remained almost unchanged. At the same time, arsenic was also adsorbed on the formed $Fe(OH)_3$ until pH of the water decreased to about 5.0. The mechanism of heavy metals (Mn, Ni, Cu and Zn) release from the ore is the same as for arsenopyrite. When the pH value falls below 5.0, their concentration noticeably increases and is: Mn from 5.21 to 20.11 ppm, Ni from 0.67 to 1.74 ppm, Cu from 99.64 to 370.42 ppm and Zn from 2.51 to 13.56 ppm. The above results showed that pH is a secondary factor, while it has a decisive influence on the release of arsenic and other heavy metals from exposed dumps of arsenopyrite ore.

The study results also showed that the release of arsenic and heavy metals in the waste ore increases over time and their concentration in the filtrate stream will increase (especially Zn and Mn) (Fig. 4). Consequently, they pose a higher risk to the environment.

Transformation of arsenic during arsenopyrite weathering

The experiment under the above conditions shows that in parallel with oxidative weathering of arsenopyrite, As(III) is oxidised and released from the ore, as well as sulphur is. The results showed that Eh of the aqueous phase in the column varied from 5 to 50 mV (Fig. 5). Over time, as the concentration of As(III) increased, the concentration of As(V) also increased. This suggests that the oxidation of As(III) to As(V) in the waste ore occurs almost continuously, at pH values between 5 and 6. There is a balance between adsorption and desorption of pentavalent arsenic on precipitated $Fe(OH)_3$ in the column as well as between As(III) and As(V) content in the aqueous phase, which is also shown by [1].

In dumps of arsenopyrite ores or sulphur-containing minerals, the actual measured pH of the filtrate has very low values (from 2.5 to 4.5) [13, 14]. This pH favours the dissolution of minerals with the formation of dissolved metals, which are toxic particles that then enter the water.

During the experiment, the pH value of the solution in the waste ore column may not have reached the actual pH values in the aqueous phase (Fig. 5).

Fig. 5 shows that pH decreased from 4.5 to 3.5 and the total iron concentration in the aqueous medium increased sevenfold. This is due to the solubility of iron in water, mainly Fe(III), by precipitation of hydroxide. At the same time weathering was stronger in the acidic environment. At pH from 3.5 to 2.5, the total iron concentration increased more slowly (about 2.2 times), since the hydroxide forms of iron are almost completely dissolved in the aqueous phase in the form of

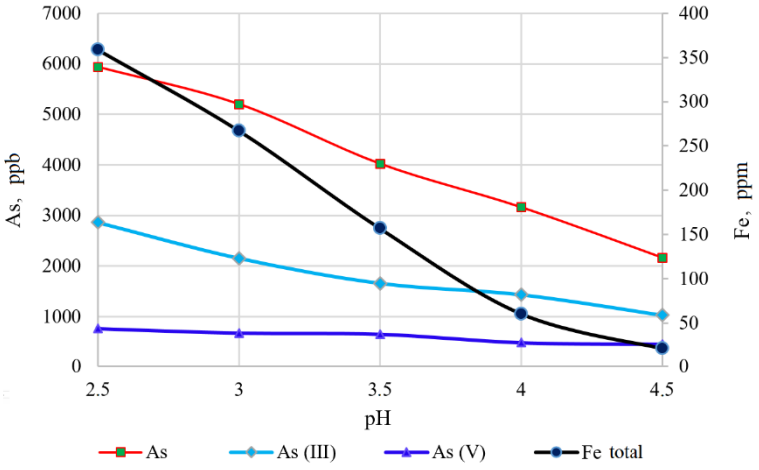

Fig. 5. Release of iron under low pH

$Fe(OH)^{2+}$ and $Fe(OH)^{2+}$ hydroxocations, as well as Fe^{3+}. As can be seen in Fig. 5, As(V) is an ion with strong adsorption capacity on Fe(III) hydroxide, so in the region of low pH values, the concentration of As(V) increased less than that of As(III)). This indicates that As(V) was not adsorbed (whereas $Fe(OH)_3$ was almost absent). When pH decreased from 3.5 to 2.5, the concentrations of Fe and As(III) increased, possibly due to an increase in the weathering rate in the acidic media, resulting in greater release of these elements into the aqueous phase.

Release rates of weathering products and some heavy metals in flooding conditions

The experiments were carried out as described in Section 2.2. The changes in pH, Eh and concentration of some typical heavy metals during the experiment are presented in Fig. 6, which shows that the pH value decreased markedly (from 6.5 to 5.0) when the ore was loaded into the column. The decrease in pH is due to the fact that dissolved oxygen in the initial aqueous phase provides the oxidative weathering of the ore. As a result, a certain amount of H^+ ions is released and pH decreases. In this condition, the Eh value decreased sharply, possibly due to the oxidation processes in the ore, which resulted in the formation of alternative forms of reduced compounds. By the end of the experiment, the Eh value decreased sharply due to the predominance of reduced forms, and no more dissolved oxygen was introduced into the column.

In flooding conditions with low water content, the pH and Eh dynamics were completely different from those under seepage conditions, and the weathering processes with release of ions into the aqueous phase also varied completely in different conditions. Concentrations of heavy metals in the water increased significantly in the first three weeks and then decreased slowly (Fig. 6, *b*). This is fully consistent with the evolution of the pH value in the aqueous phase. As mentioned above,

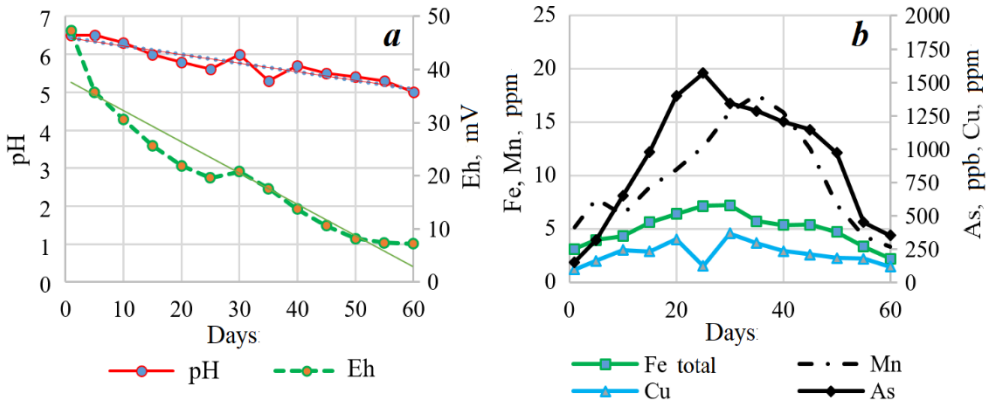

Fig. 6. Dynamics of pH и Eh (*a*) and concentrations of some elements (*b*) under flooding conditions

oxidative weathering occurs at this stage under the influence of initially dissolved oxygen. However, with a gradual decrease in oxygen content, the pH increased, Eh decreased, the concentration was almost constant, as with other metals, and then gradually decreased. This reduction process occurs because the amount of generated metal ions decreases while pH increases, which favours the adsorption of metal ions and their stronger binding to the newly formed $Fe(OH)_3$. This is also in agreement with the results of similar studies [5, 13].

In conditions of oxygen deficiency in water, the concentration of As(V) in the aqueous phase tended to decrease gradually with decreasing dissolved oxygen, while the concentration of As(III) increased gradually (Fig. 7). In this case,

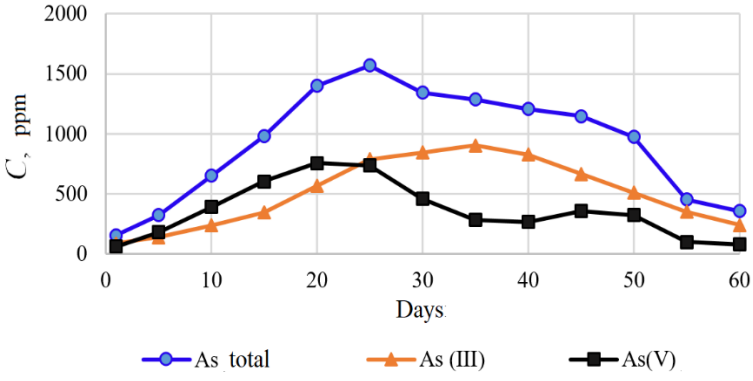

Fig. 7. Transformation of arsenic under flooding conditions

it can be clearly seen that the total concentration increased only in the first days when oxidative weathering process mainly occurred. Consequently, the concentration of metals increased in the aqueous environment. Then, with decreasing oxygen content, the total concentration hardly changed. Only the transformation of As(V) to As(III) in the aqueous phase took place with the predominance of reducing ions such as sulphite ions.

The above experimental results show that in the open air the dumped arsenopyrite ore is able to oxidise with the release of iron and other heavy metals. However, at pH value > 5 heavy metals are easily adsorbed and bound to Fe(III) hydroxide, which results in reduction of their ability to enter the environment. In the pH range from 2.5 to 5.0, large amounts of iron and other heavy metals are released.

Under flooding conditions, due to oxygen deficiency, the weathering process only occurs initially, when there is still enough oxygen in the aqueous phase as well as in the dumped ore mass. After that, the weathering process almost stops, instead reactions between the previously formed products take place, with the ion concentration in the aqueous phase almost unchanged.

If tailings of arsenopyrite or other sulphide minerals are left submerged, the potential for environmental contamination from weathering will be greatly reduced.

Conclusion

In order to assess the environmental safety of storage conditions of arsenopyrite waste ore dumps, the paper presents the results of laboratory experiment in two conditions: under seepage (modelling of an exposed ore dump with rainwater seepage) and flooding (modelling of ore dumps stored in flooded lowland areas). The obtained data allowed assessment of the influence of storage conditions on the release of arsenic and other heavy metals into environmental objects.

Laboratory modelling of weathering of arsenopyrite waste ore in seepage conditions shows that the pH value gradually decreases with time; while the content of released elements gradually increases. At lower pH values (4.5÷2.5), the concentration of elements in the aqueous phase noticeably increases. This is explained by the effects of adsorption, desorption, dissolution of Fe(III) hydroxide formed due to weathering of ore, and formation of acid in the process of weathering.

In flooding conditions, the elements are released from arsenopyrite ore only in the initial period, then weathering almost does not occur and the concentration of the elements in the aqueous phase almost does not increase.

Weathering of arsenopyrite ore is one of the pathways for metals to enter the aquatic environment and is a cause of environmental pollution. Thus, limiting the As release process by storing waste ore and ore tailings in a flooded form will significantly reduce environmental pollution during mining of arsenopyrite and sulphur-containing ores in general.

Thus, As(III) dominates the weathering process. It is toxic to the environment, so further research is needed to propose solutions for its conversion to As(V).

REFERENCES

1. Burnol, A., Garrido, F. and Charlet, L., 2008. Release of As(III) in the Groundwater: An Energy Driven Model Tested Synthetic Ferrihydrite and on Bengan Delta Sediments. In: Valencia, 2008. *Proceedings of As 2008: Arsenic in the Environment, Arsenic from Nature to Humans, the 2nd International Congress, Valencia, Spain*. Valencia, pp. 19–20.
2. Dang Van Can Đ. N. P., 2000. Assessment of the Arsenic Impact on the Environment and Human Health in Hydrothermal Deposits with High Arsenic Content. *Geology and Minerals Journal (Institute of Engineering and Technology, Hanoi)*, VII, pp. 199–204 (in Vietnamese).
3. Sherwood Lollar B., 2005. *Environmental Geochemistry*. Elsevier, 648 p.
4. Camm, G.S., Glass, H.J., Bryce, D.W. and Butcher, A.R., 2004. Characterisation of a Mining-Related Arsenic-Contaminated Site, Cornwall, UK. *Journal of Geochemical Exploration*, 82(1–3), pp. 1–15. doi:10.1016/j.gexplo.2004.01.004
5. Armienta, M.A. [et al.], 2008. Arsenic Mobilization Within Tailings of two Historical Mexican Mining Zone. In: Valencia, 2008. *Proceedings of As 2008: Arsenic in the Environment, Arsenic from Nature to Humans, the 2nd International Congress, Valencia, Spain.* Valencia, pp. 45–46.
6. Bobos, I, Durães, N. and Noronha, F., 2006. Mineralogy and Geohemistry of Mill Tailings Impoundments from Algares (Aljustrel), Portugal: Implication for Acid Sulfate Mine Water Formation. *Journal of Geochemical Exploration*, 88(1–3), pp. 1–5. doi:10.1016/j.gexplo.2005.08.004
7. Ceniceros, N. [et al.], 2008. Impact of Tallings on Arsenic and Heavy Metal Contaminated of a Mexican River. In: Valencia, 2008. *Proceedings of As 2008 : Arsenic in the Environment, Arsenic from Nature to Humans, the 2nd International Congress, Valencia, Spain*. Valencia, pp. 149–150.
8. Hu, Q.H., Sun, G.X., Gao, X.B. and Zhu, Y.G., 2012. Conversion, Sorption, and Transport of Arsenic Species in Geological Media. *Applied Geochemistry*, 27(11), pp. 2197–2203. doi:10.1016/j.apgeochem.2012.01.012
9. Hu, G.P., Balasubramanian, R. and Wu, C.D., 2003. Chemical Characterization of Rainwater at Singapore. *Chemosphere*, 51(8), pp. 747–755. https://doi.org/10.1016/S0045-6535(03)00028-6
10. Bui Xuan Dung, 2016. The water infiltration under some types of land use in Luot mountain, Xuan Mai, Hanoi. *Journal of Forestry Science and Technology*, 4, pp. 47–58 (in Vietnamese).
11. Le Tu Hai, Tran Hong Con and Pham Hong Chuyen, 2014. Investigation of Retention and Separation of As(III) away from As(V) in the Same Water Solution Bay Anionic Exchange Resin. *VNU Journal of Science, Natural Science and Technology*, 30(5S), pp. 190–195 (in Vietnamese).
12. Tran Cao Son, Pham Xuan Da, Le Thi Hong Hao and Nguyen Thanh Trung, 2010. *Expertise Method in Analysis of Chemical and Micro-Biological*. Science and Technics Publishing House, pp. 32–48 (in Vietnamese).
13. Silva, A., Delertue-Matos, C. and Fiúza, A., 2008. Arsenic Leaching in the Tailing Material of Vale das Gatas Abandoned Mine (Northern Portugal) – A Case Study. In: Valencia, 2008. *Proceedings of As 2008 : Arsenic in the Environment, Arsenic from Nature to Humans, the 2nd International Congress, Valencia, Spain.* Valencia, pp. 145–146.
14. Ho Si Giao and Mai The Toan, 2010. *Pollution Point in Mining of Vietnam International Cooperation*. Vietnam Mining Science and Technology Association (VMSTA) (in Vietnamese).

Submitted 20.04.2023; accepted after review 28.10.2023;
revised 27.12.2023; published 25.06.2024

About the authors:
Le Thu Thuy, Lecturer, Department of Environment, Hanoi University of Natural Resources and Environment (No. 41A, Phu Dien Street, Bac Tu Liem District, Hanoi city, Vietnam), *ltthuy.mt@hunre.edu.vn*
Tran Hong Con, Lecturer, Chemistry Department, Hanoi University of Science, Vietnam National University (No. 334, Nguyen Trai Street, Thanh Xuan District, Hanoi city, Vietnam)
Nguyen Trong Hiep, Head of Laboratory of Environmental Analysis, Southern Branch of Joint Vietnam-Russia Tropical Science and Technology Research Center (No. 3, 3/2 Street, 10 District, Ho Chi Minh city, Vietnam)
Vu Thi Minh Chau, Research Associate, Laboratory of Environmental Analysis, Southern Branch of Joint Vietnam-Russia Tropical Science and Technology Research Center (N o. 3, 3/2 Street, 10 District, Ho Chi Minh city, Vietnam)
Le Minh Tuan, Research Associate, Institute of science and technology for energy and environment, Vietnam Academy of Science and Technology (No. 1, Mac Dinh Chi Street, 1 District, Ho Chi Minh city, Vietnam)
Do Hoang Linh, Student, Chemistry Department, Hanoi University of Science, Vietnam National University (No. 334, Nguyen Trai Street, Thanh Xuan District, Hanoi city, Vietnam)

Contribution of the authors:

Le Thu Thuy – study planning, experiment idea development, experiment design, heavy metal analysis, results processing and article writing

Tran Hong Con – experiment idea development, experiment design

Nguyen Trong Hiep – conducting experiments on arsenic analysis, reading and commenting on the article

Vu Thi Minh Chau – conducting experiments, reading and commenting on the article

Le Minh Tuan – conducting experiments, reading and commenting on the article

Do Hoang Linh – conducting experiments, data processing

All the authors have read and approved the final manuscript.

Original article

Influence of Sedimentation Processes on the Dynamics of Cadmium Compounds in Water and Bottom Sediments of the Sea of Azov in 1991–2020

M. V. Bufetova

Sergo Ordzhonikidze Russian State Geological Exploration University (MGRI), Moscow, Russia
e-mail: mbufetova@mail.ru

Abstract
Cadmium is a highly toxic metal actively migrating in the system water–suspended sediments–bottom sediments. The paper aims to study the Cd content in the water and bottom sediments of the Sea of Azov in 1991–2020 and to evaluate the process of sedimentation self-purification of waters. The data on Cd distribution showed that from 1991 to 2009 its concentration decreased slowly in the water of the open part of the sea and in Taganrog Bay with an increase in 2010–2016. Cd concentration in the Sea of Azov water did not exceed the maximum permissible concentration (10 μg/L) for marine waters of fisheries. Levels of Cd contamination in bottom sediments were assessed by comparison with the soil contamination criteria according to the *Dutch List*. The Cd content in the bottom sediments had been decreasing until 2010 followed by its increase in the open sea and in Taganrog Bay. The Cd content exceeded its clarke value throughout the study period. Cd elimination from the waters of the open sea was 0.9–6.0 tons/year, that from the waters of Taganrog Bay was 0.5–2.4 tons/year. These estimates of Cd fluxes into the bottom sediments can characterize sedimentation self-purification of waters. The period of sedimentation turnover of Cd in the open sea and Taganrog Bay at different Cd concentrations in water during the study period averaged 70 and 13.7 years, respectively, taking into account the differences in the volume of the studied water areas. Dependence of the coefficient of Cd accumulation by bottom sediments on its concentration in water showed that the increased intensity of sedimentation self-purification of waters at low Cd concentrations in water was provided by high concentrating ability of the bottom sediments associated with their granulometric composition. In the Sea of Azov, clay and silt sediments (fraction 0.01 mm) make up over 70%. With increasing degree of Cd contamination of waters, the accumulation coefficient value decreased and accordingly the contribution of sedimentation processes to water self-purification decreased. The assimilation capacity of the bottom sediments with respect to Cd amounted to 3.8 t/year in the open Sea of Azov and 0.7 t/year in Taganrog Bay.

Keywords: Sea of Azov, cadmium, water pollution, bottom sediments, accumulation coefficient, water body self-purification, assimilation capacity

Acknowledgements: The author is grateful to *Azovmorinformtsentr*, a branch of *Zentrregionvodkhoz*, for the provided data and to the reviewers for their useful comments.

For citation: Bufetova, M.V., 2024. Influence of Sedimentation Processes on the Dynamics of Cadmium Compounds in Water and Bottom Sediments of the Sea of Azov in 1991–2020. *Ecological Safety of Coastal and Shelf Zones of Sea*, (2), pp. 122–136.

Влияние седиментационных процессов на динамику содержания соединений кадмия в воде и донных отложениях Азовского моря в 1991–2020 годах

М. В. Буфетова

Российский государственный геологоразведочный университет имени Серго Орджоникидзе (МГРИ), Москва, Россия
e-mail: mbufetova@mail.ru

Аннотация

Кадмий – высокотоксичный металл, активно мигрирующий в системе вода – взвешенные наносы – донные отложения. Цель работы – изучить его содержание в воде и донных отложениях Азовского моря в 1991–2020 гг. и оценить процесс седиментационного самоочищения вод. Данные о распределении кадмия показали, что в воде Таганрогского залива и открытой части моря наблюдалось медленное снижение его концентрации с 1991 по 2009 г. и увеличение в 2010–2016 гг. Концентрация кадмия в воде Азовского моря не превышала предельно допустимую концентрацию (10 мкг/л) для морских вод объектов рыбохозяйственного назначения. Уровень загрязнения донных осадков кадмием в работе оценивался путем сравнения с критериями экологической оценки загрязненности грунтов по «голландским листам». Содержание кадмия в донных осадках до 2010 г. снижалось, после чего было отмечено его увеличение и в открытой части моря, и в Таганрогском заливе. Содержание кадмия превышало значение кларка этого металла на протяжении всего периода исследования. Элиминация кадмия из вод открытой части моря составляла 0.9–6.0 т/год, из вод Таганрогского залива – 0.5–2.4 т/год. Данные оценки потоков кадмия в донные отложения могут характеризовать седиментационное самоочищение вод. Период седиментационного оборота кадмия в открытой части моря и Таганрогском заливе при различных его концентрациях в воде за исследуемый период в среднем составлял 70 и 13.7 лет соответственно с учетом различий в объеме исследуемых акваторий. Зависимость коэффициента накопления кадмия донными отложениями от его концентрации в воде показала, что повышенная интенсивность седиментационного самоочищения вод при низких концентрациях кадмия в воде обеспечивалась высокой концентрирующей способностью донных отложений, связанной с их гранулометрическим составом. В Азовском море глинисто-илистые осадки (фракция 0.01 мм) составляют более 70 %. С увеличением степени загрязнения вод кадмием коэффициент накопления уменьшался и, соответственно, снижался вклад седиментационных процессов в самоочищение вод. Ассимиляционная способность донных отложений в отношении Cd составила в открытой части Азовского моря 3.8 т/год, а в Таганрогском заливе – 0.7 т/год.

Ключевые слова: Азовское море, кадмий, загрязнение воды, донные отложения, коэффициент накопления, самоочищение водоемов, ассимиляционная емкость

Благодарности: автор благодарит филиал «Азовморинформцентр» ФГБВУ «Центррегионводхоз» за предоставленные данные и рецензентов за полезные замечания.

Для цитирования: *Буфетова М. В.* Влияние седиментационных процессов на динамику содержания соединений кадмия в воде и донных отложениях Азовского моря в 1991–2020 годах // Экологическая безопасность прибрежной и шельфовой зон моря. 2024. № 2. С. 122–136. EDN RRZLMA.

Introduction

The Sea of Azov is an almost isolated shelf water body surrounded by fertile steppe. Limited dimensions, shallow depths, clearly expressed continental climate with its characteristic uneven moisture all together form a unique thermohaline structure of waters and determine the rich biological productivity of the basin [1]. With the status of a fishery reservoir of the highest category, the Sea of Azov has significant economic and recreational potential, therefore, the study of this water body pollution seems to be an urgent task.

Heavy metals are among the most significant ecological pollutants entering the waters of the Sea of Azov. One of the priority metals for environmental monitoring of the sea water area is cadmium, which is classified as hazard class 2 (highly hazardous) and has a toxicological limiting index of harm [1)]. A distinctive feature of Cd is its high biochemical and physiological activity, the ability not only to be accumulated in various environments, plants and living organisms, but also to spread through food chains. Work [2] shows that Cd is actively accumulated by aquatic organisms even at its low concentrations in water. It can cause morphological, physiological and biochemical disturbances in aquatic organisms when being accumulated in them [3].

Cd is located in the same group of the periodic table with zinc and mercury occupying an intermediate position between them. This is the reason why it is similar to these elements in a number of chemical properties [4]. Cd is a relatively rare and dispersed element concentrated in zinc minerals in the field [5]. Cd can be found in the environment in the form of free hydrate ions and in complex compounds with inorganic ligands (in forms such as complexes of chlorides, carbonates, sulfides and hydroxides) and organic ligands (fulvic, amino and nucleic acids) [6]. Currently, pollution of natural ecosystems with Cd remains one of the serious environmental problems worldwide [7]. In total, the World Ocean waters contain approximately 140 million tons of Cd with its average concentration of 0.1 μg/L [5].

The Cd content in the water and bottom sediments of the Sea of Azov and its basin has been studied by many researchers. The most significant results can be found in [8–12]. It should be noted that significant gaps in the time series of

---

[1)] Ministry of Agriculture of Russia, 2016. *On the Approval of Water Quality Standards for Water Bodies of Commercial Fishing Importance, Including Standards for Maximum Permissible Concentrations of Harmful Substances in the Waters of Water Bodies of Commercial Fishing Importance*: Order of the Ministry of Agriculture of Russia dated December 13, 2016, No. 552. Moscow: Ministry of Agriculture of Russia (in Russian).

observations are found in the array of literature data on the Cd concentration in the components of the Sea of Azov ecosystem. The most detailed data on the Cd content in water and bottom sediments of the Sea of Azov from 1986 to 2006 are given in the monograph [9] and on that of Taganrog Bay from 2002 to 2011 are presented in [13, 14]. It is possible to find fragmentary data for some subsequent years in the literature, for example, on the Cd content in the water and bottom sediments of the Temryuk-Akhtarsk region of the Sea of Azov within the licensed area of *PRIAZOVNEFT Oil Company* LLC in 2013 [15], in the Don Delta in 2012–2014 [16]. General trends in the pollution of the Sea of Azov with heavy metals from 1986 to 2017 are stated in [17]. The information in [12] on the content of heavy metals in water and bottom sediments, including Cd, in dissolved and suspended forms is of great interest. It was also noted in [12] that the distribution of Cd concentration can be somewhat influenced by the hydrometeorological situation along with physicochemical and biochemical factors. It plays an important role for the ecosystem of the Sea of Azov due to its shallow waters and tendency to resuspension of the upper layer of bottom sediments. Article [18] studied the distribution of total Cd concentrations, as well as the dissolved and suspended forms of its migration along the continuum the Mius River estuary – Taganrog Bay of the Sea of Azov, within which two barrier zones are located: the mixing zone of the Mius River waters with the waters of the Mius Estuary and the mixing zone of the Estuary waters with the Taganrog Bay waters.

When studying literature sources, we recorded discrepancies in data on the Cd concentration in the water or bottom sediments of the sea in the same period, which can be stipulated by the use of different methods of sampling and sample preparation. To identify and describe the characteristic trends in the change of Cd pollution in the Sea of Azov over time, we needed a dynamic series, i.e. a series of homogeneous statistical values showing the change of some phenomenon over time. In our case, we needed data obtained from the same observation stations over several years in the same seasons using standard methods of sampling and analysis. The data array on the Cd concentration in the water and bottom sediments of the Sea of Azov in the period from 2010 to 2020 provided to the author by *Azovmorinformtsentr*, a branch of *Zentrregionvodkhoz*, under cooperation with the Department of Ecology and Environment Management of Sergo Ordzhonikidze Russian State Geological Exploration University (MGRI) served as such a dynamic series.

As is known, the establishment of maximum permissible concentrations (MPCs) of certain metals in Russia, as well as in Western countries (Guideline concentration for aquatic life, GL), is based on experimental work in aquaria with test objects. Experiments are conducted according to the principle “one metal – organisms of one species” (2–3 test objects are possible). Experimental work to determine the toxic properties of elements on test objects (aquatic organisms) provides information on the relative danger of elements in comparison with each other. Nevertheless, the experimental parameters and test organisms under study have little in common with natural conditions and populations. Standardization is

carried out by comparing the measured concentrations of individual metals in a water body with the data obtained in an experiment on test objects [19]. In Russia, these data are provided in the Order of the Ministry of Agriculture of the Russian Federation [1)]. MPCs do not take into account the properties of water and the sensitivity of organisms; they are used to evaluate the quality of all types of water, from arctic regions with extremely low mineralization to steppe regions where water contains high concentrations of salts [8, p. 676]. Therefore, recently, in addition to the MPCs, biogeochemical criteria for the standardization of the flows of maximum permissible water pollution [20, 21] based on theoretical and empirical evaluation of the ability of the marine environment self-purification have been developed. The use of these criteria makes it possible to manage the marine environment quality in accordance with the objectives of sustainable development of regions by standardizing the maximum permissible volume of flows of chemicals and their compounds in the water area [22].

The paper aimed to study the Cd content in the water and bottom sediments of Taganrog Bay and the central Sea of Azov for 1991–2020 and to determine the time scale of the processes of sedimentation self-purification of waters.

At this, the following tasks were solved:

1) to track the dynamics of the water and bottom sediment pollution in Taganrog Bay and the open Sea of Azov (the sea itself) with Cd;

2) to study the dependence of Cd concentration in the bottom sediments on its concentration in the water based on the accumulation coefficient value;

3) to evaluate the flows of Cd deposition from the water to the bottom sediments;

4) to determine the period of sedimentation turnover of Cd in the aquatic environment;

5) to calculate the assimilation capacity of the bottom sediments with respect to Cd.

This study continues the series of works initiated by [22].

Materials and methods

The Cd MPC [1)] is 10 μg/L for sea waters of fishery facilities. No MPCs for heavy metals in the bottom sediments of marine waters have been established. Therefore, it is possible to apply a comparison either with the natural clarke of metals in the Earth's crust, or with the permissible concentration levels according to the *Dutch List* [2)] to evaluate the pollution of bottom sediments. The clarke values of the upper continental Earth's crust proposed by different authors differ significantly for individual elements. The quantitative measure of differences is the geochemical range of the content of a chemical element, calculated as the ratio between the maximum and minimum clarke values of this element. Thus, it is advisable to use the value proposed by R.L. Rudnick (0.09 μg/g) as the Cd clarke [24, 25].

[2)] Ministerie van Volkshuisvesting, Ruimtelijke Ordening en Milieubeheer, 2000. *Dutch Target and Intervention Values (2000) (the New Dutch List) : Circular on Target Values and Intervention Values for Soil Remediation*. Annexes A: Target Values, Soil Remediation Intervention Values and Indicative Levels for Serious Contamination. P. 8. Available at: https://www.yumpu.com/en/document/read/44815398/dutchtarget-and-intervention-values-2000-esdat/13 [Accessed: 20 May 2024].

Comparison of the concentration of heavy metals with the *Dutch List* is generally accepted in geochemical and hydrochemical field and is carried out in accordance with the SP11-102-97 recommendations. According to the *Dutch List*, the Cd permissible concentration in the bottom sediments is 0.8 μg/g dry weight.

Water samples for analysis were collected with the PE-1220 sampling system in accordance with GOST 31861-2012 and RD 52.24.309-2016 from the surface horizon at 32 points (Fig. 1). The studies were conducted in the central and eastern Sea of Azov and in Taganrog Bay. Water samples were collected in spring (March–April), summer (June–July), autumn (September–October) and winter (December). The outboard works were carried out using standard methods. Chemical analysis of water samples for Cd content was carried out in accordance with the PND F 14.1:2:4.140-98 method where the lower limit of sensitivity was 0.00001 mg/dm^3.

Bottom sediment samples for analysis were collected at the same stations as water samples with a DCh-0.034 bottom sampler in accordance with GOST 17.1.5.01-80 in the surface layer of soils (0–2 cm). Bottom sediment samples were collected annually in summer. Chemical analysis of bottom sediment samples for Cd content was performed in accordance with the M-MVI-80-2008 method where the lower limit of Cd sensitivity was 0.00005 mg/g. The Cd content in the water and bottom sediments was measured by the AAS KVANT-Z-ETA device. The error in determining Cd in the water did not exceed 15%, in the bottom sediments – 10%. Water temperature, salinity, pH and dissolved oxygen were also measured at each point.

Retrospective data on the Cd content in the water and bottom sediments of the Sea of Azov in 1991–2006 were additionally used to determine interannual trends [9]. In [9], the studies were conducted according to FR.1.31.2005.01514 – this method preceded that of PND F 14.1:2:4.140-98, according to which the Cd concentrations were determined *Azovmorinformtsentr*, the branch of *Zentrregionvodkhoz*. Taking this into account, the data from [9] were used in our work for comparison.

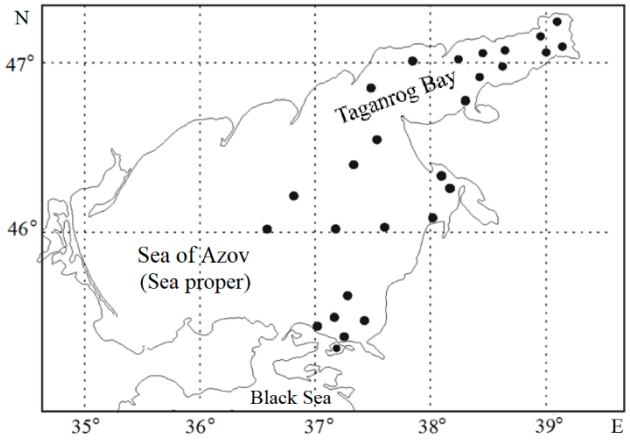

Fig. 1. Map of sampling of water and bottom sediments in 2010–2020

Parameters of the studied areas

Area	Total area, km^2 [26]	Volume, km^3 [26]	Average depth, m [26]	Average rate of sedimentation [3)], g/m^2/year
Taganrog Bay	5600	25	4.9	700
Open part of the sea	33400	231	7.0	300

Mathematical processing of analytical data was carried out using the standard Excel package. In this work, the study was conducted with average annual fairing of parameters.

Two areas were identified for work in the Sea of Azov: Taganrog Bay and the open Sea of Azov (the sea itself), which is associated with their morphometric and hydrological features (Table).

Main results

Cd enters the Sea of Azov from both natural and anthropogenic sources, such as atmospheric precipitation, river runoff, coastal abrasion with the influx of terrigenous material, intensification of shipping, construction of new and reconstruction of existing ports, wastewater from settlements located on the coast, dumping of contaminated bottom sediments of port waters and approach channels, discharge of drilling fluids and sludge during drilling of oil and gas wells. Cd is contained in fuel oil and diesel fuel (and is released when the fuel is burned), it is used as an additive to alloys, in the application of galvanic coatings (Cd plating of base metals), to obtain Cd pigments needed in the production of varnishes, enamels and ceramics, as a stabilizer for plastics (for example, polyvinyl chloride) in electric batteries, etc. As a result, Cd is emitted in these industries into the atmosphere and wastewater discharges as part of compounds and can enter the marine ecosystem.

Large industrial enterprises, which can be potential sources of Cd entering the sea due to their production cycles, are located on the coast of the Sea of Azov. These include: Taganrog Metallurgical Plant (*TAGMET* JSC), Taganrog Boiler-Making Plant

[3)] Sorokina, V.V., 2006. [*Peculiarities of Terrigenous Sedimentation in the Sea of Azov in the Second Half of the 21st Century*]. Ph.D. Thesis. Rostov-on-Don, 216 p. (in Russian).

(*Krasny Kotelshchik TKZ* PJSC), *Taganrog Commercial Sea Port* JSC, *Yeisk Sea Port* OJSC, *Azov Shipyard* JSC (Town of Azov), *Azovstal Iron and Steel Works* (City of Mariupol), *Azovmash* PJSC (City of Mariupol), *Ilyich Iron and Steel Works* LLC (City of Mariupol), *Temryuk Shipyard* LLC (Town of Temryuk), *Gazprom Neft* OJSC (Town of Primorsko-Akhtarsk), Kerch Sea Port. It should also be noted that 14 soil dumps are located in the waters of the Sea of Azov, 9 of which – in Taganrog Bay. Therefore, they can be a source of Cd pollution.

Based on the results of consideration of the characteristics of the distribution of Cd concentration in the water (C_w) of the open Sea of Azov, two phases of water pollution were recorded (Fig. 2, *a*): from 1991 to 2009, period of their low pollution, up to 5% of the MPC level, and from 2010 – a relatively higher level, although the C_w value of Cd did not exceed the MPC in all cases. The highest concentrations over the entire observation period were recorded in the summer of 2010 in the Kerch Strait (8.2 μg/L), in the summer of 2012 in the central part of the sea (7.1–9.2 μg/L) and in the spring of 2014 in the area of the Dolgaya Spit (up to 9.7 μg/L). In 2019–2020, Cd levels in water in all sea areas were low and ranged from 0.1 to 3.1 μg/L. Materials on changes in the Cd distribution characteristics in Taganrog Bay showed that its concentration in the water was minimal (up to 5% of the MPC) from 1991 to 2009, then an increase was noted (up to 30% of the MPC) from 2010 to 2014 and a decrease after 2017.

One of the most significant factors determining the ability of bottom sediments to concentrate and retain microelements is their granulometric composition. Metals are accumulated well in the finely dispersed fraction of sediments with a particle size of less than 0.05 mm. Clay and silt sediments dominate in the Sea of Azov (fraction 0.01 mm makes up over 70%). They are distributed mainly in the central sea and also accumulated locally in the depressions of estuaries and bays, in elongated troughs among banks. A characteristic narrow area of silts lines the bottom of the Taganrog Bay axial trough at a depth of 5–10 m. All silt sediments are highly organic. The Sea of Azov is characterized by such a sedimentogenesis phenomenon as mixed type of bottom sediments. Their distinctive feature is a mixture in close proportions (from 25 to 40%) of silt, siltstone and sand fractions, including detritus. Areas of mixed sediments tend to be located on the coastal shelf, at the foot of all significant banks of the open sea, and also at the center of the bottom depression in large bays. The sand zone (fraction 1.0–0.1 mm – more than 50%) extends on the Azov shelf as a narrow trail in the coastal area at a depth of up to 2–6 m, as well as on the underwater coastal slope of the spits. Sand and shell deposits form underwater banks at depths of 1–9 m, as well as narrow gentle sandy banks and ridges. In many places where banks are located the deposits are represented by shell rock filled with sand and silt [27, p. 90–91].

The Cd average concentration in the bottom sediments (C_{BS}) of the open sea varied from 20 to 85% of the permissible concentration according to the *Dutch List* (Fig. 2, *b*). Nevertheless, the Cd permissible concentration was recorded in some samples every year, mainly in summer. Thus, the permissible concentration in the area of Port Kavkaz in 2011 was 0.8 μg/g and in 2012 – 1.1 μg/g,

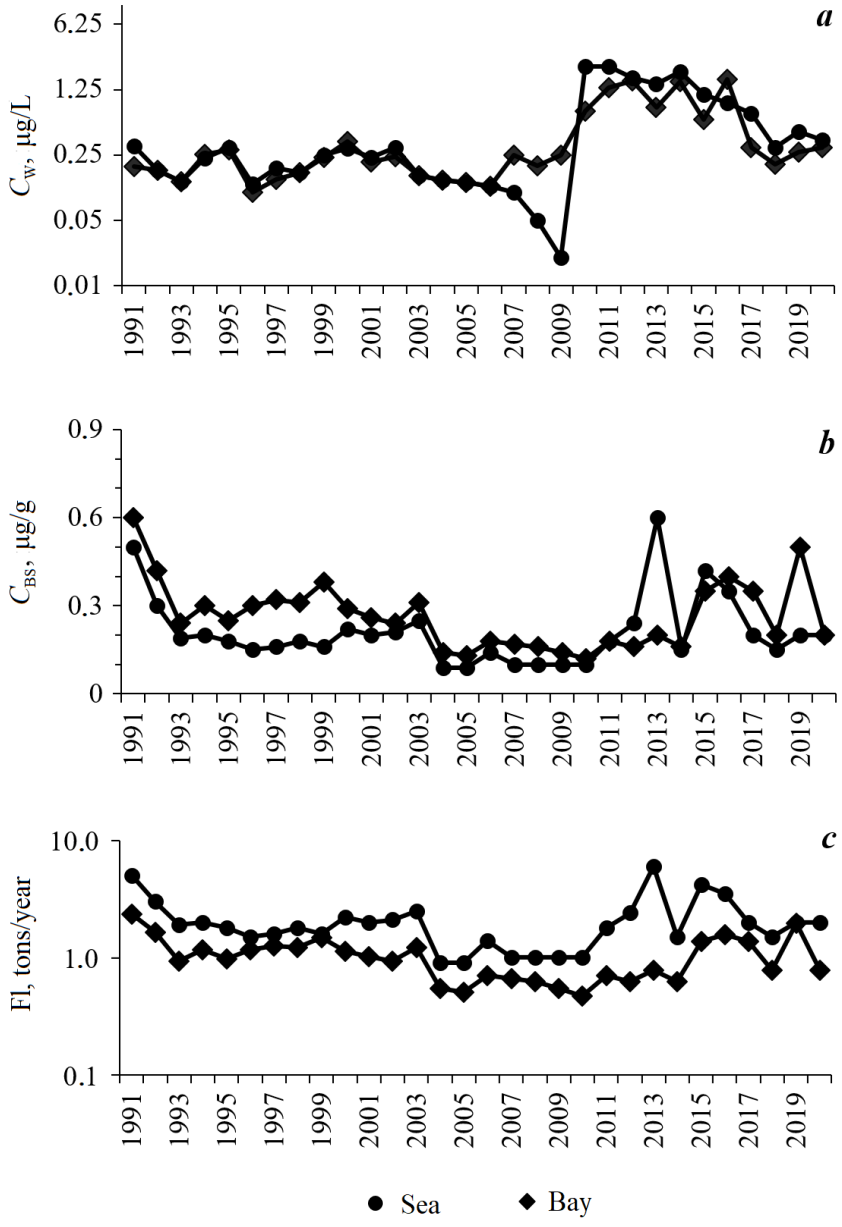

Fig. 2. Characteristics of cadmium distribution in the open sea and Taganrog Bay: concentration in water, µg/L, (*a*) and in the surface layer of bottom sediments, µg/g dry weight (*b*); cadmium deposition flux in the bottom sediment column, tons/year (*c*); sedimentation turnover period of cadmium in water, years (*d*); dependence of the coefficient of cadmium accumulation by bottom sediments on its concentration in water (*e*)

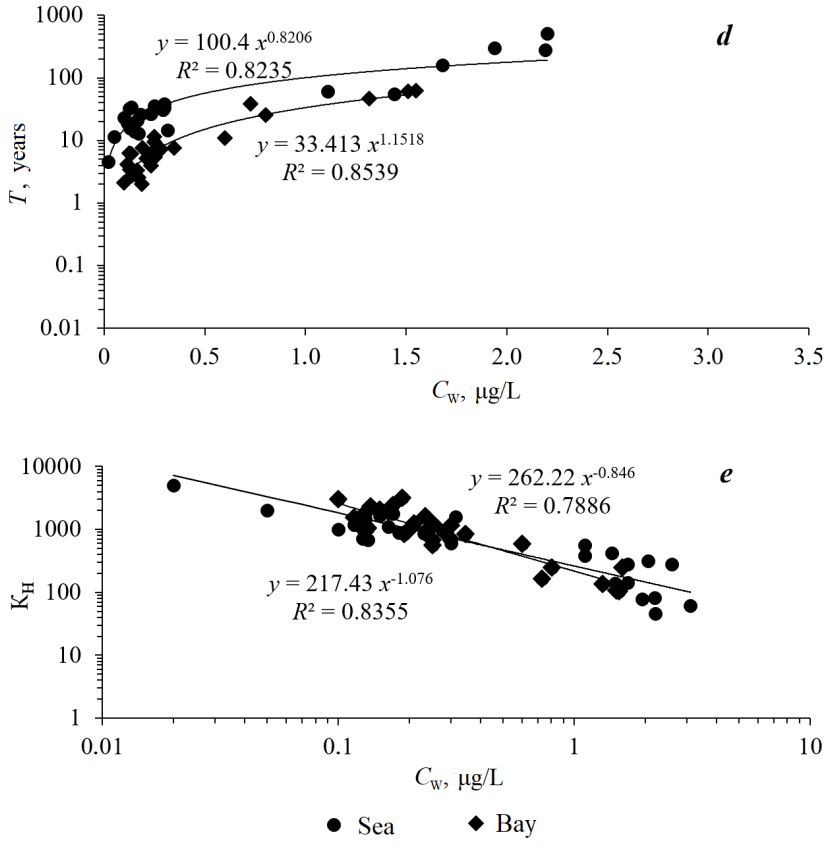

Fig. 2. Continued

in the area of the Tuzla Spit in 2018 – 3.1 μg/g, in 2019 – 0.9 μg/g, in 2013 in the area of the Dolgaya Spit (Zhelezinskaya Gully) – 1.1 μg/g, in the Kuban-Akhtarsky district – up to 1.5 μg/g. In the Taganrog Bay bottom sediments, the Cd concentration varied from 0.05 to 1.10 μg/g over the entire observation period. The maximum values exceeding the permissible concentration were recorded in the silt sediments of the central bay in 2016 (1.3 μg/g) and in 2019 (the Mius Estuary – 0.9 μg/g), in 2017 and 2019 in the eastern bay (0.9 and 1.0 μg/g, respectively), in 2019 in the Taganrog port area (1.1 μg/g). If the Cd content in the bottom sediments of the Sea of Azov is evaluated by its clarke, then a widespread excess of the clarke value of this metal is observed throughout the period under study.

Increased concentrations of Cd in some bottom sediment samples can be explained by both anthropogenic influence and changes in the physicochemical environment and dynamics of water masses. As is known, the mobility of metals changes as a result of such physicochemical processes as adsorption, sedimentation and filtration, formation of geochemical (complexation and sedimentation) and biological barriers. Studies of many contaminated natural systems have shown that adsorption/desorption is one of the most significant geochemical processes influencing the migration of inorganic pollutants. Cd sorption depends largely on the composition

of the solution in the equilibrium water – rock. When studying the factors influencing the process of Cd distribution in the system water – rock, special attention is paid to the pH, the values of which in the Sea of Azov were in the range of 6.5–9.3 during the observation period. The pH is one of the determining parameters of Cd adsorption, which is about to double with each increase in pH by 0.5 units in the pH range from 4 to 7 [28]. Conversely, Cd associated with suspended matter or bottom sediments can be extracted and pass back to water with a decrease in pH [18]. Studies show that as a result of sedimentation of finely dispersed suspensions, the removal of adsorbing substances from water occurs at a significantly higher rate compared to their chemical destruction.

The behavior of Cd can also be influenced by the amount of O_2 and the oxidation-reduction potential (Eh). If only about 2% of Cd can pass from bottom sediments into the pore solution under anaerobic conditions (Eh = −150 mV) and about 20% under moderately reducing conditions (Eh = +50 mV), then about 64% of this metal passes into the pore solution under oxidizing conditions (Eh = +500 mV) [29]. Thus, in the same sea area, when anaerobic conditions of bottom sediments change to aerobic ones, the Cd concentrations in water and bottom sediments can change significantly. Under the conditions of water saturation with oxygen due to photosynthesis and active aeration of waters, Cd is removed as part of iron and manganese oxides and hydroxides with high sorption properties, which are deposited on the surface of bottom sediments in a slightly alkaline environment (pH> 8), thus increasing the Cd content [18].

Expression [30] was used to evaluate the fluxes (Fl) of the Cd annual deposition into the bottom sediments

$$\mathrm{Fl} = C_{\mathrm{BS}} \cdot S \cdot v_{\mathrm{sed}}, \quad (1)$$

where C_{BS} is metal concentration in the surface layer of bottom sediments, μg/g; S is square of the water area under consideration, km^2; v_{sed} is specific sedimentation rate, g/m^2/year.

Fig. 2, *c* shows the results of calculations of the inflow of Cd fluxes into the bottom sediments of Taganrog Bay, the sea itself according to formula (1). The Cd elimination from the waters of the open Sea of Azov was within 0.9–6.0 tons/year, its deposition in the bottom sediments of Taganrog Bay was from 0.5 to 2.4 tons/year. These estimates of Cd deposition fluxes into the bottom sediments can characterize the sedimentation self-purification of waters from this metal.

The period of heavy metal sedimentation turnover in the aquatic environment (T, years) equal to the ratio of its pool in water to the flux of deposition into the bottom sediments reflects the time scale of the processes of sedimentation self-purification of waters [20]:

$$T = C_{\mathrm{w}} \cdot S \cdot h_{\mathrm{ave}}/\mathrm{Fl} \quad \text{or} \quad T = C_{\mathrm{w}} \cdot V/\mathrm{Fl}, \quad (2)$$

where S, V, h_{ave} and C_{w}, respectively, are square, km^2, volume, km^3, average depth, m, and heavy metal concentration, μg/L, in the analyzed water area.

Calculated according to formula (2), the average period of Cd sedimentation turnover in the open sea and in Taganrog Bay at various concentrations in water during the period under study was 70 and 13.7 years, respectively (Fig. 2, *d*). In general, the process of sedimentation turnover is complex and diverse: before passing into bottom sediments, some chemical elements and their compounds pass from one form to another up to 30–40 times [31].

Study of the trend of change in the Cd accumulation coefficient value by bottom sediments ($Co_{ACC} = C_{BS}/C_W$) depending on its concentration in water showed that this dependence with a high degree of statistical reliability (determination coefficient R^2 is 0.83 in Taganrog Bay and 0.78 in the sea itself) lay on a straight line on a graph with logarithmic scales along the ordinate axes (Fig. 2, *e*).

Fig. 2, *e* shows that the increased intensity of sedimentation self-purification of waters at low concentrations of Cd in the water was ensured by sufficiently high (at $Co_{ACC} > n \cdot 10^3$ units) concentrating capacity of bottom sediments. With an increase in the degree of water pollution by Cd, the value of Co_{ACC} decreased and, accordingly, the contribution of sedimentation processes to the self-purification of water decreased.

The obtained materials make it possible to estimate the assimilation capacity of the bottom sediments in relation to Cd. Using the calculation method presented in [31], we found that the assimilation capacity of the bottom sediments in relation to Cd in the open Sea of Azov is 3.8 tons/year and in Taganrog Bay – 0.7 tons/year.

Conclusions

During the period under study, the Cd concentration in the water of the open Sea of Azov and Taganrog Bay did not exceed the MPC. Average annual values of Cd in the bottom sediments of the open sea varied within the range from 20 to 85% of the permissible concentration according to the *Dutch List*. In in some years, excesses of the permissible concentration were recorded in central and eastern Taganrog Bay. If the Cd content in the bottom sediments of the Sea of Azov is estimated by its clarke, then an excess of concentration is observed throughout the period under study.

Estimates of the annual deposition fluxes of Cd into the bottom sediments showed that the elimination of Cd from the waters of the open Sea of Azov was within 0.9–6.0 tons/year, its deposition in the bottom sediments of Taganrog Bay was from 0.5 to 2.4 tons/year. These estimates of Cd fluxes into the bottom sediments can characterize the sedimentation self-purification of waters from this metal.

The period of Cd sedimentation turnover in the open sea and in Taganrog Bay at various concentrations in water during the period under study averaged 70 and 13.7 years, respectively.

The study of the trend of changes in the Cd accumulation coefficient by the bottom sediments depending on its concentration in water showed that the increased intensity of sedimentation self-purification of water at low concentrations of Cd in water was ensured by high (at $Co_{ACC} > n \cdot 10^3$ units) concentrating capacity of bottom sediments. With an increase in the degree of water pollution by Cd, the value

of Co_{ACC} decreased and, accordingly, the contribution of sedimentation processes to the self-purification of water decreased.

The assimilation capacity of the bottom sediments in relation to Cd is 3.8 tons/year in the open Sea of Azov and 0.7 tons/year in Taganrog Bay. The observed differences in the periods of Cd sedimentation turnover in the Sea of Azov and in Taganrog Bay, as well as in the magnitude of the assimilation capacity of the bottom sediments in relation to Cd are determined mainly by the area and volume of the water areas under study.

REFERENCES

1. Matishov, G.G., ed., 2002. [*Ecosystem Studies of the Sea of Azov and its Coastline*]. Apatity: Izd-vo KNTS RAN, Vol. IV, 447 p. (in Russian).
2. Moiseenko, T.I., Gashkina, T.I. and Dinu, M.I., 2021. Distribution of Metal Species and the Assessment Their Bioavailability in the Surface Waters of the Arctic: Proposals for the Water Quality Standards. *Geochemistry International*, 59(7), pp. 683–698. https://doi.org/10.1134/S0016702921070053
3. Sharov, A.N., Berezina, N.A., Kuprijanov, I., Sladkova, S.V., Kamardin, N.N., Shigaeva, T.D., Kudryavtseva, V.A. and Kholodkevich, S.V., 2022. Cadmium in the Eastern Gulf of Finland: Concentrations and Effects on the Mollusk Limecola balthica. *Geochemistry International*, 60(7), pp. 702–710. https://doi.org/10.1134/S0016702922060076
4. Petrova, A. and Stefunko, M., 2016. Mining and Processing Facilities as Sources of Cadmium Contamination of the Environment. *Mine Surveying and Subsurface Use*, (1), pp. 52–55 (in Russian).
5. Izrael, Yu.A. and Tsyban, A.V., 2009. *Anthropogenic Ecology of Ocean*. Moscow: Flinta; Nauka, 529 p. (in Russian).
6. Efremova, M.A., Sladkova, N.A. and Vyalshina, A.S., 2013. The Dynamics of Cadmium and Potassium Accumulation in Wheat on Soddy-Podzolic and Lowland Peat Soils. *Agrohimiâ*, (11), pp. 86–96 (in Russian).
7. Moiseenko, T.I., 2019. Bioavailability and Ecotoxicity of Metals in Aquatic Systems: Critical Contamination Levels. *Geochemistry International*, 57(7), pp. 737–750. https://doi.org/10.1134/S0016702919070085
8. Bespalova, L.A., 2006. [*Ecological Diagnostics and Sustainability Assessment of the Azov Sea Landscape Structure*]. Rostov-on-Don: Izd-vo Rostovskogo un-ta, 271 p. (in Russian).
9. Klenkin, A.A., Korpakova, I.G., Pavlenko, L.F. and Temerdashev, Z.A., 2007. [*Ecosystem of the Sea of Azov: Anthropogenic Pollution*]. Krasnodar: OOO "Prosvesh-cheniye-Yug", 324 p. (in Russian).
10. Fedorov, Yu.A., Mikhailenko, A.V. and Dotsenko, I.V., 2012. Biogeochemical Conditions and Their Role in Mass Transfer of Heavy Metals in Aquatic Landscapes. In: MSU, 2012. *Landscape Geochemistry and Soil Geography*. Moscow: APR, pp. 332–334 (in Russian).
11. Fedorov, Yu.A., Dotsenko, I.V. and Mikhailenko A.V., 2015. The Behaviour of Heavy Metals in Water of the Sea of Azov During a Wind-Driven Activity. *Bulletin of Higher Education Institutes North Caucasus Region Natural Sciences*, (3), pp. 108–112 (in Russian).
12. Mikhailenko, A.V., Fedorov, Yu.A. and Dotsenko, I.V., 2018. [*Heavy Metals in Landscape Components of the Sea of Azov*]. Rostov-on-Don; Taganrog: Izd-vo Yuzhnogo Federalnogo Universiteta, 214 p. (in Russian).

13. Dovlatyan, I.V. and Korolev, A.N., 2002. [Results of the Study of Heavy Metal Pollution in the Taganrog Bay]. *Izvestiya SFedU. Engineering Sciences*, (1), pp. 255–257 (in Russian).
14. Vishnevetskiy, V.Yu. and Ledyaeva, V.S., 2014. Ecological Forecasting of Water Pollution Heavy Metal. *Engineering Journal of Don*, 4(2), 15 (in Russian).
15. Korpakova, I., Larin, A., Korablina, I., Malkhasyan, E. and Temerdashev, Z., 2014. The Content of Heavy Metals in the Water and Bottom Sediments of the Licensed Site of LLC "NK "Priazovneft" in the Sea of Azov in 2013. *Environmental Protection in Oil and Gas Complex*, (11), pp. 25–29 (in Russian).
16. Berdnikov, S.V., Sorokina, V.V., Povazhnyy, V.V., Tkachenko, A.N. and Tkachenko, O.V., 2015. Seasonal and Spatial Dynamics of Total Suspended Matter, Nutrients and Heavy Metals Concentrations in the Don Delta in 2012–2014. In: Federal Service for Hydrometeorology and Environmental Monitoring, 2015. [*Modern Problems of Hydrochemistry and Surface Water Quality Monitoring : Proceedings of the Scientific Conference with International Participation. Part 1*]. Rostov-on-Don, pp. 141–145 (in Russian).
17. Korablina, I.V., Sevostyanova, M.V., Barabashin, T. O., Gevorgyan, J.V., Katalevsky, N.I. and Evseeva, A.I., 2018. Heavy Metals in the Ecosystem of the Azov Sea. *Problems of Fisheries*, 19(4), pp. 509–521 (in Russian).
18. Fedorov, Yu.A., Gar'kusha, D.N., Chepurnaya, V.I., Dotsenko, I.V. and Kostenko, D.F., 2021. Cadmium in Water along the Continuum 'the Mius Estuary – the Taganrog Bay of the Azov. *Geographical Bulletin*, 3(58), pp. 115–129. https://doi.org/10.17072/2079-7877-2021-3-115-129
19. Moiseenko, T.I. and Gashkina, N.A., 2018. Biogeochemistry of Cadmium: Anthropogenic Dispersion, Bioaccumulation, and Ecotoxicity. *Geochemistry International*, 56, pp. 798–811. https://doi.org/10.1134/S0016702918080062
20. Egorov, V.N., 2019. *Theory of Radioisotope and Chemical Homeostasis of Marine Ecosystems*. Sevastopol: IBSS, 356 p. https://doi.org/10.21072/978-5-6042938-5-0 (in Russian).
21. Pospelova, N.V., Egorov, V.N., Proskurnin, V.Yu. and Priymak, A.S., 2022. Suspended Particulate Matter as a Biochemical Barrier to Heavy Metals in Marine Farm Areas (Sevastopol, The Black Sea. *Marine Biological Journal*, 7(4), pp. 55–69. https://doi.org/10.21072/mbj.2022.07.4.05 (in Russian).
22. Matishov, G.G., Bufetova, M.V. and Egorov, V.N., 2017. The Regulation of Flows of Heavy Metals into the Sea of Azov According to the Intensity of Sedimentation of Water Self-Purification. *Nauka Yuga Rossii*, 13(1), pp. 44–58. https://doi.org/10.23885/2500-0640-2017-13-1-44-58 (in Russian).
23. Bufetova, M.V., 2015. Pollution of Sea of Azov with Heavy Metals. *South of Russia: Ecology, Development*, 10(3), pp. 112–120. https://doi.org/10.18470/1992-1098-2015-3-112-120) (in Russian).
24. Kasimov, N.S., Vlasov, D.V., 2015. Clarkes of Chemical Elements as Comparison Standards in Ecogeochemistry. *Moscow University Bulletin. Series 5, Geography*, (2), pp. 7–17 (in Russian).
25. Rudnick, R.L. and Gao, S., 2003. *Composition of the Continental Crust*. In: H. D. Holland, K. K. Turekian , 2003. Treatise on Geochemistry, Vol. 3: The Crust. Pergamon, pp. 1–64. https://doi.org/10.1016/B0-08-043751-6/03016-4
26. Goptarev, N.P., Simonov, A.I., Zatuchnaya, B.M. and Gershanovich, D.E., eds., 1991. [*Hydrometeorology and Hydrochemistry of Seas of the USSR. Vol. 5. The Sea of Azov*]. St. Petersburg: Gidrometeoizdat, 236 p. (in Russian).

27. Arkhipova, O.E., Bulysheva, N.I., Gargopa, Yu.M., Golubeva, N.I., Inzhebeikin, Yu.I., Kovaleva, G.V., Kondakov, A.A., Krasnorutskaya K.V.1, Lebedeva N.V. [et al.], 2011. *Ecological Atlas of the Sea of Azov*. Rostov-on-Don: SSC RAS, 328 p. (in Russian).
28. Putilina, V.S., Galitskaya, I.V. and Yuganova, T.I., 2012. *Sorption when Groundwater Contaminating by Heavy Metals and Radioactive Elements*. *Cadmium*. Novosibirsk, 110 p. (in Russian).
29. Papina, T.S., 2001. *Transport and Peculiarities of Heavy Metals Distribution in the Row: Water* ï *Suspended Substance* ï *River Ecosystems Sludge*. Novosibirsk, 58 p. (in Russian).
30. Polikarpov, G.G. and Egorov, V.N., 1986. [*Marine Dynamic Radiochemoecology*]. Moscow: Energoatomizdat, 176 p. (in Russian).
31. Khrustalev, Yu.P., 1999. *The Fundamental Problems of the Sedimentogenesis Geochemistry in the Azov Sea*. Apatity: Publishing house of the KSC RAS, 247 p. (in Russian).
32. Bufetova, M.V. and Egorov, V.N., 2023. Lead Contamination of Water and Sediments of Taganrog Bay and the Open Part of the Sea of Azov in 1991ï 2020. *Ecological Safety of Coastal and Shelf Zones of Sea*, (2), pp. 105ï 119. doi:10.29039/2413-5577-2023-2-105-119

Submitted 11.01.2024; accepted after review 5.02.2024;
revised 27.03.2024; published 25.06.2024

About the author:

Marina V. Bufetova, Associate Professor of the Department of Ecology and Nature Management, Faculty of Ecology, Sergo Ordzhonikidze Russian State Geological Exploration University (MGRI) (23 Miklukho-Maklaya St., Moscow, 117997, Russian Federation), Associate Professor, Ph.D. (Geogr.), **ORCID ID: 0000-0002-6247-1698**, *mbufetova@mail.ru*

The author has read and approved the final manuscript

Original article

Safety Assessment of the Ultrasound Equipment Effect on the State of Some Fish Species of the Black Sea

T. B. Sigacheva [1]*, T. V. Gavruseva [1], E. N. Skuratovskaya [1], M. P. Kirin [1], N. A. Moroz [2]

[1] *A.O. Kovalevsky Institute of Biology of the Southern Seas of RAS, Sevastopol, Russia*
[2] *«All-Russian Research Institute for Nuclear Power Plants Operation», Moskow, Russia*
* *e-mail: mtk.fam@mail.ru*

Abstract
For the commissioning of ultrasound equipment effective for the microphytofouling control of nuclear power plant hydraulic facilities, field studies are needed to confirm its safety for aquatic organisms, in particular for fish exposed to ultrasound. The paper aims to assess the effect of ultrasound equipment (power 500 W, frequency 27 kHz, current 3 A) on the behavioral response, biochemical and histopathological parameters of some Black Sea fish species in the marine environment (Karantinnaya Bay, Black Sea). The experiment was carried out over three days. In each day the ultrasound equipment was switched on for 1 h at an exposure frequency of 27 kHz. Afterwards, the individuals were kept in tanks for another five days to assess possible delayed effects. The irritating and deterrent influences were established at a short distance (10–30 cm) from the ultrasound equipment. The most pronounced behavioral reactions were recorded in red mullet *Mullus ponticus*, Black Sea horse mackerel *Trachurus ponticus*, picarel *Spicara flexuosum* and common stingray *Dasyatis pastinaca*, the least pronounced ones were noted in European black scorpionfish *Scorpaena porcus*. At the same time, fish mortality was not observed in the experimental and control tanks throughout the entire experiments. There were no significant differences between the biochemical parameters in the blood serum and liver, histopathological alteration indices in liver, gills and kidneys, as well as the total indices of alterations in fish from the experimental and control tanks. The obtained results indicate that the ultrasound equipment with the defined characteristics has no negative influence on fish that allows us to recommend this equipment for the application in the technical water supply system of nuclear power plants.

Keywords: ultrasound exposure, Black Sea fish, behavioral response, survival, fish survival, biochemical parameters, histopathological parameters

Acknowledgments: the work was carried out under state assignment of IBSS “Biodiversity as the basis for the sustainable functioning of marine ecosystems, criteria and scientific principles for its conservation” № 124022400148-4.

For citation: Sigacheva, T.B., Gavruseva, T.V., Skuratovskaya, E.N., Kirin, M.P. and Moroz, N.A., 2024. Safety Assessment of the Ultrasound Equipment Effect on the State of Some Fish Species of the Black Sea. *Ecological Safety of Coastal and Shelf Zones of Sea*, (2), pp. 137–152.

Оценка безопасности воздействия ультразвуковой установки на состояние некоторых видов рыб Черного моря

Т. Б. Сигачева [1]*, Т. В. Гаврюсева [1], Е. Н. Скуратовская [1], М. П. Кирин [1], Н. А. Мороз [2]

[1] *ФГБУН ФИЦ «Институт биологии южных морей им. А.О. Ковалевского РАН», Севастополь, Россия*

[2] *АО «Всероссийский научно-исследовательский институт по эксплуатации атомных электростанций», Москва, Россия*

* *e-mail: mtk.fam@mail.ru*

Аннотация

Для введения в эксплуатацию ультразвуковой установки, эффективной для борьбы с микрофитообрастаниями гидротехнических сооружений атомных электростанций, необходимо проведение натурных исследований, подтверждающих ее безопасность для гидробионтов, в частности рыб, попадающих в зону действия ультразвука. Цель работы состоит в оценке воздействия ультразвуковой установки (мощностью 500 Вт, частотой 27 кГц, силой тока 3 А) на поведенческие реакции, биохимические и гистопатологические показатели некоторых видов рыб Черного моря в условиях морской акватории (б. Карантинная, Черное море). Эксперимент проводили в течение трех дней, в каждый из которых ультразвуковую установку включали на 1 ч при частоте воздействия 27кГц. После этого особи содержались в садках еще на протяжении пяти дней для оценки возможных отсроченных эффектов. Установлено, что на небольшом расстоянии (10–30 см) ультразвуковая установка оказывает на рыб раздражающее и отпугивающее воздействие. Наиболее выраженные поведенческие реакции были отмечены у султанки *Mullus ponticus*, ставриды *Trachurus ponticus*, смариды *Spicara flexuosum* и морского кота *Dasyatis pastinaca*, наименее выраженные – у морского ерша *Scorpaena porcus*. При этом на протяжении всего эксперимента гибели рыб не наблюдали ни в опытном, ни в контрольном садках. Достоверные различия между биохимическими показателями в сыворотке крови и печени анализируемых видов рыб из опытного и контрольного садков отсутствуют. Сравнительный анализ индексов гистопатологических изменений печени, жабр и почек, а также общих индексов альтераций у рыб из опытного и контрольного садков не показал достоверных различий. Полученные результаты свидетельствуют, что ультразвуковая установка с заданными характеристиками воздействия не влияет на состояние рыб из опытной группы, что позволяет рекомендовать данную установку к использованию в системах технического водоснабжения атомных электростанций.

Ключевые слова: ультразвуковое воздействие, черноморские рыбы, поведенческие реакции, выживаемость, выживаемость рыб, биохимические параметры, гистопатологические изменения

Благодарности: работа выполнена в рамках темы государственного задания ФИЦ ИнБЮМ РАН «Биоразнообразие как основа устойчивого функционирования морских экосистем, критерии и научные принципы его сохранения» № 124022400148-4.

Для цитирования: Оценка безопасности воздействия ультразвуковой установки на состояние некоторых видов рыб Черного моря / Т. Б. Сигачева [и др.] // Экологическая безопасность прибрежной и шельфовой зон моря. 2024. № 2. С. 137–152. EDN WLEUIH.

Introduction

Today, during operation of nuclear power plants (NPPs) and floating nuclear thermal power plants (FNPPs), deviations in their operation are recorded, caused by accumulation of living organisms (sources of bio-interference) in technological systems. This significantly affects the operational characteristics of technical water supply systems, leads to equipment failure, power reduction of NPP/FNPP power units and, as a consequence, to underproduction of electric power and to economic losses associated with repair, unscheduled maintenance and replacement of process equipment [1].

One of the effective and reagent-free methods of biological interference control is ultrasonic water treatment. Specialists of the Department of Biochemical Technologies and Technological Support of JSC VNIIAES developed ultrasonic equipment (USE) with various radiation modes for protection of hydraulic structures from microphytofouling. As a result of joint work with the staff of the Benthos Ecology Department of A. O. Kovalevsky Institute of Biology of the Southern Seas of the Russian Academy of Sciences (IBSS), the high efficiency of the USE against fouling was established, as well as the optimal mode and frequencies of exposure [1]. At the same time, no field studies confirming the safety of the equipment for hydrobionts, in particular fish, falling within the zone of action of the USE, have been carried out so far. Such studies are a necessary stage of work for safe application of USE at NPPs, heat sinks of which belong to the objects of fishery importance, including sea water areas. The interest in conducting this kind of research in marine waters is generated due to the operation of two NPPs (Leningrad and Kola) and the Akademik Lomonosov FNPP on the territory of the Russian Federation, which use coastal marine areas as heat sinks, as well as the active construction of NPPs by Rosatom in the marine areas of Turkey, Bangladesh, Egypt and India.

To date, the effects of sound and ultrasound on the sensory systems of fish [2] as well as those of focused ultrasound on the peripheral structures of animal and human sensory organs [3] have been well studied. At the same time, information on the effect of ultrasound on fish health in general is still limited in the literature. Most works, as a rule, are aimed at studying the effect of fish barrier ultrasonic devices only on the behavioral responses of fish [4], as well as on studying the effectiveness of ultrasound to control fish ectoparasites [5]. To evaluate the effect of ultrasound on fish reared in offshore structures or on offshore multipurpose platforms combining renewable energy production and aquaculture, S. Knobloch et al. studied the growth, survival and microbiota of laboratory-reared European sea bass (*Dicentrarchus labrax*) [6]. Ultrasound between 17.5 and 49.7 kHz was found to have no effect on growth and survival of sea bass. However, microbiological analysis using the plate count method and 16S rRNA gene based metataxonomics

showed an impaired microbiota of the gills and skin, including an increase in the number of potential pathogenic bacteria [6]. Other researchers ran a long-term 30-day experiment to assess the effects of low-power (7–9 W) dual-frequency anti-cyanobacterial USE (23 and 46 kHz) under freshwater conditions on growth, blood cortisol levels and antioxidant enzyme activities in carp liver homogenates. The insignificant changes in biochemical parameters noted in the work, according to the authors, indicated the absence of stress conditions in fish and, therefore, any negative effect of the low-power USE with these frequencies of exposure [7].

At the same time, the impact of effective for biofouling control USE (power 500 W, frequency 27 kHz, current 3 A) on behavioral responses of fish, biochemical and histopathological parameters of their tissues/organs in marine conditions has not been assessed so far.

Thus, the work aims to assess the effect of the USE (power 500 W, frequency 27 kHz, current 3 A) on behavioral, biochemical and histopathological parameters of some fish species of the Black Sea in marine conditions.

Material and methods

Experimental studies were carried out in the coastal water area of Sevastopol (Karantinnaya Bay, Black Sea) to assess the impact of USE (developer JSC VNIIAES, Moscow) with a power of 500 W, frequency of 27 kHz, current of 3 A on behavioral responses as well as biochemical and histopathological indicators of fish.

To perform the experiment, the following tasks were set: 1) installation of the experimental equipment (control and experimental cages) and the USE; 2) catch of fish; 3) assessment of the USE effect on behavioral responses of fish and their distribution in the cages, as well as survival rate using video recording equipment; 4) assessment of the USE effect on biochemical and histopathological parameters of fish.

Two cages (control and experimental) were prepared for the experiment. The cages were polypropylene pipe frames with flip lids (length – 4 m, width – 2 m, height – 1 m) covered with 10 mm mesh capron netting. The bottom of the cages was made of reinforced perforated polyvinyl chloride cloth with a mesh of 1.5 mm. To raise the upper edge of the cages 10–15 cm above the water surface, polystyrene foam floats were attached to the upper part of the cages and weights were attached to the lower part. The cages were submerged in the coastal sea area near the laboratory building of IBSS. The control cage was towed away from the experimental area at a distance of 30 m. The experimental cage was secured near the pier for placing the radiating equipment in it. The depth under the cages was 5 m.

In the Sevastopol water area (Black Sea) some species of fish of the Black Sea were caught using bottom traps: red mullet *Mullus ponticus* Essipov, 1927 – 120 individuals, peacock wrasse *Symphodus tinca* (Linnaeus, 1758) – 60 individuals,

European black scorpionfish *Scorpaena porcus* Linnaeus, 1758 – 60 individuals, common stingray *Dasyatis pastinaca* (Linnaeus, 1758) – 4 individuals, thornback ray *Raja clavata* Linnaeus, 1758 – 2 individuals, Black Sea horse mackerel *Trachurus ponticus* Aleev, 1956 – 20 individuals, annular seabream *Diplodus annularis* (Linnaeus, 1758) – 4 individuals, brown meagre *Sciaena umbra* Linnaeus 1758 – 6 specimens, picarel *Spicara flexuosum* Rafinesque, 1810 – 6 individuals, damselfish *Chromis chromis* (Linnaeus, 1758) – 2 individuals.

The fish were equally divided between two cages. The fish were kept in the cages for five days before the experiment in order to adapt the individuals to the conditions in the cages, as well as to exclude from the experiment the individuals injured during catching. The experiment was conducted for three days, on each of which the ultrasound was on for 1 h with a frequency of 27 kHz.

The behavior and distribution of the fish in the experimental and control cages were assessed using an underwater video camera (7/9/10 inch AHD Underwater Fishing Camera, China) and visually by the distance between the fish shoal front and the USE. Fish survival in the experimental cage was assessed by counting dead fish specimens during and after exposure to the USE, while in the control cage it was assessed throughout the experiment. After the end of the three-day experiment on the effect of the USE on the behavioral responses of the fish, individuals remained in the cages for another five days to assess possible delayed effects.

The effect of the USE on biochemical and histopathological parameters was assessed on representatives of different ecological groups of fish – red mullet and European black scorionfish. After removing the fish from the cages, a standard biological analysis of 21 individuals of red mullet and 20 individuals of European black scorionfish was carried out: the main linear and weight characteristics [1)] as well as clinical and pathological features [8, 9] were determined. The age of the fish was determined from otoliths [1)].

Fish liver and blood serum served as materials for biochemical studies. The content of products of oxidized proteins (OP), lipid peroxidation (LPO), as well as the activity of superoxide dismutase (SOD), catalase (CAT), peroxidase (PER) and cholinesterase (ChE) were determined in fish liver. In liver and serum, alanine aminotransferase (ALT) and aspartate aminotransferase (AST) activities were determined by the methods we described previously [10].

All determinations were performed on a spectrophotometer SF-2000 (OKB Spectr, St. Petersburg, Russia).

For histological analysis, samples of gills, liver and kidneys were fixed for 24–48 h in Davidson's solution and then placed in 70% alcohol. Further processing of histological samples was carried out according to the generally accepted method [2)]. Sections 4–5 μm thick were stained with hematoxylin-eosin according to Mayer and Romanowsky–Giemsa [2)]. The histopathological changes detected in fish were analysed using a modified semiquantitative analysis of alterations according to the method of D. Bernet et al. [11], in which the severity factor (w)

[1)] Pravdin, I.F., 1966. [*Guideline for Fish Studies (Mainly Freshwater Fish)*]. Moscow: Pishchevaya Promyshlennost, 374 p. (in Russian).

[2)] Bancroft, J.D. and Gamble, M., 2008. *Theory and Practice of Histological Techniques*. New York; London: Churchill Livingstone, 744 p.

and the prevalence of lesions in organs (*a*) were taken into account. Using the above values, the organ index was calculated [11, p. 30]

$$I_{org} = \sum_{rp} \sum_{alt} (a_{org\ rp\ alt} \times w_{org\ rp\ alt}),$$

where *org* – organ; *rp* – reaction pattern; *alt* – change; *a* – score value; *w* – importance factor. A high index value indicates a significant degree of damage. The total alteration index *IT* was calculated as the sum of organ indices.

The significance of differences between the samples was evaluated using the Mann–Whitney U-test. Differences were considered reliable at a significance level of $p \leq 0.05$. The statistical analysis was performed using computer programmes Past 3 and Microsoft Office Excel 2016.

Results and discussion

Behavioral responses, distribution and survival of fish

The first day of the experiment. 30 min before the start of the experiment, a radiating device was placed in the experimental cage. The fish moved freely inside the cage without fear of a floating object on the water surface. The red mullet were at the bottom in a group, part of which was under the USE. The peacock wrasses, European black scorpionfish and brown meagres were located in the corners between the cage bottom and the wall. The thornback rays were located at the bottom. The Black Sea horse mackerels, picarels and annular seabreams were grouped together and stayed near the cage wall. The common stingray individuals and damselfish were actively moving in the water column throughout the cage area.

After turning on the USE in the experimental cage, the fish (picarels, annular seabreams, Black Sea horse mackerels, peacock wrasses, European black scorpionfish, brown meagres, a thornback ray), which were not directly exposed to the USE, did not change their behavior and location. Individuals of the common stingray, when approaching the USE again, sharply turned and swam away in the opposite direction, avoiding getting into the radiation zone under the equipment. The red mullets, located at the bottom of the cage under the equipment, began to move towards individuals of their own species, which were out of the range of the equipment.

During the operation of the equipment, the fish tried to avoid the ultrasound zone. While outside the area of the USE, they behaved in the same way as before the start of the equipment.

The second day of the experiment. No fish mortality was observed in the experimental and control cages.

When turning on the USE, the fish were distributed throughout the volume of the cage. At an attempt to drive the group of red mullets into the ultrasound zone, they moved under the equipment, where they stayed for a long time, sometimes rising from the bottom trying to relocate and then again going to the bottom. Visually, these behavioral responses of the red mullets in the exposed area could be characterised as loss of orientation / being stunned. Similar behavioral responses were observed in the horse mackerels, picarels and common stingray. Other fish species that were not in the USE zone moved freely around the cage. The common stingrays occasionally swam under the equipment, but stayed near the bottom, avoiding the water column closer to the equipment. After turning off the radiating equipment, the fish did not change their behavior or location in the cage.

The third day of the experiment. No fish mortality was observed in the experimental and control cages. After turning on the USE in the experimental cage, there was no noticeable effect on fish of all species. They moved calmly throughout the cage area without signs of agitation or loss of orientation.

After the end of the three-day experiment on the effect of USE on the behavioral responses of fish, the individuals were kept in the cages for five days more to assess possible delayed effects. No fish mortality was observed in the experimental and control cages.

Thus, the 27 kHz USE can irritate and repel fish at a short distance (10–30 cm) from the equipment. The most pronounced behavioral responses were observed in the red mullets, horse mackerel, picarels and common stingray, which avoided the area exposed to the USE. The common stingray does not have scales, which probably makes it more sensitive to the effects of the USE. The least pronounced behavioral responses were observed in the European black scorpion fish. Assessment of the survival rate of individuals in the control and experimental cages exposed to ultrasound with a frequency of 27 kHz revealed no negative effect (death of fish). The absence of negative effects on growth and survival of fish was also noted in a 72-day experiment on exposure of sea bass (*Dicentrarchus labrax*) to ultrasound with a frequency in the range from 17.5 to 49.7 kHz in the form of randomly alternating sequences of cycles [6]. At the same time, the results of our studies allowed us to establish that a more powerful source of radiation (> 500 W) is required to assess the repellent effect of ultrasound at distances greater than 30 cm.

Biochemical studies

The results of biochemical studies showed that there were no significant differences between all analysed parameters in tissues of the red mullet and European black scorpionfish from the experimental and control groups (Table 1).

Analysis of the correlation between the intensity of POL and OP and the reactions of the antioxidant (AO) system allows us to assess the nature of the organism's response to a certain stress factor or their complex. The increase in the activity of AR enzymes under the influence of unfavourable environmental factors is a non-specific adaptive reaction of the organism aimed at neutralization of reactive oxygen species.

Reduced or relatively low activity of AO enzymes against the high content of LPO and OP products, on the contrary, indicates a shift of pro-oxidant-antioxidant reactions towards free-radical oxidation of biomolecules and development of oxidative stress preceding pathological conditions in the organism [12–15]. In our studies, the absence of significant differences between the indicators of oxidative stress (content of TBARS, OP products) and the activity of AO enzymes (SOD, CAT, PER) in the liver of fish from the experimental and control groups can indicate that USE (500 W) with a given frequency, periodicity and duration of work did not have any effect on the state of the pro-oxidant-antioxidant system of fish liver. The absence of significant differences between the activity of AO enzymes (SOD, glutathione peroxidase, glutathione-S-transferase) in the liver of carp (*Cyprinus carpio*) from the experimental and control groups was also noted

Table 1. Some biochemical parameters (M ± m) in tissues of red mullet *M. ponticus* under ultrasound exposure

Parameter	Red mullet		European black scorpionfish	
	Control	Experiment	Control	Experiment
Liver				
TBARS, nmol TBARS/mg protein	2.370 ± 0.240	3.000 ± 0.39	4.240 ± 0.700	4.020 ± 0.490
C_{356}, optical units/mg protein	0.039 ± 0.007	0.049 ± 0.006	0.057 ± 0.009	0.059 ± 0.012
C_{370}, optical units/mg protein	0.037 ± 0.006	0.047 ± 0.006	0.052 ± 0.008	0.055 ± 0.011
C_{430}, optical units/mg protein	0.014 ± 0.004	0.020 ± 0.003	0.022 ± 0.005	0.024 ± 0.005
C_{530}, optical units/mg protein	0.004 ± 0.002	0.006 ± 0.001	0.008 ± 0.003	0.009 ± 0.001
SOD, arbitrary units/mg protein/min	15.450 ± 2.730	23.110 ± 3.710	27.300 ± 3.900	34.460 ± 2.450
CAT, mcat/mg protein	0.143 ± 0.022	0.160 ± 0.016	0.090 ± 0.014	0.080 ± 0.009
PER, optical units/mg protein/min	0.025 ± 0.009	0.016 ± 0.006	0.023 ± 0.006	0.028 ± 0.005
ALT, μmol/h mg protein	0.430 ± 0.080	0.370 ± 0.030	0.200 ± 0.020	0.160 ± 0.020

Continued Table 1

Parameter	Red mullet		European black scorpionfish	
	Control	Experiment	Control	Experiment
AST, μmol/h mg protein	0.120 ± 0.025	0.190 ± 0.030	0.057 ± 0.009	0.054 ± 0.007
ChE, μcat/g protein	0.360 ± 0.090	0.440 ± 0.050	0.350 ± 0.060	0.031 ± 0.040
Glucose, mmol/g tissue	190.390 ± 37.660	182.840 ± 18.700	106.640 ± 15.830	120.020 ± 18.800
Blood serum				
ALT, μmol/h mg protein	0.013 ± 0.006	0.019 ± 0.005	0.017 ± 0.007	0.010 ± 0.0002
AST, μmol/h mg protein	0.040 ± 0.028	0.026 ± 0.010	0.007 ± 0.002	0.013 ± 0.004

Note: TBARS – thiobarbituric acid reactive substances, C_{356} – neutral aldehydes, C_{370} – neutral ketones, C_{430} – basic aldehydes, C_{530} – basic ketones, SOD – superoxide dismutase, CAT – catalase, PER – peroxidase, ALT – alanine aminotransferase, AST – aspartate aminotransferase, ChE – cholinesterase.

under the action of low-power ultrasound (7–9 W; 23 and 46 kHz) under freshwater conditions [7].

Other informative biomarkers recommended for the assessment of cytolytic organ damage under oxidative stress are ALT and AST [16, 17]. As a result of cell membrane integrity disruption, aminotransferases are released into the blood. At the same time their activity decreases in the organ and increases in the serum. In our studies, the ALT and AST activity in the liver and serum of the fish from the compared groups did not differ, which also indicates the absence of any effect of ultrasound (with the given characteristics of the equipment, frequency and mode of exposure) on the fish organism.

In combination with the above markers, as a rule, the liver glucose content, an indicator of carbohydrate metabolism, is analysed [18]. The absence of reliable differences between the analysed groups of red mullet and European black scorpionfish may indicate the absence of adaptive/compensatory restructuring of metabolic processes, which is typical for organisms under stress factors of different nature and intensity.

Another important indicator recommended to assess the functioning of the nervous system and protein synthesising function of the liver under stress factors is the enzyme ChE [19]. In our studies, ChE activity in the liver of two fish species from the experimental group did not differ from that of fish from the control group. The obtained results may indicate the absence of ultrasound influence (with the given characteristics of the equipment, frequency and mode of exposure) on the protein synthesising function of the liver.

Histological studies

The integral result of physiological and biochemical changes are histopathological alterations reflecting the severity of pathological processes at the level of tissues and organs [9, 20]. Histological methods of investigation in the fish revealed the following changes.

Red mullet. Melanomacrophage centres were most frequently observed in the **liver** parenchyma (33.3% in the control group and 41.7% in the experimental group) (Fig. 1, *a*; 2, *a*). The incidence of lipoid vacuolization of hepatocytes differed insignificantly (22.2 and 25%) (Fig. 2, *a*). The local inflammatory reaction near blood vessels (Fig. 1, *b*) was more often observed in the fish of the control group (33.3 vs. 16.7%), and dilation of hepatic sinusoids and blood vessels (8.3% each) was detected in the fish only after exposure to ultrasound. Localised moderate hyperplasia of the respiratory epithelium of the gill lamellae was recorded in the **gills**, the incidence of which differed insignificantly (22.2 and 25%) (Fig. 1, *c*; 2, *c*). Single parasitic protozoa were found on the gill lamellae in the control and experimental groups (66.7 and 33.3%, respectively) (Fig. 1, *d*; 2, *c*). Chondroma, a benign tumour of cartilage tissue, was diagnosed in 8.3% of the fish in the experimental group (Fig. 2, *c*). In the **kidneys**, no significant differences were found between the analysed groups (Fig. 2, *e*).

European black scorpionfish. In the **liver**, the incidence of lipoid vacuolization of hepatocytes and melanomacrophage centres differed insignificantly (Fig. 2, *b*),

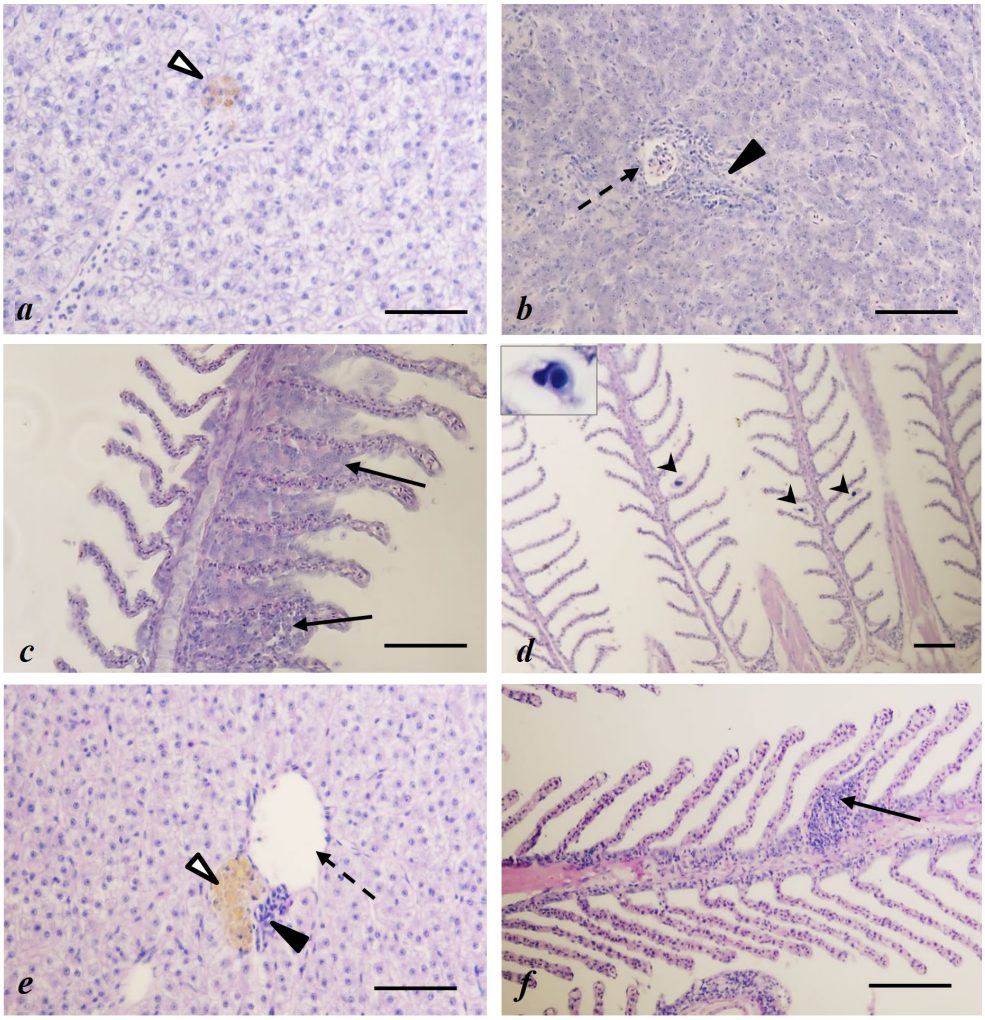

F i g . 1 . Histological structure of liver (*a, b*) and gills (*c*, *d*) of red mullet *M. ponticus* and of European black scorpionfish *S. porcus* (*e* – liver, *f* – gills) under ultrasound exposure. Note: △ – melanomacrophage center; ↟ – blood vessel dilation; ▲ – local inflammatory reaction; ↑ – epithelial hyperplasia in gill lamellae; ➤ – parasitic protozoa on gill lamellae. Scale bar: 50 μm

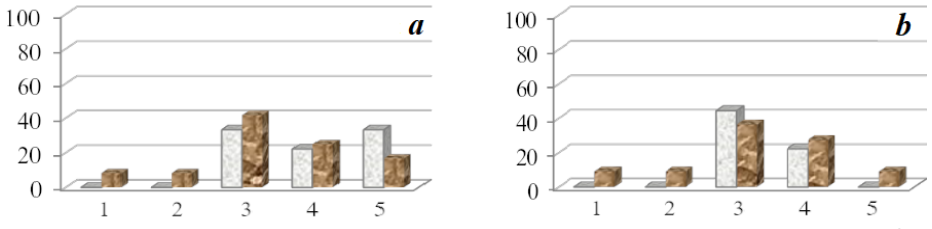

1 – Dilation of blood vessels
2 – Dilation of hepatic sinusoids
3 – Melanomacrophage centers
4 – Lipoid vacuolization of hepatocytes
5 – Local inflammatory reaction

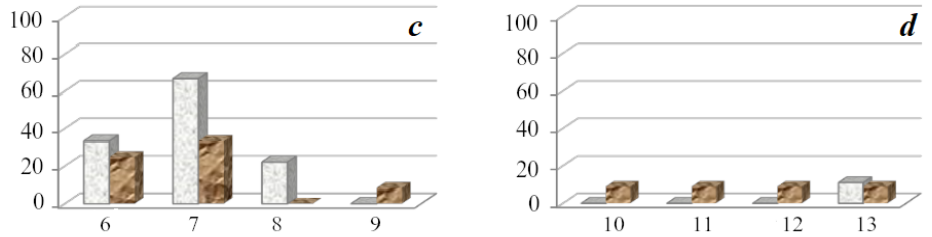

6, 11 – Local hyperplasia of respiratory epithelium of gill lamellae
7, 13 – Single protozoa on gill lamellae
8 – *Epitheliocystis* sp. on gill lamellae
9 – Chondroma
10 – Dilation of blood vessels
12 – Local fusion of gill lamellae

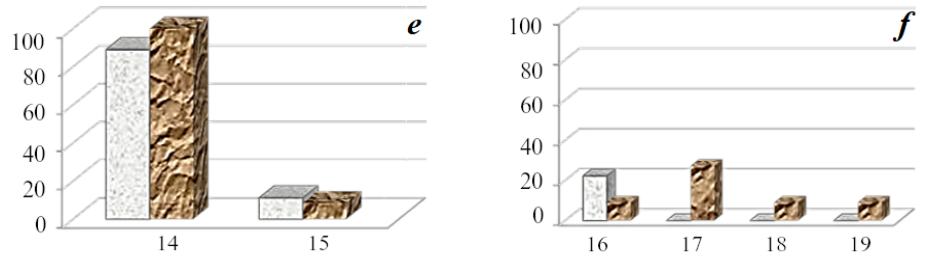

14, 16 – Melanization of macrophages
15 – Intercellular edema
17 – Hyaline drop dystrophy of nephrocytes
18 – Local necrosis of renal tubules
19 – Local inflammatory reaction

F i g . 2 . Incidence (%) of histopathological changes in liver (*a, b*), gills (*c, d*) and kidneys (*e, f*) of red mullet *M. ponticus* (*left*) and European black scorpionfish *S. porcus* (*right*) under ultrasound exposure

whereas dilation of the hepatic sinusoids (9.1%) and blood vessels (18.2%), as well as local inflammatory reaction (9.1%) were observed only in the fish of the experimental group (Fig. 1, *e*; 2, *b*). In the **gills**, local hyperplasia of the epithelium and fusion of the gill lamellae, as well as dilation of blood vessels were detected only in fish of the experimental group (9.1% each) (Fig. 1, *f*; 2, *d*). In the **kidneys**, melanization of macrophages was most frequently observed (22.2 and 9.1% in the control and experimental groups, respectively). Local inflammatory reaction, hyaline-drop degeneration and necrosis of renal tubule cells were recorded only in the fish of the experimental group (9.1, 27.3 and 9.1%) (Fig. 2, *f*).

The revealed disorders of the histological structure of organs mainly belong to the first group of severity [11] and are reversible. It should be noted that the occurrence of protozoan parasites on the gill lamellae of the red mullets in the control group was twice higher than that in the experimental group (Fig. 2, *c*). Probably, exposure to ultrasound reduced the parasitic load on the gills of the fish. Similar studies were conducted on the salmon reared in marine cages in Southern Chile. It was found that ultrasound reduced the total ectoparasitic load of *Caligus rogercresseyi* without the use of chemical antiparasitic agents [3)].

The comparative analysis of indices of histopathological alterations of the liver, gills and kidneys of the control and experimental groups in two fish species did not reveal reliable differences. The statistical analysis of total alteration indices of the control and experimental groups of the red mullet and European black scorpion fish also showed no significant differences (Table 2).

T a b l e 2 . Values of indices of histopathological alterations in organ (M ± m) of red mullet *M. ponticus* and European black scorpionfish *S. porcus* under ultrasound exposure

Parameter	Red mullet		European black scorpionfish	
	Control	Experiment	Control	Experiment
Organ alteration index				
of liver I_l	0.88 ± 0.78	1.00 ± 0.85	1.33 ± 1.58	1.45 ± 1.69
of gills I_g	1.50 ± 1.33	1.16 ± 1.33	0.11 ± 0.33	0.45 ± 0.07
of kidneys I_k	1.00 ± 0.50	1.08 ± 0.28	0.22 ± 0.47	0.73 ± 1.48
Total pathology index *IT*	3.44 ± 1.58	3.25 ± 2.17	1.67 ± 1.50	2.18 ± 2.31

[3)] Aquavitro. [*Use of Ultrasound in the Control of the Chilean Sea Louse Caligus Rogercresseyi*]. [online] Available at: https://aquavitro.org/2016/11/17/ispolzovanie-ultrazvuka-v-kontrole-chilijskoj-morskoj-vshi-caligus-rogercresseyi [Accessed: 24 May 2024].

Conclusion

The analysis of behavioral responses of Black Sea fish species (red mullet, peacock wrasse, European black scorpion fish, common stingray, thornback ray, Black Sea horse mackerel, annular seabream, brown meagre, picarel, damselfish) under the action of ultrasound (JSC VNIIAES, Moscow) (power 500 W, frequency 27 kHz, strength 3 A) allowed establishing an irritating and repelling effect on fish at a small distance (10–30 cm) from the equipment. The most pronounced behavioral responses were observed in the red mullet, Black Sea horse mackerel, picarel and common stingray, the least pronounced ones were in the European black scorpion fish. No fish mortality was observed.

The results of biochemical studies showed that there were no significant differences between the analysed parameters (level of OP and POL, activity of AO enzymes, aminotransferases and ChE, and glucose content) in tissues of the European black scorpion fish and red mullet from the experimental and control cages. Indices of histopathological changes in the liver, gills and kidneys, as well as values of the total alteration index in the compared groups of red mullet and European black scorpionfish also did not differ.

Thus, the analysis of behavioral, biochemical and histological parameters of some fish species of the Black Sea suggests absence of negative influence of the USE (JSC VNIIAES, Moscow) (power 500 W, frequency 27 kHz, current 3 A) on the state of health of fish from the experimental group. This allows us to recommend this equipment for use in NPP technical water-supply systems.

References

1. Moroz, N.A., Nevrova, E.L., Zamyslova, T.N., Kasyanov, A.B., Petrov, A.N. and Revkov, N.K., 2021. [Methods of Fouling Control at Nuclear Power Plants]. In: M. I. Orlova and V. A. Rodionov, eds., 2021. [*Problems of Development of New Generation Protective Coatings against Corrosion, Biofouling and Icing for Marine, Coastal and Terrestrial Objects*]. Saint Petersburg: Izd-vo SPbGEU, pp. 94–103 (in Russian).
2. Akoev, G.N., ed., 1990. [*Sensory Physiology of Sea Fishes (Methodological Aspects)*]. Apatity: Kolsky Filial AN SSSR, 128 p. (in Russian).
3. Vartanayan, I.A., Gavrilov, L.R., Gershuni, G.V., Rozenblum, A.S. and Tsirulnikov, E.M., 1985. [*Sensory Perception (First Effort of Research with Focused Ultrasound)*]. Leningrad: Nauka, 189 p. (in Russian).
4. Kudryavtsev, V.I., 2002. [On the Problem of Using Acoustic Fields to Control the Behaviour of Fish and Other Aquatic Animals]. In: TRTU, 2002. [*Izvestiya TSURE. Proceedings of the Second All-Russian Conference with International Participants Ecology 2002 – Sea and Human*]. Taganrog: Izd-vo TRTU, pp. 132–136 (in Russian).
5. Svendsen, E., Dahle, S.W., Hagemann, A., Birkevold, J., Delacroix, S. and Andersen, A.B., 2017. Effect of Ultrasonic Cavitation on Small and Large Organisms for Water Disinfection During Fish Transport. *Aquaculture Research*, 49(3), pp. 1–10. https://doi.org/10.1111/are.13567
6. Knobloch, S., Philip, J., Ferrari, S., Benhaim, D., Bertrand, M. and Poirier, I., 2021. The Effect of Ultrasonic Antifouling Control on the Growth and Microbiota of Farmed European Sea Bass (*Dicentrarchus labrax*). *Marine Pollution Bulletin*, 164, pp. 112072. https://doi.org/10.1016/j.marpolbul.2021.112072
7. Techer, D., Milla, S. and Banas, D., 2017. Sublethal Effect Assessment of a Low-Power and Dual-Frequency Anti-Cyanobacterial Ultrasound Device on the Common Carp (*Cyprinus Carpio*): A Field Study. *Environmental Science and Pollution Research*, 24, pp. 5669–5678. https://doi.org/10.1007/s11356-016-8305-6

8. Gavruseva, T.V., 2020. The Study of External Pathologies in Fish of the South-Western Coast of the Black Sea. *South of Russia: Ecology, Development*, 15(1), pp. 118–129. https://doi.org/10.18470/1992-1098-2020-1-118-129
9. Au, D.W.T., 2004. The Application of Histocytopathological Biomarkers in Marine Pollution Monitoring: A Review. *Marine Pollution Bulletin*, 48(9–10), pp. 817–834. https://doi.org/10.1016/j.marpolbul.2004.02.032
10. Sigacheva, T. and Skuratovskaya, E., 2022. Application of Biochemical and Morpho-physiological Parameters of Round Goby *Neogobius melanostomus* (Pallas, 1814) for Assessment of Marine Ecological State. *Environmental Science and Pollution Research*, 29(26), pp. 39323–39330. https://doi.org/10.1007/s11356-022-18962-0
11. Bernet, D., Schmidt, H., Meier, W., Burkhardt-Holm, P and Wahli, T., 1999. Histo-pathology in Fish: Proposal for Protocol to Assess Aquatic Pollution. *Journal of Fish Diseases*, 22(1), pp. 25–34. https://doi.org/10.1046/j.1365-2761.1999.00134.x
12. Van der Oost, R., Beyer, J. and Vermeulen, N.P.E., 2003. Fish Bioaccumulation and Biomarkers in Environmental risk assessment: a review. *Environmental Toxicology and Pharmacology*, 13(2), pp. 57–149. https://doi.org/10.1016/s1382-6689(02)00126-6
13. Stoliar, O.B. and Lushchak, V.I., 2012. Environmental Pollution and Oxidative Stress in Fish. In: V. I. Lushchak, ed., 2012. *Oxidative Stress – Environmental Induction and Dietary Antioxidants*. London: IntechOpen, pp. 131–166. https://doi.org/10.5772/38094
14. Regoli, F. and Giuliani, M., 2014. Oxidative Pathways of Chemical Toxicity and Oxidative Stress Biomarkers in Marine Organisms. *Marine Environmental Research*, 93, pp. 106–117. https://doi.org/10.1016/j.marenvres.2013.07.006
15. Sigacheva, T.B., Chesnokova, I.I., Gostyukhina, O.L., Kholodkevich, S.V., Kuznetsova, T.V., Andreenko, T.I., Kovrigina, N.P., Gavruseva, T.V., Kirin, M.P. and Kurakin, A.S., 2021. Assessment of Recreational Potential of Sevastopol Bays Using Bioindication Methods. *South of Russia: Ecology, Development*, 16(1), pp. 151–167. https://doi.org/10.18470/1992-1098-2021-1-151-167 (in Russian).
16. Tkachenko, H., Kurhaluk, N. and Grudniewska, J., 2013. Effects of Chloramine-T Exposure on Oxidative Stress Biomarkers and Liver Biochemistry of Rainbow Trout, *Oncorhynchus mykiss* (Walbaum), Brown Trout, *Salmo trutta* (L.), and Grayling, *Thymallus thymallus* (L.). *Archives of Polish Fisheries*, 21(1), pp. 41–51. https://doi.org/10.2478/aopf-2013-0005
17. El-Khayat, H.M.M., Hamid, H.A., Gaber, H.S., Mahmoud, K.M.A. and Flefel, H.E., 2015. Snails and Fish as Pollution Biomarkers in Lake Manzala and Laboratory A: Lake Manzala Snails. *Fisheries and Aquaculture Journal*, 6(4), pp. 1–9. https://doi.org/10.4172/2150-3508.1000153
18. Gharaei, A., Ghaffari, M., Keyvanshokooh, S. and Akrami, R., 2011. Changes in Metabolic Enzymes, Cortisol and Glucose Concentrations of Beluga (*Huso huso*) Exposed to Dietary Methylmercury. *Fish Physiology and Biochemistry*, 37(3), pp. 485–493. https://doi.org/10.1007/s10695-010-9450-3
19. Gad, N.S., 2009. Determination of Glutathione Related Enzymes and Cholinesterase Activities in *Oreochromis niloticus* and *Clarias gariepinus* as Bioindicator for Pollution in Lake Manzala. *Global Veterinaria*, 3(1), pp. 37–44. Available at: http://www.idosi.org/gv/gv3(1)09/7.pdf [Accessed: 26 April 2024].
20. Mineev, A.K., 2013. Nonspecific Reactions in Fish from Waters Middle and Lower Volga. *Izvestia of Samara Scientific Center of the Russian Academy of Sciences*, 15(3-7), pp. 2301–2309 (in Russian).

Submitted 15.01.2024; accepted after review 02.02.2024;
revised 27.03.2024; published 25.06.2024

About the authors:

Tatyana B. Sigacheva, Senior Research Associate, A. O. Kovalevsky Institute of Biology of the Southern Seas of RAS (2 Nakhimova Ave, Sevastopol, 299011, Russian Federation), PhD (Biol.), **ORCID ID: 0000-0003-3125-898X, Scopus Author ID: 36990852700, ResearcherID: AAP-9877-2020,** *mtk.fam@mail.ru*

Tatyana V. Gavruseva, Senior Research Associate, A. O. Kovalevsky Institute of Biology of the Southern Seas of RAS (2 Nakhimova Ave, Sevastopol, 299011, Russian Federation), PhD (Biol.), **ORCID ID: 0000-0002-9102-0861, Scopus Author ID: 16202640900, ResearcherID: AAP-9893-2020,** *gavrt2004@mail.ru*

Ekaterina N. Skuratovskaya, Leading Research Associate, A. O. Kovalevsky Institute of Biology of the Southern Seas of RAS (2 Nakhimova Ave, Sevastopol, 299011, Russian Federation), PhD (Biol.), **ORCID ID: 0000-0003-4501-5065, Scopus Author ID: 12241009500, ResearcherID: U-9246-2019,** *skuratovskaya@ibss-ras.ru*

Maksim P. Kirin, Leading Engineer, A. O. Kovalevsky Institute of Biology of the Southern Seas of RAS (2 Nakhimova Ave, Sevastopol, 299011, Russian Federation), **ORCID ID: 0000-0002-4214-565X**, **Scopus Author ID: 57502865700,** *kirinmaxim@mail.ru*

Natalia A. Moroz, Head of the Department of Biochemical Technologies and Engineering Support, VNIIAES JSC (25 Ferganskaya St, Moscow, 109507, Russian Federation), PhD (Tech.), *sv_nata@mail.ru*

Contribution of the authors:

Tatyana B. Sigacheva and Ekaterina N. Skuratovskaya – analysis of biochemical parameters in fish tissues, writing the article

Tatyana V. Gavruseva – histopathological analysis of fish organs and semiquantitative analysis of alterations, writing the article

Maksim P. Kirin – conduction of the experiment to study the USE effect on the fish behavior and survival, writing the article

Natalia A. Moroz – ensuring the operation and maintenance of the USE during the experiment, writing the article

All the authors have read and approved the final manuscript.

Original article

Dynamics of Allometric and Weight Parameters of the Black Sea Scallop *Flexopecten glaber ponticus* (Bucquoy, Dautzenberg & Dollfus, 1889) During Cage Farming

L. V. Ladygina *, A. V. Pirkova

A.O. Kovalevsky Institute of Biology of the Southern Seas of RAS, Sevastopol, Russia
* *e-mail: lvladygina@yandex.ru*

Abstract
The scallop *Flexopecten glaber ponticus* (Bucquoy, Dautzenberg & Dollfus, 1889), which is endemic to the Black Sea, can be classified as a mollusk species potentially cultivable in the coastal waters of Crimea. Recent data indicate emerging trends in the scallop population recovery off the Crimean coast. The scallop settles in large quantities into nursery cages together with the giant oyster *Crassostrea gigas* (Thunberg, 1793), which suggests the scallop can be reared in suspended culture due to its availability and ease of collection. We studied the seasonal dynamics of allometric growth and weight increase of the Black Sea scallop *F. glaber ponticus* during cage farming off the coast of Crimea. For the first time, a growth model is presented that adequately describes the linear growth of the mollusk. The linear relationship between shell height and age of the scallop and the exponential relationship between the total live weight and shell height were found. It was shown that the commercial quality indices of *F. glaber ponticus* – meat yield, condition index and gonadosomatic index – vary with season. The maximum values of the condition index and meat yield were noted in April, 63.40 and 33.01%, respectively. The gonadosomatic index increased from January to June (from 6.8 to 13.14%) and decreased from July to November, which trends are associated with the gametogenesis and spawning of the mollusk. The percentage of dry matter in soft tissues was 16.5%. We propose the cultivation duration (2.5–3 years) and optimal timing for harvesting marketable Black Sea scallop as a promising mariculture species. Winter and spring can be the best period for collection of the Black Sea scallop of marketable size.

Keywords: scallop *Flexopecten glaber ponticus,* growing, linear growth, condition index, meat yield, gonadosomatic index, Black Sea, mariculture, commercial mollusks

Acknowledgments: This work was carried out within the framework of IBSS state research assignment “Comprehensive study of the functioning mechanisms of marine biotechnological complexes with the aim of obtaining bioactive substances from hydrobionts” (No. 124022400152-1). We express our gratitude to the director of the Research Association “Marikul'tura” LLC V. D. Shinyavsky for the opportunity to rear Black Sea scallop on a marine farm in suspended culture.

For citation: Ladygina, L.V. and Pirkova, A.V., 2024. Dynamics of Allometric and Weight Parameters of the Black Sea Scallop Flexopecten glaber ponticus (Bucquoy, Dautzenberg & Dollfus, 1889) During Cage Farming. *Ecological Safety of Coastal and Shelf Zones of Sea*, (2), pp. 153–164.

Динамика линейных и весовых параметров черноморского гребешка *Flexopecten glaber ponticus* (Bucquoy, Dautzenberg & Dollfus, 1889) при садковом выращивании

Л. В. Ладыгина *, А. В. Пиркова

ФГБУН ФИЦ «Институт биологии южных морей им. А. О. Ковалевского РАН», Севастополь, Россия

* *e-mail: lvladygina@yandex.ru*

Аннотация

Плоский гребешок *Flexopecten glaber ponticus* (Bucquoy, Dautzenberg & Dollfus, 1889), являющийся эндемиком Черного моря, может быть отнесен к потенциальным объектам культивирования у берегов Крыма. Данные последних лет свидетельствуют о восстановительных процессах в популяции гребешка на Крымском побережье. В массовом количестве гребешок оседает в выростные садки с гигантской устрицей *Crassostrea gigas* (Thunberg, 1793), что позволяет выращивать его в подвесной культуре благодаря доступности и простоте сбора. Цель работы – изучить сезонную динамику линейного и весового роста черноморского гребешка *F. glaber ponticus* при садковом выращивании у берегов Крыма. Впервые представлена модель роста, адекватно описывающая линейный рост моллюсков. Определена линейная зависимость высоты раковины гребешка от возраста и экспоненциальная зависимость общего живого веса гребешков от высоты раковины. Показано, что индексы товарного качества *F. glaber ponticus*: выход мяса, индекс кондиции и гонадосоматический индекс – изменяются в зависимости от сезона. Максимальные значения индекса кондиции и выхода мяса отмечены в апреле и составляли соответственно 63.40 и 33.01 %. Гонадосоматический индекс увеличивался с января по июнь (от 6.8 до 13.14 %) и уменьшался с июля по ноябрь, что связано с процессами гаметогенеза и нереста моллюсков. Доля сухого вещества в мягких тканях составила 16.5 %. Рекомендована продолжительность выращивания (2.5–3 года) и сроки сбора товарной продукции черноморского гребешка как перспективного объекта марикультуры. Для сбора урожая черноморского гребешка товарного размера может быть оптимальным зимне-весенний период.

Ключевые слова: гребешок, *Flexopecten glaber ponticus,* марикультура, рост, индекс кондиции, выход мяса, гонадосоматический индекс, Черное море, промысловые моллюски

Благодарности: работа выполнена в рамках государственного задания ФИЦ ИнБЮМ по теме «Комплексное исследование механизмов функционирования морских биотехнологических комплексов с целью получения биологически активных веществ из гидробионтов» (№ гос. регистрации 124022400152-1). Выражаем благодарность директору ООО НИО «Марикультура» В. Д. Шинявскому за предоставленную возможность выращивания черноморского гребешка на морской ферме в подвесной культуре.

Для цитирования: *Ладыгина Л. В., Пиркова А. В.* Динамика линейных и весовых параметров черноморского гребешка *Flexopecten glaber ponticus* (Bucquoy, Dautzenberg & Dollfus, 1889) при садковом выращивании // Экологическая безопасность прибрежной и шельфовой зон моря. 2024. № 2. С. 153–164. EDN ERRZYM.

Introduction

The mollusk aquaculture includes approximately 65 registered species represented mainly by bivalves (clams, oysters, scallops and mussels), which account for 89% of global marine aquaculture production, while 11% comes from wild capture. The largest producers of marine bivalves are Asian countries, especially China, where 85% of the world production is grown [1]. The world seafood market considers scallops, along with other commercial bivalves (mussels and oysters), to be a valuable delicacy due to their excellent taste and nutritional properties. High-quality protein, polyunsaturated omega-3 fatty acids in high concentrations necessary for human activity, as well as macro- and microelements (iodine, selenium, calcium), vitamins A and D make a major contribution to the nutritional value of the mollusk [2].

In the Black Sea, commercial harvesting and cultivation of bivalves are not particularly developed. Only five mollusk species are of commercial importance: *Mytilus galloprovincialis* (Lamarck, 1819), *Crassostrea gigas* (Thunberg, 1793), *Chamelea gallina* (Linnaeus, 1758), *Donax trunculus* (Linnaeus, 1758) and *Anadara kagoshimensis* (Tokunaga, 1906) [3]. The scallop *Flexopecten glaber ponticus* (Bucquoy, Dautzenberg & Dollfus, 1889), which is endemic to the Black Sea, can be classified as a mollusk species potentially cultivable in the Crimean coastal waters. It lives at depths of up to 30 m on the surface of silty, sandy and shelly ground, as well as on oyster beds [1)]. The scallop can attach itself temporarily to the thalli of vegetation located above the ground. The color of the shells varies from white or yellow to red and brown, the right valve is often lighter than the left one. The length and height of the mollusk shell is up to 55 mm, its width is up to 13 mm. Until recently, the Black Sea scallop was included in the Red Book of the Republic of Crimea as a subspecies declining in numbers [2)]. However, recent literature and our own data [3, 4] indicate emerging trends in the scallop population recovery off the Crimean coast. The scallop settles in large quantities into nursery cages together with the giant oyster *C. gigas*, which suggests the scallop can be reared in suspended culture due to its availability and ease of collection.

During cage farming, *F. glaber ponticus* has a relatively high growth rate in its first year of life and reaches a length of about 42 mm by the end of the second year. The largest mollusk specimens at the age of three years had a shell height of more than 55 mm. As for the scallops from natural Black Sea settlements, this size is close to the limit [3]. The scallops *F. glaber* with a shell height of more than 50 mm are considered to be commercial ones [5]. This species is promising for the Black Sea mariculture due to its high growth rate.

[1)] Skarlato, O.A., 1972. [Class Bivalvia]. In: V. A. Vodyanitskiy, 1972. [*Field Guide for the Black Sea and the Sea of Azov*]. Kiev: Naukova Dumka, pp. 178–249. Vol. 3 (in Russian).

[2)] Ivanov, S.P. and Fateryga, A.V., eds., 2015. *Red Book of the Republic of Crimea. Animals*. Simferopol: ARIAL, 440 p. (in Russian).

The Black Sea scallop is a synchronous hermaphrodite. The gonad is two-colored: the male part of the gonad is cream-colored, the female part is orange. It reproduces in June and July. Spawning is partial. The Black Sea scallops become reproductive in the first year of their life [6].

According to N. Berik [6], the scallop *F. glaber* farmed in the Canakkale Strait (the northern Aegean Sea) also reproduces in June and July. The scallop *F. glaber* from the northwestern Adriatic Sea has two spawning periods: in April and May, as well as from June to September (with maximum gonadosomatic index values in June) [5].

The cultivation of *F. glaber ponticus* along the Crimean coast of the Black Sea is at an early stage, so the data concerning the biotechnology of cultivating this species and its nutritional properties are very little.

The paper aims at the study of the seasonal dynamics of allometric growth, determination of the relationship between the total weight and shell height and evaluation of commercial quality indices (meat yield (MY), condition index (CI) and gonadosomatic index (GSI)) of the Black Sea scallop *F. glaber ponticus* as a promising mariculture species during cage farming.

Materials and methods of study

The material of the study was the scallop spat collected in nursery cages with the giant oyster *C. gigas* grown on an oyster farm (Sevastopol Bay outer roadstead: 44°37′13.4″ N; 33°30′13.6″ E). The mollusk specimens were then grown with the use of suspended culture at a depth of 3–5 m for 2.5 years.

The growth dynamics and determination of the total weight of scallops of different ages (from 0.5 to 2.5 years) were studied over a year selecting 10 pcs. monthly. The mollusk specimens were cleaned of fouling organisms, washed in sea water and then their size and weight characteristics were determined [7]. The length (L, mm), height (H, mm), width (D, mm) of the *F. glaber ponticus* shell were measured with a digital caliper (*Zubr* ShTs-1) with an accuracy of 0.01 mm. Total wet weight of the scallop (W_{total}, g – total weight with mantle fluid), weight of soft tissue ($W_{s.t}$, g), weight of gonads (W_{gon}, g) were determined according to method [7] on electronic scales (OHAUS) with an accuracy of 0.01 g.

Dry matter of soft tissues and dry matter of gonads were determined on AXIS ANG200C electronic scales (to 0.0001 g) after drying in a thermostat to a constant dry matter at a temperature of 60 °C for 48 h. CI, MY and GSI indices (%) were calculated using formulas [8]:

$$CI = \text{meat wet weight (g)} / \text{shell wet weight (g)} \cdot 100;$$

$$MY = \text{meat wet weight (g)} / \text{total wet weight (g)} \cdot 100;$$

$$GSI = \text{gonad wet weight (g)} / \text{meat wet weight (g)} \cdot 100.$$

The moisture content of the sample was determined as the difference in weight before and after drying in a thermostat at 60 °C to constant weight and was shown as percentage. Ash content was determined by burning samples in a TEMOS-Express muffle furnace at a temperature of 600 °C for 2 h [3)]. The mean values of allometric and weight parameters and confidence intervals were calculated in Excel.

[3)] Horwitz, W., 2000. *Official Methods of Analysis of the AOAC International.* Gaithersburg, USA.

Empirical data on allometric growth were approximated with the von Bertalanffy growth model – the Ford–Walford equation [9, 10]

$$H_t = H_\infty \cdot (1 - e^{-kt}),$$

where H_t is actual size of an individual, mm, at age t, years; H_∞ is theoretically maximum shell height, mm; k is growth constant, year^{-1}; e is base of natural logarithm (2.71828…).

Results and discussion

As a result of the analysis of size-frequency distributions, modal sizes of mollusk specimens in age groups of 0.5–2.0 years were obtained. They were then used to create an allometric growth model. The height of the scallop spat shell immediately after the larvae metamorphosis is 0.3 mm [4)]. The values of the parameters of this equation were found graphically. To construct the graph, the average values of the scallop shell height at age t were plotted on the abscissa axis, and at age $t + 1$ – on the ordinate axis (Fig. 1).

These points are located on one straight line. The intersection of the line with the right angle bisector determines the theoretically maximum size of an individual in the settlement. Fig. 1 shows that the line intersects the bisector at 57.0 mm. The slope angle ($\alpha = 26°$) makes it possible to evaluate the growth constant:

$$k = -\lg \operatorname{tg} \alpha / \lg e,$$

where tg α is tangent of the slope angle of a straight line, which is equal to 0.4877, then $k = -\lg 0.4877 / 0.4343 = -03118 / 04343 = -0.718$. We obtain the following relationship:

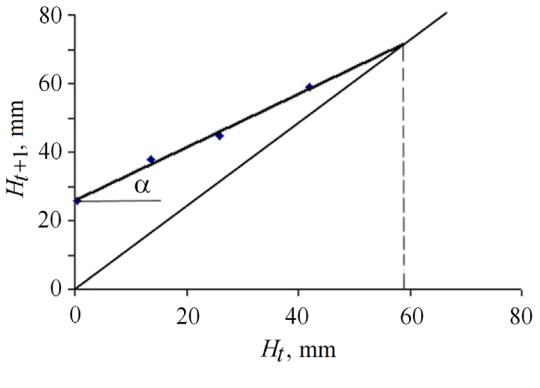

Fig. 1. Graphical determination of parameters of the von Bertalanffy growth equation

$$H_t = 57.0 \cdot (1 - e^{0.718t}),$$
$$0.5 \le t \le 2.0.$$

Using this formula, we calculated the theoretically expected average values of the scallop shell height (Table).

The formula describes the mollusk allometric growth adequately. Thus, the theoretically expected modal classes coincide completely with the actual average values of the shell height for the age of 1.5 and 2.0 years.

[4)] Zakhvatkina, K.A., 1972. [Larvae of Bivalvia]. In: V. A. Vodyanitskiy, 1972. [*Field Guide for the Black Sea and the Sea of Azov*]. Kiev: Naukova Dumka, pp. 250–270. Vol. 3 (in Russian).

Parameters of the growth equation for the scallop *Flexopecten glaber ponticus* and theoretically expected modal sizes of mollusk specimens aged 0.5–2 years

t, years	k_t	e^{-kt}	$1 - e^{-kt}$	H_t (theoretically expected), mm	$H \pm i$ (actual), mm
0.5	0.359	0.698	0.302	17.21	13.71 ± 0.76
1.0	0.718	0.487	0.513	29.24	25.88 ± 0.67
1.5	1.077	0.341	0.659	37.56	37.96 ± 0.75
2.0	1.436	0.238	0.762	43.43	42.12 ± 1.02

Note: $\pm i$ – confidence interval, mm.

The relationship between the average value of the scallop shell height (H, mm) and age ($0.5 \geq t \geq 2.5$) is also described by a linear function with a high value of the correlation coefficient ($r = 0.9841$):

$$H = 19.514\, t + 4.8472.$$

Fig. 2 shows the graph of relationship.

As the shell height increased, the total weight of the scallop increased exponentially (Fig. 3).

The results of our studies showed that the relationship between the wet weight of soft tissues and the total wet weight of the Black Sea scallop was described by a linear function (Fig. 4).

The values of the *F. glaber ponticus* weight indicators (MY, CI and GSI) show the mollusk commercial quality. Weight indicators can vary depending on the season, presence and availability of food, reproductive cycle stages and are the result of a complex interaction among these factors [11]. These indicators reflect the mollusk ecophysiological characteristics (gametogenesis and metabolism processes) and are of great importance when harvesting marketable products.

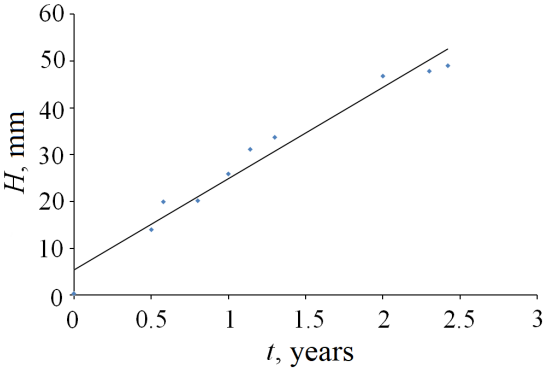

Fig. 2. Dynamics of growth of the scallop *Flexopecten glaber ponticus* during cage farming

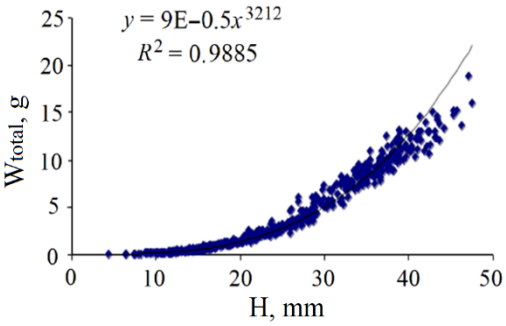

Fig. 3. Dependence of the total weight of the scallop *Flexopecten glaber ponticus* on the shell height

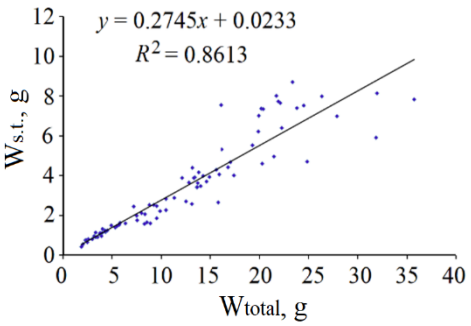

Fig. 4. Correlation of the soft tissue wet weight with the total weight of the Black Sea scallop *Flexopecten glaber ponticus*

We established that changes in the weight indicators of the scallop *F. glaber ponticus* were seasonal. The maximum CI and MY values were noted in April, 63.40 ± 6.54% and 33.01 ± 5.06% (p = 0.05), respectively, while the minimum values of these indicators were recorded in October: 41.39 ± 5.15% and 22.71 ± 2.80% (Fig. 5). The CI increase from January to May is obviously related to the gonad maturation dynamics. The CI values dropped sharply in June during the spawning period and remained low from July to December. The MY values increased from January to April due to an increase in somatic tissue weight. These values then decreased during the spawning period and remained low during the resting period. The processes of somatic tissue growth slowed down and the CI increased due to the increase in the weight of the gonads in April–June. For the same scallop species grown in the Çardak Lagoon on the shore of the Canakkale Strait (Turkey), similar results were obtained for MY: 39.69% in spring and 29.96% in summer [6].

It is known that the decrease in the CI and MY indices in summer and autumn is caused by unfavorable hydrological conditions, as well as a decrease in the qualitative and quantitative composition of phytoplankton necessary for somatic and generative growth [12]. Thus, the concentration of microalgae decreased in August to minimum values (26 thousand cells·L^{-1}) in the water area of the mussel and oyster farm (location of nursery cages with the scallops) with water warming up to 25 °C. It was the period of domination of large-celled forms of algae, which are not food for bivalves [13]. The maximum values of phytoplankton abundance were typical for February, when food species of microalgae predominated: the diatom *Skeletonema costatum* (Greville, 1865) and the coccolithophore *Emiliania huxleyi* (Lohmann, 1967). From April to July, the number of phytoplankton changed slightly, from 100 to 124 thousand cells·L^{-1}.

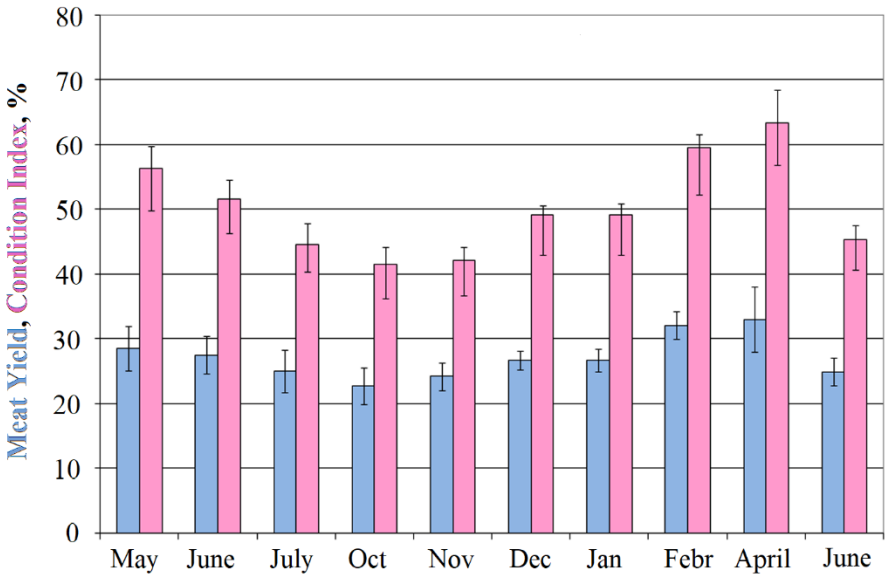

F i g . 5 . Seasonal dynamics of mean values of condition index and meat yield of the scallop *Flexopecten glaber ponticus* during cage farming

According to literature data, seasonal fluctuations in seawater parameters can affect the physiological functions and survival of the scallops negatively [14]. Due to a lack of food, metabolic energy is redirected mainly to maintaining reproductive processes, which leads to a decrease in the condition index value, while high food availability enhances tissue and gonad growth [15].

The increase in the scallop GSI values from February (6.8 ± 1.86%) to June (13.14 ± 1.52%) with its maximum in April (13.5 ± 1.44%) indicates the maturation of the gonads (Fig. 6). In parallel with the development of the gonads, the total weight of the scallop soft tissue and the CI values also increased. The Black Sea scallop spawning was noted in June – early July and the GSI value was 10.25 ± 2.0% at the end of July. From October to December, the GSI values were declining and reached their minimum in December (5.9 ± 0.74%).

Changes in the MY and GSI indices are directly related to the reproductive cycle. The weight of gonads increases before spawning, while the weight of the somatic tissue decreases. It is known that glycogen accumulated in the adductor is used as an energy source to increase the weight of gonads. Thus, reproduction affects significantly the adductor weight and, consequently, the total weight of the soft tissue [16, 17]. By the reproduction period, the relative weight of the somatic tissue decreases due to the increase in the weight of gonads [17].

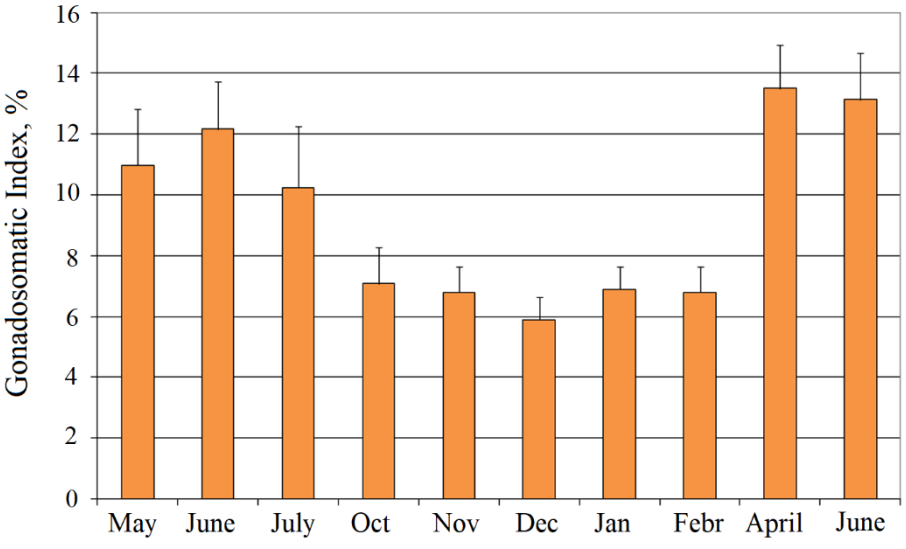

Fig. 6. Seasonal dynamics of the gonadosomatic index of the Black Sea scallop *Flexopecten glaber ponticus* during cage farming

According to our data, the weight of gonads changed insignificantly from December to February (from 0.136 g to 0.152 g). However, the weight of the gonads increased to maximum values (0.343 g) from April to June, possibly due to the accumulation of a sufficient amount of lipids [5]. Therefore, high CI values in April are stipulated by an increase in the weight of the somatic tissue, and in June – an increase in the weight of gonads. Gametogenesis processes depend on biotic and abiotic factors [18]. The mollusk gametogenesis occurs with a sufficient amount of trophic resources necessary for the energy-consuming reproduction process. With an insufficient amount of food, the mollusk experiences catabolism of such reserve tissue as the adductor [18]. According to T. Marceta [5], the tendency toward decreased weight and energy content in the somatic tissue and gonads indicates a gradual depletion of energy stored in the somatic tissue for use in the reproductive process.

The MY, CI and GSI indices reflect the ecophysiological state of bivalves. Changing the index values adjusts significantly the cultivation biotechnology and harvesting dates. The MY values of the scallop *F. glaber ponticus* increased from autumn to early spring. Therefore, the commercial value of the mollusk decreases sharply during and after the spawning period when the scallop gonads are freed from reproductive bodies and the weight of the soft tissue decreases.

The dry matter content in the soft tissue of the scallop *F. glaber ponticus* averaged 16.5% and the proportion of water was 83.5%, with its maximum content in February (83.81%). Similar values were obtained for other bivalves: *M. galloprovincialis, Limaria tuberculata* (Olivi, 1792) [19]. The water content in the soft

tissue influences physical and chemical characteristics of the mollusk and is considered to be a good indicator of seafood freshness and quality. Its content depends on the physical structure since water is involved in many physiological processes such as nutrient transport, waste removal, transmission of nerve impulses and muscle contractions [20].

The relationship between the dry weight of the scallop soft tissues and the wet weight is expressed by the following linear function:

$$W_{\text{dry s.t.}} = 0.1601 \cdot W_{\text{meat s.t.}} + 0.0127,$$
$$0.18 \geq W_{\text{meat s.t.}}\ \text{g} \geq 4.42; \quad R^2 = 0.9912.$$

The ash content in the soft tissues of the Black Sea scallop indicating the amount of inorganic compounds in the tissues ranged from 1.85 g / 100 g to 2.36 g / 100 g. Similar average ash content values were determined for bivalves from the Adriatic Sea: *F. glaber* – 2.11 g / 100 g, *Chlamys varia* (Linnaeus, 1758) – 2.49 g / 100 g, *Ostrea edulis* (Linnaeus, 1758) – 2.18 g / 100 g [21] and from the Mediterranean Sea: *M. galloprovincialis* – 2.62 g / 100 g [19].

Conclusion

Recently, the population of the Black Sea scallop *F. glaber ponticus* has been recovering resulting in an increase in the amount of settled spat, which makes it possible to study the allometric and weight parameters. When grown in suspended culture, the weight of the Black Sea scallop increased exponentially with its shell height. The mollusk commercial indicators varied depending on the season. The highest CI and MY values were noted from December to April (49.13−63.4 and 26.71−33.01%, respectively), and the lowest ones – in the summer months. The maximum GSI values were obtained in June during the pre-spawning period. Therefore, winter and spring can be the best periods for collection of the Black Sea scallop of marketable size.

References

1. Wijsman, J.W.M., Troost, K., Fang, J. and Roncarati, A., 2019. Global Production of Marine Bivalves. Trends and Challenges. In: A. Smaal, J. Ferreira, J. Grant, J. Petersen and Ø. Strand, eds., 2019. *Goods and Services of Marine Bivalves.* Springer: Cham, pp. 7–26. https://doi.org/10.1007/978-3-319-96776-9_2
2. Prato, E., Biandolino, F., Parlapiano, I., Papa, L., Kelly, M. and Fanelli, G., 2018. Bioactive Fatty Acids of Three Commercial Scallop Species. *International Journal of Food Properties*, 21(1), pp. 519–532. https://doi.org/10.1080/10942912.2018.1425703
3. Revkov, N.K., Pirkova, A.V., Timofeev, V.A., Ladygina, L.V. and Schurov, S.V., 2021. Growth and Morphometric Characteristics of the Scallop *Flexopecten glaber* (Bivalvia: Pectinidae) Reared in Cages off the Coast of Crimea (Black Sea). *Ruthenica: Russian Malacological Journal*, 31(3), pp. 127–138. https://doi.org/10.35885/ruthenica.2021.31(3).3 (in Russian).
4. Pirkova, A.V. and Ladygina, L.V., 2017. Meiosis, Embryonic, and Larval Development of the Black Sea Scallop Flexopecten glaber ponticus (Bucquoy, Dautzenberg & Dollfus, 1889) (Bivalvia, Pectinidae). *Marine Biological Journal*, 2(4), pp. 50−57. https://doi.org/10.21072/mbj.2017.02.4.05 (in Russian).

5. Marceta, T., Da Ros, L., Marin, G.M., Codognotto, V.F. and Bressan, M., 2016. Overview of the Biology of *Flexopecten glaber* in the North Western Adriatic Sea (Italy): A Good Candidate for Future Shellfish Farming Aims? *Aquaculture*, 462, pp. 80–91. https://doi.org/10.1016/j.aquaculture.2016.04.036
6. Berik, N., Çankiriligil, E.C. and Gülc, G., 2017. Meat Yield and Shell Dimension of Smooth Scallop (*Flexopecten glaber*) Caught from Çardak Lagoon in Canakkale, Turkey. *Journal of Aquaculture and Marine Biology*, 5(3), 00122. https://doi.org/10.15406/jamb.2017.05.00122
7. Alimov, A.F., Lvova, A.A., Makarova, G.E. and Soldatova, I.N., 1990. [Height and Age]. In: G. L. Shkorbatov and Ya. I. Starobogatov, eds., 1990. [*Methods to Study Bivalves*]. Leningrad: ZIN, pp. 121−141 (in Russian).
8. Okumus, I. and Stirling, H.P., 1998. Seasonal Variations in the Meat Weight, Condition Index and Biochemical Composition of Mussels (*Mytilus edulis* L.) in Suspended Culture in Two Scottish Sea Lochs. *Aquaculture*, 159(3–4), pp. 249−261. https://doi.org/10.1016/S0044-8486(97)00206-8
9. Walford, L.A., 1946. A New Graphic Method of Describing the Growth of Animals. *The Biological Bulletin*, 90(2), pp. 106–109. https://doi.org/10.2307/1538217
10. Zaika, V.E., 2004. Weight Allometry of Shells in Bivalve Mollusks. *Marine Ecological Journal*, 3(1), pp. 47–50 (in Russian).
11. Çelik, M.Y., Karayücel, S., Karayücel, İ., Öztürk, R. and Eyüboğlu, B., 2012. Meat Yield, Condition Index, and Biochemical Composition of Mussels (*Mytilus galloprovincialis* Lamarck, 1819) in Sinop, South of the Black Sea. *Journal of Aquatic Food Product Technology*, 21(3), pp. 198–205. https://doi.org/10.1080/10498850.2011.589099
12. Biandolino, F., Prato, E. and Caroppo, C., 2008. Preliminary Investigation on the Phytoplankton Contribution to the Mussel Diet on the Basis of Fatty Acids Analysis. *Journal of the Marine Biological Association of the United Kingdom*, 88(5), pp. 1009–1017. https://doi.org/10.1017/S0025315408001598
13. Pospelova, N.V. and Priimak, A.S., 2021. The Feeding of Mytilus galloprovincialis Lam. Cultivating in Coastal Waters of Sevastopol. *Proceedings of the T.I.Vyazemsky Karadag Scientific Station – Nature Reserve of the Russian Academy of Sciences*, 6(1), pp. 24–34. https://doi.org/10.21072/eco.2021.17.03 (in Russian).
14. Rahman, M.A., Henderson, S., Miller-Ezzy, P.A., Li, X.X. and Qin, J.G., 2020. Analysis of the Seasonal Impact of Three Marine Bivalves on Seston Particles in Water Column. *Journal of Experimental Marine Biology and Ecology*, 522, 151251. https://doi.org/10.1016/j.jembe.2019.151251
15. Delgado, M. and Camacho, A.P., 2005. Histological Study of the Gonadal Development of *Ruditapes decussatus* (L.) (Mollusca: Bivalvia) and its Relationship with Available Food. *Scientia Marina*, 69, pp. 87–97. Available at: https://scientiamarina.revistas.csic.es/index.php/scientiamarina/article/download/235/232/232 [Accessed: 20 April 2024].
16. Topić Popović, N., Beer Ljubić, B., Strunjak-Perović, I., Babić, S., Lorencin, V., Jadan, M., Čižmek, L., Matulić, D., Bojanić, K. [et al.], 2020. Seasonal Antioxidant and Biochemical Properties of the Northern Adriatic *Pecten jacobaeus. PLoS ONE*, 15(3), e0230539. https://doi.org/10.1371/journal.pone.0230539
17. Veske, E., Çankırılıgil, E.C. and Yavuzcan, H., 2022. Seasonal Proximate Composition, Amino Acid and Trace Metal Contents of the Great Mediterranean Scallop (*Pecten jacobaeus*) Collected from the Gulf of Antalya. *Journal of Anatolian Environmental and Animal Sciences*, 7(3), pp. 358–366. https://doi.org/10.35229/jaes.1111135
18. Pichaud, N., Briatte, S., Desrosiers, V., Pellerin, J., Fournier, M. and Blier, P.U., 2009. Metabolic Capacities and Immunocompetence of Sea Scallops (*Placopecten magellanicus*, Gmelin) at Different Ages and Life Stages. *Journal of Shellfish Research*, 28, pp. 865–876. https://doi.org/10.2983/035.028.0416

19. Biandolino, F., Leo, A.D., Parlapiano, I., Papa, L., Giandomenico, S., Spada, L. and Prato, E., 2019. Nutritional Quality of Edible Marine Bivalves from the Southern Coast of Italy, Mediterranean Sea. *Polish Journal of Food and Nutrition Sciences*, 69(1), pp. 71–81. https://doi.org/10.31883/pjfns-2019-0001
20. Aberoumad, A. and Pourshafi, K., 2010. Chemical and Proximate Composition Properties of Different Fish Species Obtained from Iran. *World Journal of Fish and Marine Sciences,* 2(3), pp. 237–239. Available at: https://www.idosi.org/wjfms/wjfms2(3)10/12.pdf [Accessed: 20 April 2024].
21. Pleadin, J., Kvrgić, K., Zrnčić, S., Lešić, T., Koprivnjak, O., Vulić, A., Džafić, N., Oraić D. and Krešić, G., 2019. Variations in Nutritive Composition of Three Shellfish Species. *Italian Journal of Food Sciences*, 31, pp. 716−730. https://doi.org/10.14674/IJFS-1502

Submitted 09.01.2024; accepted after review 26.02.2024;
revised 27.03.2024; published 25.06.2024

About the authors:

Lyudmila V. Ladygina, Senior Research Associate, A.O. Kovalevsky Institute of Biology of the Southern Seas of RAS (2 Nakhimov Av., Sevastopol, 299011, Russian Federation), Ph.D. (Biol.), *lvladygina@yandex.ru*

Anna V. Pirkova, Senior Research Associate, A.O. Kovalevsky Institute of Biology of the Southern Seas of RAS (2 Nakhimov Av., Sevastopol, 299011, Russian Federation), Ph.D. (Biol.), *avpirkova@mail.ru*

Contribution of the authors:

Lyudmila V. Ladygina − material processing, analysis and discussion of results, manuscript writing

Anna V. Pirkova − material processing, analysis and discussion of results, manuscript editing

All the authors have read and approved the final manuscript.